Evaluating quinone based compounds for their anti-trypanosomatid properties

Submitted in partial fulfilment of the requirements

of the Degree of Doctor of Philosophy

Emma Louise Meredith

Statement of originality

I, Emma Louise Meredith, confirm that the research included within this thesis is my own work or that where it has been carried out in collaboration with, or supported by others, that this is duly acknowledged below and my contribution indicated. Previously published material is also acknowledged below.

I attest that I have exercised reasonable care to ensure that the work is original, and does not to the best of my knowledge break any UK law, infringe any third party's copyright or other Intellectual Property Right, or contain any confidential material.

I accept that the College has the right to use plagiarism detection software to check the electronic version of the thesis.

I confirm that this thesis has not been previously submitted for the award of a degree by this or any other university.

Signature: 

Date: 14th July 2015

Details of collaborations:

Dr Sam Alsford, London School of Hygiene and Tropical Medicine (LSHTM)

Dr Karin Seifert, London School of Hygiene and Tropical Medicine(LSHTM)

Details of publications to date:

Sullivan, J.A., J.L. Tong, M. Wong, A. Kumar, H. Sarkar, S. Ali, I. Hussein, I. Zaman, E.L. Meredith, N.A. Helsby, L. Hu and S.R. Wilkinson. Unravelling the role of SNM1 in the DNA repair system of *Trypanosoma brucei*.*Molecular Microbiology* 96, 827-838.

Hall, B., E.L.Meredith., S.R.Wilkinson. Targeting the substrate preference of a type I nitroreductase to develop antitrypanosomal quinone-based prodrugs.*Antimicrobial agents and chemotherapy* 56, 5821-5830

Funding:

The funding for this project was provided by the BBSRC Doctorial Training Studentship.

Abstract

Human African trypanosomiasis (HAT) is caused by the protozoan parasite *Trypanosoma brucei*. The use of existing drug regimens is controversial as they are toxic, have limited efficacy with resistance on the rise. Therefore, there is an urgent need for new therapies. One group of compounds that are being exploited or evaluated in treating infectious diseases and cancer are the quinones, with these agents mediating their cytotoxic activities by acting as prodrugs or inhibiting key metabolic pathways. Here, we report the screening of a quinone-based compound library against bloodstream form *T. brucei* and against the related parasites *Trypanosoma cruzi* and *Leishmania major*, the causative agents of Chagas disease and cutaneous leishmaniasis, respectively. This analysis demonstrated that the most potent compounds were those that possessed an aziridinyl 1,4-benzoquinone (ABQs) core with the most effective displaying a 50% growth inhibitory concentrations of < 1 μM against all three pathogens. Using RH1, the archetypal ABQ, as a selective agent, a combination of a *T. brucei* whole genome loss of function assay and drug selection studies demonstrated that these compounds function as prodrugs with the activation mechanism catalysed by a type I nitroreductase (NTR). Functional studies using *T. brucei* that express altered levels of NTR further demonstrated the importance of this enzyme in activating the majority of quinone-based moieties tested. Using genetic approaches, we next demonstrated that following NTR-mediated activation the resultant products go on to promote formation of interstrand crosslinks (ICLs) within the parasites' genomes: *T. brucei* lacking the DNA repair enzyme SNM1, a nuclease that specifically fixes ICL damage, were more susceptible to ABQs than controls. In conclusion, ABQs are potent antiparasitic prodrugs although mammalian toxicity studies indicate these compounds may not be suitable potential therapies for systemic infections although they are of interest as genetic tools for probing gene function.

Acknowledgements

I would like to thank Dr Shane Wilkinson for his supervision and support throughout this process. I am also very grateful to the following members of staff at the London School of Hygiene and Tropical Medicine: Professor John Kelly for use of the Amaxa system; Dr Martin Taylor for his useful advice on qRT-PCR techniques; Dr Sam Alsford for carrying out the three RNAi library screens presented here and Dr Karin Seifert for screening a selection of the quinone based compounds against mouse macrophages. Thanks also goes out to Drs Andrew Voak and Ricardo de Pádua for their help and support at the beginning of my PhD. Also I need to thank them both for the most unusual birthday present I have ever received, a flask of promastigote form *Leishmania major* for drug assays. I am also very appreciative of members past and present of office 4.36 as well as the tea group (and June) for teaching me that most issues can be resolved over tea and cake.

I am indebted to my parents for their constant support throughout my PhD. I promise I will one day sit down and talk you through this thesis. Also I need to thank my good friends for keeping me sane- usually over food, cocktails or both. I hope one day I can return the support you all have provided me. Finally, to the members past and present of the 1st Woodford St Mary's Brownies and the Guiders in Woodford South district for reminding me that laughter is certainly the best medicine!

Contents

List of figures contained within this thesis

List of tables contained within this thesis

Abbreviations used in this thesis

ABQ	Aziridinyl 1,4-benzoquinone
BSF	Bloodstream form
CDC	Centre for Disease control
CSF	Cerebal spinal fluid
CPR/P450R	Cytochrome P450 reductase
HAT	Human African trypanosomiasis
IC_{50}	Inhibitory concentration at 50% cell growth
ICL	Interstrand cross link
LD_{50}	Concentration which kills 50% of cells
LS-BSF	Long slender blood stream form
LSHTM	London School of Hygiene and Tropical Medicine
MCT	Metacyclic trypomastigote
MGMT	Methylguanine methyltransferase
NER	Nucleotide excision repair pathway
NGO	Non-Government Organisation
NQO1	NAD(P)H:quinone oxidoreductase 1
NQO2	NAD(P)H: quinone oxidoreductase 2
NTD	Neglected tropical diseases
NTR	Type 1 nitroreductase
PCF	Procyclic form
Pso2p	Sensitive to psoralen
qRT-PCR	quantitative real time PCR
SNM1	Sensitive to nitrogen mustards
SSF	Short stumpy form
VSG	Variable surface antigen
WHO	World Health Organisation
WT	Wild type

Chapter 1: Introduction

1.1 Introduction to Trypanosomatid parasites

Trypanosomatids represent a monophyletic order of protozoa belonging to the Class Kinetoplastida (Stevens *et al*. 2001). The trypanosomatids are obligate parasites primarily of insects although several genera are heteroxenous, having complex life cycles involving a secondary plant, invertebrate or vertebrate host (Lopes 2010). During their life cycles, trypanosomatids are characterised by having at least one form with a long slender morphology and single flagellum that together give the cell a corkscrew-like motion (*trypano* = borer, *soma* = body). As eukaryotes, trypanosomatid cells possess membrane bound organelles such as the nucleus, endoplasmic reticulum and Golgi bodies, peroxisomes and mitochondrion although the specific arrangement and function of some of these structures can be unusual (Lopes 2010) (Figure 1.1). For example, the peroxisomes of trypanosomatids are known as glycosomes as several enzymes of the glycolytic pathway are compartmentalised in this organelle (Barrett *et al*. 2003; Parsons 2004; Stuart *et al*. 2008; Lopes 2010), while they only contain one mitochondrion whose genome, known as the kinetoplast, is composed of a highly complex interconnected network of mini and maxi circle DNAs known as ktDNAs (Stevens *et al*. 2001; Barrett *et al*. 2003; Stuart *et al*. 2008; Lopes 2010).

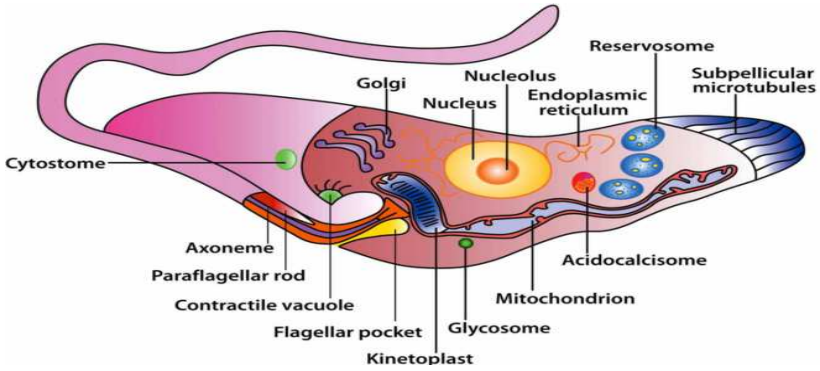

Figure 1.1: Structure of trypanosomatid cell. Trypanosomatid cells contain a range of organelles including a large single mitochondrion and its associated kinetoplast (the mitochondrial genome), the flagellum and flagellum pocket, nucleus, ribosomes, endoplasmic reticulum, Golgi apparatus and glycosomes (modified peroxisomes that contain glycolytic enzymes) (Image taken from Lopes (2010))

Trypanosomatids cause several major infections in humans and animals. It is estimated that 22 million people worldwide are infected by these microbes (Barrett *et al*. 2003; Stuart *et al*. 2008; Lopes 2010) with the parasites responsible for three human diseases namely human African trypanosomiasis (HAT), Chagas disease (also known as American trypanosomiasis) and Leishmaniasis, which are caused by *Trypanosoma brucei*, *Trypanosoma cruzi* and *Leishmania* species, respectively. All three of these infections are transmitted by the blood feeding habits of an insect vector with the pathogens causing predominantly chronic infections that can be lead to longer term disability, disfigurement, neurological abnormalities and death. These three diseases are classified by the World Health Organisation (WHO) as 'Neglected Tropical Diseases' (NTDs). In total, there are seventeen such conditions caused by various agents including helminths, protozoa, viruses and bacteria. This diverse group of illnesses principally affects low-income populations in developing regions of the World and causing substantial illness in more than 1.4 billion people globally (CDC 2011). Besides being responsible for the deaths of over 500,000 people

worldwide every year these infections often impair the physical and cognitive development of children, making it difficult to farm or earn a living, and limit productivity in the workplace. As such NTDs often trap the most vulnerable individuals within a community in a cycle of poverty and disease. As the cost of new drug innovations is now estimated to be greater than US$2.5 billion (Tufts Center for the Study of Drug Development 2014), pharmaceutical companies are unwilling to invest in therapeutic development specifically targeting diseases that affect the world's poorest communities as the returns do not justify such a financial outlay. Of the 1393 new drugs that came onto the market between 1975 and 1999 only 16 were developed for treating NTDs (Pécoul 2004).Therefore, there is an urgent need for new safer drugs against these debilitating conditions.

1.2 Human African trypanosomiasis

Human African trypanosomiasis, also known as African sleeping sickness, is a public health problem across sub-Saharan Africa. First recorded by the physician Thomas Winterbottom in 1734 (Steverding, 2008), this infection along with Nagana, the equivalent disease found in ungulate animals, has affected the development of this region of the World essentially making vast tracts of land ranging from south of the Sahara to north of the Kalahari desert economically unviable in terms of farming. Currently over 60 million people are at risk of infection, especially poor rural communities in areas such as Sudan, Angola and the Democratic Republic of Congo, where agriculture, fishing and hunting are the main sources of income (World Health Organisation 2011).

The improving political situation and the ability of non-governmental organisations (NGOs) such as WHO, Médecins Sans Frontières and Drugs for Neglected Diseases Initiative to access the above regions and thus safely implement diagnosis and treatment programmes has resulted in the number of reported new cases falling to below 10,000 (Simarro *et al*. 2011; Franco *et al*. 2014). The success of these schemes has prompted Dr Jean Jannin, Coordinator of the Innovative and Intensified Disease Management unit of the WHO Department of Control of Neglected Tropical Diseases in Geneva, to state that "The target is to eliminate the *gambiense* (West African) form of the disease (HAT) as a public-health problem by 2020" and "It means bringing down the incidence of the disease to less than 1 case per 10 000 of the population in at least 90% of the areas where cases exist." (World Health Organisation 2013) with the ultimate goal of a sustainable disease elimination by 2030 (Franco *et al*. 2014). However, history has demonstrated that such aspirations will only prevail if effective diagnosis and treatment programmes are maintained. Over the last 120 years there have been several HAT epidemics. The first of these occurred at the turn of the 20th century (1896-1906) and affected mainly the northern shore of Lake Victoria where up to two thirds of the population in the affected region died: this equates to an estimated 250,000 people (Lundkvist *et al*. 2004). This alarming situation promoted an increase in research targeting HAT resulting in the development of the arsenic-based trypanocidal therapy tryparsamide and eventually suramin, a drug that is still in use today. A second major epidemic which started in 1920 and came to an end in the late 1940's, resulted to the then governing colonial powers to instigate systematic screening, treatment and surveillance strategies using experiences learnt from the 1896-1906 outbreak. As a result from the 1940s through to the 1970s the estimated number of new cases fell to levels on par with the

situation we are seeing today. However, as many African countries gained independence during the late 1960's and the early 1970's, the resultant social upheaval and political instability caused the public health services and control programmes previously used by the colonial powers to control HAT to collapse. As a consequence there was a dramatic increase in the number of new cases and deaths directly attributable to this disease, peaking during the mid-1990s where in one year (1996) alone, estimates indicated that there were approximately 450,000 new cases of the disease and causing approximately 50,000 deaths. It was in light of these worrying statistics coupled with a decline in civil unrest, several NGOs were promoted to initiate many of the screening, treatment and surveillance strategies used today.

1.3 The causative agent

The pathogen responsible for causing HAT is the protozoan parasite *T. brucei*, that dependent on geographical location, is transmitted *via* anthropomorphic and zoonotic cycles by the haematophagous behaviour of the tsetse fly (*Glossina* genus). Unlike the other human infective trypanosomatid parasites *Trypanosoma cruzi* and *Leishmania*, this protozoan does not invade cells instead lives extracellularly in various body fluids such as the bloodstream, lymphatic system and cerebral spinal fluid (CSF). Analysis of *T. brucei* from different sites in Africa has shown that this species can be split into two distinct sub-species with each grouping showing differences in disease progression, epidemiology, mechanisms of transmission *etc* (Table 1.1).

	West African HAT	East African HAT
Causative agent	*T.b. gambiense*	*T.b. rhodesiense*
Vector	Riverine (*Glossina palpalis)*	Savannah (*Glossina morsitans)*
Ecology	Rainforest, rivers and lakes	Woodland and dry bush
Location	West and Central Africa	East and Southern Africa
Transmission	Anthropomorphic	Zoonotic
Epidemiology	Endemic, some epidemics	Sporadic outbreaks
Prognosis	Slow progression to chronic disease	Rapid progression to death
Parasitaemia	Low	High
Asymptomatic carriers	Common	Rare
Non-human hosts	Rare	Wild and domestic animals (ungulates)

Table 1.1: Differences between the different forms of human African trypanosomiasis. Adapted from Wiser, M. Protozoan and Human diseases (2011).

In West and Central Africa, a form of HAT known as West African trypanosomiasis predominates (Figure 1.2). This chronic infection, caused by *T.b. gambiense* and transmitted mainly *via* an anthropomorphic cycle, accounts for the vast majority (98%) of HAT cases (World Health Organisation 2014). However, recent data indicates that the disease prevalence figures may be higher than those quoted by WHO as infected individuals having an active immune system are usually able to

suppress the parasitemia to levels that fails to promote disease symptoms for periods longer than originally thought (Wastling *et al.* 2011; Jamonneau *et al*. 2012): in one case, a patient was infected by *T.b. gambiense* for nearly 30 years before developing the cerebral symptoms associated with HAT (Sudarshi *et al*. 2014). As such it is now apparent that there are significantly more asymptomatic carriers than previously thought with many individuals leading a full and productive life, unaware that they are infected but still acting as a reservoir for this form of the disease.

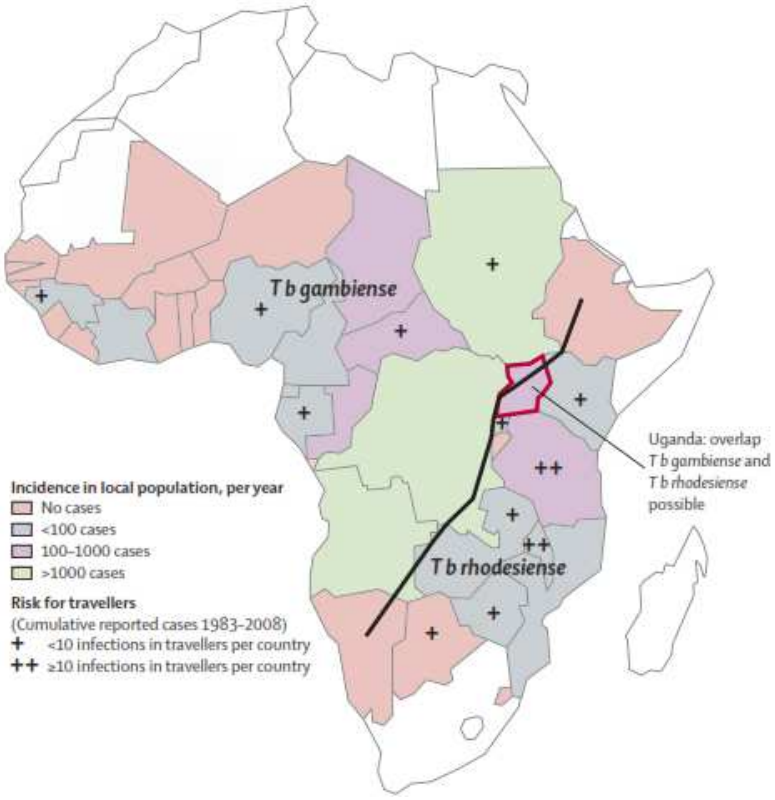

Figure 1.2:Distribution and incidence of the different human African trypanosomiasis forms. The white countries represent areas where the tsetse vectors are not found and no cases of HAT have been reported.Image taken fromBrun *et al*. (2010)**.** Available from: http://www.thelancet.com/journals/lancet/article/PIIS0140-6736(09)60829-1/fulltext.Copyright © 2016 Elsevier Limited.

Endemic in East and Southern Africa the second HAT variant known as East African trypanosomiasis is prevalent (Figure 1.2). Caused by *T.b. rhodesiense*, this predominantly zoonotic infection only accounts for 2% of HAT cases. In contrast to *T.b. gambiense*, the parasite loads in a *T.b. rhodesiense*-infected individual can reach

high levels and can result in the rapid death of the host. As such East African trypanosomiasis is said to be an acute infection. Although the two *T. brucei* sub-species are found at different geographical sites, there now appears to be an emerging overlap of the endemic areas in Uganda, potentially through the movement of *T. b. rhodesiense* animal reservoirs to non-zoonotic *T.b. gambiense* endemic sites (Picozzi *et al*. 2005). This is of particular concern as *T. brucei* does undergo genetic exchange that in theory could result in the hybridization of the different *T. brucei* sub-species to generate new trypanosome variants (Picozzi *et al*. 2005; Franco *et al*. 2014).

1.4 *Trypanosoma brucei* life cycle

To deal with the various environments *T. brucei* is exposed to during its life cycle, the parasite exhibits several distinct forms (Figure 1.3).

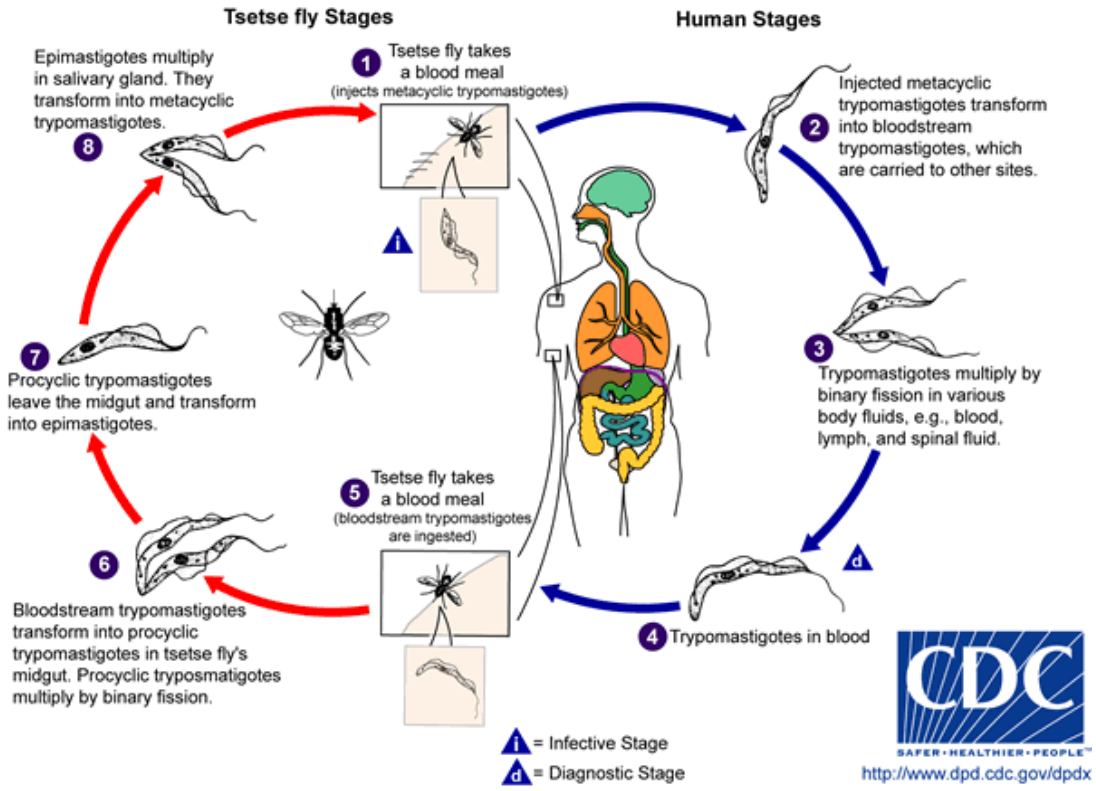

Figure 1.3: Life cycle of *T. brucei*. Image sourced from (Center for disease control (CDC) 2015). Available from: http://www.cdc.gov/parasites/sleepingsickness/biology.html.

When taking a blood meal, the tsetse fly punctures the skin of a mammalian organism causing blood and lymph to rise and pool at the bite site. If the insect is infected with *T. brucei*, saliva containing the parasite in its highly infectious metacyclic trypomastigote (MCT) form can be transferred into this pool with the pathogen then gaining accessing to the bloodstream of the host. Once inside the vertebrate, the non-dividing MCT differentiates to a long, slender bloodstream form (LS-BSF) trypomastigote that start to divided by binary fission and commence colonising the various bodily fluids of host. During the initial stages of infection the parasites are confined to the blood and lymph systems but as the disease progresses they can cross the blood brain barrier and enter the cerebrospinal fluid. While in the blood and lymphatic systems, the parasite number fluctuates to generate a characteristic "wave of parasitemia" profile. A quorum sensing-like mechanism driven by the so-called "stumpy induction factor" operating towards the peak of each wave that promotes differentiation of the LS-BSF to a short stumpy form (SSF) trypomastigote form, which is pre-adapted for conditions inside the insect (Mony *et al*. 2014; Mony & Matthews 2015). When another tsetse fly takes a blood meal, the vector ingests blood or lymph containing LS-BSF and SSF parasites. In the insect's gut, conditions that kill LS-BSF stimulate differentiation of SSF trypanosomes into procyclic trypomastigotes (PCF). The PCFs multiply by binary fission, colonize this part of the insect's digestive tract before eventually migrating, possibly *via* the insect's haemcoel, to the salivary glands of the vector. Once in the salivary glands, the PCFs transform into the epimastigote form and using their flagellum, adhere to epithelial cells of this organ (Ralston *et al*. 2009). At this point genetic exchange can take place, although this is not an obligatory part of the *T. brucei* life cycle (Peacock *et al*. 2014). Eventually, in response to unknown conditions and factors,

epimastigotes mature into metacyclic trypomastigotes (MCTs) that detach from the salivary glands' epithelial layer and enter this duct's lumen ready to infect a new host when the fly feeds.

1.5 Disease staging and pathologies of human African trypanosomiasis.

The pathologies associated with HAT occur through two distinct stages known as the early (or haemolymphatic) stage that then develops into the late (or meningoencephalitic) staging (Figure 1.4). For *T.b. gambiense* infections progression from the early to late disease staging takes on average 3 years, although recent findings have questioned these values (Jamonneau *et al*. 2012; Wastling *et al*. 2011; Sudarshi *et al*. 2014), while in the case of *T.b. rhodesiense* infections this usually weeks-months after the initial infection (Brun *et al*. 2010).

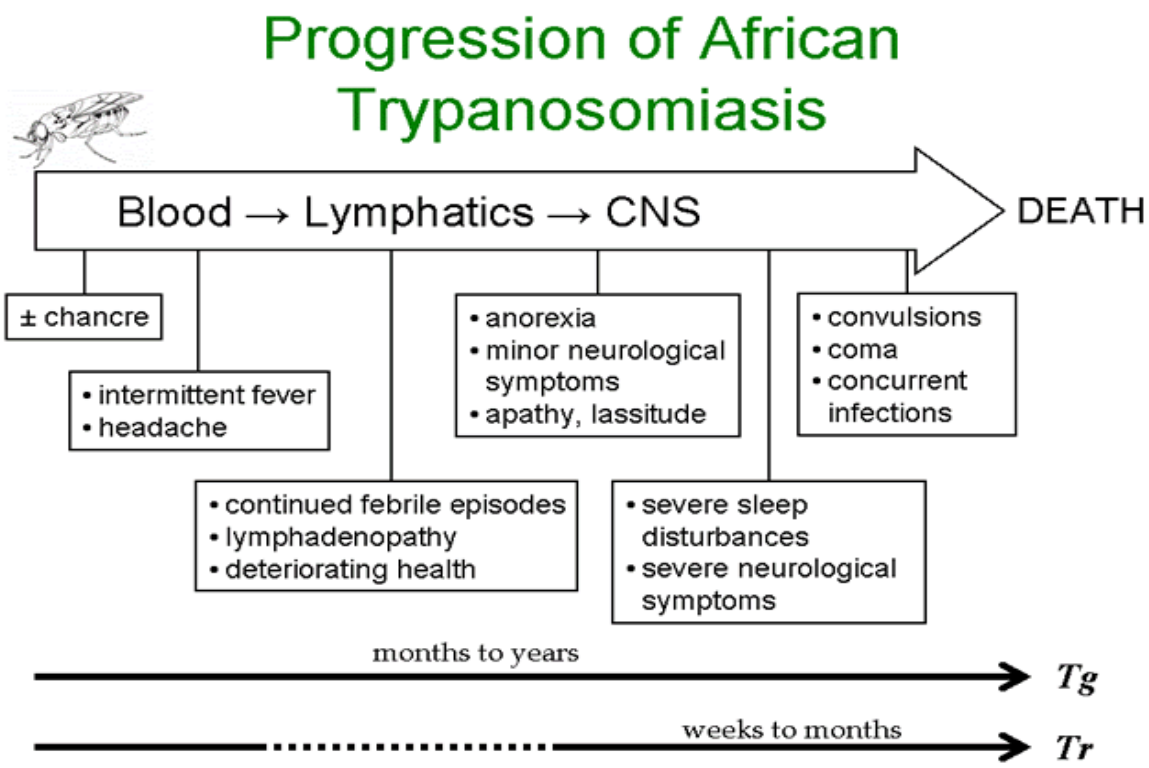

Figure 1.4: Progression of human African trypanosomiasis.*Tr:T.b. rhodesiense. Tg:T.b. gambiense*. Image sourced from Wiser (2011).

Early stage HAT starts upon infection and continues while the parasites remain restricted to the blood or lymphatic systems of the human host (Malvy & Chappuis 2011). In most cases this disease staging is asymptomatic although for 19% of patients harbouring *T.b. rhodesiense*, a painful, localised skin inflammatory, known as a trypanosomal chancre, may develop at the site of the insect bite (Figure 1.5) (Brun *et al*. 2010). As the early stage develops the patient presents with a range of symptoms including headaches, adenopathy and characteristically a relapsing fevers, with the latter condition directly associated with the fluctuating parasitemia found in the patient's bloodstream (Stuart *et al*. 2008). Trypanosomes possess immunogenic proteins known as variable surface glycoproteins (VSG) with roughly 10^7 copies per cells and estimates suggest that 10% of the trypanosome genome is assigned to *vsg* encoding genes (Berriman *et al*. 2005; Stuart *et al*. 2008; Bacchi 2009; Lopes 2010; Wiser 2011). The host immune system will mount a specific antibody response against trypanosomes expressing one VSG, leading to parasite elimination of those expressing that protein. However, parasites that have switched expression to a new VSG protein, survive and rapidly replicate until the host mounts an immune response against the VSG (Vincendeau & Bouteille 2006; Wiser 2011). This sequence of events in repeated.

Figure 1.5: Chancre at the site of the tsetse fly bite in *T. b rhodesiense* infections. Left image sourced from http://www.microbiologybook.org/parasitology/blood-proto.htm and right image sourced from Moore *et al*. (2002)

Eventually, trypanosomes cross the blood brain barrier and accesses the CSF with the patient entering the late stage of the disease. Here, symptoms include a range of neurological conditions such as impaired mental function, weight loss, altered sleeping patterns and personality changes with the patient eventually slipping into coma and then dying. It is not fully understood how or why the parasites enters the CSF, although one current thought could be that the parasite manipulates host behaviour in order to aid its transmission: the daytime sleeping patterns displayed by patients exhibiting late stage HAT may increase the chance that the host will be bitten by the tsetse fly as the person will not react to the pain of an insect bite (Wolburg *et al*. 2012). Interestingly, prostagladin D_2 induces sleep if injected into the ventricle system and it has been demonstrated this hormone-like compound is significantly elevated in the CSF of patients in the late stage HAT with this helping to regulate parasite cell density (Wolburg *et al*. 2012).

1.6 Current treatments

Currently, five chemotherapeutic regimens are available for use against HAT with treatment determined by which *T. brucei* sub-species an individual is infected with and the presented disease stage (drug structures shown in Figure 1.6). When treating the early stage, pentamidine is given as the frontline drug targeting West African trypanosomiasis while suramin is used against the East African form of the disease. These treatments if appropriately administered are usually effective. However, once the pathogen has cross the blood brain barrier and the patient has entered the late disease stage, treatment success declines and unfortunately, it is at this point when most patients present themselves to a clinician. The therapies available to target the late stage HAT consist of melarsoprol, which can be used against both *T.*

*brucei*variants, and eflornithine, which although used as a monotherapy, is now routinely employed to treat patients infected with *T.b. gambiense* in a nifurtimox-eflornithine combinatorial therapy (NECT). Key features of the drug treatments are outlined in Table 1.2.

The use of the above therapies is problematic. Most of the available chemotherapies require hospitalisation while being administered and for follow up screens aimed at determining whether the treatment has worked. This in addition to compound synthesis, transportation and storage *etc*, all contribute to the treatment cost which is generally prohibitive to most HAT suffers(Barrett *et al*. 2003). As a consequence, most treatments are administered through the actions of NGO funded mobile schemes. Additionally, resistance to some of the treatments, particularly melarsoprol and to a lesser extent pentamidine, is on the rise such that these are becoming ineffective in certain countries such as Uganda (Matovu *et al*. 2003; Bernhard *et al*. 2007; Nerima *et al*. 2007; Robays *et al*. 2008; Pyana *et al*. 2011; Graf *et al*. 2013). Perhaps the most worrying issue regarding the front line HAT treatments stems from their toxicities. For suramin, which can cause problems including nephrotoxicity, bone marrow toxicity, anaphylactic shock, skin lesions and neurological complications, and pentamidine, which often leads to hypoglycaemia and hypotension, these side effects are generally not a major problem with any complications generally clearing up after cessation of treatment (Legros *et al*. 2002; Brun *et al*. 2010; Wilkinson *et al*. 2011; Kennedy 2013). However, the use of melarsoprol, an arsenic-based compound, is controversial as this can cause reactive encephalopathy. This issue arises in 5 to 8% of HAT patients and results in the death of 45 to 60% in such individuals (Legros *et al*. 2002; Burri 2010). This adverse side

effects appears to be associated with activation of the melarsoprol prodrug to melarsen oxide, with this toxophore responsible for other side effects such as convulsions, loss of consciousness, rashes and vomiting (Bouteille *et al*. 2003; Nok 2003; Wilkinson & Kelly 2009).

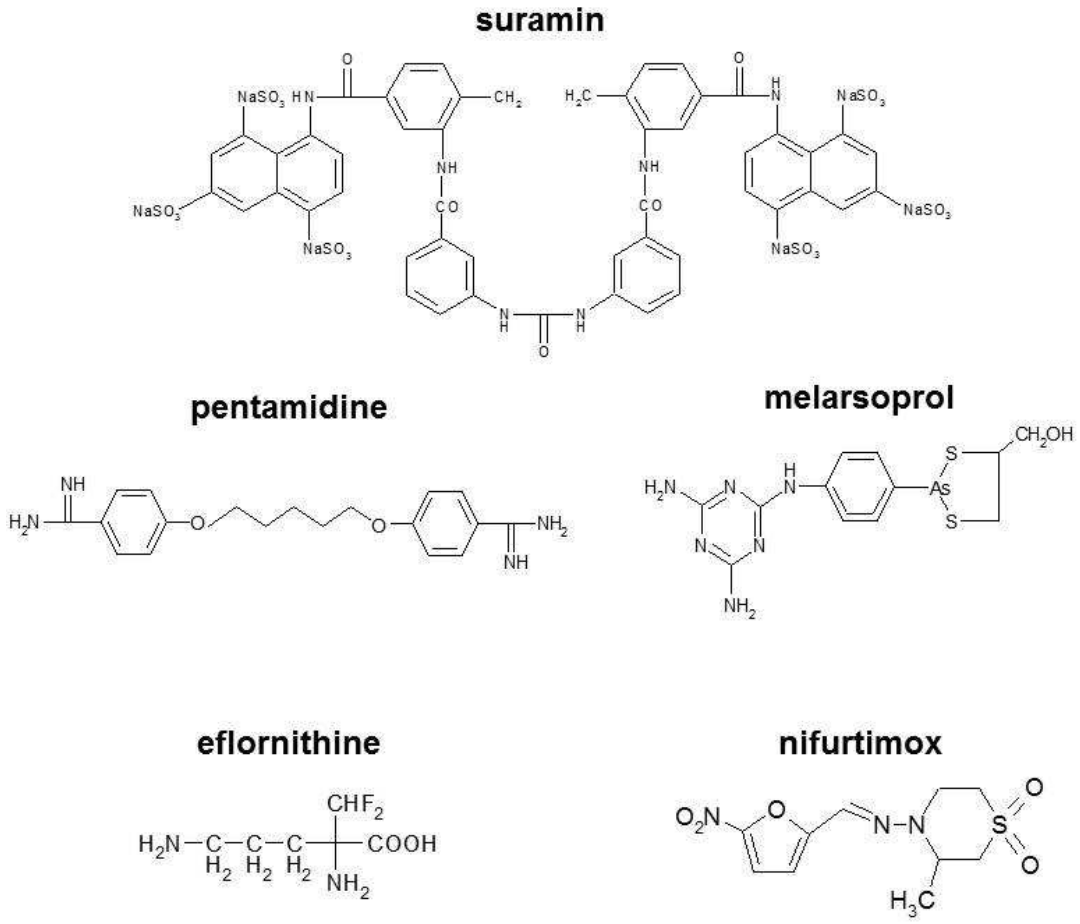

Figure 1.6. Structure of the drugs used against human African trypanosomiasis.

Drug (class)	Mode of action	Uses	Obstacles	References
Suramin (Polysulphonated napthalene)	Glycoprotein ISG75 and four lysosomal proteins have been linked with efficacy and resistance. Function unclear 'promiscuous' inhibitor of an array of glycolytic and pentose phosphate pathway enzymes	First line of treatment for early stages of *T.b. rhodesiense* infections	Negatively charged cannot cross the blood-brain barrier; Administratedintravenously; Skin reactions, nerve damage and haematological toxicity.	Nok 2003; Legros *et al*. 2002; Bacchi 2009; Wilkinson & Kelly 2009; Alsford *et al*. 2012
Pentamidine (Aromatic diamidine)	P2 adenoside transporter 1 (AT1) and an aquaglyceroporin (AQP2/3) linked with uptake and resistance. Readily metabolised by human cytochrome P450 reductase. Accumulation of drug collapses trypanosome mitochondrial membrane potential. Binds to the minor groove of mitochondrial DNA minicircles.	First line of treatment for early stages of *T.b. gambiense* infections	Does not readily pass through the blood brain barrier; Generally well tolerated	Shapiro & Englund 1990; Wilkinson & Kelly 2009; Alsford *et al*. 2012; Baker *et al*. 2013
Melarsoprol (trivalent arsenical)	P2 adenoside transporter 1 (AT1) and an aquaglyceroporin (AQP2/3) linked with uptake and resistance. Prodrug with activation leading to formation of melarsen oxide (MelOx) and hinders adenine uptake. Inhibits a range of glycolytic enzymes and forms stable adducts with trypanothione thus block activity of trypanothione reductase.	Second line treatment for haemolymphatic stages of *T.b. rhodesiense* and *T.b. gambiense* The only treatment for late stages of *T.b. rhodesiense* infections.	Highly toxic causing 10% of patients to develop reactive encephalitis; Side effects include convulsions, loss of consciousness and vomiting.	Fairlamb *et al*. 1989; Stich *et al*. 2002; Bacchi 2009; Wilkinson & Kelly 2009; Schumann Burkard *et al*. 2011Alsford *et al*. 2012; Baker *et al*. 2013

Drug (class)	Mode of action	Uses	Obstacles	References
Eflornithine (Fluorinated amino acid)	Uptake *via* amino acid transporter (AAT6). Inhibitor of ornithine decarboxylase (ODC),prevents production of putrescine. Inactivation of ODC transforms the trypanosome into forms not capable of modifying VSG or dividing allow immune clearance	Early and late stage of *T.b. gambiense* infections. Used for melarsoprol refractory cases.	Poor transport across blood-brain barrier; Costly, complicated and difficult to administer; Side effects include GI problems, convulsions and fever.	Steverding 2008; Bacchi 2009; Vincent *et al*. 2010; Wiser 2011; Alsford *et al*. 2012; Alirol *et al*. 2013
Nifurtimox Eflornithine combination therapy (NECT)	Combination therapy. Nifurtimox partner is a drug used to treat Chagas disease. Nifurtimox is a prodrug and activated by a type I NTR leading to cytotoxic products. Reduction of type I NTR activity linked to resistance.	Replaced melarsoprol in late stage *T.b. gambiense* infections.	Gastrointestinal disturbances, abdominal pain and vomiting common. Convulsions, tremor and agitation and polyneuropathy have been reported.	Checchi *et al*. 2007; Wilkinson & Kelly 2009; Burri 2010; Franco *et al*. 2012; Alirol *et al*. 2013

Table 1.2: Summary of drug treatments available to treat human African trypanosomiasis.

1.7 Quinones

Quinone-based compounds encompass a range of chemical moieties characterised by the presence of two carbonyl groups linked to a carbocyclic backbone. They can be divided into several classes dependent on the relative positions of the carbonyl-groups on the ring, either in 1,2 (ortho), 1,3 (meta) or 1,4 (para) positions, and whether the carbocyclic core is part of another ring system.

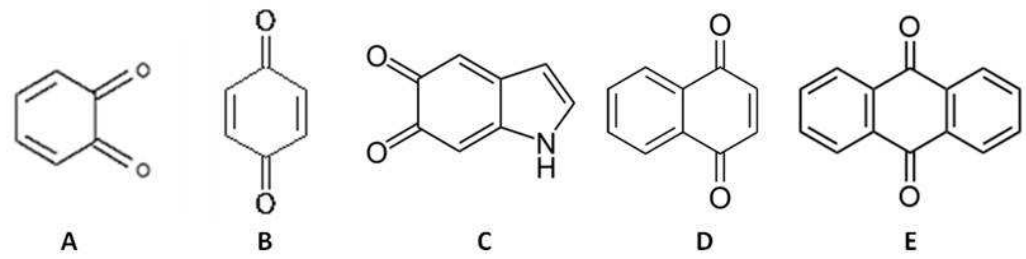

Figure 1.7: Examples of basic quinone structures. A corresponds to a 1,2-benzoquinone, B to a 1,4-benzoquinone, C represents an indolequinone, D a 1,4-naphthoquinone and E a 9,10-anthraquinone

Quinone compounds are found throughout nature, functioning as electron acceptors in crucial oxidoreductase cascades such as in the mitochondrial electron transport chain and photosystem II in chloroplasts. Additionally, natural and synthetic quinones are of pharmacological interest, functioning either as inhibitors of essential redox pathways or as pro-drugs. In the latter case, the compound must undergo activation before mediating its cytotoxic effects, reactions catalysed by quinone oxidoreductases (Koster 1991; Danson *et al*. 2004; Hall *et al*. 2012). Based on oxygen-sensitivity, such enzymes can be divided into two groups (Figure 1.8). Under hypoxic conditions, oxygen-sensitive quinone oxidoreductases such as NADH cytochrome b_5 reductase and cytochrome P450 reductases mediate the 1-electron reduction of the quinone to an unstable semiquinone radical (Koster 1991; Long II & Jaiswal 2000; Fang & Beattie 2002a; Begleiter *et al*. 2007; Avendano & Menendez 2008). This can then be further reduced to the hydroquinone derivative. However, in

the presence of oxygen, formation of the hydroquinone product is inhibited, with the radical undergoing futile cycling to produce superoxide & regeneration of the parent compound. In contrast, the oxygen-insensitive quinone oxidoreductases including NAD(P)H quinone oxidoreductase 1 and 2 (NQO1; (also known as DT-diaphorase) and NQO2) catalyse the 2-electron reduction of the quinone to form the hydroquinone directly.

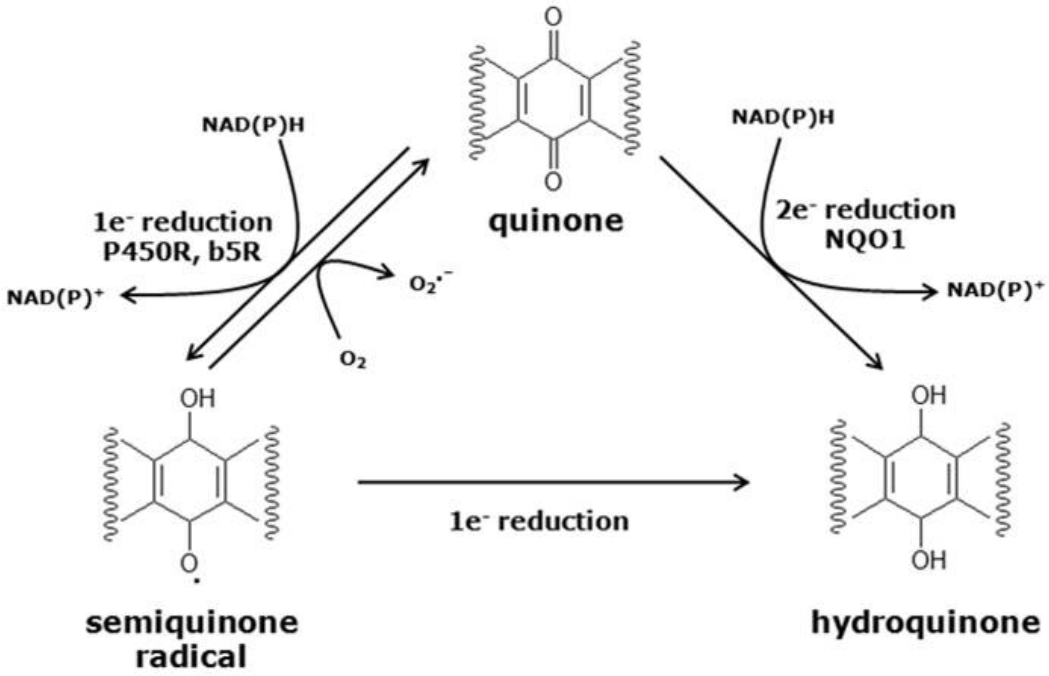

Figure 1.8: Quinone reduction pathways. Quinones can be reduced to hydroquinones by two distinct pathways. In one system, enzymes such as cytochrome P450 reductase (P450R) & cytochrome b5 reductase (b5R) mediate the $1e^-$ reduction of the quinone to a semiquinone radical. This then undergoes further reduction to the hydroquinone. In the presence of O_2, the semiquinone can undergo futile cycling to form $O_2^{\cdot-}$& the parental quinone. In the other pathway, reduction of the quinone to the hydroquinone occurs directly, via a $2e^-$ reduction event as typified by NAD(P)H:quinone oxidoreductase 1 (NQO1). ≀ represents R groups on the quinone backbone.

1.7.1 Quinones as anti-cancer agents

Quinones have been extensively studied as potential anticancer agents. This was stimulated by observations that expression of the quinone oxidoreductase NQO1, a predominately cytosolic enzyme thought to exert a protective effect by detoxifying

toxins and mutagens, is low in normal tissues but elevated in cancer cells (Danson *et al*. 2004). This interest resulted in development of several NQO1 activated quinone-based compounds including EO9, mitomycin C, β-lapachone and gelanamycin, agents that show promising antitumor activities although some of these do promote unwanted side effects. (Siegel *et al*. 1990; Berardini *et al*. 1993; Maliepaard *et al*. 1995; Tudor *et al*. 2005). Through a ping-pong mechanism and utilising NAD(P)H as donor of reducing equivalents, NQO1 mediates conversion of the quinone to the hydroquinone derivative, resulting in a redistribution of electrons within the carbocyclic backbone. Dependent on the initial structure this can then promote different downstream effects (Figure 1.9).

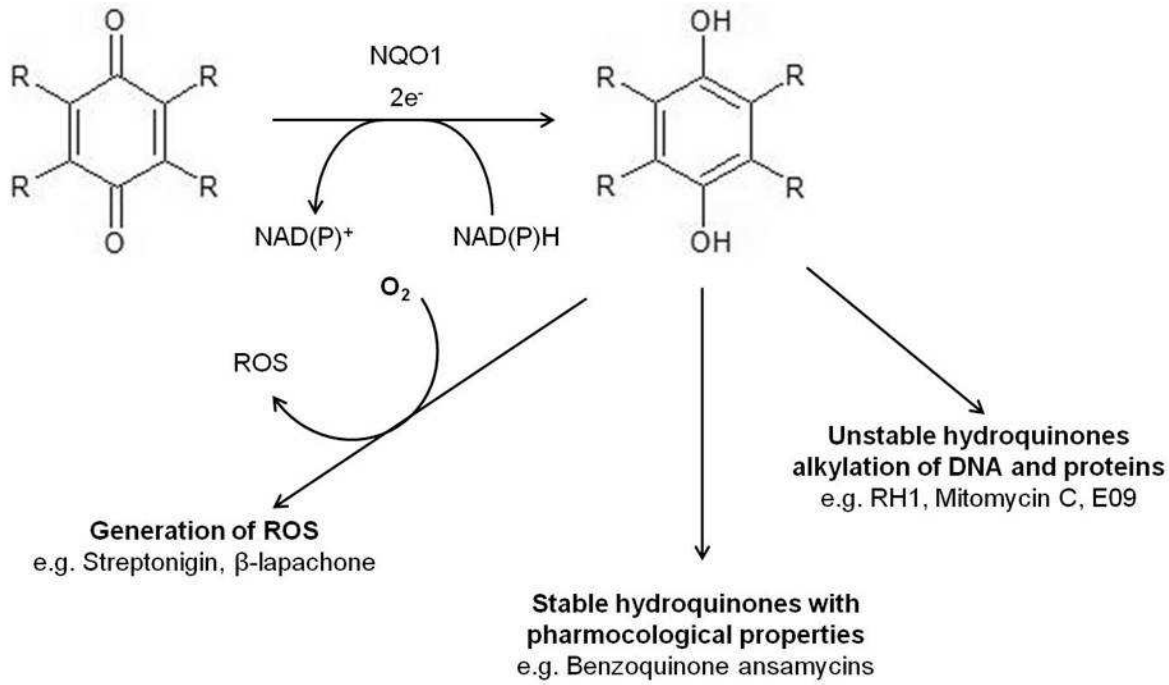

Figure 1.9: Pathways quinone based compounds can take after activation by NQO1 to form hydroquinones. Image modified from Siegel *et al*. (2012).

For compounds such as streptonigin and β-lapachone, the NQO1 generated hydroquinone can undergo redox cycling with oxygen leading to the formation of reactive oxygen species. If generated at significant levels, these can then cause a cell to enter a state of oxidative stress that can lead to cell death (Dzielendziak *et al*.

1990; Siegel *et al*. 2012; Parkinson *et al*. 2013). Alternatively, reduction of some quinones generates stable hydroquinone metabolites that can exert an inhibitory effect on other enzymes. For example the hydroquinones of the ansamycin natural products can interact with and bind to the ATP binding pocket of heat shock protein 90 (hsp90) preventing this enzyme from folding newly synthesized proteins including oncoproteins such as HER2 and Raf-1 (Whitesell *et al*. 1994; Reigan *et al*. 2011; Siegel *et al*. 2012). Finally, some quinones following NQO1 activation generate unstable hydroquinones. The resultant electron redistribution within the carbocyclic backbone promotes exposure of biological active moieties that lead to conjugation of the agent to a target substrate. For azirinidyl agents such as mitomycin, EO9 & AZQ (+ analogues), the conjugating moieties remains attached to the carbocyclic core whereas in other compounds, such as the *phosphoramidate mustards & indolequinone-camptothecins*, cleavage of specific bonds in the structure results in compound fragmentation and release of the adduct forming component.

In addition to NQO1, quinones can undergo bioactivation by other routes. Enzymes such as cytochrome P450 reductase (P450R), cytochrome B5 reductase and xanthine oxidase can mediate a one electron reduction of the pharmacophore resulting in the production of a semiquinone radical (Begleiter & Leith 1990; Maliepaard *et al*. 1995; Bolton *et al*. 2000; Yan *et al*. 2008; Phillips *et al*. 2013). In the presence of oxygen, the radical can undergo futile cycling, as described above, leading to the formation of reactive oxygen species that promote oxidative stress in a cell. However, whether this mechanism is responsible for cytotoxicity of a given compound cytotoxicity is open for debate as cancerous tissue from lung and breast biopsies express P450R at equivalent levels to non-cancerous controls (Lopez 1999).

Quinones can also undergo reduction *via* the activity of the catechol quinone reductase, also known as NQO2, an enzyme having 49% identity to NQO1 (Wu *et al*. 1997; Long II & Jaiswal 2000; Dufour *et al*. 2012). However, in contrast to NQO1, NQO2 does not use NAD(P)H as a source of reducing equivalents. At present NQO2's physiological reductant is unknown although it can utilise the synthetic compound dihydronicotinamide riboside to catalyse the two electron reduction of quinones including RH1, and nitrobenzamides such as CB1954 (Wu *et al*. 1997; Yan *et al*. 2008). For indolequinone-based compounds, this activation generates derivatives that promote binding to and inhibition of NQO2 itself (known as suicide inhibition)(Dufour *et al*. 2012). This approach has attracted considerable interest in relation to various neurodegenerative disorders such as Alzheimer's and Parkinson's disease, malaria and leukaemia, all conditions where NQO2 is believed to play a role in mediating drug resistance (Long II & Jaiswal 2000; Graves *et al*. 2002; Winger *et al*. 2009; Benoit *et al*. 2010; Hashimoto & Nakai 2011; Leung & Shilton 2013). It is envisaged that development of inhibitors targeting NQO2 may be able to reverse the resistance phenotype

1.7.2 Quinones and trypanosomes

Quinone-based compounds have been screened for their antimicrobial properties (Baggish & Hill 2002; Kayser *et al*. 2003; Tran *et al*. 2004; Grellier *et al*. 2010; Lizzi *et al*. 2012; Hall *et al*. 2012; Lam *et al*. 2013; Pieretti *et al*. 2013). The quinone pharmacore exhibits redox potential and electrophilicity which makes them ideal drug candidates for treating cancers as well as infective agents such as *Mycobacterium*, *Plasmodium* and *Trypanosoma*(Tran *et al*. 2004; Pinto & de Castro 2009; Grellier *et al*. 2010; Hall *et al*. 2012; Lizzi *et al*. 2012; Pieretti *et al*. 2013). In

the case of trypanosomes, screening programs using natural & synthetic quinones have identified a number of lead compounds although how these structures mediate their anti-parasitic activity is unclear (Pinto & de Castro 2009; Romas *et al*. 2009; Lizzi *et al*. 2012; Pieretti *et al*. 2013). Several theories accounting for their trypanocidal properties have been proposed with some postulated to inhibit key essential enzymes such as trypanothione reductase or lipoamide dehydrogenase, while others are thought to induce oxidative stress within the parasite (Henderson *et al*. 1988; Fang & Beattie 2002a; Fang & Beattie 2002b; Kubata *et al*. 2002; Romas *et al*. 2009; Garavaglia *et al*. 2010). These proposals were made based on *in vitro* enzyme studies and the belief that trypanosomes had a limited enzymatic capacity to metabolise reactive oxygen species (Boveris *et al*. 1980; Fairlamb & Cerami 1992). However, no direct link between the trypanocidal activity of quinone-based agents & a proposed protein target within the parasite itself has been established and it is now known that trypanosomatids actually possess a series of novel oxidative defence pathways (Rahlfs *et al*. 2002; Wilkinson & Kelly 2003; Wilkinson *et al*. 2006; Irigoín *et al*. 2008).

Work conducted in the Wilkinson group has focused on the activity of a type I nitroreductase (NTR), a class of oxidoreductase reductase limited to bacteria and absent from most eukaryotes, with a subset of protozoan parasites being major exceptions (Wilkinson *et al*. 2008). Analysis of this NADH-dependent, FMN-containing mitochondrially targeted enzyme has shown that it can readily activate the trypanocidal prodrugs nifurtimox and benznidazole, as well as reduce a range of nitrofuran-, nitroimidazole-, nitrotriazole- and nitrobenzyl-based antiparasitic agents (Wilkinson *et al*. 2008; Bot *et al*. 2010; Hall *et al*. 2010; Hu *et al*. 2011;

Papadopoulou *et al*. 2011; Papadopoulou *et al*. 2012; Yang *et al*. 2012; Bot *et al*. 2013; Papadopoulou *et al*. 2013; Voak *et al*. 2013; Voak *et al*. 2014; Papadopoulou *et al*. 2015). In addition to metabolising nitroaromatic agents the trypanosomal NTR was shown to preferentially interact with quinones, particularly benzoquinones, leading to the proposal that the biological role for the enzyme was as a ubiquinone oxidoreductase (Hall *et al*. 2012). This hypothesis was supported by analysis of a nifurtimox selected population obtained using a whole genome loss of function (RNAi) assay where several gene hits that are postulated to encode for proteins involved in ubiquinone biology were identified (Alsford *et al*. 2012). The reactions catalysed by the parasite type I NTR appear to be analogous to those outline above regarding NQO1 activity (Hall *et al*. 2012).

1.8 DNA alkylating agents and repair mechanisms

Alkylating agents are defined as *"compounds capable of covalently binding an alkyl group* (C_nH_{2n+1}) *to a biomolecule under physiological conditions"*(Avendano & Menendez 2008). These structures tend to be electrophilic in nature and can readily interact with and bind to nucleophilic centres. For more than 60 years aziridine-containing compounds have formed the basis for the treatment of certain cancers with many of these prescribed drugs mediating the covalent attachment of binding groups to specific nucleotides, usually guanine, within the DNA backbone. As a result, cellular processes such as DNA transcription and DNA replication can be blocked, potentially leading to DNA fragmentation when the repair mechanisms used to fix such damage do not respond appropriately. Alkylating moieties exhibit their highest toxicity during that late G1 and S phases of the cell cycle with any

resulting DNA damage promoting cell cycle arrest (Avendano & Menendez 2008; Genois *et al*. 2014).

DNA alkylating agents fall into several types dependent on the number of functional groupings present in the compound's backbone (Figure 1.10). For the so-called monofunctional agents, structures that contain a single alkylating substituent, specific residues within one strand of the DNA double helix become alkylated such that a bulky side grouping is tagged onto the DNA structure. Such lesions can be highly mutagenic leading to coding errors with cells evolving repair mechanisms such as the base excision repair (BER) or nucleotide excision repair (NER) to fix such damage. For example, dacarbazine methylates guanine residues at the oxygen of the carbonyl grouping of purine ring resulting in O^6-methylguanine derivatives (Valavanis *et al*. 1993; Avendano & Menendez 2008), with the adduct removed by O^6-methylguanine-DNA alkyltransferase (MGMT) (Drabløs *et al*. 2004).

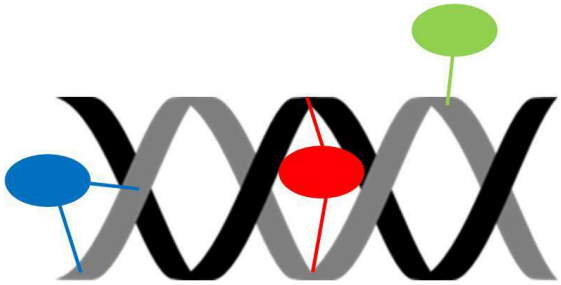

Figure 1.10: Different types of DNA alkylating agent. Intrastrand (shown in blue) covalently bond to one DNA strand in two places. Interstrand (shown in red) form covalent bonds across the double helix. Monofunctional DNA adducts (shown in green) only bind to one of the stands.

In contrast multifunctional agents, structures that contain several alkylating substituents, can interact with and covalently bind to multiple (usually two) residues within a single strand of the DNA double helix leading to formation of intrastrand cross links or bond to nucleotides on opposing strands to generate interstand cross

links (ICLs) (Figure 1.10). The latter are a particularly dangerous lesion as they physically link the two complementary strands within the DNA double helix together. This blocks essential cellular process that require DNA strand separation, including DNA replication and transcription, leading to chromosomal breakage, rearrangements, or cell death (Dronkert & Kanaar 2001; McHugh *et al*. 2001; Deans & West 2011; Sengerová *et al*. 2011). Estimates indicate that a single ICL can kill a unicellular microbe with as few as 20 being fatal to a mammalian cell (Magaña-Schwencke *et al*. 1982; Lawley & Phillips 1996).

One substituent that is effective at promoting DNA alkylation is the aziridine grouping, a three-membered heterocycle containing one amine group (-NH-) bound to two methylene bridges. As these moieties are highly reactive they must be attached to an electron withdrawing backbone to be of any medicinal value. This attachment functions to reduce the overall reactivity of the pharmacore while still preserving their DNA alkylating capabilities (Avendano & Menendez 2008). For prodrugs such as RH1 and CB1954, the two electron reduction reaction mediated by enzymes such as NQO1 or type I NTRs results in an increase in the pKa of the aziridine nitrogen to restore the reactiveness of the aziridinyl group (Figure 1.11). The resultant hydroquinone facilitates protonation of the aziridine nitrogen, thus forming an aziridinium cation, which then acts as an electrophilic centre targeting the nucleobase guanine. Interaction between the cation and the nucleophile causes the aziridinyl ring to open, thus releasing the strain within this moiety, with the now linear alkyl side chain binding covalently binding to the N7 position of purine ring on guanine. If a compound contains a single aziridinyl grouping then a monoalkylation will occur while structures that have multiple aziridinyl substituents

can be generated intra- or inter-strand DNA cross links (Avendano & Menendez 2008).

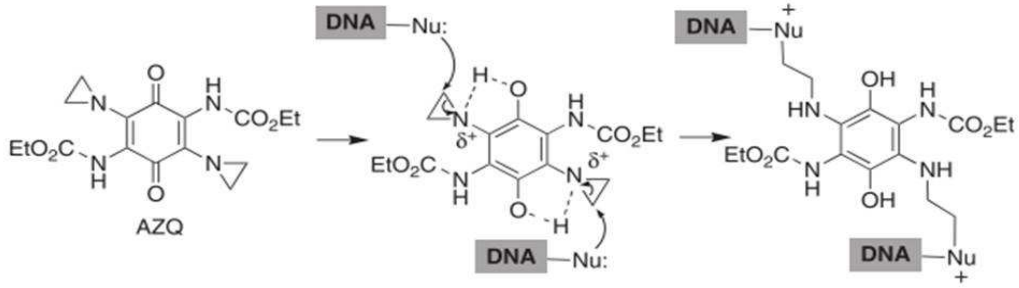

Figure 1.11: Schematic of DNA alkylation by the aziridinyl 1,4-benzoquinone AZQ (Image sourced from Avendano & Menendez 2008). Available from: http://store.elsevier.com/Medicinal-Chemistry-of-Anticancer-Drugs/Carmen-Avendano/isbn-9780080559629/Copyright © 2015 Elsevier B.V

In order to preserve the integrity and functionality of their genomes, all eukaryotic cells have evolved a series of complementary and overlapping pathways to function in the repair of ICLs. However, the exact enzymatic makeup of these systems are not fully understood (Deans & West 2011). In yeast many of the major DNA repair pathways (NER, mismatch repair, post-replication repair/translesion synthesis and homologous recombination) have been implicated in fixing ICL damage although only a few proteins specifically involved in this repair have been identified (Barber *et al*. 2005; Lehoczký *et al*. 2007; Daee *et al*. 2012; Ward *et al*. 2012). The best characterised of these are members of the Pso2p/SNM1 family of enzymes as cells lacking this activity are specifically and highly susceptible to ICL-inducing agents, such as the nitrogen mustards and aziridines, but not to any other forms of DNA damage (Henriques & Moustacchi 1981): note Pso2p (sensitive to PSORalen) refers to the yeast enzyme with SNM1 (Sensitive to Nitrogen Mustard) being the name given to plant/mammalian homologues. The role played by Pso2p/SNM1 in these repair systems remains unknown although biochemical studies have shown that it displays a 5' exonuclease activity (Dronkert & Kanaar 2001; Li *et al*. 2005). This coupled with the observation that *pso2Δ* cells exposed to ICL-inducing compounds

tend to accumulate DNA double stranded breaks indicates that Pso2p does not function in the initial identification/incision events, which in yeast occurs *via* the NER pathway, but may be involved in the processing of DNA ends created during the generation of ICL-associated DNA double stranded breaks (Li & Moses 2003; Li *et al*. 2005; Barber *et al*. 2005; Dudáš *et al*. 2007). Intriguingly, Pso2p also displays a structure-specific DNA hairpin opening endonuclease activity providing evidence that it may have other functions outside ICL repair (Tiefenbach & Junop 2012).

All members of the Pso2p/SNM1 family contain a non-canonical metallo-ß-lactamase (MBL) domain containing four motifs including a characteristic HxHxDH signature, which cooperate to facilitate zinc co-factor binding (Figure 1.12) (Cattell *et al*. 2010). Additionally, and in contrast to other MBL-containing proteins, Pso2p/SNM1 members also contain a characteristic β-CASP (named after its representative member **C**PSF, **A**rtemis, **S**NM1 and **P**SO2) region, which in addition to possessing elements that function in metal binding, also harbours regions which are important in substrate interactions and specificity. *In silico* studies have shown that a range of protozoan parasite including *Plasmodium, Leishmania* and *Trypanosoma*, all possess a member of the Pso2p/SNM1 family of nucleases (Bonatto *et al*. 2005; Sullivan *et al*. 2015). For the *T. brucei* homologue, the function of this enzyme was established using yeast complementation with gene deletion studies demonstrating that the Pso2p/SNM1 activity was non-essential to the medically relevant life cycle stage (Sullivan *et al*. 2015). As with yeast *pso2* null mutants, trypanosomes lacking SNM1 were specifically more susceptible to DNA alkylating agents that promote ICL formation, a phenotype that could be readily complemented by ectopic expression of Tb*snm1*.

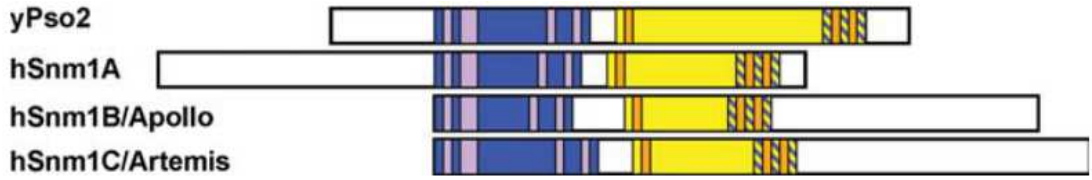

Figure 1.12. Schematic of representatives from the SNM1/PSO2 family of proteins. Alignment of the yeast (yPSO2) and three human (SNM1A, SNM1B/Apollo and SNMC/Artemis) proteins are shown revealing the conserved MBL (blue/purple) and β-CASP (yellow/orange) domains. Adapted from Cattell *et al*. (2010). Available from http://onlinelibrary.wiley.com/doi/10.1002/em.20556/abstract.

1.9 Research aims

The treatment regimes for the treatment of HAT are controversial as they are toxic and have limited efficacy. This, coupled with the emergence of resistant/non-responsive parasite strains, has led to an urgent need for new, safer therapies targeting this infection. Quinone based compounds represent a group of moieties that are being exploited and/or evaluated in treating infectious diseases and hypoxic cancers. Here, I explore whether these agents could signify a new group of treatments for trypanosomatid diseases, focusing on HAT.

The specific aims were to:

1. Determine the anti-trypanosomatid properties of selection of compounds containing benzo-, indole- or naphtho-quinone backbones.
2. Investigate the mode(s) of action of the most potentagents, assessing whether they function as prodrugs and/or promote DNA damage
3. Understand how *T. brucei*might gain resistance towards the most active quinone.
4. Explore the mechanism of action of the nitroaromatic trypanocidal agents CB1954 and BG-M2

Chapter 2: Materials and Methods

2.1 Stocks

2.1.1 Cell stocks

The wild type organisms and cell lines used in this study are listed in Table 2.1.

Table 2.1: Organisms used in this study

Organism name	Source
Leishmania major MHOM/IL/80/Friedlin	D. Smith, University of York
Trypanosoma brucei brucei Lister 427; clone 221a	D. Horn, University of Dundee
Trypanosoma brucei brucei Lister 427; clone 2TAG1 (2T1)	Alsford & Horn (2008)
Trypanosoma brucei brucei single marker bloodstream (SMB)	Wirtz*et al*. (1999)
Trypanosoma cruzi CL-Brener	J. Kelly, LSHTM
Escherichia coli XL-1 Blue	Laboratory stock
Human acute monocytic leukaemia line (THP-1)	K. Seifert, LSHTM
BALB/c mice	K. Seifert, LSHTM

2.1.2 Quinone based compounds used in this study

The quinone-based compounds (**1**-**4**; **6**-**36**; **47**-**51**) used in this study were obtained from the Drug Synthesis and Chemistry Branch, Developmental Therapeutics Program, Division of Cancer Treatment and Diagnosis, National Cancer Institute with the exception of RH1 (compound **5**) and the 1,4 benzoquinone mustards (**52**-**56**), which were donated by Frank Guziec, Jr. (Southwestern University,

Georgetown, TX), and the napthoquinones (**37**-**46)** which were supplied by Mohammed Jaffar (Morvus Technology Ltd, UK). Compounds were resuspended in dimethyl sulfoxide (DMSO) (Sigma Aldrich) at a concentration of 10 mM unless otherwise stated. The structures and chemical/physical properties of the compounds are listed in the Appendices**.**

2.1.3 Non-quinone based compounds used in this study

LH37 and LH33 were obtained from Longqin Hu (Rutgers, The State University of New Jersey, New Jersey, USA) and nifurtimox supplied by Simon Croft (LSHTM, UK). Megazol and DFMO were obtained from Mike Barrett (University of Glasgow, Glasgow, UK). BG-M2, KS90 and KS900 supplied by Phillip Penketh (Yale, Connecticut, USA) and NH10 was donated by Nuala Helsby (University of Auckland, Auckland, New Zealand). Nitrofurazone and CB1954 were purchased from Sigma-Aldrich while G418, phleomycin, puromycin, blasticidin and hydromycin were sourced from PAA Laboratories Ltd or Melford Laboratories Ltd.

2.2 Cell culture and storage

2.2.1 Maintenance of *Trypanosoma brucei brucei*

The bloodstream form (BSF) of *T. brucei* was grown in HMI-11 which consists of HMI-9 media (Invitrogen) supplemented with 3 g L^{-1} sodium bicarbonate, 0.014% (v/v) β-mercaptoethanol (both from Sigma-Aldrich) and 10% (v/v) heat-inactivated foetal calf serum (PAA Laboratories Ltd) at 37ºC in a 5% (v/v) CO_2 atmosphere (Hirumi and Hirumi, 1989). Derivatives of this cell line (designated 2T1 and SMB) that constitutively express the tetracycline repressor protein, were grown in this medium supplemented with 1 µg mL^{-1} phleomycin (2T1) or 2 µg mL^{-1} G418 (SMB).

T. brucei 2T1 parasites transformed to express elevated levels of TbNTR (a type I nitroreductase), TbCPRII or TbCPRIII (both cytochrome P450 reductase enzymes) and *T. brucei* SMB parasites transformed to undergo inducible RNA interference towards various genetic targets were further selected by the addition of 2.5 µg mL^{-1} hygromycin (Wilkinson *et al*. 2008; Bot *et al*. 2013). *T. brucei* (wild type and 2T1) null mutant cells lacking the nuclease TbSNM1 were cultured in medium supplemented with 10 µg mL^{-1} blasticidin and 2 µg mL^{-1} puromycin (Sullivan *et al*. 2015). In over expression and complementation experiments, wild type and TbSNM1 null mutant parasites expressing elevated levels of TbSNM1 were grown in the presence of 2 µg mL^{-1} phleomycin (Sullivan *et al*. 2015). *T. brucei* heterozygous cells expressing lowered levels of the type I nitroreductase TbNTR were cultured in HMI-11 containing10 µg mL^{-1} blasticidin (Wilkinson *et al*. 2008). To select *T. brucei* lines displaying resistance to the quinone RH1 (**5**), parasites in the logarithmic phase of growth were continually cultured in the presence of compound starting at 5 nM and increasing in a stepwise fashion over a period of 3 months to 40 nM.

2.2.2 Maintenance of *Leishmania major*

The promastigote form of *L. major* MHOM/IL/80/Friedlin was cultured at 25°C in modified M199 medium (Invitrogen) supplemented with 4 mM sodium bicarbonate, 40 mM HEPES pH 7.4, 0.1 mM adenine, 0.005% (w/v) haemin (all Sigma-Aldrich), 25000 U L^{-1} penicillin, 25 mg L^{-1} streptomycin (both PAA Laboratories Ltd) and 10% (v/v) heat-inactivated foetal bovine serum (PAA Laboratories Ltd). The medium was filter sterilized and stored at 4°C.

2.2.3 Maintenance of *Trypanosoma cruzi*

The epimastigote form of *T. cruzi* was cultured in RPMI-1640 medium (PAA Laboratories Ltd) supplemented with 5 g L^{-1} trypticase, 5 g L^{-1} HEPES pH 8.0, 20 mg L^{-1} haemin, 0.34 g L^{-1} sodium glutamate, 0.22 g L^{-1} sodium pyruvate, 2500 U L^{-1} penicillin, 0.25 g L^{-1} streptomycin (all Sigma-Aldrich) and 10% (v/v) heat-inactivated foetal calf serum (PAA Laboratories Ltd) and incubated at 25°C (Kendall *et al*., 1990).

2.2.4 Maintenance of *Escherichia coli*

Escherichia coli XL-1 blue strains were maintained at 37°C in NZCYM (10 g L^{-1} enzymatic casein digest, 1 g L^{-1} casamino acids, 5 g L^{-1} yeast extract, 5 g L^{-1} NaCl, 0.98 g L^{-1} $MgSO_4$) (Sigma-Aldrich or Melford Laboratories Ltd), supplemented with 100 µg mL^{-1} ampillicin (Sigma-Aldrich) where appropriate. In some experiments, the growth medium was solidified with 1.5% (w/v) Agar no.1 (Oxoid).

2.2.5 Mammalian cells

The THP-1 cell line was grown at 37°C under a 5% (v/v) CO_2 atmosphere in RPMI-1640 medium (PAA Laboratories Ltd.) supplemented with 2 mM pyruvate, 2 mM sodium glutamate, 25000 U L^{-1} penicillin and 2.5 mg L^{-1} streptomycin, 20 mM HEPES (pH 8.0) (all Sigma-Aldrich) and 10% (v/v) foetal calf serum (PAA Laboratories Ltd).

2.2.6 Cell storage

For long term storage, cells were deposited as frozen stocks in liquid nitrogen (parasite lines) or at -80°C (prokaryotic strains) in growth medium containing 20% (v/v) glycerol (Sigma-Aldrich). Bacterial strains were frozen directly at -80°C in 1.2 mL cryogenic vials (Nunc). Parasite lines, in 1.2 mL cryogenic vials (Nunc), were frozen slowly (1-2 days) to -80ºC using a Cryo 1°C Freezing Container (Nalgene) containing isopropanol (VWR International), then transferred to liquid nitrogen for long-term storage. Mammalian (THP-1) cells were frozen in fresh growth medium containing 20% (v/v) DMSO (Sigma-Aldrich) at a density of 1 x 10^5 cells mL^{-1}. Frozen stocks were generated as described for parasite lines using the Cryo 1°C Freezing Container (Nalgene).

Eukaryotic cell lines were revived by quickly thawing the contents of the frozen vial. Thawed cells were pelleted by centrifugation for 5 minutes (parasites at 1640 x*g*, mammalian cells at 400 x *g*) and washed in 10 mL of the appropriate medium. Cells were then re-suspended in fresh medium as per normal culturing.

2.3 Anti-parasitic and toxicity screens

2.3.1 Bloodstream form *Trypanosoma brucei brucei*

All growth inhibition assays were carried out in 96-well plates (PAA Laboratories Ltd). *T. brucei* BSF parasites in the logarithmic phase of growth were seeded at 1 x 10^4 cells mL^{-1} in 200 µL of HMI-11 medium containing various concentrations of the compound under study. Other assays performed included culturing cells grown in the absence of drug (100% growth) and a medium background control. After incubation at 37°C for 3 days, resazurin (Sigma Aldrich) was added to each well at a final concentration of 12.5 mg L^{-1} (or 2.5 µg resazurin per well). The plates were

further incubated for 8-24 hours at 37°C before measuring the fluorescence using a Gemini Fluorescent Plate reader (Molecular Devices) at λ_{EX} =530 nM and λ_{EM} =585 nM with a filter cut off at 550 nM. The colour change (and subsequent fluorescence) is a result of the reduction of the dye by living cells therefore the change is proportional to the amount of cells present. Therefore, the highest fluorescence was observed in untreated cells, whereas the lowest was observed in the absence of cells.

To calculate the fluorescence value at each compound concentration (fl_v) the following calculation was used:

equation 1: $fl_v = fl_{raw} - fl_{background}$

where fl_{raw} is the raw fluorescence value at a given compound concentration and $fl_{background}$ is the average background fluorescence value of the medium control.

The fluorescence value at a given compound concentration (fl_v) was then expressed as % growth relative to the average fluorescence value at a compound concentration equal to 0 ($fl_{drug=0}$) (i.e. no drug control)

equation 2: % growth at given [compound] = $fl_v/fl_{drug=0}$ x 100

The % growth data at a given compound concentration was then expressed as % growth inhibition at a given compound concentration

equation 3: % growth inhibition = 100 - % growth at given [compound]

Data expressed as % growth or % growth inhibition was used to construct dose response curves and establish the compound concentration that inhibits cell growth by 50% (IC_{50}) using the non-linear regression tool on GraphPad Prism (GraphPad Software Inc).

2.3.2 *Leishmania major* promastigotes

L. major promastigotes in the logarithmic phase of growth were seeded at 5 x 10^5 cells mL^{-1} in 200 µL M199 growth medium containing various concentrations of the compound under study. Other assays performed included culturing cells grown in the absence of drug (100% growth) and a medium background control. After incubation at 27°C for 6 days, resazurin (Sigma-Aldrich) was added to each well at a final concentration of 12.5 mg L^{-1} (or 2.5 µg resazurin per well). The plates were further incubated for 8-24 hours at 27°C before measuring the fluorescence using the Gemini Fluorescent Plate reader as previously described and growth inhibition curves were calculated as described.

2.3.3 *Trypanosoma cruzi* promastigotes

T.cruzi epimastigotes in the logarithmic phase of growth were seeded at 5 x 10^5 cells mL^{-1} in 200 µL of modified RPMI growth medium containing various concentrations of the compound under study. Other assays performed included culturing cells grown in the absence of drug (100% growth) and a medium background control. After incubation at 27°C for 12-14 days, resazurin (Sigma Aldrich) was added to each well at a final concentration of 12.5 mg L^{-1} (or 2.5 µg resazurin per well). The plates were further incubated for 24-48 hours at 27°C before measuring the fluorescence using a Gemini Fluorescent Plate reader (Molecular Devices) and calculating IC_{50} values as described.

2.3.4 Mammalian cells

THP-1 cells were seeded at 2.5 x 10^4 cells mL^{-1} in 200 µL modified RMPI-1640 growth medium and incubated at 37°C in a 5% (v/v) CO_2 atmosphere for 3 days in

the presence of 20 ng mL^{-1} phorbol 12-myristate 13-acetate (Sigma Aldrich). On day 4, the medium was carefully removed, the cells washed in pre-warmed medium lacking PMA and the cells treated with growth medium various concentrations of the compound under study. The plates were incubated for a further 3 days at 37°C under a 5% (v/v) CO_2 atmosphere before addition of resazurin to a final concentration of 12.5 mg L^{-1} (or 2.5 μg per well) to each culture. Plates were incubated for a further 8-12 hours before determining the fluorescence of each culture as described.

Peritoneal macrophages isolated from mice were used in growth inhibition assays. Briefly, macrophages seeded at 4 x 10^5 mL^{-1} in mammalian growth medium were incubated overnight at 37°C in a 5% (v/v) CO_2 atmosphere to facilitate attachment of the cells onto a slide in a 16-well chamber slide. The following day the medium was carefully removed, the cells washed in pre-warmed RPMI-1640, then treated with various concentrations of the compound under study diluted in the growth medium. The plates were incubated for a further 5 days at 37°C under a 5% (v/v) CO_2 atmosphere before washing the slide in 100% (v/v) methanol for 2 minutes, briefly rinsing in 100% (v/v) methanol and then air drying. The slide was then washed with 10% (w/v) Giemsa stain diluted in tap water for 10 minutes before briefly rinsing in tap water and air drying. The above cell isolation, drug treatments and cell staining were all performed by Karin Seifert (LSHTM, UK). Slides were visualized with Leica DMRA2 light microscope with Retiga EXi Fast 1394 digital camera and Velocity software package using at x100 oil immersion objective and the number of cells per field of view determined. A minimum of 10 fields of view per drug treatment were examined and the average number of cells per field of view calculated. The values obtained for each drug-treated culture were then expressed as

a % growth relative to untreated controls. Photographs of the slides were taken using the same microscope with a x20 objective.

2.4 Nucleic acid extraction techniques

2.4.1 Parasite genomic DNA

Parasite genomic DNA (gDNA) was extracted using two methods. In the first protocol, gDNA was harvested using a sodium dodecyl sulfate (SDS)-based lysis/phenol:chloroform protocol adapted from Kelly *et al*(1993). Parasites in the logarithmic phase of growth were pelleted (1640 g for 10 minutes), washed in phosphate buffered saline (PBS) (137 mM NaCl, 2.7 mM KCl, 10 mM Na_2HPO_4, 1.76 mM KH_2PO_4, pH 7.6) and resuspended in TEN lysis buffer (50 mM Tris-Cl pH 8.0, 50 mM EDTA, 50 mM NaCl) containing 100μg mL^{-1} proteinase K (Sigma-Aldrich). SDS was then added to a final concentration of 1% (w/v) and the mixture incubated at 54^{o}C for 2 hours. An equal volume of phenol:chloroform (1:1) was added to the lysate, the contents mixed by inversion of the tube and the aqueous/organic phased partitioned by centrifugation (3,500 g for 10 minutes). The upper aqueous layer was carefully removed, dispensed into a fresh tube and if required, the phenol/chloroform step repeated. The 'cleaned' nucleic acid-containing aqueous phase was finally transferred to a fresh tube. A few drops (~20-30 μL) of 1 M $MgCl_2$ was then added and the chromosomal DNA precipitated using an equal volume of isopropanol. The resultant fibrous material was collected, transferred to a fresh 1.5 mL centrifuge tube, washed with 70% (v/v) ethanol and left to air dry. The gDNA was then dissolved in low salt buffer (10 mM Tris HCl,1 mM EDTA pH8.0)

containing 30 μg mL^{-1} heat-treated (100ºC for 10 minutes) RNase A (Sigma-Aldrich).

The second gDNA extraction method was carried out using the DNeasy Blood and Tissue Kit (Qiagen) following the manufacturer's protocol. Briefly, parasites in the logarithmic phase of growth were pelleted (1640 g for 10 minutes) then resuspended in PBS containing 1-2 mg mL^{-1} proteinase K. An equal volume of RNase-containing lysis buffer was then added to the mixture and the mixture incubated at 60°C for 10 minutes. A volume of ethanol (96-100 % (v/v)) equal to that used to initially resuspend the cells was added to the lysate, the contents mixed and passed through a QIAprep spin column by centrifugation (20,238 g for 1 minute), such that the genomic DNA binds to the silica membrane of the column. The DNA was then washed using an ethanol-based buffer, removing any residual salts and other precipitates, with the gDNA finally eluted off the silica membrane in 50-200 μL a low salt buffer (10 mM Tris HCl,1 mM EDTA pH8.0). The gDNA was stored at 4°C until use.

2.4.2 Total RNA extraction

Total RNA was extracted from *L. major* promastigotes or BSF *T. b. brucei* in the logarithmic phase of growth using the RNeasy Extraction kit (Qiagen) as per the manufacturer's instructions. Parasite cultures were pelleted by centrifuged (1,640 g for 10 minutes) and any residual growth media removed. The pellet was resuspended and cells disrupted using a guanidinium thiocyanate (GTC)-containing lysis buffer before being passed through QIAshredder spin column (Qiagen) by centrifugation (20,238 g for 2 minutes). The flow through was collected to which ethanol (70%

(v/v)) was added and the homogenized lysate passed through an RNeasy Mini Column by centrifugation (20,238 g for 15 seconds) such that the RNA binds and becomes entrapped in the silica membrane of the column. The RNA sample was then washed with GTC, the column dried by centrifugation (20,238 g for 15 seconds) and any contaminating DNA removed by digestion with on column DNase I (Qiagen) for 15 minutes at room temperature. The column was then washed again firstly with the GTC-containing buffer then twice using an ethanol based buffer before eluting the total RNA into 30-50 µL RNase-free water. The RNA is stored at -20°C until use.

2.4.3 Plasmid DNA

Small scale plasmid DNA (5-20 µg) extractions from *E. coli* were performed using the QIAprep Spin Miniprep kit (Qiagen) according to the manufacturer's instructions. Briefly, NZCYM broth supplemented with 100 µg ml^{-1} ampillicin was inoculated with the desired *E. coli* strain and grown overnight at 37°C with aeration. The bacteria were harvested (20,238 g for 1 minutes), residual growth medium removed and the cells resuspended then lysed in an RNase A-containing alkali buffer. The pH of the lysate was adjusted using a neutralisation buffer and the resultant cell debris/chromosomal DNA removed by centrifugation (20,238 g for 10 minutes). The supernatant was passed through to QIAprep spin column by centrifugation (20,238 g for 1 minute) such that the plasmid DNA binds to the silica membrane of the column. The DNA was then washed using an ethanol-based buffer, removing any residual salts and other precipitates with the plasmid DNA finally eluted off the silica membrane in 40-60 µL a low salt 10 mM Tris HCl, 1 mM EDTA pH 8.0 buffer. Plasmid DNA was stored at -20°C until use.

2.5 DNA manipulation techniques

2.5.1 cDNA synthesis

Complementary DNA (cDNA) was synthesized from total RNA using the Superscript® VILO™ cDNA synthesis kit (Invitrogen). A typical 20 µL reaction contained 1X VILO reaction mix (formulation includes random hexamers, $MgCl_2$, dNTPs), 2.5 ng uL^{-1} total RNA and 1X SuperScript® enzyme mix (formulation includes Superscript III reverse transcriptase, RNase OUT™, Recombinant Ribonuclease Inhibitor, and a proprietary helper protein). Using a Techne TC-412 thermocycler, a single cycle at 25°C for 10 minutes followed by 42°C for 60 minutes was performed and the reaction halted by an 85°C treatment for 5 minutes. Samples were then stored at -20ºc until use.

2.5.2 DNA amplification

DNA fragments were amplified using primers purchased from Sigma-Aldrich (see Appendix) with dNTPs and DNA polymerases (plus associated buffers) sourced from New England Biolabs. In a typical 50 µL amplification the reaction contained 1x Thermopol buffer (20 mM Tris-HCl, 10 mM $(NH_4)_2SO_4$, 10 mM KCl, 0.1% (v/v) Triton X-100, 1.5 mM $MgSO_4$), 200 µM dNTPs, 0.1 ng μL^{-1} template DNA, 0.5 µM forward & reverse primers and 20 U mL^{-1} DNA polymerase (*Taq* or Vent *pfu* were used dependent on whether the fragment required proof reading). On occasions additional $MgSO_4$ was added to the reaction.

Using a Techne TC-412 thermocycler, a standard PCR program consisted of one cycle at 96 °C for initial melting, followed by 30 cycles of: 96°C for 30 seconds (denaturing step), 55°C for 30 seconds (annealing) and 72°C for 60 seconds

(extension time). A further extension of 10 minutes at 72°C was usually added at the end of the 30th cycle. The temperatures and times were dependent on the oligonucleotide primer properties, therefore these conditions were varied as necessary.

2.5.3 Quantitative real time PCR (qRT-PCR)

DNA fragments were amplified from cDNA employing the QuantiTect® SYBR® Green PCR kit (Qiagen) and primers obtained from Sigma-Aldrich (see Appendix 3). A typical 10 µL reaction contained 1X QuantiTect® SYBR® Green PCR buffer (20 mM Tris-HCl, 10 mM $(NH_4)_2SO_4$, 10 mM KCl, 0.1% (v/v) Triton X-100, 2.5 mM $MgSO_4$, 200 µM dNTPs and HotStarTaq® DNA polymerase), 1000 ng μL^{-1} template cDNA and a pre-determined amount of forward & reverse primers. Samples were loaded onto 384 well plates and sealed using an adhesive qPCR seal (both donated by Dr M.Struebig).

Using an Applied Biosystems 7900HT system, a standard PCR program consisted of one cycle at 95°C for 15 minutes to activate the HotStarTaq® DNA polymerase followed by 40 cycles of 95°C for 10 seconds (denaturing), 60°C 10 seconds (annealing) and 72°C for 10 seconds (extension). Following completion of the amplification step a dissociation curve analysis was carried out to ensure target specificity. Fluorescence data collected during the amplification was analyzed using SDS version 2.4 software (Applied Biosystems) and exported into Excel 2007 (Microsoft). From the resultant sigmoidal curves, the cycle threshold (C_T) value was determined and normalized against standardized control (TbTERT)(Brenndörfer

&Boshart 2010) using the comparative C_T method as described by Schmittgen & Livak (2008).

2.5.4 DNA purification

DNA fragments were purified using a GeneJET™ DNA gel extraction kit (Fermentas Life Science) in accordance with the manufacturer's protocols. For DNA samples in liquid, a high salt buffer containing chaotropic salts was applied to the sample before passing it through a GeneJET™ purification column by centrifugation (20,238 g for 1 minute) such that the nucleic acid binds to the column's silica membrane: the chaotropic salts promote binding of DNA to the silica membrane as well as denaturing associated proteins. Following a series of ethanol washes and centrifugation steps, the DNA was eluted from the silica membrane using 30-60 µL low salt elution buffer. The DNA is stored at -20°C until use.

To purify DNA fragments embedded in agarose, the weight (and hence volume) of the DNA-containing agarose slice was determined to which an equal volume ofsolubilisation buffer was added. The mixture was then incubated at 60°C for 10 minutes or until the agarose had completely dissolved. An equal volume of isopropanol was added to the DNA-containing solution and the mixture applied to a GeneJET™ purification column. The binding/wash steps were carried out as described as above.

2.5.5 DNA ligation

DNA ligation reactions were varied dependent on the ratio of insert to vector present. The relative amounts of each DNA sample was judged following visualization of an ethidium bromide stained agarose gel. A typical ligation reaction was set up as

follows: in a 30 µL reaction, varying amounts of purified DNA (vector & insert) and 3 µL 10X T4 DNA ligation buffer (500 mM Tris-HCl pH 7.5, 100 mM $MgCl_2$, 10 mM ATP, 100 mM dithiothreitol (DTT)) (Biolabs New England) were mixed and the volume of the ligation reaction adjusted to 29 µL with sterile distilled H_20. T4 DNA ligase (1 µL: 400 units) was added to the reaction, the mixture consolidated then incubated at room temperature for 2-4 hours or at 4°C overnight.

In some cases, ligations were carried out using the pGEM®-T-Easy vector system (Promega). Here, a typical 20 µL reaction was set up containing 1 µL pGEM®-T-Easy vector (50 ng), 10 µL 2X Rapid Ligation Buffer (60 mM Tris-HCl pH 7.8, 20mM $MgCl_2$, 20mM DTT, 2mM ATP, 10% (w/v) polyethylene glycol MW8000), 1 µL pGEM®-T-Easy T4 DNA ligase (3 U) and 8 µL insert DNA. The ligation mix was consolidated then incubated at room temperature for 2-4 hours or at 4°C overnight.

2.5.6 DNA restriction digests

The restriction enzymes (Table 2.2) used in this study were purchased from New England Biolabs or Thermo Fisher Scientific. A typical plasmid restriction digestion was set up as follows: in a total volume of 20 µL, plasmid DNA (10 µL) was mixed with 2 µL 10X restriction enzyme buffer appropriate for the restriction enzyme(s) being used and the volume adjusted to 19 µL with sterile distilled H_2O. In some cases bovine serum albumin was added to the reaction to a final concentration of 100 µg mL^{-1}. Restriction enzyme (1 µL: 10-20 units) was then added to the reaction and the contents consolidated by centrifugation. The reaction mixture was incubated at the recommended temperature for the restriction enzyme, generally 37°C, for 1-2

hours. The reaction was halted by addition of 6X DNA loading dye (10 mM Tris.HCl pH 7.6, 0.03% (w/v) bromophenol blue, 0.03% (w/v) xylene cyanol FF, 60% (v/v) glycerol, 60 mM EDTA) (Thermo Fisher Scientific) and the DNA fragments fractionated on an agarose gel.

Table 2.2:Restriction enzymes used in this study. The cleavage site for each enzyme indicated by '/'

Enzyme	Restriction site	Enzyme	Restriction site
ApaI	GGGCC/C	NotI	GC/GGCCGC
BamHI	G/GATCC	SacI	GAGCT/C
EcoRI	G/AATTC	XbaI	T/CTAGA
HindIII	A/AGCTT	XhoI	C/TCGAG

Restriction digestion analysis of gDNA (generally for Southern hybridization studies) was set up as described above except a larger total reaction volume (100 µL) and more DNA (30-60 µL) were used. Generally, multiple aliquots of the restriction enzyme were added to each reaction to ensure that the digestion had gone to completion.

2.5.7 Bacterial DNA transformation

Competent *E. coli* were prepared as follows: a bacterial stock culture was diluted 1:20 into fresh NZCYM medium (generally 0.5 mL stock in 10 mL fresh medium) and the new culture grown with aeration at 37°C for two hours: at this point the optical density at 600 nm of the culture was between 0.6-1.0). Aliquots (generally 1 mL) of the bacterial cells were pelleted (20,238 g for 1 minute), resuspended in an equal volume (generally 1 mL) ice cold 0.1 M $CaCl_2$ and then incubated on ice for 10

minutes. The bacteria were harvested (20,238 g for 1 minute) and the pellet resuspended in a $1/10^{th}$ volume (generally 0.1 mL) ofice cold 0.1 M $CaCl_2$. The DNA to be transformed (15- 30 μL of a ligation or 1 μL of pure plasmid DNA) was added to the $CaCl_2$ resuspended competent cells, the mixture held on ice for 10-30 minutes then heat shocked at 42°C for 2 minutes before being immediately returned to ice for a further 2 minutes. The transformed bacteria were plated onto NZCYM agar plates containing an appropriate antibiotic for plasmid selection and left to incubate overnight at 37°C to allow growth of colonies.

2.5.8 Parasite DNA transformation

T. brucei were transformed using the Amaxa® nucleofection system (Lonza). Parasites (~$2x10^7$ per transfection) in the exponential phase of growth were harvested by centrifugation (1,640 x *g* for 10 minutes at room temperature), residual growth medium removed and the pellet resuspended in 100 μL Human T-cell Nucleofector® solution (Lonza): this solution was made no more than 5 minutes before use by combining 82 μL of reagent A with 18 μL reagent B in the Human T-cell Nucleofector® kit. The cell suspension was immediately transferred to a nucleofection cuvette containing ~10 μg DNA (in 10μL) to be transformed and parasite electroporation performed using the Amaxa Nucleofector® device set to programme X-001. The cells were then transferred into pre-warmed HMI-11 (generally 48 mL) medium and left at 37°C. After at least 6 hours, selective antibiotics (see section 2.2.1) were added to the transformed culture, aliquots (generally 2 mL) transferred into the wells of a 24 well plate and the parasites incubate at 37°C under a 5% (v/v) CO_2 atmosphere. In some cases 1:10 and 1:100

dilutions of the transformed culture were set up prior to addition of the selective antibiotics. Drug-resistant *T.brucei* were usually apparent 5-7 days post-transfection.

2.5.9 DNA sequencing

For custom DNA sequencing Eurofins MWG operon (for single reads) or the Beijing Genome Institute (BGI) (for high throughput multi-read sequences) were used. Samples such as PCR products or plasmids were sent at a concentration of 50-100 ng μL^{-1} whilst the corresponding oligonucleotides were sent at a final concentration of 10 pmol μL^{-1}. Results were usually received within 48 hours where single sequence reads were performed or 2 months for high throughput multi-read sequencing.

2.5.10 Bioinformatic analysis

The primer prediction algorithm RNAit (Redmond *et al*. 2003) was used to predict specific regions of opening reading frames suitable for RNAi. Trypanosomal and *Leishmania*DNA/protein sequences were identified following text or BLAST searches using algorithms housed at the Kinetoplastid genome resource TritrypDB (http://tritrypdb.org/tritrypdb/) or NCBI (http://blast.ncbi.nlm.nih.gov/Blast.cgi). PSORT (http://psort.hgc.jp/) was used as a predictor of localisation. Analysis of high throughput multi-read sequencing data was carried out by Dr Sam Alsford (LSHTM) as described (Glover *et al*. 2015).

2.6 Nucleic acid separation and hybridization

2.6.1 DNA by conventional gel electrophoresis

Conventional agarose gel electrophoresis was used to fractionate DNA molecules between 200 bp to 10 kbp. The size of the gel, agarose concentration, voltage and

times were optimized to achieve the desired result. A standard agarose gel 0.8-1.2% (w/v) was made by dissolving agarose powder (Bioline) in 1X TAE (40 mM Tris base, 40 mM acetic acid, 1 mM EDTA) by boiling using a microwave. After the agarose had cooled, ethidium bromide (0.1 mg L^{-1}) was added. Once gels were cast, the solidified agarose was placed into a gel electrophoresis tank containing 1X TAE supplemented with 0.1mg L^{-1} ethidium bromide. DNA samples (containing DNA loading dye) and a 1 kb GeneRuler™ (Thermo Fischer Scientific) were loaded onto the gel and the samples fractionated through the gel by applying a constant voltage (70-100 V) across the gel for 40 minutes to 2 hours. Migration of the samples through the agarose matrix was followed by monitoring the bromophenol blue and xylene cyanol dye fronts present in the samples loading buffer. When the DNA had migrated the desired distance, the agarose gel was visualized on a UV transluminator and documented (Syngene).

2.6.2 DNA blotting

DNA-containing agarose gels were depurinated for 10-15 minutes, bathed in denaturation buffer (0.5 M NaOH, 1.5 M NaCl (Sigma Aldrich)) for 30 minutes and washed again in distilled water. The gel was transferred into neutralisation buffer (0.5 M Tris-HCl, 1.5 M NaCl at pH 7.5) for an hour before washing again in distilled water.

The nucleic acids were transferred onto MAGNA nylon membrane (MSI 0.45µ) by capillary action using 20X SSC solution (3M NaCl; 0.3M sodium citrate) using the method described by Southern (Southern 1975). 3MM filter paper was wrapped around a support (usually a gel casting tray) and placed in a large plastic container. The filter paper was then soaked with 20X SSC onto which the gel containing the

nucleic acid to be transferred was placed. The gel was wetted with 20X SSC, covered with nylon membrane on top of which were place additional pieces of dry 3MM filter paper, a paper towel 'wicks', a flat tray and finally a weigh. The large plastic container was then filled with 20X SSC and the whole arrangement left overnight. Following transfer, the nucleic acids were cross linked to the nylon membrane using a UV cross-linker (Stratagene) set at a pre-determined algorithm, with the nucleic acid side of the membrane positioned toward the UV blubs. The fixed membrane was put into pre-hybridisation solution or stored in 3MM paper at room temperature.

2.6.3 DNA probe synthesis

Non-radioactive DNA were synthesized using the PCR DIG Probe Synthesis Kit (Roche) according to the manufacturer's protocol. For a 50 µL reaction, 5 µL 10X PCR buffer (containing 15 mM $MgCl_2$) and 5 µL PCR DIG probe synthesis mix (2 mM dATP, dGTP and dCTP; 1.3 mM dTTP; 0.7 mM DIG labelled dUTP) were added to a 0.2 ml tube containing the template DNA and the forward/reverse primers (0.5 µM each). The reaction volume was adjusted to 49.25 µL with sterile distilled water to which 0.75 µL (2.6 units) of DNA polymerase was added. Using a Techne TC-412 thermocycler, a standard PCR program consisting of one cycle at 96°C for initial melting followed by 30 cycles of 96°C for 30 seconds (denaturing), 55°C for 30 seconds (annealing) and 60°C for 60 seconds (extension), was performed. A further extension 10 minutes at 72°C was usually added to the program. The temperatures and times used were varied dependent on the oligonucleotide primer combinations and template. After the amplification, the reactions products were fractionated on a 0.8% (w/v) agarose gel and bands of the expected size gel purified.

The probe was then stored at -20°C or denatured at 95°C for 5 minutes then used immediately for hybridization.

2.6.4 DNA hybridization

Nylon membranes containing immobilized DNA were incubated in pre-hybridization solution (5X SSC buffer; 0.5% (w/v) SDS**,** 1X Denhardts solution (200 mg L^{-1} Ficoll® 400, 200 mg L^{-1} polyvinylpyrrolidone, 200 mg L^{-1} bovine serum albumin) containing 0.2 g L^{-1} sonicated denatured salmon sperm DNA (Sigma Aldrich) at 65°C for a minimum of 1 hour. The denatured probe was immediately added to the pre-hybridization solution and then membrane incubated at 65°C overnight. The following morning, the membrane was copiously washed with 2X SSC containing 0.2% (w/v) SDS at room temperature for 15 minutes then twice with 0.1X SSC containing 0.2% (w/v) SDS for 15 minutes at 65°C.

Detection of the hybridizing probe was carried out using the DIG Luminescent Detection Kit (Roche) as per the manufacturer's instructions. Briefly, the membrane was washed with Blocking Solution (1% (w/v) Blocking Reagent (Roche) in 0.1 M maleic acid, 0.15 M NaCl pH 7.5) before challenging for 30 minutes with an alkaline phosphatase conjugated anti-DIG antibody diluted 1:10 000 in Blocking Solution. Following two 15 minute washes in Wash Buffer (0.1 M maleic acid, 0.15 M NaCl, pH 7.5, 0.3% (v/v) Tween 20) and equilibration in Detection Buffer (0.1 M Tris-HCl, 0.1 M NaCl, pH 9.5), the DNA side of the membrane was covered with CPSD® solution diluted 1:100 with Detection Buffer and incubated firstly for 5 minutes at room temperature then for 5 to 15 minutes at 37°C. In a dark room, the membrane was then placed in an X-Ray cassette and exposed to X-Ray film (SLS). The film

was washed in RG Universal Ready to Use Developer and Fixer solutions (Champion Photochemistry) and water before being documented.

Chapter 3: Screening quinone-based compounds for anti-parasitic activity

Parasites belonging to the order Trypanosomatida cause three of the seventeen infections referred to as neglected tropical diseases (NTDs) (Molyneux *et al*. 2005; World Health Organisation 2015). Because this collection of maladies primarily affect people living in the poorest regions of the World, such ailments are not deemed commercially viable by pharmaceutical companies in terms of drug development: the developmental costs required to bring a new drug to market outweigh any potential finacial return (Feasey *et al*. 2010). As such only 16 of the 1393 new drugs coming to market between 1975 and 1999 actually target NTDs (Pécoul 2004). In the case of trypanosomatid diseases, existing chemotherapies are problematic as they are costly, generally require medical supervision for their administration, often cause numerous severe side effects and may have limited efficacy (Wilkinson & Kelly 2009). Because of these issues the recommended drug regimens are frequently not completed resulting in the selection of parasite strains refractory to certain front-line drugs (Barrett *et al*. 2003; Wilkinson & Kelly 2009; Baker *et al*. 2013; Mohapatra 2014). Against this backdrop there is an urgent need for cheap, safe agents that can be administrated orally towards NTDs in general.

Quinone-based compounds encompass a range of molecules characterised by 2 carbonyl-groups linked to a carbocyclic backbone. They can be divided into several classes dependent on the number/type of ring(s) present in the basic structure & the relative positions of the carbonyl-groups on the ring (Figure 3.1).

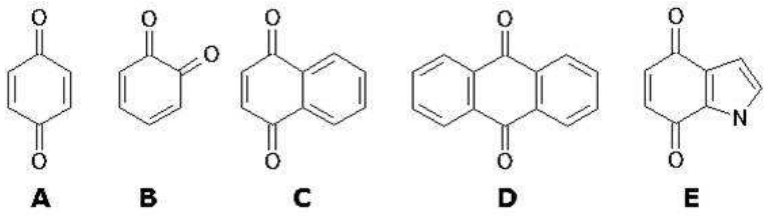

Figure 3.1: Examples of basic quinone structures. A shows a 1,4-benzoquinone, B a 1,2-benzoquinone, C is a 1,4-naphthoquinone, D a 9,10-anthraquinone & E an indolequinone.

Widely distributed in nature, quinones participate in a number of crucial biological cascades serving as electron acceptors and donators in the photosynthesis (plastoquinone, phylloquinone) and aerobic respiration (ubiquinone) electron transport chains and in blood coagulation and bone formation (vitamin K_1 and K_2) (Figure 3.2). Additionally, several natural & synthetic quinones have been used or are undergoing clinical evaluation in medicine as antimicrobial & anticancer agents. These usually function as inhibitors of essential redox pathways or as pro-drugs. For example, atovaquone, used as part of malarone combinational therapy to treat malaria, binds to and blocks the cytochrome bc1 complex in the *Plasmodium* mitochondrial electron transport chain while the anti-cancer drug mitomycin C following bioreductive activation, covalently binds to DNA strands leading to formation of inter- and intra-strand crosslinkages (Figure 3.2) (Iyer & Szybalski 1963; Mather *et al*. 2005).

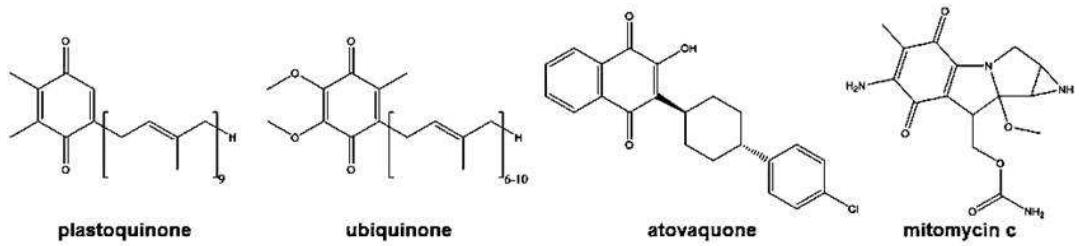

Figure 3.2: Examples of biologically active quinone-based molecules

Here, we report the antimicrobial screening of several different types of quinone-based molecules against the protozoan parasites *L. major*, *T. brucei* and *T. cruzi* and for one group of compounds evaluate their toxicity toward mammalian cells.

3.1 Anti-parasitic and toxicity properties of aziridinyl 1,4-benzoquinones

Aziridinyl 1,4-benzoquinones lacking substitutions on the aziridinyl ring are of pharmacological interest because these compounds are reported to have potent anticancer activities (Lin *et al*. 1972; Lusthof *et al*. 1989). For RH1 (**5**) and AZQ (**20**) this has resulted in these agents undergoing clinical evaluation for use as treatments to target hypoxic solid malignancies including tumours associated with the breast, liver and colon (Schilsky *et al*. 1982; Tan *et al*. 1984; Falletta *et al*. 1990; Danson *et al*. 2011). In these situations, the cancerous cells have been shown to express elevated levels of the enzyme NADPH quinone oxidoreductase 1 (NQO1; also known as DT-diaphorase). In the absence of oxygen, this enzyme catalyses the 2 electron reduction of the ABQ prodrug to generate metabolites that then mediate their cytotoxic effect by promoting DNA damage through the formation of DNA cross links (Danson *et al*. 2004; Dehn *et al*. 2005; Danson *et al*. 2007).

Recently, the anti-microbial activities of ABQs towards the *Plasmodium falciparum* and *Trypanosoma brucei* parasites have been investigated with several potential lead compounds identified (Grellier *et al*. 2010; Hall *et al*. 2012). Here, we have expanded on these initial screens to evaluate the anti-kinteoplastid activities of 22 ABQs (compounds **1-22**; appendix 1) against *T. brucei*, *T. cruzi* and *L. major*. As an initial step a series of primary screens were performed aimed at determining the growth inhibitory activity of a fixed concentration of compound (10 µM) against

BSF *T. brucei*, *T. cruzi* epimastigotes or *L. major* promastigotes (Materials and Methods). In these assays a fixed number of parasites (1 x 10^4*T. brucei* ml^{-1}; 5 x 10^5*T. cruzi* or *L. major* ml^{-1}) were grown for three (*T. brucei*), fourteen (*T. cruzi*) or six (*L. major*) days at 37 ºC (*T. brucei*) or at 27 ºC (*T. cruzi* and *L. major*) and then the cell number determined using the vital dye resazurin as reporter. All treatments were performed in quadruplicate. The resultant fluorescence values for each compound treated culture was transformed (subtraction of a background medium-control florescence) and the data for each treatment expressed as % growth inhibition relative to untreated parasites analysed in parallel (data not shown). To demonstrate the validity of this assay system the growth inhibitory effects of nifurtimox on all three parasites was also determined. Based on these initial screens twelve, nine and twelve structures yielded high or moderate fluorescence values indicating they exhibited no or low growth inhibitory activity against *T. brucei*, *T. cruzi* and *L. major*, respectively. These were excluded from further studies.

To further evaluate the anti-microbial activities of the remaining ABQs a series of secondary screens were performed aimed at determining the growth inhibitory activities of a range of compound concentrations (typically 3 nM to 10 µM for *T. brucei* and *L. major*, and 1 to 500 nM for *T. cruzi*). The resultant fluorescence values were transformed as previously described and compared against untreated parasites grown in parallel, with the finalised data expressed as % cell growth. Dose response curves for each agent were drawn (Figure 3.3) from which compound IC_{50} valueswere determined (Table 3.1). Together the data demonstrated the ABQs to be a potent anti-parasitic class of compounds. Of those compounds tested MeDZQ (**2**), RH1 (**5**), **6** and **8** all yielded IC_{50} values<100 nM against BSF *T. brucei* with DZQ

(**1**), **3**, TZQ (**21**) and **22** exhibitingvalues <500 nM. For *T. cruzi*, three agents (DZQ (**1**), RH1 (**5**) and TZQ (**21**)) displayed extremely potent activity against the epimastigote stage yielding IC_{50}'s <10 nM with a further two (MeDZQ (**2**) and **22**) and three (**4**, **6** and **14**) generating values <100 and <500 nM, respectively. Against *L. major* promastigotes TZQ (**21**) exhibited an IC_{50} of <10 nM with DZQ (**1**) and RH1 (**5**) generating values of <100 nM with **3** and **22** yielding IC_{50}'s <500 nM. Of all the ABQs analysed RH1 (**5**) was the most potent agent tested against all three parasite yielding IC_{50} values of 19 ± 1, 3 ± 1 and 68 ± 1 nM against *T. brucei*, *T. cruzi* and *L. major*, respectively.

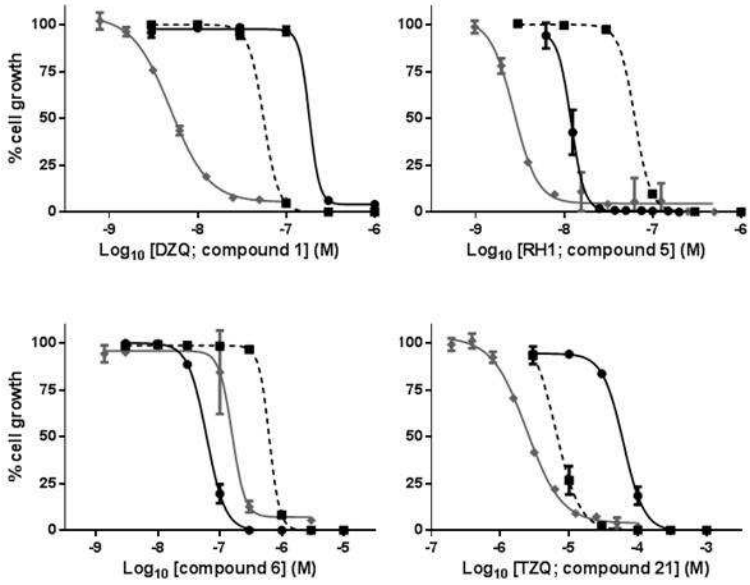

Figure 3.3: Dose response curvesof trypanosomatid parasites towards selected aziridinyl 1,4-benzoquinone compounds. The growth inhibitory effects ofDZQ (**1**), RH1 (**5**), **6** and **21** towards wild type bloodstream form *T. brucei* (circles, black solid line), *L. major* promastigote (squares, black dotted line) or *T. cruzi* epimastigote (diamonds grey solid line) cells was evaluated. Dose response curves were constructed from which the IC_{50} was calculated using non-linear regression analysis. Data points are averages from experiments performed in triplicate (*T. brucei* and *L. major*) or quadruplicate (*T. cruzi*) ± standard deviation.

Compound	IC_{50} values (μM) ± standard deviation		
	T. brucei	***T. cruzi***	***L. major***
Nifurtimox[a]	2.700 ± 0.100	2.600 ± 0.400	6.280 ± 0.040
7, **9-12**, **16-19**	>10.000	>10.000	>10.000
DZQ (**1**)	0.272 ± 0.001	0.005 ± 0.001	0.060 ± 0.001
MeDZQ (**2**)	0.018 ± 0.001	0.055 ± 0.002	0.560 ± 0.139
3	0.400 ± 0.03	6.200 ± 1.160	0.199 ± 0.004
4	1.180 ± 0.160	0.106 ± 0.025	0.663 ± 0.006
RH1 (**5**)	0.019 ± 0.001	0.003 ± 0.001	0.068 ± 0.001
6	0.066 ± 0.002	0.205 ± 0.053	0.664 ± 0.002
8	0.058 ± 0.001	1.300 ± 0.108	1.870 ± 0.184
13	>10.000	5.550 ± 0.240	>10.000
14	>10.000	0.445 ± 0.030	2.270 ± 0.017
15	>10.000	3.310 ± 0.200	>10.000
AZQ (**20**)	8.233 ± 0.272	6.000 ± 0.283	>10.000
TZQ (**21**)	0.179 ± 0.001	0.003 ± 0.001	0.009 ±0.001
22	0.148 ± 0.001	0.055 ± 0.002	0.218 ± 0.02

Table 3.1: Anti-parasitic activity of aziridinyl 1,4-benzoquinones. Data represent the growth-inhibitory effect as judged by the IC_{50} values of aziridinyl 1,4-benzoquinones on wild-type BSF *T. brucei*, *L. major* promastigotes and *T. cruzi* epimastigotes. All values are means ± standard deviation from three or four independent experiments. [a]*T. brucei* and *T. cruzi* IC_{50} towards nifurtimox were obtained from Wilkinson *et al*. (2008).

To evaluate whether those ABQs that displayed anti-parasitic activity against all three kinteoplastid parasitesexhibited toxicity to mammalian cells we determined the cell killing properties of each agent against differentiated THP-1 cells: note this assay is not a growth inhibitory experiment as THP-1 cells once differentiated into macrophage-like cells are unable to divide. As for the parasite growth assays resazurin was used as reporter with the mammalian fluorescence values transformed as described previously and expressed as % viable cells relative to untreated control cultures. Values were then used to plot dose responses curves (Figure 3.4) from which the compound concentration that kills 50% of the mammalian cells (LD_{50}) was determined (Table 3.2).

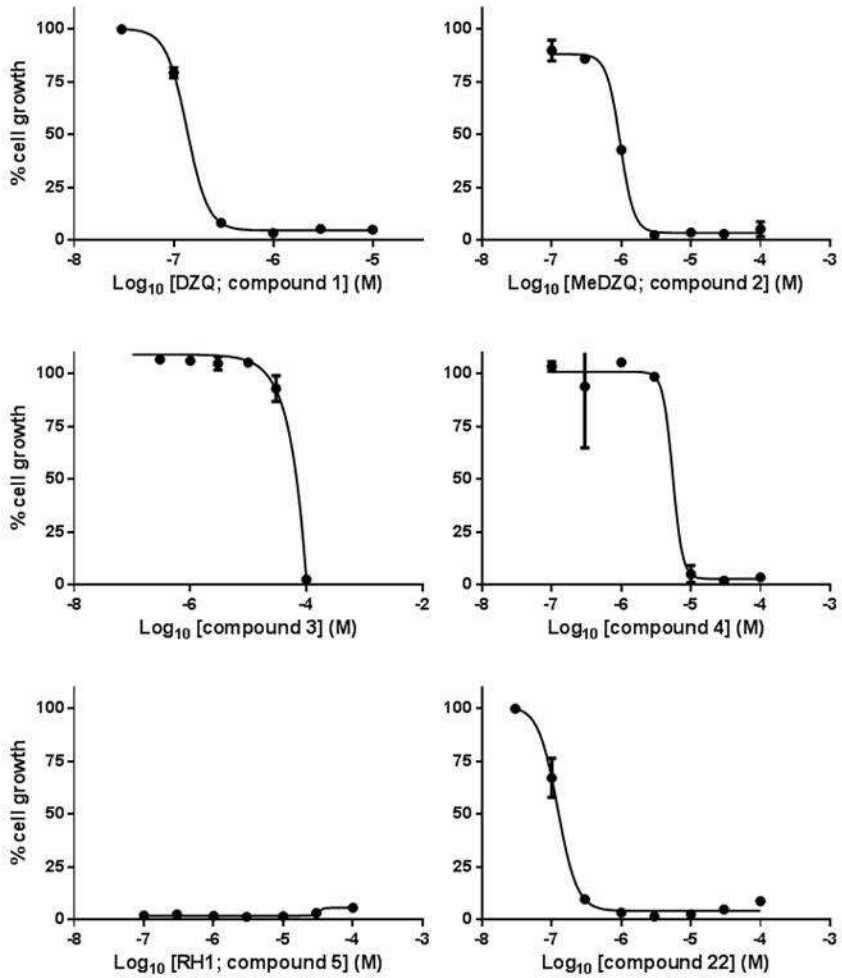

Figure 3.4: Dose response curves of differentiated THP-1 cells towards aziridinyl 1,4-benzoquinones compounds. The growth inhibitory effects ofselectedaziridinyl 1,4-benzoquinones (DZQ (**1**), MeDZQ (**2**), **3**, **4**, RH1 (**5**) and **22**) towards differentiated THP-1 cells was evaluated. Dose response curves were constructed from which the LD_{50} was calculated using non-linear regression analysis. Data points are averages from experiments performed in triplicate ± standard deviation. Experiments were conducted by Ms J. Szular, QMUL.

Compound	LD_{50}(µM) ± standard deviation
DZQ (**1**)	0.181 ± 0.005
2	0.885 ± 0.023
3	63.170 ± 0.176
4	6.633 ± 0.176
RH1 **(5)**	<0.100
6	1.067 ± 0.159
8	2.950 ± 0.770
TZQ (**21**)	<0.100
22	0.138 ± 0.025
Nifurtimox[a]	>100.000

Table 3.2: Toxicity of aziridinyl 1,4-benzoquinones towards cultured mammalian macrophages. Data represent the growth-inhibitory effect as judged by their IC_{50}'s of selected aziridinyl 1,4-benzoquinones on differentiated THP-1 macrophage cells. All values are means ± standard deviation from three independent experiments. [a]Differentiated THP-1 LD_{50} valuetowards nifurtimox taken from Voak *et al* (2013).

Under these conditions eight of the ABQs tested showed significant toxicity *in vitro* yielding LD_{50}'s <10 µM with two compounds, including RH1 (**5**), being extremely toxic yielding values <100 nM. Comparison of the mammalian toxicity LD_{50} data with the IC_{50} values observed against the parasites allowed a crude measure of that agents' selectively toward the pathogen(Table 3.3). In many cases the ABQ displayed a higher potency against the mammalian cell line relative to the parasite: the observed LD_{50} value towards the differentiated THP-1 line was lower than the calculated IC_{50} value against the parasite resulting in a selective toxicity value <1. Of those that did display preferential activity toward the parasite the observed selective toxicity (<50) was equivalent to that noted using nifurtimox, an agent who use in humans is problematic (Wilkinson & Kelly 2009). Only compound **3** showed reasonable selectivity against BSF *T. brucei* and *L. major* promastigotes yielding selective toxicity values of 158 and 317, respectively.

Compound	Selective toxicity (LD_{50} THP-1/IC_{50} parasite)		
	T. brucei	***T. cruzi***	***L. major***
DZQ (**1**)	<1	36	3
2	49	16	2
3	158	10	317
4	6	63	10
RH1 **(5)**	5	<33	1
6	16	<1	<1
8	51	<1	<1
TZQ (**21**)	<1	<33	<11
22	<1	3	<1
Nifurtimox	>37	>38	>16

Table 3.3: Selective toxicity of aziridinyl 1,4-benzoquinones

As THP-1 cells are an immortal human monocytic cell line derived from an acute monocytic leukaemia patient and that ABQs have potent activity against cancerous cells (AZQ was trialled as a treatment against leukaemia) (Tan *et al*. 1984; Lee *et al*. 1986; Moore *et al*. 1997), it was decided that selected compounds should be screened for their toxicity against non-cancerous mouse peritoneal macrophages. The compounds (TZQ (**1**), RH1 (**5**), TZQ (**21**) and **22**) analysed all displayed potency against all parasites screened with three of the four agents differing only in the number of aziridinyl groups attached to the benzoquinone ring thus allowing a crude structure activity relationship study to be performed: DZQ (**1**) contains two aziridinyl substituents, TZQ (**21**) contains three and **22** has four. Peritoneal macrophages obtained from BALB/c mice (Dr Karin Seifert, LSHTM) were adhered onto a microscope slide, treated with different concentrations (100 to 1000 nM) of the selected ABQ and incubated at 37ºC. The cells were then fixed, Giemsa stained and the average number of cells per field of view determined (Figure 3.5): routinely 10 fields of view were counted. For each drug treated sample the % of stained cells relative to untreated controls was determined and plotted as a dose response curve (data not shown) from which the LD_{50} was calculated. Under these conditions TZQ

(**1**), RH1 (**5**), TZQ (**21**) and **22** displayed LD_{50} values of 255, <100, <100 and 120 nM, respectively.

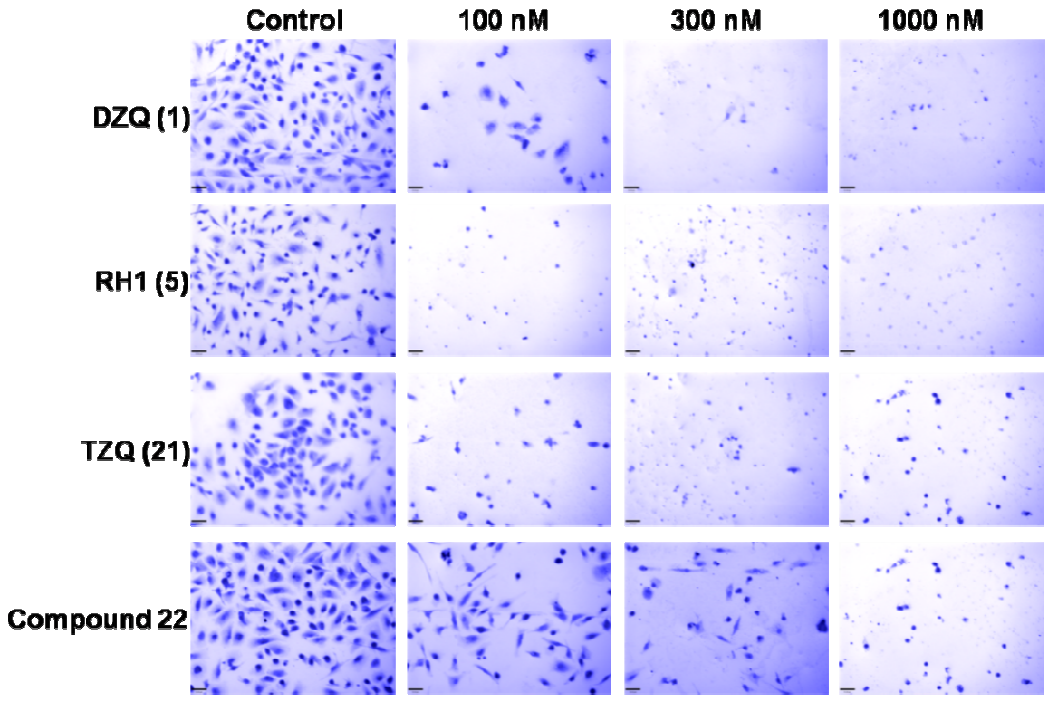

Figure 3.5: Susceptibility of primary spleen macrophages to aziridinyl 1,4-benzoquinones. Peritoneal macrophages extracted from BALB/c mice were adhered onto microscope slides then treated with different concentrations of selected ABQs. Cells were Giemsa stained and visualized by light microscopy. A typical field using a x20 objective is shown.

Our data clearly demonstrates that ABQs are extremely toxic to primary cells thus confirming our THP-1 studies and shows that this class of compound are unlikely to be beneficial in targeting systemic trypanosomal and leishmanial infections. However, they may still be useful in the therapy of cutaneous lesions. As such our focus on ABQs switched from exploiting these as potential treatments to using them as chemical tools to understand their mechanisms of action against the pathogen.

3.2 Trypanocidal and leishmanicidal properties of methyl substituted aziridinyl 1,4-benzoquinones

Searches of the PubChem database (http://pubchem.ncbi.nlm.nih.gov/) identified several additional ABQs that all contained mono- or di-methyl substitutions on the aziridinyl groups attached to the 1,4-benzoquinone core which were freely available from the National Cancer Institute. In this study these agents represent a second class of compounds referred to as methyl aziridinyl 1,4-benzoquinones (MeABQs). Many of these chemicals were originally synthesised while searching for anti-cancer agents, screens in which many were deemed to be inactive.

Here, a total of 12 MeABQs (**23**-**34**) were assayed for anti-parasitic activity using the primary and secondary screening procedures outlined previously. From the primary screens, five, five and four compounds failed to display any activity against BSF *T. brucei*, *T. cruzi* epimastigotes or *L. major* promastigotes, respectively (Table 3.4). Subsequent secondary screening generating dose response curves (Figure 3.6) from which IC_{50} values were determined (Table 3.4). Generally, these compounds appeared to be less toxic to the parasites than the non-methylated ABQ group of compounds with no chemical yielding an IC_{50} value of <500 nM against *T. brucei*, one (**24**) against *T. cruzi* and six (**23**-**25**, **27**, **29** and **30**) against *L. major*. In light of the cytotoxicity displayed by ABQs to mammalian cells and because no one MeABQ agent displayed activity against all three parasite lines, this class of compound was not analysed further.

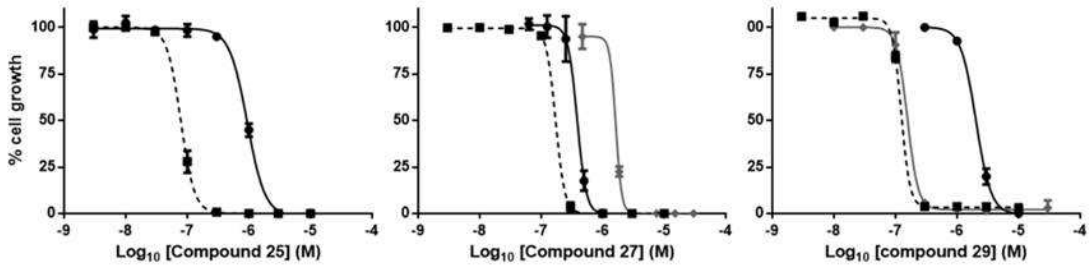

Figure 3.6: Susceptibility of trypanosomatid parasites towards selected methyl and di-methyl substituted aziridinyl 1,4-benzoquinones. The growth inhibitory effects of **25, 27** and **29** towards wild type bloodstream form *T. brucei* (circles, black solid line), *L. major* promastigote (squares, black dotted line) or *T. cruzi* epimastigote (diamonds grey solid line) cells was evaluated. **25** did not show activity against *T. cruzi* epimastigotes at 10 µM therefore was not screened further. Dose response curves were constructed from which the IC_{50} was calculated using non-linear regression analysis. All data points are averages from experiments performed in triplicate ± standard deviation

Compound	**IC_{50} values (µM) ± standard deviation**		
	T. brucei	***T. cruzi***	***L. major***
23	>10.000	2.180 ± 0.670	0.348 ± 0.166
24	>10.000	0.037 ± 0.001	0.473 ± 0.123
25	0.920 ± 0.050	-	0.080 ±0.006
26	>10.000	8.638 ± 0.736	2.360 ± 0.230
27	0.540 ± 0.040	0.620 ± 0.180	0.210 ± 0.01
28	2.850 ± 0.260	>10.000	>10.000
29	2.160 ± 0.079	0.975 ± 0.025	0.175 ± 0.005
30	0.700 ± 0.053	0.980 ± 0.025	0.174 ± 0.01
31	>10.000	>10.000	>10.000
32	2.873 ± 0.042	>10.000	>10.000
33	>10.000	>10.000	8.157 ± 0.080
34	2.923 ± 0.065	>10.000	>10.000

Table 3.4: Anti-parasitic activity of methyl substituted aziridinyl 1,4-benzoquinones. Data represent the growth-inhibitory effect as judged by their IC_{50}'s of methylated aziridinyl 1,4-benzoquinones on wild-type BSF *T. brucei*, *L. major* promastigotes and *T. cruzi* epimastigotes. All values are means ± standard deviation from three or four independent experiments.

3.3 Trypanocidal and leishmanicidal properties of naphthoquinone.

Naphthoquinone-based compounds are of biological importance playing key roles in process requiring oxidoreductase shuttles or as enzyme cofactors (*e.g.* the K vitamins). Additionally, they have been exploited as antimicrobial agents primarily as inhibitors of the above systems (*e.g.*atovaquone is used to treat malaria)

(Srivastava *et al*. 1997; Srivastava *et al*. 1999). In the search for anti-kinetoplastid agents approximately 100 publications detailing the synthesis and evaluation of naphthoquinone derivatives have been reported with such compounds targeting a range of different biological processes within the parasites including energy production, generators of mitochondrial oxidative stress, ergosterol biosynthesis, cytoskeleton assembly, protein metabolism and biosynthesis and chaperones modulation (Menna-Barreto *et al*. 2010; Pieretti *et al*. 2013; Salomão *et al*. 2013). Here, we evaluated a series of naphthoquinones (**35**-**51**), many of which contained nitrogen mustard and aziridinyl groupings that may promote DNA damage, for their trypanocidal and leishmanicidal properties. After conducting growth inhibition screens, dose response curves were drawn (Figure 3.7) from which IC_{50} values calculated (Table 3.5). Out of the seventeen compounds tested, fifteen (**36**-**45** and **47**-**51**) were active against *T. brucei* yielding IC_{50}'s ranging from ~0.1 to ~2.7 µM while fourteen (**36**-**44** and **47**-**51**) displayed potency against *L. major*, generating IC_{50}'s from ~0.3 to 8.7 µM. Invariably, compounds that exhibited trypanosomal growth inhibitory properties were active against the leishmanial species. Only **45** did not follow this trend although this agent displayed a relatively low activity against *T. brucei* (IC_{50} of 1.91 ± 0.21 µM) while no having an effect on *L. major* at 10 µM. In contrast, *T. cruzi* was generally less susceptible to this class of quinone with only five (**35**, **36**, **38**, **40** and **41**) agents displaying anti-Chagasic properties producing IC_{50}'s ranged from to 0.7 to 7.7 µM).

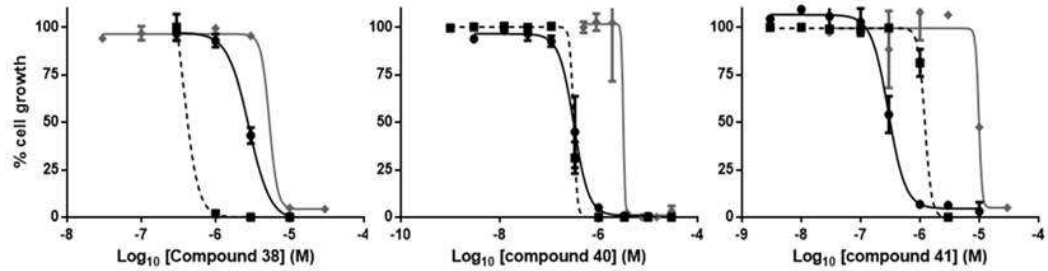

Figure 3.7: Dose response curvesof trypanosomatid parasites towards selected naphthoquinones. The growth inhibitory effects of **38**, **40** and **41** towards wild type bloodstream form *T. brucei* (circles, black solid line), *L. major* promastigote (squares, black dotted line) or *T. cruzi* epimastigote (diamonds grey solid line) cells was evaluated. Dose response curves were constructed from which the IC_{50} was calculated using non-linear regression analysis. All data points are averages from experiments performed in triplicate ± standard deviation.

Compound	**IC_{50} values (µM) ± standard deviation**		
	T. brucei	***T. cruzi***	***L. major***
Menadione (**35**)	>10.000	7.710 ± 0.090	>10.000
Plumbagin (**36**)	0.640 ± 0.015	2.360 ± 0.310	0.410 ± 0.040
37	2.170 ± 0.070	>10.000	8.700 ± 1.050
38	2.700 ± 0.100	7.090 ± 0.730	0.730 ± 0.020
39	1.890 ± 0.030	>10.000	7.600 ± 0.030
40	0.200 ± 0.040	0.700 ± 0.070	0.288 ± 0.010
41	0.300 ± 0.067	7.000 ± 0.180	1.780 ± 0.130
42	0.630 ± 0.010	>10.000	1.300 ± 0.040
43	0.107 ± 0.149	>10.000	0.650 ± 0.006
44	0.670 ± 0.010	>10.000	0.900 ± 0.006
45	1.910 ± 0.210	>10.000	>10.000
Lapachol (**46**)	>10.000	>10.000	>10.000
47	0.197 ± 0.030	>10.000	5.667 ± 0.379
48	0.721± 0.004	>10.000	6.717 ± 0.029
49	0.660 ± 0.070	>10.000	2.000 ± 0.080
50	6.333± 0.247	>10.000	6.310 ± 0.277
51	0.198 ± 0.010	>10.000	1.187 ± 0.018

Table 3.5:Anti-parasitic activity of naphthoquinones. Data represent the growth-inhibitory effect as judged by their IC_{50}'s of naphthoquinones on wild-type BSF *T. brucei*, *L. major* promastigotes and *T. cruzi* epimastigotes. All values are means ± standard deviation from three or four independent experiments.

3.4 Trypanocidal and leishmanicidal properties of benzoquinone nitrogen mustards

Nitrogen mustard-containing compounds such as chlorambucil, mechlorethamine**,** cyclophosphamide, melphalan, prednimustine, bendamustine etc have been trialled and used extensively to treat a range of cancers (Mouridsen *et al*. 1980; Dighiero *et al*. 1998; Moreau *et al*. 1999; Skinner *et al*. 2004; Tashkin *et al*. 2006; Leoni *et al*. 2008). In most cases, the biologically active $N(CH_2CH_2Cl)_2$ grouping is attached to a cyclic structure such as a benzyl (chlorambucil, melphalan, prednimustine), oxazaphosphorine (cyclophosphamide) or benzimidaozle (bendamustine) ring. Previous work conducted in the Wilkinson lab has shown that nitrobenzylphosphoramide-containing nitrogen mustards are potent trypanocidal and leishmanicidal compounds with the activities of such agents dependent on type I NTR(Hall *et al*. 2010; Hu *et al*. 2011; Voak *et al*. 2014). Based on the above lines of evidence we evaluated a small collection of 1,4-benzoquinone nitrogen mustards (**52**-**56**) for their anti-parasitic properties (Figure 3.8; Table 3.6). Out of the five compounds tested, one (**54**) failed to display activity against any of the parasites screened at 10 µM. From the remaining agents four (**52**, **53**, **55** and **56**) showed activity against both *T. brucei* and *L. major* with only one (**52**) displaying anti-*T. cruzi* effects. Where an anti-microbial property was observed the leishmanial parasite was generally more susceptible to a given agent than the trypanosome *e.g.* based on IC_{50} values *L. major* was 7.5- and 2.8-fold more susceptible to **52** as compared to *T. brucei* and *T. cruzi*, respectively.

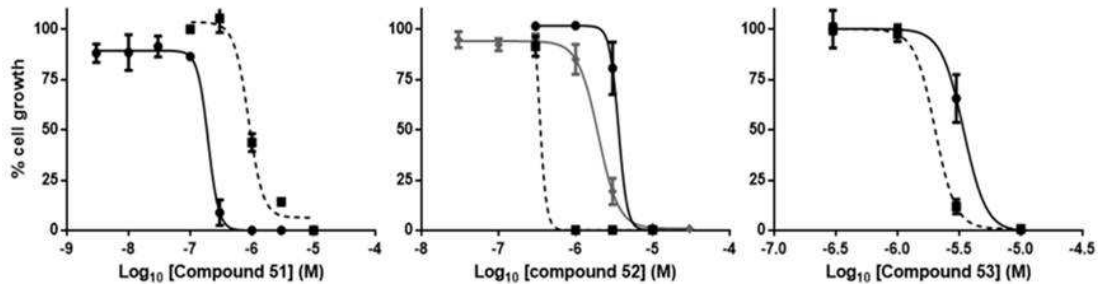

Figure 3.8: Dose response curvesof trypanosomatid parasites towards 1,4-benzoquinone nitrogen mustards. The growth inhibitory effects of **51**, **52** and **53** towards wild type bloodstream form *T. brucei* (circles, black solid line), *L. major* promastigote (squares, black dotted line) or *T. cruzi* epimastigote (diamonds grey solid line) cells was evaluated. Dose response curves were constructed from which the IC_{50} was calculated using non-linear regression analysis. All data points are averages from experiments performed in triplicate ± standard deviation

Compound	IC_{50} values (µM) ± standard deviation		
	T. brucei	***T. cruzi***	***L. major***
52	5.433 ± 0.764	2.023 ± 0.080	0.720 ± 0.030
53	4.483 ± 0.993	>10.000	2.270 ± 0.090
54	>10.000	>10.000	>10.000
55	2.023 ± 0.008	>10.000	0.610 ± 0.020
56	1.727 ± 0.096	0.668 ± 0.050	0.668 ± 0.050

Table 3.6: Anti-parasitic activity of 1,4-benzoquinone nitrogen mustards. Data represent the growth-inhibitory effect as judged by their IC_{50}'s of 1,4-benzoquinone nitrogen mustards on wild-type BSF *T. brucei*, *L. major* promastigotes and *T. cruzi* epimastigotes. All values are means ± standard deviation from three or four independent experiments.

3.5 Trypanocidal and leishmanicidal properties of other aziridinyl-containing quinones

Several other classes of quinones that contain aziridinyl groupings have been used or are under clinical evaluation as therapeutic agents. One of the best known is mitomycin C, an indolequinone being used to treat a range of tumours including cancers of the bladder, breast, lung, liver and stomach (see http://www.cancerresearchuk.org/about-cancer/cancers-in-general/treatment/ cancer-

drugs/mitomycin-c) and its derivatives porfiromycin and apaziquone which have or are undergoing clinical evaluation to treat hypoxic tumours (Keyes *et al*. 1985; Puri *et al*. 2006; Phillips *et al*. 2013; Guise *et al*. 2014). The compounds all function as prodrugs undergoing NQO1-mediated activation that results in products which promote DNA damage (Iyer & Szybalski 1964; Siegel *et al*. 2012). Interestingly, novel indolequinone prodrugs have been developed that function to inhibit NADPH quinone oxidoreductase 2 (NQO2), an enzyme of unknown function whose expression is upregulated in some cancers (Yan *et al*. 2011; Dufour *et al*. 2012). In this case, activation of these prodrugs occurs *via* NQO2 bioreduction to produce metabolites that actually alkylate and inhibit NQO2 itself (Dufour *et al*. 2012).

Here, we evaluated the efficacy of three further aziridinyl-containing quinones including mitomycin C (**57**) and two benzimidazoles (**58** and **59**) against *T. brucei*, *T. cruzi* and *L. major* (Figure 3.10; Table 3.7). Mitomycin C (**57**) displayed growth inhibitory activity against all three parasites displaying a particularly high degree of potency towards *T. brucei* (IC_{50} of 20 nM). As with this indolequinone, the two benzimidazoles were extremely effective against *T. brucei* with **58** and **59** yielding IC_{50} values of 211and 6 nM, respectively but less so against *T. cruzi* and *L. major*.

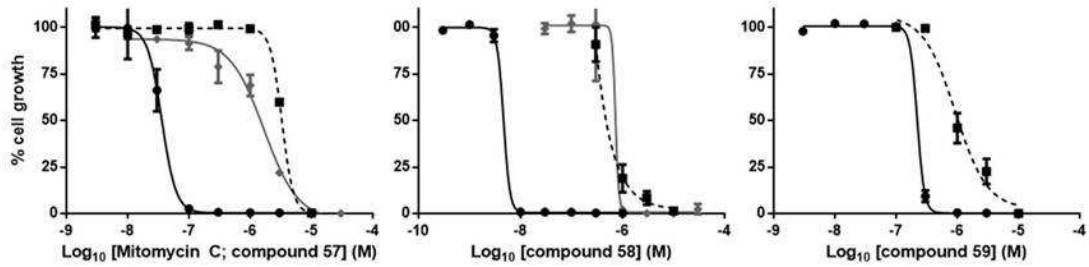

Figure 3.9: Dose response curvesof trypanosomatid parasites towards other aziridinyl-containing quinones. The growth inhibitory effects of **57**, **58** and **59** towards wild type bloodstream form *T. brucei* (circles, black solid line), *L. major* promastigote (squares, black dotted line) or *T. cruzi* epimastigote (diamonds grey solid line) cells was evaluated. Dose response curves were constructed from which the IC_{50} was calculated using non-linear regression analysis. All data points are averages from experiments performed in triplicate ± standard deviation.

Compound	**IC_{50} values (µM) ± standard deviation**		
	T. brucei	***T. cruzi***	***L. major***
Mitomycin c (**57**)	0.020 ± 0.015	2.063 ± 0.380	4.200 ± 0.029
58	0.211 ± 0.005	>10.000	2.800 ± 0.200
59	0.006 ± 0.001	0.773 ± 0.128	0.680 ± 0.060

Table 3.7: Anti-parasitic activity of other aziridinyl containing quinones. Data represent the growth-inhibitory effect as judged by their IC_{50}'s of the remaining aziridinyl containing quinones on wild-type BSF *T. brucei*, *L. major* promastigotes and *T. cruzi* epimastigotes. All values are means ± standard deviation from three or four independent experiments.

Chapter 3 summary

This chapter has focused on evaluating the trypanocidal and leishmanicidal activities of a small (59) compound library made up of chemicals that all contain a quinone-containing backbone. We demonstrated that:

1. Most compounds tested displayed anti-parasitic activity at 10 µM, with ~1/3rd (21/59) exhibiting growth inhibitory effects against all three parasites studied.

2. Several compounds yielded very low IC_{50} values (<100nM) indicating that these were of promise in treatment development targeting trypanosomiasis and leishmaniasis: six compounds (MeDZQ (**2**), RH1 (**5**), **6**, **8**, mitomycin C (**57**) and **59**) generated IC_{50}'s <100 nM against *T. brucei*, five (DZQ (**1**), MeDZQ (**2**), RH1 (**5**), TZQ (**21**) and **22**) against *T. cruzi* and four (DZQ (**1**), RH1 (**5**), TZQ (**21**) and **25**) against *L. major*.

3. As a class the aziridinyl 1,4 benzoquinones that lacked methyl substituents on their aziridinyl groupings were the most effect against all three parasites tested, with RH1 (**5**) being the most effective of all.

4. When tested against primary and secondary mammalian cell lines (macrophages and macrophage-like cells) all the compounds tested, including RH1 (**5**), displayed significant toxicity.

5. In light of the observed toxicity, aziridinyl 1,4 benzoquinones are unlikely to be beneficial in targeting systemic trypanosomal and leishmanial infections although may still be of use in treating cutaneous lesions.

6. The focus on ABQs in this thesis should switch from exploiting these as potential anti-parasitic treatments to using them as chemical tools to understand their mechanisms of action against the pathogen.

Chapter 4: Unravelling the trypanocidal mode of action of the aziridinyl benzoquinones

Understanding how various compounds may mediate their cytotoxic effects has helped in deciphering key biological and biochemical process within a given cell or organism. This information has not only informed future drug design but also allows for the identification of potential resistance mechanisms. In trypanosomes, one way in which a compound's mode of action can be identified is through the generation of genetically modified parasites that express altered levels of a given gene with the susceptibility of the resultant recombinant lines evaluated against the chemical understudy. One drawback of this approach is that certain assumptions about the compound's mode of action are required at the onset thus potentially biasing the study. Recently, the application of high throughput whole genome loss of function (RNAi) and whole genome gain of function (over expression) screening strategies for use in *T. brucei* have been described with these approaches partially circumventing the above issue (Alsford *et al*. 2012; Begolo *et al*. 2014). Here, using an RNAi library screening technique we evaluate whether the trypanocidal benzoquinone-based compounds described in Chapter 3 function as prodrugs that forms metabolites which go on to promote DNA damage through a mechanism that can be repaired by a trypanosomal nuclease belonging to the SNM1/PSO2 family, enzymes that are only implicated in the repair of interstrand crosslinks (ICLs).

4.1 Identifying the RH1 activation mechanism.

In conjunction with Dr Sam Alsford (LSHTM) a whole genome loss of function assay was conducted on BSF *T. brucei* using RH1, the archetypal ABQ, as selective

agent. The library consists of a population of *T. brucei* parasites which have been genetically modified to contain a tetracycline inducible RNAi construct plus a fragment of the *T. brucei* genome. The library exhibits > 5 times coverage of the *T. brucei* genome (Alsford *et al* 2011). The whole loss-of-function library screens have been used to identify key proteins which confer resistance towards a particular agent. Previous work by Horn and Alsford groups have identified AAT6 as a key uptake mechanism for eflornithine resistance whilst NTR was identified as a mediator of nifurtimox resistance (Baker *et al*, 2011; Alsford *et al*, 2014).

To summarise the experiment, an aliquot of the *T. brucei* RNAi library stock was induced to undergo RNAi by addition of tetracycline (1 µg ml^{-1}) one day (-1 day) prior to setting up the selection. At day 0, 30 nM RH1 (a concentration 1.5 times the IC_{50} (see Table 3.1)) was added to a culture containing 2 x 10^5 *T. brucei* ml^{-1} and over the course of the next 12 days the cell density of the treated culture followed (Figure 4.1): When appropriate the culture was diluted to 2 x 10^5*T. brucei* ml^{-1} in medium containing fresh tetracycline (1 µg ml^{-1}) and RH1 (30nM). The above treatment initially resulted in a reduced growth rate as compared to non-induced and non-RH1 controls, followed by an outgrowth from day 8 onwards of an RH1 resistant population, a pattern has been previously observed using other selective conditions (Baker *et al*. 2011; Alsford *et al*. 2013; Alsford *et al*. 2014). The outgrowth represents theparasites which contain a fragment of the genome, which under RNAi conditions confers resistance towards the selective agent.

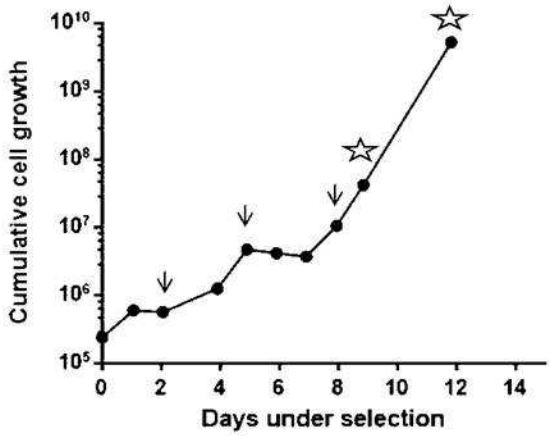

Figure 4.1: Screening for RH1 resistant determinants using a genome wide *T. brucei* RNAi library. The BSF *T. brucei* RNAi library (Alsford *et al*. 2012; Glover *et al*. 2015) was co-treated with tetracycline (1 µg ml^{-1}) to induce RNAi, and RH1 (30 nM) with the cumulative cell growth of the culture followed**.** The arrows correspond to culture dilution and addition of fresh RH1 (30 nM) and tetracycline (1 µg ml^{-1}). Genomic DNA (as indicated by stars) was extracted from parasites at days 9 and 12. The above data was collected by Dr S. Alsford, LSHTM.

Towards the end of the selection, at days 9 and 12, genomic DNA was extracted from the RH1 selected parasite population and used as template in a PCR-based low resolution screen. This screen was carried out in accordance to Baker *et al* (2011). To summarise this low resolution screen, the genomic DNA was used in a standard PCR reaction (30 cycles of 95ºc for 30s, 57ºc for 30s and 72ºc for 130s) containing the primers LIB2f and LIB2r (See Appendix 3). These primers are designed to amplify the fragment found in the RNAi construct. The PCR products were separated on a 1% agarose gel (Figure 4.2). The hits that are pulled out of a low resolution screen are those that yield the highest amounts of reads from the high throughput sequencing of the genomic DNA.

Analysis of the resultant amplification products identified one major fragment of ~1.1 kbp and a background non-descript smear. Sequence analysis of the major band and comparison against the reference genome database revealed that the RH1-

resistance-associated fragment mapped to a region that spanned the 5' untranslated/5' coding sequence of the type I nitroreductase (Tb*ntr*) gene (Gene ID: Tb927.7.7230 on TriTRypDB). This was not unexpected given that the encoded protein, TbNTR, had been previously associated with the activation of trypanocidal nitroheterocyclic-based prodrugs nifurtimox and benznidazole (Wilkinson *et al*. 2008; Baker *et al*. 2011; Hall *et al*. 2011; Hall & Wilkinson 2011) and been postulated to function as a NADH dependent quinone oxidoreductase (Wilkinson *et al*. 2008; Alsford *et al*. 2012; Hall *et al*. 2012).

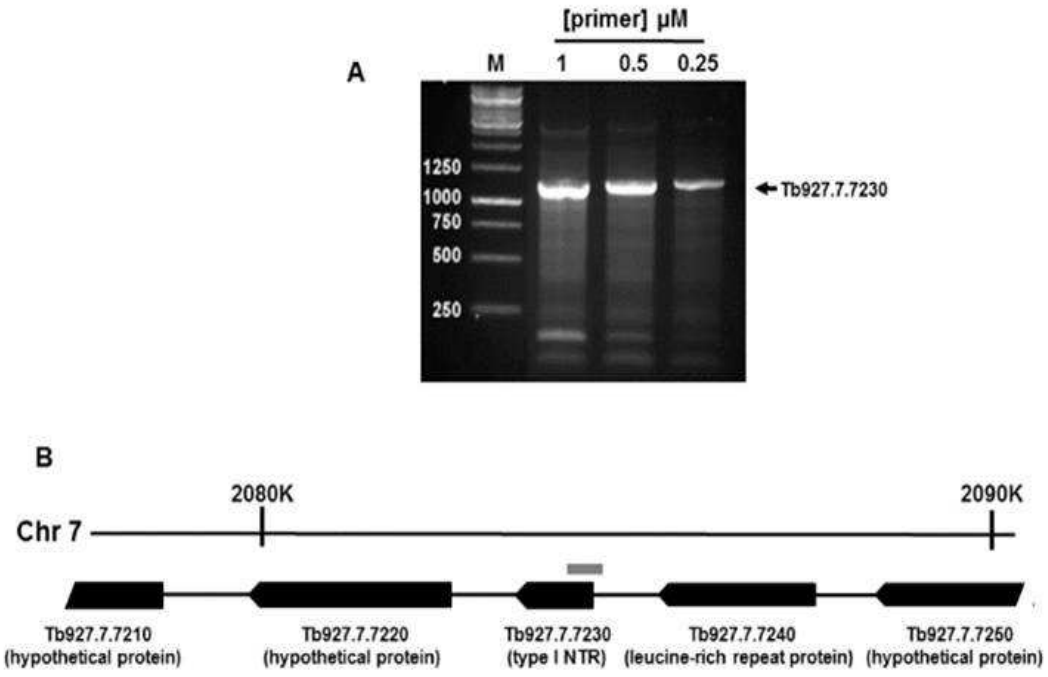

Figure 4.2: Identification of RH1 resistance determinants. (A) Amplification of the RNAi target from the RH1 screen using gDNA extracted on day 9 of the selection and different primer concentrations produced several bands with the major fragment mapping to the type I nitroreductase (Tb*ntr*) loci. M indicates a size marker in bp. (B) The position of the DNA fragment recovered from the RH1 RNAi screen, mapping to the Tb*ntr* loci is indicated by grey box.

In addition to facilitating the low resolution PCR screens, the extracted template genome DNA can also serve as starting material for a more in-depth analysis.Such analysiscan reveal other genes associated with conferring resistance towards the

selecting agent. For example the in-depth analysis of nifurtimox resistant library carried out by Alsford *et al* (2012) identified putative flavokinases which convert riboflavin to FMN, the cofactor for the nifurtimox prodrug activator NTR. This would involve the high throughput sequencing of the PCR products to generate any hits coupled with extensive bioinformatics used to map such hits against the reference genome sequence. Prior to conducting such a study the inducibility of the RNAi screen needs to be determined. The percentage inducibility effectively functions as a measure as to how much of the outgrowth observed for a given selection is actually due to the RNAi effect and not as a result of some other process such as selection of background mutations. This value can be readily calculated by firstly comparing the cumulative growth of non-induced (*i.e.* not undergoing RNAi) parasites grown in the presence of drug treatment against non-induced parasites grown in the absence of drug treatment (equation 4):

$$\text{Equation 4: } \frac{\text{non induced with drug treatment}}{\text{non induced with no drug treatment}}$$

Next, the cumulative growth of parasites induced to undergo RNAi grown in the presence of drug treatment is compared the cumulative growth of parasite induced to undergo RNAi grown in the absence of drug treatment (equation 5):

$$\text{Equation 5: } \frac{\text{induced with drug treatment}}{\text{induced with no drug treatment}}$$

Then, the two above equations are compared against each other and transformed by subtraction form 1 (equation 6);

$$\text{Equation 6: } \quad 1\text{-} \frac{\text{value of equation 4}}{\text{value of equation 5}}$$

For RH1 a % inducibility value of 12% was observed (Figure 4.3). This figure is low in comparison to most other selective challenged used against the RNAi library screen with compounds such as eflornithine and pentamidine yielding

inducibilityvalues >80% (Alsford *et al* 2012). However, for the nifurtimox screens reported by Alsford *et al* (2012) an inducibility value of <20% was recorded (Alsford *et al.* 2012). This value reflects how much of the observed phenotype is down to the effect of RNAi. Low values suggest that background mutations are responsible for the resistance rather than the effect of RNAi. One possible explanation for such low values could reflect a possible mode of action for RH1 and nifurtimox. Potentially both agents may promote the formation of mutations in the genome of the *T. brucei* RNAi library parasites such that these resultant mutants are resistant to the selective pressure producing the observed outgrowth.

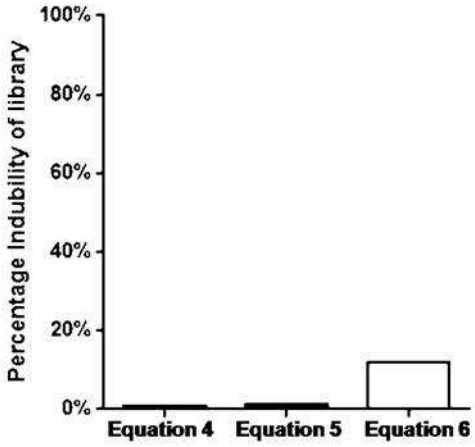

Figure 4.3: Inducibility of the RH1 resistance phenotype of the selected library. Data was collected by Dr S. Alsford, LSHTM.

4.2 Validating TbNTR as an activator of RH1

To conclusively demonstrate that TbNTR is the key activator of RH1 we evaluated the susceptibility of *T. brucei* cells engineered to express reduced levels of the encoding gene. Initially, we developed two DNA constructs that facilitate RNAi targeting the Tb*ntr* transcript. In one vector, based on p2T7^{TA}, formation of double strand RNA that drives the RNAi process is driven by two head to head promoters (see Chapter 6) (Wilkinson *et al*. 2003), while in the other, based on pRPa^{SL}, formation of double strand RNA is caused by

expression from a single promoter of repeat sequences from the target gene that form a stem loop structure (Alsford & Horn 2008). Despite it being documented that the TbNTR activity is essential for BSF *T. brucei* viability (Wilkinson *et al*. 2008), RNAi targeting the Tb*ntr* transcript using either system had no effect on parasite growth or on the susceptibility of the parasite to nifurtimox or RH1. To overcome this we used a *T. brucei* line (Tb*ntr*$^{+/-}$) where one of the Tb*ntr* alleles had been replaced with a puromycin resistance cassette (Wilkinson *et al*. 2008). When the susceptibility of these recombinant parasites towards RH1 was assessed the heterozygote cells displayed an IC_{50} approximately 2.5-fold greater than that observed towards wild type cells (Figure 4.4). Likewise, parallel studies involving nifurtimox displayed a similar result with the Tb*ntr*$^{+/-}$ line being more resistant to this 5-nitrofuran than controls (data not shown) and is in keeping with previous observations (Wilkinson *et al* 2008). This confirmed that reduction of Tb*ntr* expression through loss of one of the alleles encoding for TbNTR is sufficient to generate resistance to RH1.

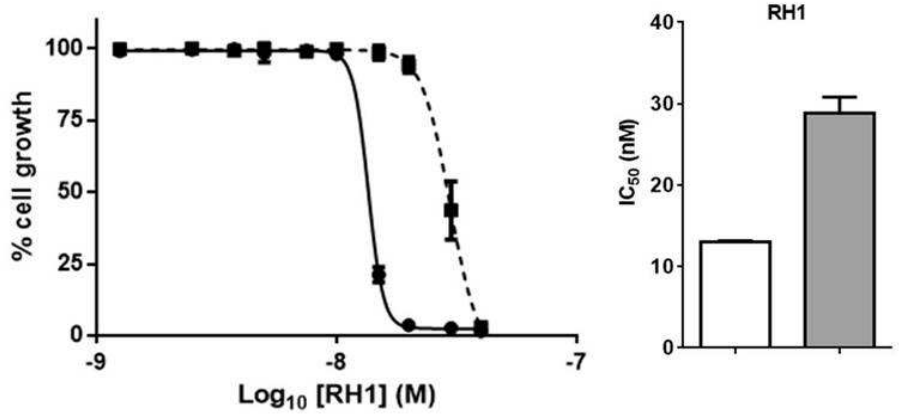

Figure 4.4: Susceptibility of *T. brucei* Tb*ntr* heterozygotes to RH1. (A) Dose response curve of wild type *T. brucei* (solid line) and parasites that are haploid for Tb*ntr* (dotted line) to RH1. (B) Susceptibility of wild type *T. brucei* (white bar) and TbNTR heterozygotes (grey bar) to RH1 as judged by the IC_{50} values (in nM). All data are means for experiments performed in quadruplicate ± standard deviation. The differences in susceptibility of wild type and TbNTR over expressing cells to RH1 was statistically significant (P <0.01), as assessed by Student's *t* test.

As reduction of TbNTR activity leads to RH1 resistance it is implicit that gain of function *via* over expression of the oxidoreductase should have the converse effect, generating cells that are more susceptible to the ABQ. To determine if this is the case, the sensitivity of a *T. brucei* line engineered to express elevated levels of the enzyme towards the quinone was evaluated (Wilkinson *et al*. 2008; Hall *et al*. 2011; Bot *et al*. 2013). This demonstrated that parasites over expressing Tb*ntr* were hypersensitive (approximately 4-fold) to this aziridinyl agent as compared to controls.

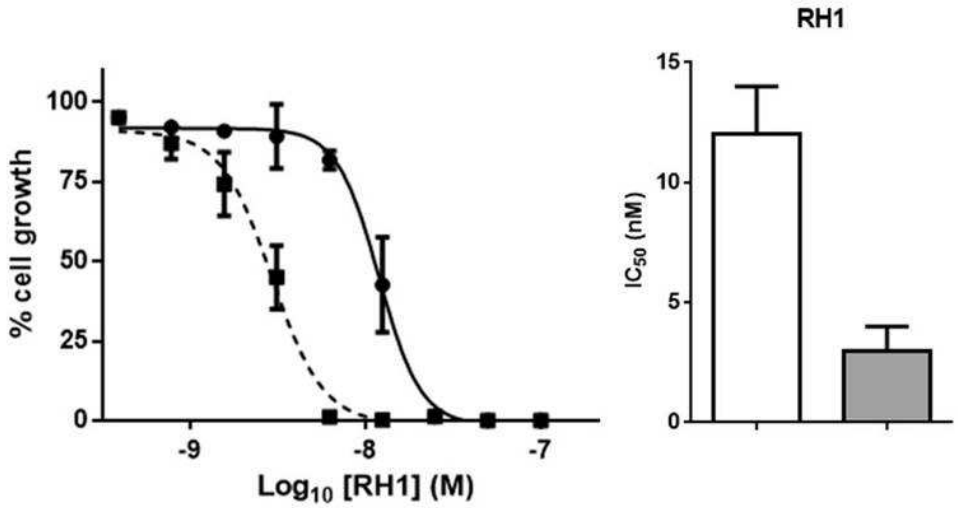

Figure 4.5: Susceptibility of *T. brucei* expressing elevated levels of TbNTR to RH1. (A). Dose response curve of wild type *T. brucei* (solid line) and parasites engineered to express elevated levels of TbNTR (dotted line) to RH1. (B). Susceptibility of wild type *T. brucei* (white bar) and TbNTR over expressing line (grey bar) to RH1 as judged by the IC_{50} values (in nM). All data are means for experiments performed in quadruplicate ± standard deviation. The differences in susceptibility of wild type and TbNTR over expressing cells to RH1 was statistically significant ($P < 0.01$), as assessed by Student's *t* test.

Together, the above functional genomic data clearly demonstrate that TbNTR is a key activator of RH1.

4.3 Does TbNTR activate other aziridinyl benzoquinones?

To determine whether TbNTR plays a role in activating other ABQs the susceptibility of the Tb*ntr* over expressing parasites towards a selected group of these compounds was tested (Figure 4.6; Table 4.1). Out of the additional compounds screened, six (DZQ, MeDZQ, **3**, **6**, **8** and TZQ) all showed the same hypersensitivity profile as RH1, being between 1.5 and 3.5-fold more susceptible to the aziridinyl agents than controls. Intriguingly, one compound (**22**), a tetra-aziridinyl ABQ, did not follow this pattern with the TbNTR over expressers exhibiting an IC_{50} equivalent to that observed against control cells.

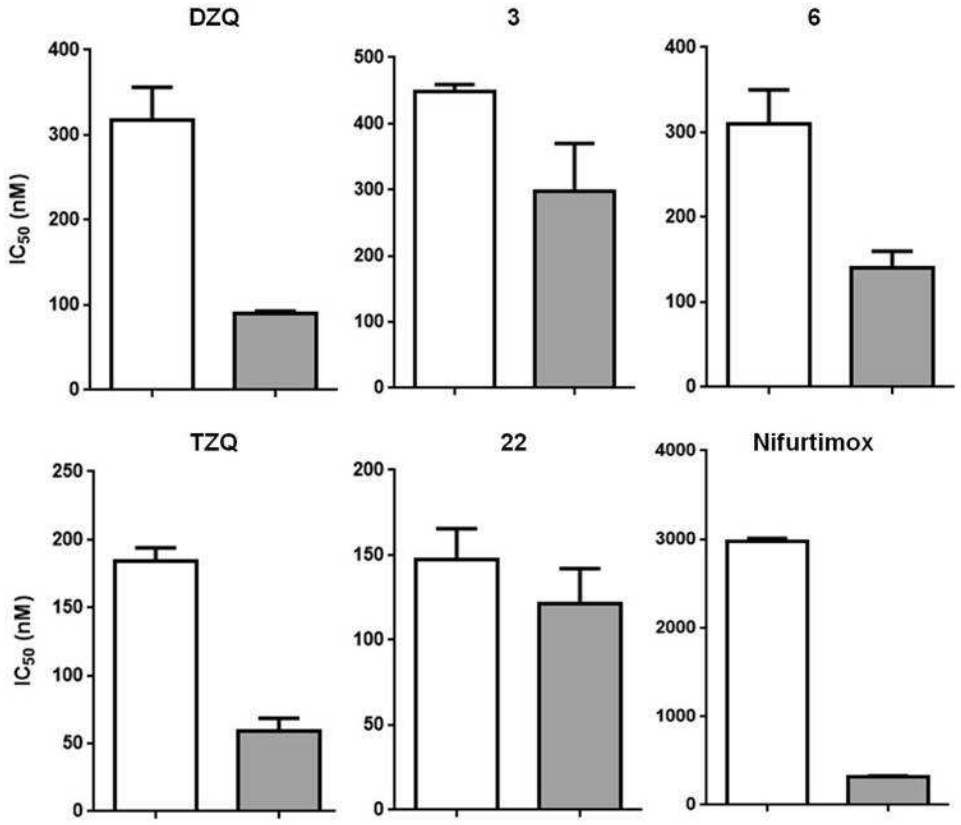

Figure 4.6: Susceptibility of *T. brucei* expressing elevated levels of TbNTR to ABQs. Dose response curves evaluating the sensitivity of wild type *T. brucei* (white bars) and parasites engineered to express elevated levels of TbNTR (grey bars) toward selected ABQs were plotted and the IC_{50} values (in nM) determined. Nifurtimox were used as control. All data are means for experiments performed in quadruplicate ± standard deviation. The differences in susceptibilities of control and TbNTR over expressing cells to all compounds except compound **22** was statistically significant (P <0.01), as assessed by Student's *t* test.

Compound	IC_{50} values (μM) ± standard deviation		Ratio
	control	over expressers	
Melarsoprol	3.750 ± 0.200	4.100 ± 0.500	0.9
Nifurtimox	2.980 ± 0.030	0.315 ± 0.015	9.5
DZQ (**1**)	0.318 ± 0.038	0.090 ± 0.003	3.5
3	0.449 ± 0.010	0.297 ± 0.073	1.5
RH1 (**5**)	0.012 ± 0.002	0.003 ± 0.001	4.0
6	0.310 ± 0.040	0.140 ± 0.020	2.2
8	0.670 ± 0.030	0.460 ± 0.010	1.5
TZQ (**21**)	0.184 ± 0.010	0.060 ±0.009	3.1
22	0.121 ± 0.021	0.148 ± 0.009	0.8

Table 4.1: The growth inhibitory effect of ABQ compounds towards *T. brucei* expressing elevated levels of TbNTR. Data represents the IC_{50} values of parasites expressing wild type and elevated levels of TbNTR. All values are means ± standard deviation of four independent experiments. The fold difference in IC_{50} values between the two treatments are given.

The above findings are further supported by *in vitro* studies where ABQs such as DZQ, MeDZQ, **3**, RH1, **6**, **8** and TZQ were shown to be substrates for purified recombinant TbNTR whereas **22** was not metabolised by parasite enzyme (Hall *et al* 2012). Therefore, based on our observations **22** is not activated by TbNTR.

4.3Assessing other aziridinyl benzoquinone activation mechanisms

The ABQs can undergo activation to form hydroquinone derivatives by two distinct pathways. As shown in figure 1.8, enzymes such as cytochrome P450 reductase (CPR) mediate the $1e^-$ reduction of the quinone to a semiquinone radical with the fate this reduction product dependent on oxygen levels. Under hypoxic conditions this radical can then undergo further reduction to the hydroquinone while in the presence of O_2, the semiquinone can undergo futile cycling to form $O_2^{\cdot-}$ and the parental quinone. In the second pathway, reduction of the quinone to the

hydroquinone occurs directly *via*a $2e^-$ reduction event as typified by NQO1. As TbNTR shares many biochemical characteristics with NQO1 it appears that the major ABQ trypanocidal mechanism for most compounds involves the second of the above pathways. However, to evaluate whether the anti-parasitic ABQs reported in Chapter 3 can undergo activation by the first pathway, the susceptibility of *T. brucei* lines engineered to express ectopic copies of the TbCPR isoforms 2 (TbCPR2) or 3 (TbCPR3) (Bot *et al*. 2013)to RH1, TZQ and **22** was evaluated (Figures 4.7). When using RH1 and TZQ, both TbCPR over expressing lines exhibited IC_{50}'s similar to that observed against control cells indicating that for these ABQs the $1e^-$ quinone reduction pathway plays no role in their trypanocidal activities. When the *T. brucei* line expressing elevated levels of TbCPR2 or TbCPR3 were tested against **22**, both recombinant lines were hypersensitive (>20-fold) to this tetra-aziridinyl agent than control cells.

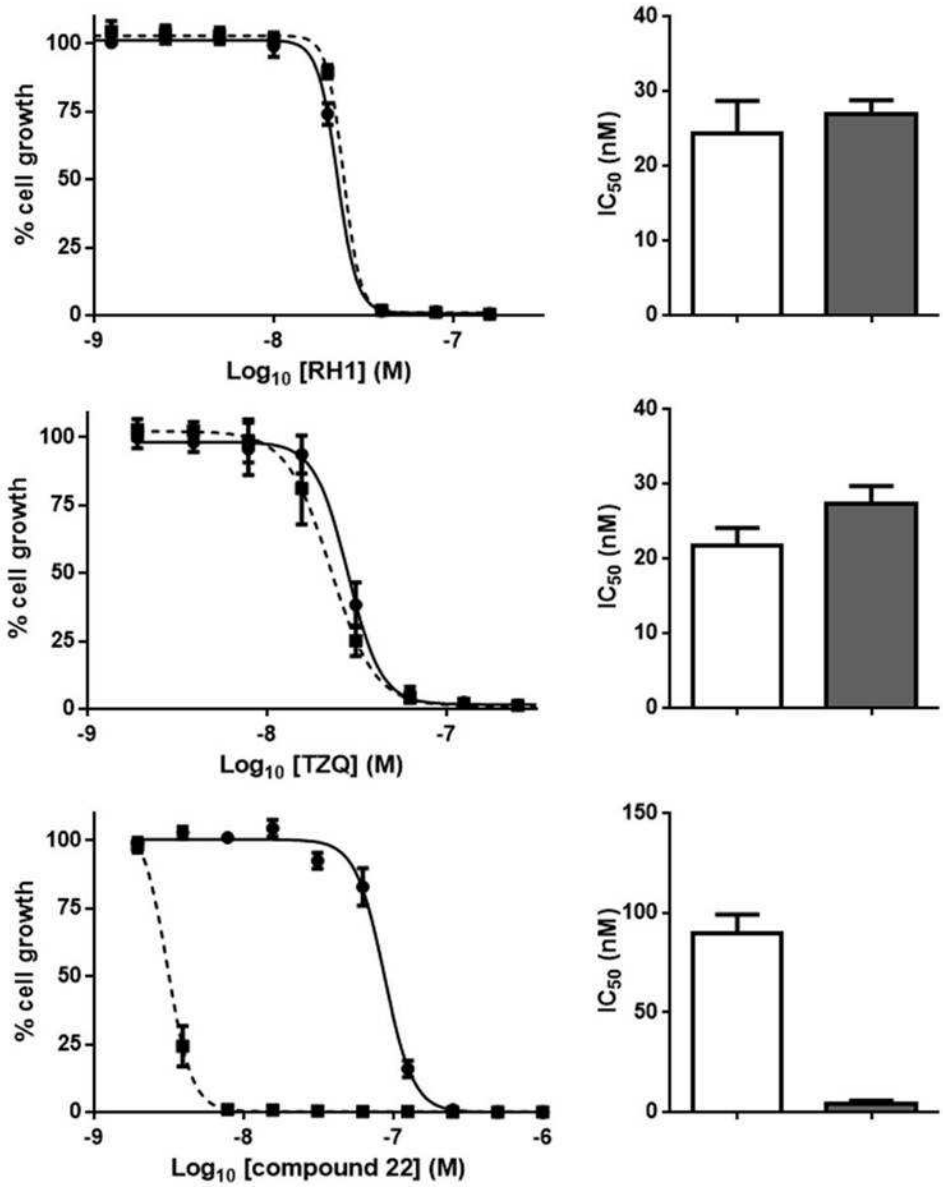

Figure 4.7: Susceptibility of *T. brucei* expressing elevated levels of TbCPR2 to ABQs. Panels on the left hand side show the dose response curve of wild type *T. brucei* (solid line) and parasites engineered to express elevated levels of TbCPR2 (dotted line) to RH1, TZQ and **22**.The panels on the right hand side show the susceptibility of wild type *T. brucei* (white bar) and TbCPR2 over expressing parasites (grey bar) to RH1, TZQ and **22** as judged by the IC_{50} values (in nM). All data are means for experiments performed in quadruplicate ± standard deviation. The differences in susceptibility of wild type and CRP2 over expressing cells to **22** was statistically significant ($P < 0.01$), as assessed by Student's *t* test.

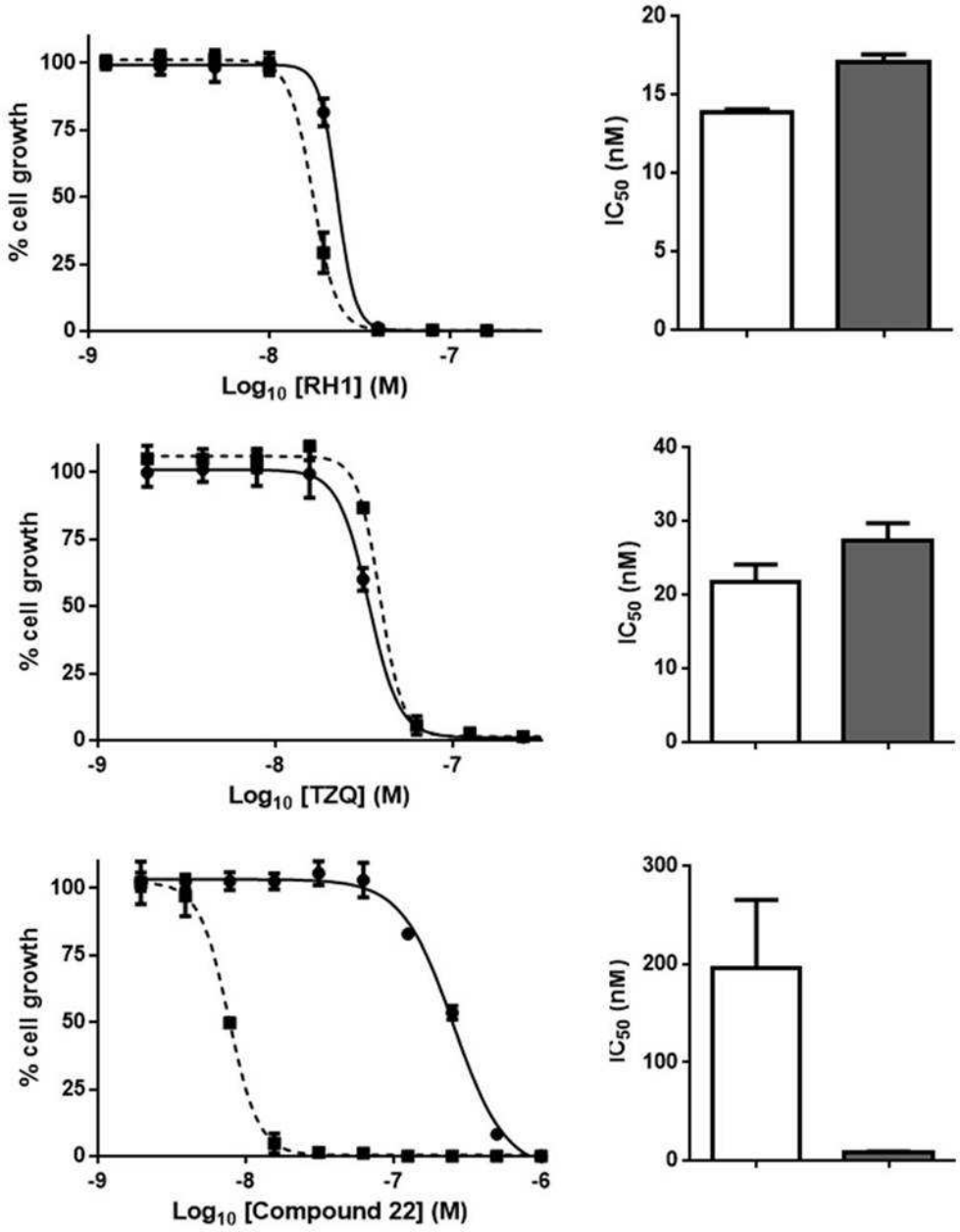

Figure 4.8: Susceptibility of *T. brucei* expressing elevated levels of TbCPR3 to ABQs. Panels on the left hand side show the dose response curve of wild type *T. brucei* (solid line) and parasites engineered to express elevated levels of TbCPR3 (dotted line) to RH1, TZQ and **22**.The panels on the right hand side show the susceptibility of wild type *T. brucei* (white bar) and TbCPR3over expressing parasites (grey bar) to RH1, TZQ and **22** as judged by the IC_{50} values (in nM). All data are means for experiments performed in quadruplicate ± standard deviation. The differences in susceptibility of control and TbCRP3 over expressing cells to **22** was statistically significant ($P < 0.01$), as assessed by Student's *t* test.

Based on the above observations, it appears that **22**, the only ABQ whose trypanocidal activity is not dependent on TbNTR, functions as a prodrug that undergoes activation *via* a mechanism in which the trypanosomal CPRs play a role. Whether other enzymes can catalyse this activity was not established here.

Chapter 4 summary

In this Chapter we have explored how the ABQs can mediate their cytotoxic effect against *T.brucei.* Specifically we have shown that:

1. Screening of the RNAi library using RH1 as selective agent determined that reduction in type I nitroreductase activity generates resistant parasites.
2. *T.brucei* Tb*ntr* heterozygote parasites are resistant to RH1.
3. *T. brucei* cells engineered to express an ectopic copy of Tb*ntr* are more susceptible to RH1 and most other ABQs tested, with compound **22** being the exception.
4. Compound **22**, a tetra aziridinyl ABQ, still functions as a prodrug and is activated by a reaction catalysed by cytochrome P450 reductase isoforms.

Chapter 5: Investigating the potential role of ABQs in promoting DNA damage in trypanosomes.

In most cells ABQs ultimately mediate their toxicity through the formation of ICLs that block processes which require separation of the DNA double helix (*i.e.* replication and transcription) (Berardini *et al*. 1993; Alley *et al*. 1994; Yan *et al*. 2008; Pierce *et al*. 2011). To combat the deleterious effects of such lesions several DNA repair pathways cooperate to recognise and then fix this damage. Of the enzymes that function in these systems, members of the so-called SNM1/Pso2p family are of particular interest as cells lacking this activity are specifically and highly susceptible to ICL-inducing agents including psoralen, cisplatin and mechlorethamine but not to any other forms of DNA damage (Henriques & Moustacchi 1980; D Bonatto *et al*. 2005). Recently, an SNM1 homologue has been identified in *T. brucei*(Sullivan *et al*. 2015). Gene disruption of the Tb*snm1* gene has revealed that this activity was non-essential to the medically relevant *T. brucei* life cycle stage although null mutant cells were more susceptible than wild type to bi- and tri-functional DNA alkylating agents, a phenotype that could be readily complemented by ectopic expression of Tb*snm1*. Here, using *T. brucei* lines expressing altered levels of Tb*snm1* we evaluated whether the trypanocidal ABQs identified in Chapter 3 mediate their anti-parasitic activities by promoting DNA damage following NTR or CPR activation.

5.1 Susceptibility of *T. brucei* expressing altered levels of Tb*snm1* to aziridinyl benzoquinones.

Functional studies aimed at investigating the role Tb*snm1* plays in *T. brucei* resulted in a series of parasites lines engineered to express different levels of this DNA repair

enzyme (Sullivan *et al*. 2015). As part of the characterisation of these lines we conducted hybridisation and PCR-based techniques to confirm the nature of the TbSNM1 null mutant background: Southern hybridisation confirmed that both copies of the *Tbsnm1* had been successfully disrupted in the parasite genome while RT-PCR and qPCR showed that null mutant cells were not expressing a full length Tb*snm1* mRNA transcript (data not shown).

To evaluate whether deletion of both copies of Tb*snm1* from the *T. brucei* genome altered the cells sensitivity to the ABQs null mutant trypanosomes were grown in the presence of DZQ, RH1, TZQ or **22** and the IC_{50} values for each compound determined (Figure 5.1; Table 5.1). For all agents tested null cells were ~3 to 7-fold more susceptible to the ABQ under study than control parasites analysed in parallel. When these growth assays were extended to look at the trypanocidal agents nifurtimox anddifluoromethylornithine (DFMO), no difference was observed in the IC_{50}'s exhibited by the engineered and control lines.

Compound	**IC_{50} values (µM) ± standard deviation**		**Ratio**
	Wild Type	**Tb*snm1*$^{-/-}$**	
DZQ	0.157 ± 0.023	0.043 ± 0.002	3.7
RH1	0.015 ± 0.001	0.005 ± 0.001	3.0
TZQ	0.202 ± 0.006	0.076 ± 0.004	2.7
22	0.138 ± 0.025	0.021 ± 0.005	6.6
DFMO	27.500 ± 0.108	27.100 ± 0.850	1.0
Nifurtimox[a]	2.850 ± 0.020	2.250 ± 0.090	0.8

Table 5.1: Susceptibility of *T. brucei* lines to ABQ compounds. Data represents the IC_{50} values in µM of *T. brucei* (wild type) and *T. brucei* Tb*snm1*$^{-/-}$ null mutants (Tb*snm1*$^{-/-}$) to selected ABQ compounds. All values are means ± standard deviation of four independent experiments. The fold difference in IC_{50} values between the two treatments are given. The differences in susceptibility of wild type and Tb*snm1*$^{-/-}$

lines to DZQ, RH1, TZQ or **22** was statisticallysignificant ($P < 0.01$), as assessed by Student's *t* test.

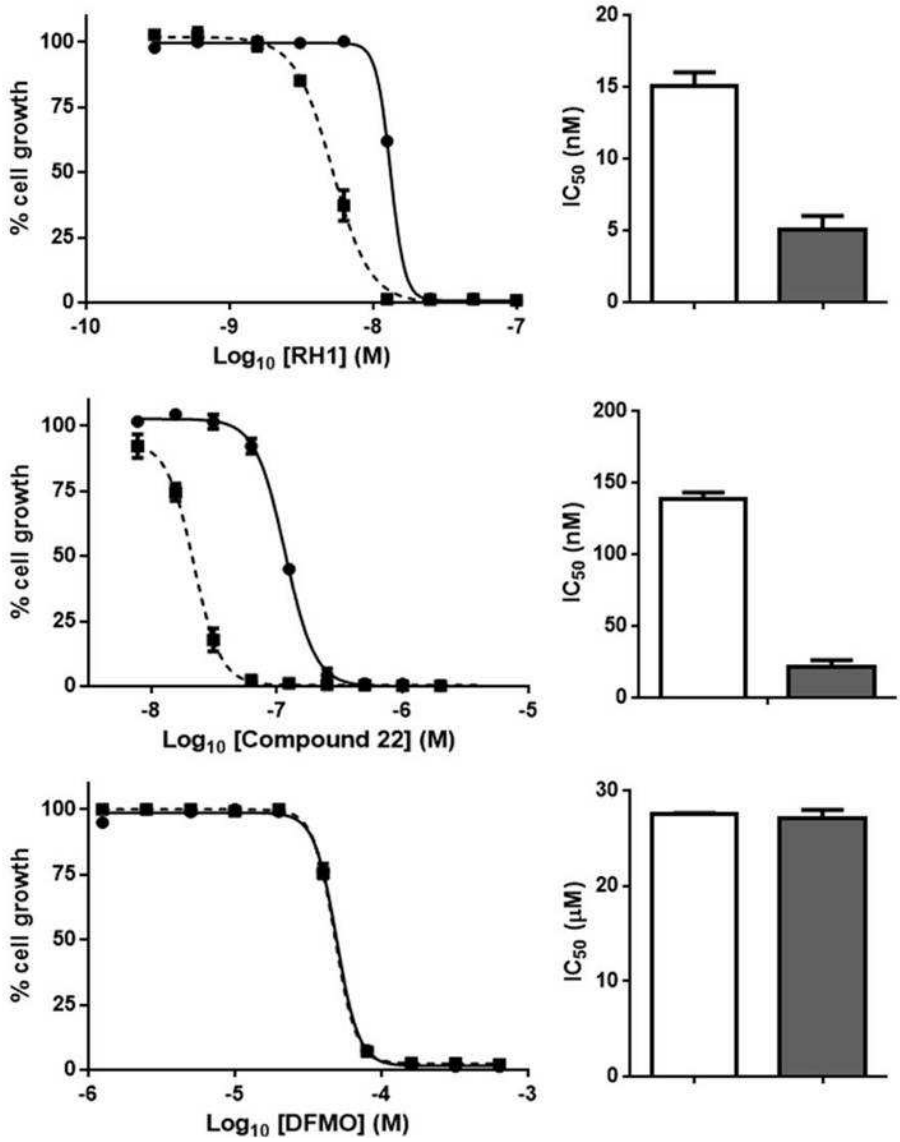

Figure 5.1: Susceptibility of *T. brucei* Tb*snm1*$^{-/-}$ null mutant cells to ABQs. Panels on the left show the dose response curves of wild type *T. brucei* (solid line) and Tb*snm1*$^{-/-}$ null mutant (dotted line) parasites to RH1, **22** and DFMO. The panels on the right show the susceptibility of wild type *T. brucei* (white bar) and Tb*snm1*$^{-/-}$ null mutant (grey bar) parasites to RH1, **22** and DFMO as judged by the IC_{50} values (in nM or µM). All data are means for experiments performed in quadruplicate ± standard deviation. The differences in susceptibility of wild type and Tb*snm1*$^{-/-}$ null mutants to RH1 and **22** was statistically significant ($P < 0.01$), as assessed by Student's *t* test.

To conclusively demonstrate that the above altered susceptibility phenotype was solely due to lack of TbSNM1 activity a complementation strategy was used. In

these experiments a vector targeted to one of the parasite's tubulin arrays and that facilitates constitutive expression of an ectopic copy of Tb*snm1* was introduced into null mutant and wild type trypanosomes. Southern hybridisation and PCR approaches were used to demonstrate integration of the ectopic Tb*snm1* into a tubulin array and gene expression (data not shown).

The susceptibility of the null mutant cells expressing an ectopic copy of Tb*snm1* towards DZQ, RH1, TZQ or **22** was then evaluated (Figure 5.2; Table 5.2). When the sensitivity of the complemented line to all four ABQs was tested the resultant dose response curves and IC_{50} values were distinct from those obtained using TbSNM1 null mutant cells and were similar to the plots and values observed using wild type parasites and wild type *T. brucei* engineered to express elevated levels of TbSNM1.

Compound	**IC_{50} values (μM) ± standard deviation**			
	wild type	**Tb*snm1*$^{-/-}$**	**Tb*snm1*$^{-/-}$ Tb*snm1*^{RV}**	**Tb*snm1*^{RV}**
DZQ	0.157 ± 0.023	0.043 ± 0.002	0.204 ± 0.022	0.206 ± 0.017
RH1	0.019 ± 0.001	0.005 ± 0.001	0.012 ± 0.001	0.011 ± 0.001
TZQ	0.253 ± 0.033	0.046 ± 0.001	0.376 ± 0.006	0.300 ± 0.023
22	0.091 ± 0.008	0.012 ± 0.001	0.069 ± 0.007	0.056 ± 0.007
DFMO	24.150 ± 3.940	24.240 ± 6.710	26.960 ± 1.400	25.410 ± 6.440

Table 5.2: Susceptibility of *T. brucei* lines expressing altered levels of Tb*snm1* to ABQ compounds. Data represents the IC_{50} values in μM of *T. brucei* wild type, Tb*snm1*$^{-/-}$ null mutants (Tb*snm1*$^{-/-}$), Tb*snm1*$^{-/-}$ expressing an ectopic copy of Tb*snm1* (Tb*snm1*$^{-/-}$ Tb*snm1*^{RV}) and *T. brucei* wild type expressing elevated levels of Tb*snm1* (Tb*snm1*^{RV}) to selected ABQs. All values are means ± standard deviation of four independent experiments. The fold difference in IC_{50} values between the two treatments are given. The differences in susceptibility of wild type and Tb*snm1*$^{-/-}$ lines to DZQ, RH1, TZQ or **22** was statistically significant ($P < 0.01$), as assessed by Student's *t* test. Ratios are shown in Appendix 3.

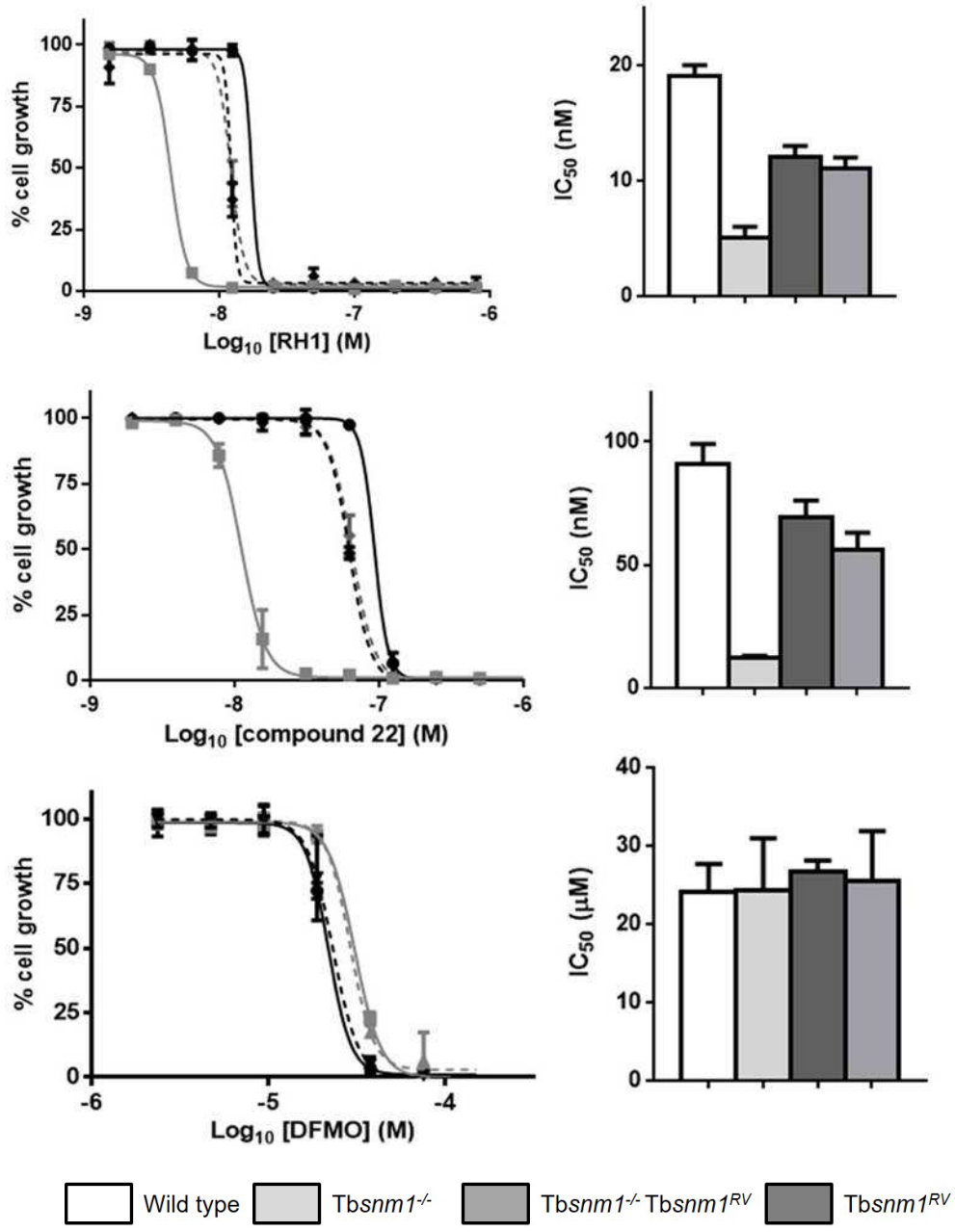

Figure 5.2: Susceptibility of *T. brucei* lines expressing altered levels of Tb*snm1* to ABQs. Panels on the left hand side show the dose response curve of wild type *T. brucei* (black solid line), Tb*snm1*$^{-/-}$ null mutants (grey solid line), Tb*snm1*$^{-/-}$ expressing an ectopic copy of Tb*snm1* (grey dashed line) and *T. brucei* wild type expressing elevated levels of Tb*snm1* (black dashed line) to RH1, **22** and DFMO. The panels on the right hand side show the susceptibility of wild type *T. brucei* (white bar), Tb*snm1*$^{-/-}$ null mutants (light grey bar), Tb*snm1*$^{-/-}$ expressing an ectopic copy of Tb*snm1* dark (grey bar) and *T. brucei* wild type expressing elevated levels of Tb*snm1* (dark grey bar) to RH1, **22** and DFMO as judged by the IC_{50} values (in nM or µM). All data are means for experiments performed in quadruplicate ± standard deviation.

The above data clearly shows that DZQ, RH1, TZQ and **22** all promote a form of DNA damage, which by analogy to other organisms is through the formation of ICLs, in the T. *brucei* genome with TbSNM1 playing a key role in the repair of such lesions.

5.2 Linking aziridinyl benzoquinone activation with DNA damage

To establish whether there was a link between activation of the trypanocidal aziridinyl benzoquinones and TbSNM1-mediated DNA damage pathways both copies of the Tb*snm1* gene were deleted from the genome of puromycin sensitive *T.brucei* parasites previously engineered to inducibly overexpress carboxyl terminal tagged ectopic copies of Tb*ntr*, Tb*cpr2* or Tb*cpr3*(Wilkinson *et al*. 2008; Hall *et al*. 2011). Using a combination of Southern hybridisation, comparative C_T analysis of the qPCR data and western blot we confirmed that: 1. the two *Tbsnm1* alleles had been successfully disrupted in the genome of the final recombinant lines, 2. the RNA transcripts of Tb*ntr*, Tb*cpr2* or Tb*cpr3* were ~13-, ~3- and ~6-fold higher, respectively, in the final recombinant lines than in wild type cells, and 3. the epitope tagged version of TbNTR, TbCPR2 or TbCPR3 were expressed within the final recombinant parasites (data not shown).

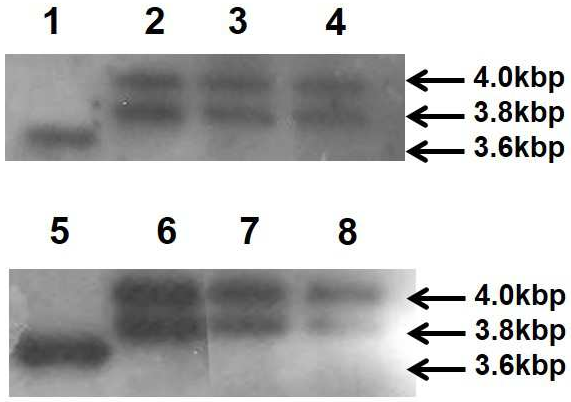

Figure 5.3: Southern hybridisation of *Mlu1* digested genomic DNA extracted from TbSNM1 samples. Lanes1 and 5: Wild type 221, Lanes 2 and 6: Tb*snm1*$^{-/-}$, Lanes 3 and 4: Tb*snm1*$^{-/-}$ Tb*ntr,* Lane 7:Tb*snm1*$^{-/-}$ Tb*cpr2 and* Lane 8: Tb*snm1*$^{-/-}$ Tb*cpr3.* Autoradiographs of samples hybirdized with the 3' UTR region of TbSNM1 resulting in two fragments corresponding to the differences in fragment size after the addition of a puromycin and blasticidin resistance cassette.

The susceptibility of *snm1* null trypanosomes expressing elevated levels of TbNTRtowards RH1 and TZQ was measured. Likewise, trypanosomes expressing elevated levels of TbCPR2 or 3 in the same background were challenged against **22**to establish a link between prodrug activation and Tb*snm1*-mediated DNA repair pathways.

When TbSNM1 null mutant parasites or cells engineered to just express an ectopic copy of Tb*ntr* were treated with RH1 and TZQ an increased susceptibility when compared against wild type *T. brucei* was observed (Figure 5.4; Table 5.3): Tb*snm1*$^{-/-}$ cells and *T. brucei* over expressing Tb*ntr* were 3.0- and 5.0-fold more susceptible to RH1, respectively, with a 2.7- and 3.4-fold increase in sensitivity noted towards TZQ. For TbSNM1 null parasites induced to express an ectopic copy of Tb*ntr* this increase in potency was magnified further with these cells showing a 15.0-fold increase in susceptibility towards both compounds, when as compared against wild

type. This alteration was specific to the ABQs as all lines tested exhibited equivalent susceptibilities to DFMO.

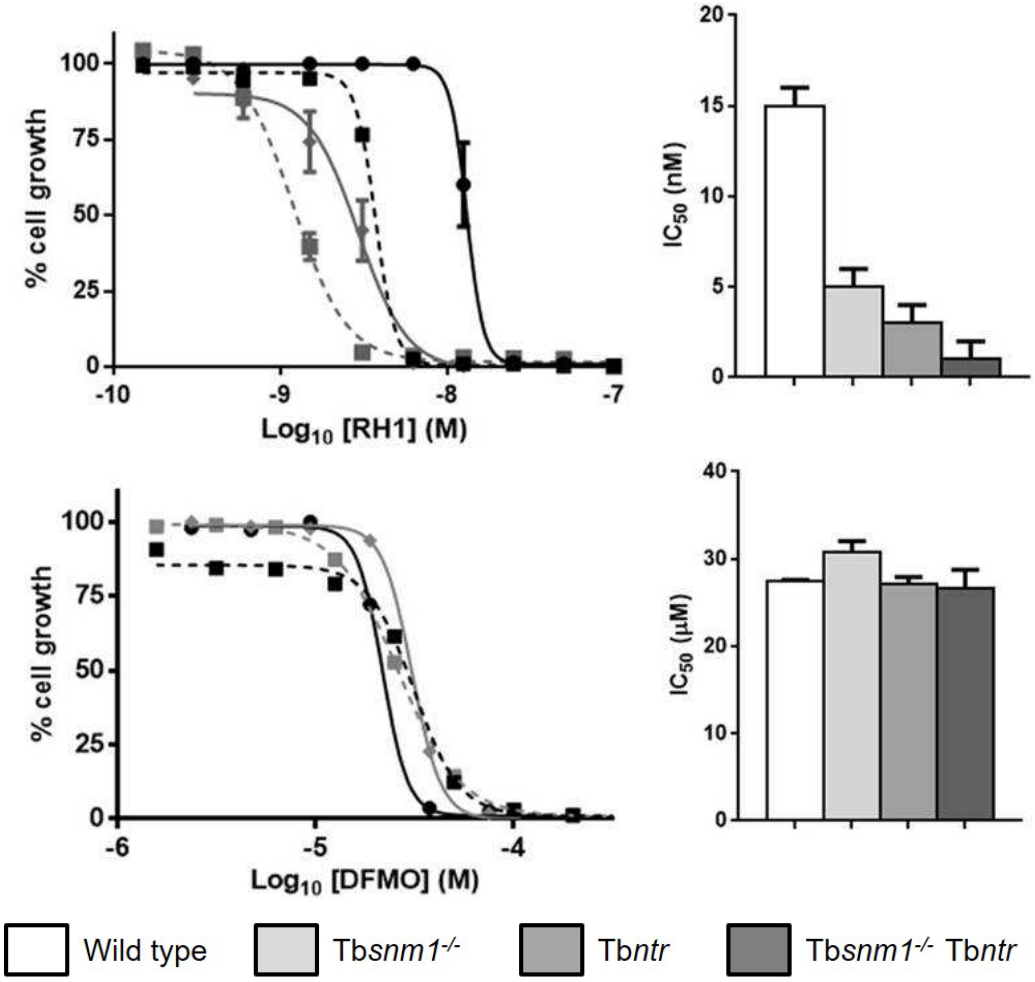

Figure 5.4:Susceptibility of *T. brucei snm1*$^{-/-}$ null mutants over expressing TbNTR to RH1. Panels on the left hand side show the dose response curve of wild type *T. brucei* (black solid line), Tb*snm1*$^{-/-}$ null mutants (black dotted line), *T. brucei* expressing elevated levels of Tb*ntr* (grey solid line) and Tb*snm1*$^{-/-}$ null mutants expressing elevated levels of Tb*ntr* (grey dotted line) to RH1 and DFMO. The panels on the right hand side show the susceptibility of wild type *T. brucei* (white bar), Tb*snm1*$^{-/-}$ null mutants (light grey bar), *T. brucei* expressing an ectopic copy of Tb*ntr* dark (grey bar) and Tb*snm1*$^{-/-}$ null mutants expressing elevated levels of Tb*ntr* (dark grey bar) to RH1and DFMO as judged by the IC_{50} values. All data are means for experiments performed in quadruplicate ± standard deviation.

Compound	IC_{50} values (μM) ± standard deviation			
	Wild Type	**Tb*ntr***	**Tbs*nm1*$^{-/-}$**	**Tbs*nm1*$^{-/-}$ Tb*ntr***
RH1	0.015 ± 0.001	0.003 ± 0.001	0.005 ± 0.001	0.001 ± 0.001
TZQ	0.202 ± 0.006	0.060 ± 0.009	0.076 ± 0.004	0.013 ± 0.001
DFMO[a]	27.500 ± 0.108	30.720 ± 1.330	27.100 ± 0.850	26.710 ± 2.060

Table 5.3: The growth inhibitory effects of selected ABQ compounds on *T. brucei snm1*$^{-/-}$ null mutants over expressing TbNTR. Data represents the IC_{50} values in μM of *T. brucei* wild type, *T. brucei* expressing elevated levels of TbNTR (Tb*ntr*), TbSNM1 null mutants (Tb*snm1*$^{-/-}$) and TbSNM1 null mutants expressing an ectopic copy of Tb*ntr* (Tb*snm1*$^{-/-}$ Tb*ntr*) to RH1, TZQ and DFMO. All values are means ± standard deviation of four independent experiments. [a] valve for DFMO taken from Sullivan *et al* (2015).Flow diagrams and ratios can be found in Appendix 4.

When these studies were extended to investigate the susceptibility of TbSNM1 null mutant parasites engineered to express an ectopic copy of Tb*cpr2* or Tb*cpr3* towards **22**a similar effect was observed (Figures 5.5 and 5.6; Tables 5.4 and 5.5). For the Tb*snm1*$^{-/-}$ cells and *T. brucei* over expressing Tb*cpr2* or Tb*cpr3*, all three lines displayed a ~7-fold increase in susceptible towards this ABQ. This fold difference increased in TbSNM1 null parasites induced to express an ectopic copy of Tb*cpr2* or Tb*cpr3* such that these cells showed a 12.5- and 13.8-fold increase in susceptibility, respectively, when as compared against wild type. Again, this alteration was specific to this particular ABQs as all lines tested exhibited equivalent susceptibilities to DFMO.

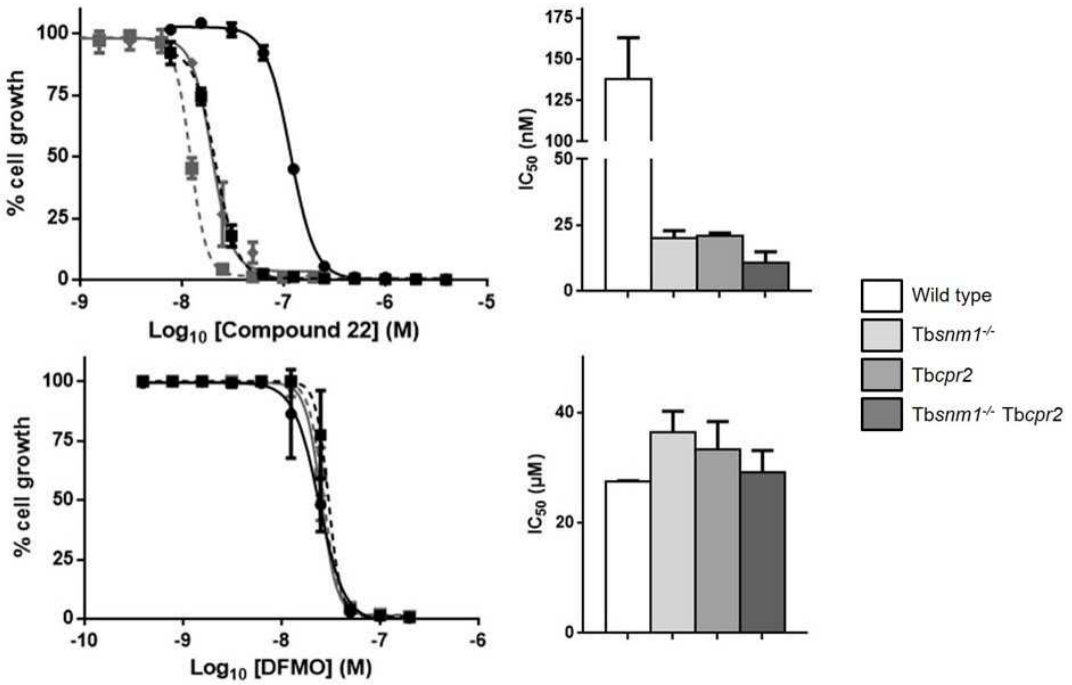

Figure 5.5: Susceptibility of *T. brucei snm1*$^{-/-}$ null mutants over expressing TbCPR2 to 22. Panels on the left hand side show the dose response curve of wild type *T. brucei* (black solid line), Tb*snm1*$^{-/-}$ null mutants (black dotted line), *T. brucei* expressing elevated levels of Tb*cpr2* (grey solid line) and Tb*snm1*$^{-/-}$ null mutants expressing elevated levels of Tb*cpr2* (grey dotted line) to **22** and DFMO. The panels on the right hand side show the susceptibility of wild type *T. brucei* (white bar), Tb*snm1*$^{-/-}$ null mutants (light grey bar), *T. brucei* expressing an ectopic copy of Tb*cpr2* dark (grey bar) and Tb*snm1*$^{-/-}$ null mutants expressing elevated levels of Tb*cpr2* (dark grey bar) to these compounds and DFMO as judged by the IC_{50} values. All data are means for experiments performed in quadruplicate ± standard deviation.

Compound	IC_{50} values (µM) ± standard deviation			
	wild type	Tb*cpr2*	Tb*snm1*$^{-/-}$	Tb*snm1*$^{-/-}$ Tb*cpr2*
22	0.138 ± 0.025	0.020 ± 0.003	0.021 ± 0.001	0.011 ± 0.004
DFMO	27.500 ± 0.108	33.250 ± 5.123	27.100 ± 0.850	29.250 ± 3.862

Table 5.4: The growth inhibitory effects of selected ABQ compounds on *T. brucei snm1*$^{-/-}$ null mutants over expressing TbCPR2. Data represents the IC_{50} values in µM of *T. brucei* wild type, *T. brucei* expressing elevated levels of TbCPR2 (Tb*cpr2*), TbSNM1 null mutants (Tb*snm1*$^{-/-}$) and TbSNM1 null mutants expressing an ectopic copy of Tb*cpr2* (Tb*snm1*$^{-/-}$ Tb*cpr2*) to **22** and DFMO. All values are means ± standard deviation of four independent experiments. . Flow diagrams and ratios can be found in Appendix 4.

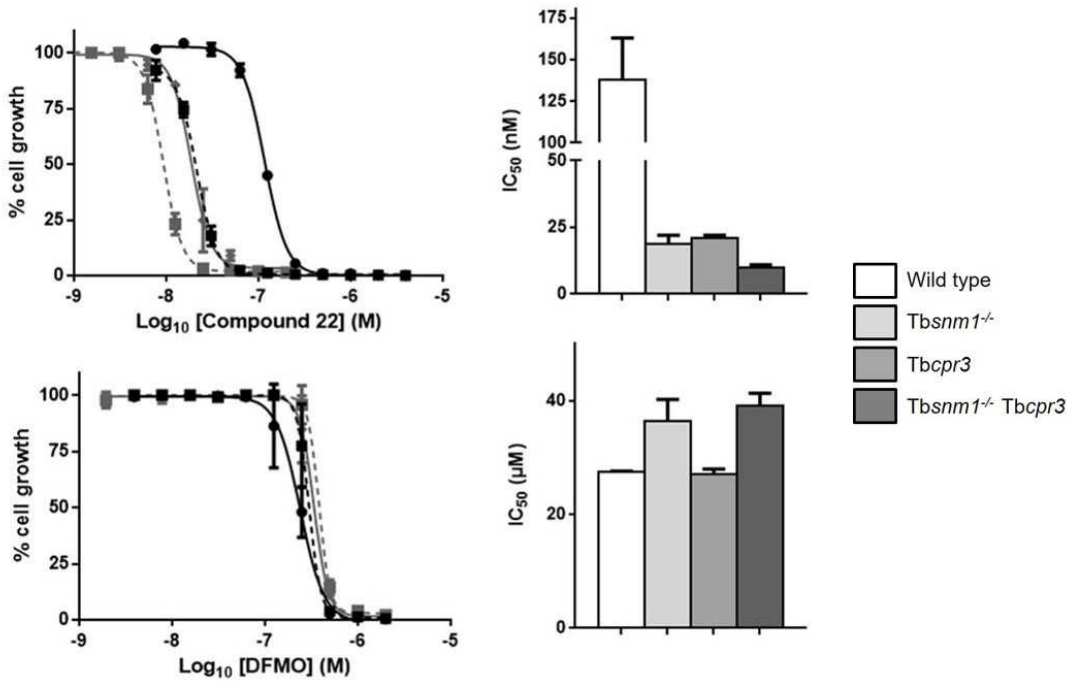

Figure 5.6: Susceptibility of *T. brucei snm1*$^{-/-}$ null mutants over expressing TbCPR3 to 22. Panels on the left hand side show the dose response curve of wild type *T. brucei* (black solid line), Tb*snm1*$^{-/-}$ null mutants (black dotted line), *T. brucei* expressing elevated levels of Tb*cpr3* (grey solid line) and Tb*snm1*$^{-/-}$ null mutants expressing elevated levels of Tb*cpr3* (grey dotted line) to **22** and DFMO. The panels on the right hand side show the susceptibility of wild type *T. brucei* (white bar), Tb*snm1*$^{-/-}$ null mutants (light grey bar), *T. brucei* expressing an ectopic copy of Tb*cpr3* dark (grey bar) and Tb*snm1*$^{-/-}$ null mutants expressing elevated levels of Tb*cpr3* (dark grey bar) to these compounds and DFMO as judged by the IC_{50} values. All data are means for experiments performed in quadruplicate ± standard deviation.

Compound	IC_{50} values (µM) ± standard deviation			
	wild type	**Tb*cpr3***	**Tb*snm1*$^{-/-}$**	**Tb*snm1*$^{-/-}$ Tb*cpr3***
22	0.138 ± 0.025	0.019 ± 0.003	0.021 ± 0.001	0.010 ± 0.001
DFMO	27.500 ± 0.108	36.500 ± 3.697	27.100 ± 0.850	39.125 ± 2.170

Table 5.5: The growth inhibitory effects of selected ABQ compounds on *T. brucei snm1*$^{-/-}$ null mutants over expressing TbCPR3. Data represents the IC_{50} values in µM of *T. brucei* wild type, *T. brucei* expressing elevated levels of TbCPR3 (Tb*cpr3*), TbSNM1 null mutants (Tb*snm1*$^{-/-}$) and TbSNM1 null mutants expressing an ectopic copy of Tb*cpr3* (Tb*snm1*$^{-/-}$ Tb*cpr3*) to **22** and DFMO. All values are means ± standard deviation of four independent experiments. Flow diagrams and ratios can be found in Appendix 4.

Here, we have explored the effect of ABQ compounds on parasites null in the DNA repair enzyme Tb*snm1*. We observe a 3.0 and 2.7 fold increase in susceptibility of these parasites when compared to wild type. We have expanded ours studies to investigate the effect of the introducing the quinone prodrug activators (*ntr*, *cypr2*, *cypr3*) into this cell line. Parasites null in repair enzyme and expressing ectopic copies of the activators are fivefold more sensitive than the *snm1* null parasites. We can therefore conclude that once the quinone based compound is activated, the activated moiety goes onto cause DNA damage through the formation of ICLs.

Concluding points of Chapter 5

In this Chapter we have explored how the ABQs can mediate their cytotoxic effect in the parasite *T. brucei.* From this we have demonstrated that:

1. ABQ compounds mediate DNA damage and cells null in the DNA repair protein *snm1*display a 2-6 fold increase in susceptibility,
2. The Tb*snm1* phenotype can be rescued using an ectopic copy of Tb*snm1*. Two of the four screened ABQ compounds screened against these lines show complete restoration of the phenotype and resistance whereas two ABQ compounds only showed a partial restoration of the Tb*snm1* phenotype.
3. When the Tb*snm1* gene is deleted from the cell line expressing increased amounts of the quinone reductases (Tb*ntr*/Tb*cypr2*/Tb*cypr3*), the cells become between two and five fold more sensitive to ABQ compounds.

Figure 5.7: Flow diagrams to summarise the susceptibility of *T. brucei* lines discussed in this chapter. IC_{50} values± standard deviation for wild type, *snm1*$^{-/-}$ null mutants, NTR/CPR2/CPR3 overexpressing lines and NTR/CPR2/CPR3 overexpressing lines in a *snm1*$^{-/-}$ null background. These values can be found in Tables 5.3, 5.4 and 5.5 as well as Figures 5.4, 5.5 and 5.6.

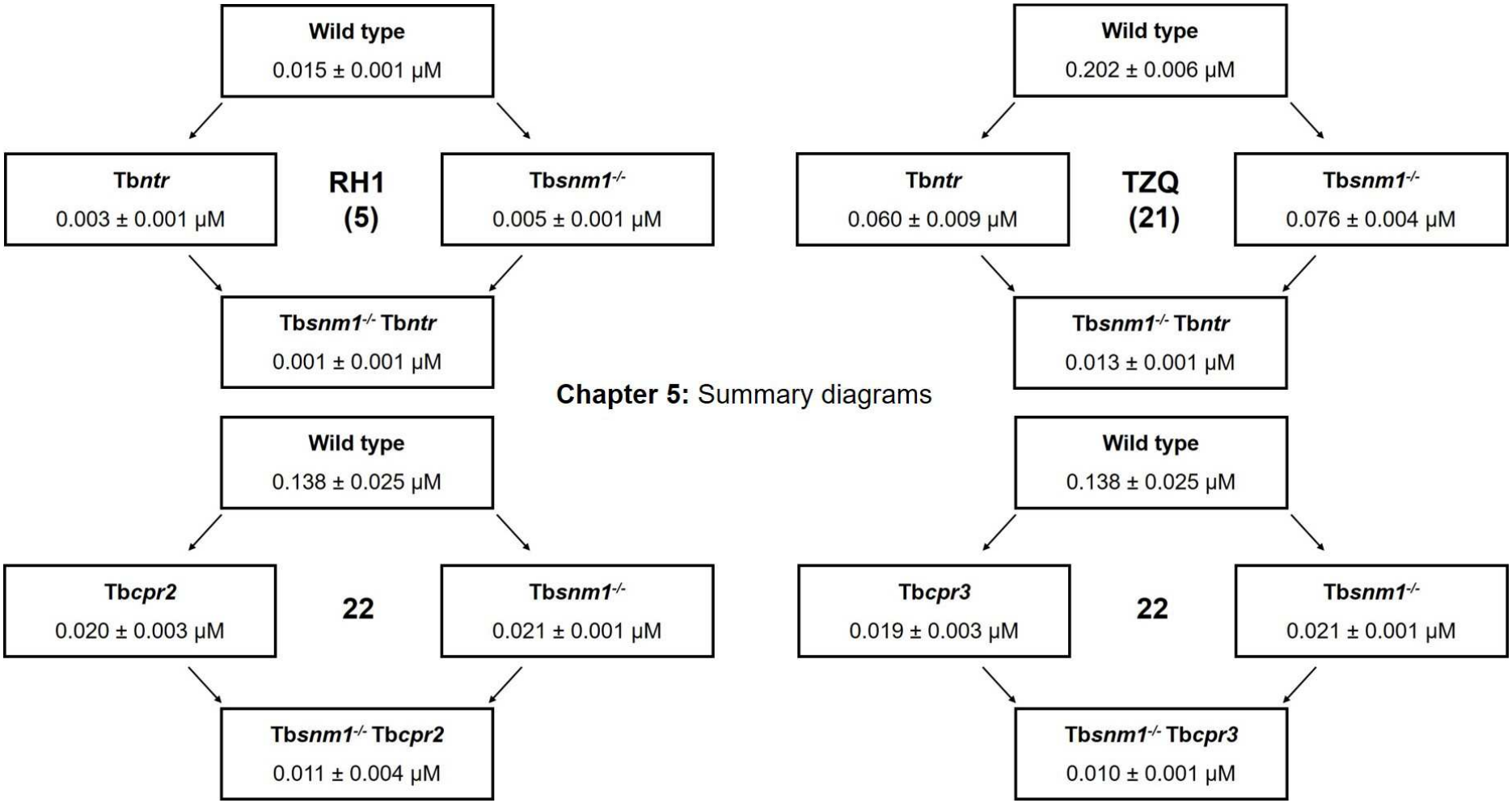

Chapter 6: Unravelling the mechanism RH1 resistance

Selection of trypanosomes lines that display resistance to clinically used trypanosomal therapies has been extensively used to provide information as to how a given agent mediates its cytotoxic effects (Carter & Fairlamb, 1993; Berger *et al* 1995; Wilkinson *et al*. 2008; Vincent *et al*. 2010; Sokolova *et al* 2010). Here we take a non-bias approach to select *T. brucei* cells that display resistance to RH1, the archetypal ABQ. As described in Chapter 3, RH1 is active against all three of the parasites studied in this thesis generating IC_{50} values of <100 nM. The IC_{50} values towards bloodstream form *T. brucei*, *T. cruzi* epimastigotes and *L. major* promastigotes are 19, 3 and 68 nM, respectively. The data presented in this section complements the observations previously outlined in Chapter 4.

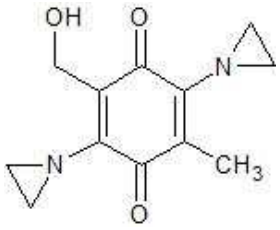

Figure 6.1: Structure of RH1

6.1 Selection of RH1 resistant *T. brucei*

To further investigate its mechanism of action we continuously cultured BSF *T. brucei* in the presence of RH1 to generate cells that display resistance to this ABQ. In preliminary selections performed in triplicate, *T. brucei* cultures containing 1 x 10^4 cells ml^{-1} were treated with RH1 at its wild type IC_{50} level (20 nM) and cell growth monitored. When the parasite density approached 1 x 10^6 cells ml^{-1}, the culture was diluted to 1 x 10^4 cells ml^{-1} in medium containing fresh RH1 (20 nM). In these initial screens, between 10 and 20 days into the selection process, the cell

numbers crashed such that no viable cells were visible under light microscopy (data not shown) and when cultures were incubated further showed no signs parasite growth were observed. From this we concluded that the exposure of the cultures to IC_{50} levels of RH1 generates a trypanocidal effect that the parasite is unable to recover from.

To overcome this a second selection protocol based on that reported by Vincent and colleagues (2010) whilst obtaining eflornithine resistant *T. brucei*, was followed. In these experiments, *T. brucei* cultures seeded at 1 x 10^4 cells ml^{-1} were initially treated with an amount of RH1 roughly equivalent to the concentration that inhibits parasite growth by 10% (5 nM), with the level of the selective agent gradually increased firstly to 10 nM (IC_{25}), approximately 1 week into the selection, and then to 20 nM (IC_{50}) two weeks into the experiment, with the cumulative cell density monitored throughout (Figure 6.2). Of the three replica cultures analysed, two stopped growing as soon as the selective pressure was increased to 20 nM. In contrast, the remaining culture was still viable even when the RH1 concentration had been increased to 30 and then 40 nM, the later value being twice the IC_{50} value observed against wild type parasites.

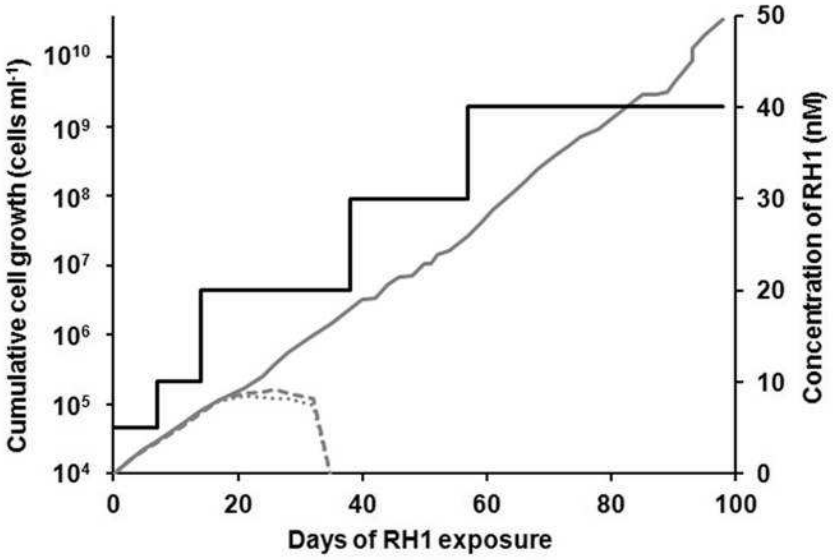

Figure 6.2: RH1 resistance selection in *T. brucei*. Selection of RH1 resistant *T. brucei* was performed by the stepwise increase of the ABQ starting at 5 nM eventually going up to 40 nM. The concentration of RH1 is the culture is displayed by the solid black line. The cumulative cell density of three independent cultures was monitored throughout the experiment: cultures 1, 2 and 3 are represented by the grey solid line, dashed grey line and dotted grey line, respectively. Cultures 2 and 3 failed to grow when the treatment was increased to 20 nM.

Throughout the selection process the susceptibility of the parasite population to RH1 was regularly monitored. For cultures maintained in low RH1 concentrations (5 or 10 nM) a susceptibility phenotype, as judged by their IC_{50} values, similar to that of the wild type was observed: wild type and selecting lines displayed IC_{50}'s of ~20 nM. When the selecting line was cultured in a higher level of ABQ, a stepwise increase in the resistance phenotype was noted such that trypanosome populations cultured in the presence of 20 nM RH1 exhibited an IC_{50} of ~35 nM while parasites grown in 40 nM RH1 displayed an IC_{50} of ~80 nM. This jump in the IC_{50} suggests that resistance to RH1 may be multifactorial. When the selective pressure was increased to beyond 40 nM, parasite numbers crashed such that no viable cells were visible under light microscopy and cultures failed to grow when incubated further (data not shown). Based on this we postulated that we were unable to go above 40

nM in our selection assay. In light of this, the polyclonal cell lines grown in 40 nM RH1 was cloned by limited dilution while still maintaining selective pressure and two lines, designated as $RH1^R$ C1 and $RH1^R$ C2, were analysed further.

6.2 Characterisation of *T. brucei* $RH1^R$ clonal lines

Firstly, we investigated the growth properties of two $RH1^R$ clones (Figure 6.3). In the absence of RH1, the doubling time of the two clones was comparable to the parental line (doubling time of ~7½ hrs). When grown in medium containing RH1 (40 nM), the doubling time of the resistant lines increased ~1.5-fold (doubling time of ~10½ hours). In comparison, no growth of wild type *T. brucei* maintained in 40 nM ABQ was detected after 24 hrs.

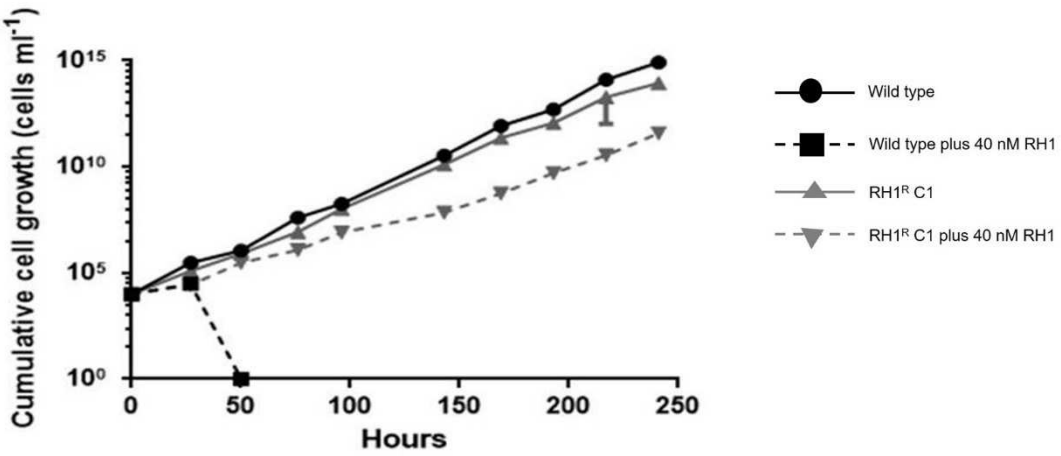

Figure 6.3: Cumulative cell growth of *T. brucei* $RH1^R$ parasites. The cumulative cell density of wild type *T. brucei* (black lines) and a laboratory-generated RH1-resistant clone ($RH1^R$ C1)(grey lines) grown in medium lacking (solid lines) or containing 40 nM RH1 (dashed lines). Data pointsare averages from experiments performed in quadruplicate *T. brucei* cumulative growth average ± standard deviation.A second RH1-resistant clone ($RH1^R$ C2)analysed in parallel displayed similar growth properties (data not shown).

To confirm that the cloning process had not altered the susceptibility of the $RH1^R$ lines to the ABQ, the dose response of the two clones towards RH1 was evaluated (Figure 6.4). Analysis of the IC_{50}'s extrapolated from the resultant plots demonstrated that $RH1^R$ C1 and C2 displayed values ~3.5-fold higher than that

observed against the wild type, being equivalent to that noted for the polyclonal RH1 selected parasites: RH1 exhibited IC_{50}'s of 25.25 ± 6.13, 82.75 ± 1.71 and 92.13 ± 0.85 nM against wild type cells, $RH1^R$ C1 and $RH1^R$ C2, respectively.

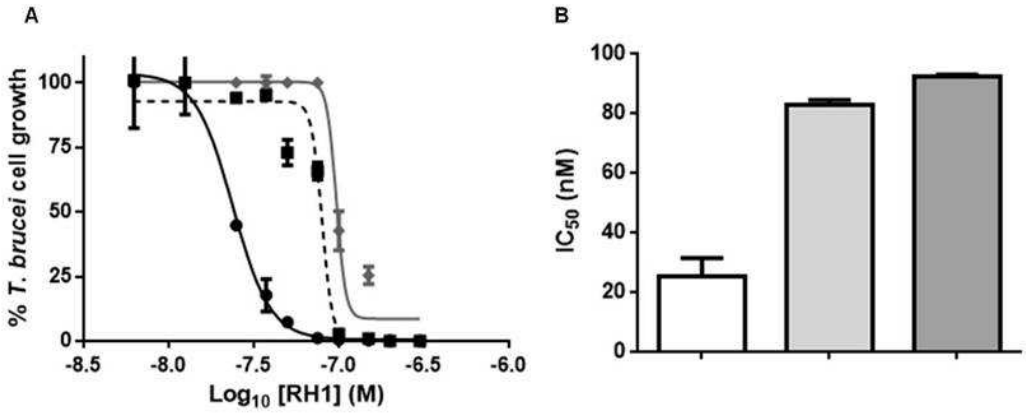

Figure 6.4:Susceptibility of the *T. brucei*$RH1^R$clones to RH1. (A) Dose response curve of wild type *T. brucei* (circles, black solid line) and two RH1 resistant clones, $RH1^R$ C1 (squares, black dashed line) and $RH1^R$ C2 (diamonds, grey solid line) to RH1. (B) Susceptibility of wild type *T. brucei* (white bar) and $RH1^R$ C1 (light grey bar) and $RH1^R$ C2 (dark grey bar) to RH1 as judged by the IC_{50} values (in nM). Data points are averages from experiments performed in quadruplicate ± standard deviation. The differences in susceptibility of wild type and the $RH1^R$ clones to RH1 was statistically significant (P <0.01), as assessed by Student's *t* test.

When analysing certain trypanosomatids, particularly *Leishmania*, that have been selected for resistance to a given drug or compound, removal of the selective agent from the growth medium for a prolonged period of time can result in a complete or partial loss of the phenotype generating revertant lines (Sereno & Lemesre 1997; Perez-Victoria *et al*. 2001; Pérez-victoria *et al*. 2003; Leprohon *et al*. 2009; Kumar *et al*. 2013; Ritt *et al*. 2013; Mukherjee *et al*. 2013). This suggests that whatever event(s) that promoted resistance is unstable and can be readily lost or replaced by a complementary pathway. To investigate the stability of the resistance phenotype displayed by the two $RH1^R$ lines, the trypanosomes were cultured for 50 and 100 generation in the absence of the ABQ and at each generation interval the susceptibility of each clone towards RH1 evaluated (Figures 6.5 and 6.6). Even when

cultured for 100 generations in medium lacking RH1 both $RH1^R$ clones still displayed the resistance phenotype being 3.5- to 6-fold less sensitive than wild type indicating that the mechanism which leads to RH1 resistance is stable in the absence of selection pressure.

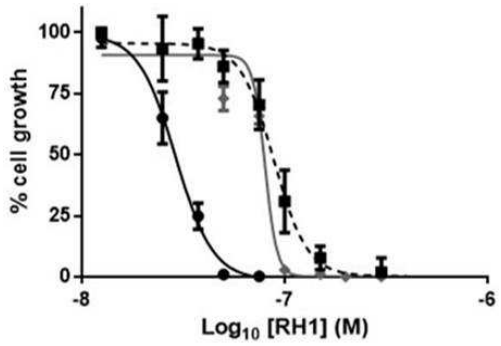

Figure 6.5: Susceptibility of *T. brucei*$RH1^R$C1 cultured in the presence and absence of selective pressure. Dose response curve of wild type *T. brucei* (circles, black solid line), $RH1^R$ C1 continuously cultured in RH1 (40 nM) (diamonds, grey solid line) and $RH1^R$ C1 cultured for 100 generations in medium lacking RH1 (squares, black dashed line) to RH1 were plotted. Data points are averages from experiments performed in quadruplicate ± standard deviation. $RH1^R$ C1 parasites cultured in the absence of RH1 for 50 generations and the $RH1^R$ C2 line (cultured in the absence of the ABQ for 50 and 100 generations) analysed in parallel displayed similar susceptibility profiles (Figure 6.5).

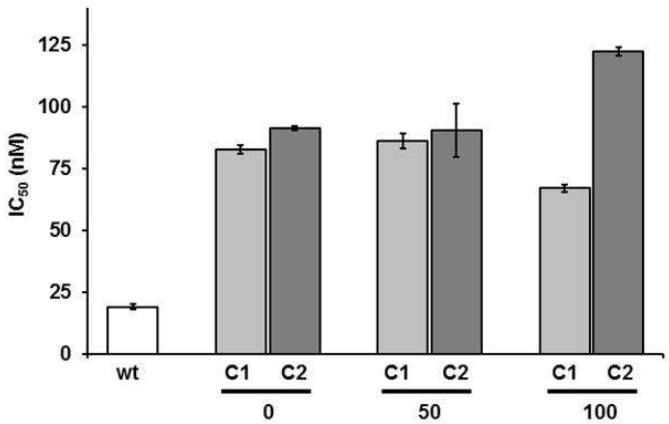

Figure 6.6: Susceptibility of *T. brucei*$RH1^R$clones cultured in the absence of selective pressure. The IC_{50} values (in nM) extrapolated from dose response curves demonstrate that $RH1^R$ C1 (C1) and $RH1^R$ C2 (C2) parasites remain RH1 resistant in comparison to wild type T. brucei (wt) even when cultured in the absence of selective agent for 50 and 100 generations. Data points are averages from experiments performed in quadruplicate ± standard deviation. The differences in susceptibility of wild type and the $RH1^R$ clones to RH1 was statistically significant ($P < 0.01$), as assessed by Student's *t* test.

6.3 Cross resistance of RH1^{R} lines to trypanocidal agents

Trypanosomatid parasites that have been selected for resistance to one compound often display reduced sensitivity to other agents (Carter & Fairlamb 1993; Berger *et al*. 1995; Wilkinson *et al*. 2008; Sokolova *et al*. 2010). To determine whether the RH1^{R} clones behave similarly, our susceptibility studies on the RH1 selected lines were extended to include a range of compounds, with many of the chemicals tested being ICL forming agents and/or type I NTR activated prodrugs (Table 6.1). For those ICL promoting compounds that contained an aziridinyl- (including other ABQs) or nitrogen mustard-moiety at their core, the RH1^{R} cells displayed a ~2- to 3.5-fold increase in resistance towards such agents as compared to the parental line. The only DNA damaging compound class that did not follow this trend were the nitrosoureas. This may be because: 1. these chemicals do not promote sufficient ICL damage to have a deleterious effect on the growth of *T. brucei* and actually may mediate their trypanocidal effect *via* some other mechanism(s) or 2. the pathway(s) invoked in RH1^{R} cells leading to RH1 resistance do not play a role in fixing any damage caused by these agents. Interestingly, the *T. brucei* TbSNM1 null mutants described by Sullivan *et al*. (2015) displayed the same susceptibilities to nitrosoureas as wild type parasites. This further suggests that if these compounds do promote ICL formation an SNM1-independent pathway functions to repair any resulting DNA damage generated by these agents and is in contrast to the SNM1-dependent mechanisms used to fix the lesions generated by aziridinyl and nitrogen mustard-based compounds.

When our susceptibility studies were extended to investigate how RH1^{R} cells responded to trypanocidal agents, cross resistance was observed towards nifurtimox

and megazol but not towards DFMO (Table 6.1). It has been postulated that both nifurtimox and megazol may mediate at least part of their anti-parasitic effects by promoting DNA damage although this mechanism is unlikely to occur *via* the formation of ICL lesions (Poli *et al*. 2002; Enanga *et al*. 2003; Buschini *et al*. 2009; Wilkinson & Kelly 2009). Additionally, these two nitroheterocyclic structures along with several of the ICL-inducing compounds (*e.g.* RH1, DZQ, carboquone, CB1954 and LH17) that $RH1^R$ cells also display cross resistance towards, also function as prodrugs with the type I NTR catalysing the activation of such agents (Wilkinson *et al*. 2008; Hall *et al*. 2010; Bot *et al*. 2010; Hall *et al*. 2012). Based on the above phenotypic screens it is tempting to speculate that the mechanism(s) invoked in $RH1^R$ cells that leads to reduced RH1 sensitivity may involve components of the ICL repair pathway and/or modulation of the type I NTR activity.

Compound	IC_{50} values (µM) ± standard deviation		
	wild type	$RH1^R$ C1	ratio
Aziridines			
DZQ	0.191 ± 0.008	0.374 ± 0.043	1.9
RH1	0.025 ± 0.006	0.083 ± 0.002	3.3
Carboquone	0.023 ± 0.001	0.066 ± 0.014	2.8
CB1954	5.275 ± 0.556	11.275 ± 1.441	2.1
Triethylenemelamine	1.970 ± 0.743	3.975 ± 0.119	2.0
ThioTEPA	37.825 ± 1.729	83.525 ± 2.401	2.2
Nitrogen mustards			
Mechlorethamine	54.750 ± 3.775	95.250 ± 0.957	1.8
Melphalan	9.650 ± 0.370	18.900 ± 0.455	1.9
LH17	5.438 ± 0.444	17.998 ± 1.106	3.6
Nitrosoureas			
Lomustine (µM)	16.650 ± 0.443	15.463 ± 0.665	0.9
Semustine (µM)	15.025 ± 3.457	17.100 ± 3.619	1.1
Other agents			
DFMO	16.763 ± 2.691	22.177 ± 0.383	1.3
Nifurtimox	1.688 ± 0.386	7.050 ± 0.311	3.6
Megazol	0.166 ± 0.001	0.454 ± 0.004	2.7

Table 6.1: Susceptibility of *T. brucei*$RH1^R$ cells to various trypanocidal agents. Data represent the growth-inhibitory effect as judged by their IC_{50}'s of various agents on BSF *T. brucei* wild type and $RH1^R$ cells. All values are means ± standard deviation from independent experiments preformed in quadruplicate. The ratio represent the fold difference in IC_{50} value between the $RH1^R$ and wild type lines to a given compound.

6.4 Evaluating the ABQ activation mechanism in $RH1^R$ cells

Based on the cross resistance profiles displayed by the $RH1^R$ clones towards a range of compounds and the stepwise increase in IC_{50} values noted during the selection process, we hypothesis that resistance to RH1 is multifactorial. As many of the agents tested are type I NTR metabolised prodrugs and/or promote some form of

DNA damage, we evaluated whether the activation mechanism identified in Chapter 4 and downstream DNA repair pathways eluded to in Chapter 5 are somehow affected within the $RH1^R$ clones, leading to the phenotypic changes noted in these resistant cells.

Reduction in gene copy number and the acquisition of mutations in *ntr* is now regarded as a key marker displayed by laboratory *T. cruzi* cells selected for resistance to nifurtimox and benznidazole (Wilkinson *et al*. 2008; Mejía-Jaramillo *et al*. 2011; Mejia *et al*. 2012; Campos *et al*. 2014). To examine whether Tb*ntr* is implicated in mediating RH1 resistance, we analysed the sequence, copy number and mRNA expression levels of this gene in $RH1^R$ cells. Initially, we amplified the region of Tb*ntr* (~720 bp) that encodes for the enzymes catalytic domain from the selected line using a high fidelity DNA polymerase. Following A-tailing, the resultant fragments were cloned into the pGEM-T-easy vector and the inserts sequenced (a total of 5 sequences were analysed from 4 independent PCRs). Examination of the nucleic acid and deduced amino acid sequences indicated that Tb*ntr* expressed by $RH1^R$ cells was identical to that in wild type (sequences on the TriTryp database and as generated in the Wilkinson laboratory). Therefore, the RH1 resistance phenotype displayed $RH1^R$ cells is not due to acquisition of mutations in the Tb*ntr* catalytic domain. Here, we did not investigate whether alterations to the nucleic acid sequence in the 5' region of Tb*ntr* lead to resistance as analysis of Tc*ntr* from *T. cruzi* nifurtimox or benznidazole resistant cells has have never shown any difference in this part of the gene.

To determine whether *T. brucei* $RH1^R$ parasites exhibited any changes to the Tb*ntr* copy number we conducted quantitative PCRs on genomic DNA extracted from wild

type and RH1 selected lines, targeting internal fragments within Tb*ntr* and Tb*tert*; Tb*tert* was used as a standardized control (described by Brenndörfer & Boshart (2010)). Using the comparative C_T method, the resultant fluorescence profiles obtained from each reaction for each DNA fragment and from each parasite line were compared with the relative levels of Tb*ntr* normalized with respect to Tb*tert*(Figure 6.7). This demonstrated that the copy number of Tb*ntr* from the $RH1^R$ line was not significantly different from that in wild type parasites.

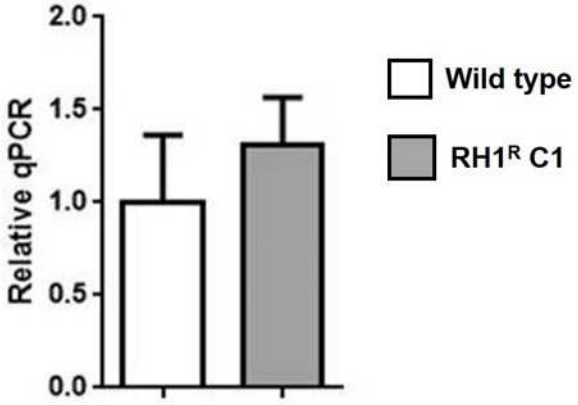

Figure 6.7: Tb*ntr* copy number in $RH1^R$ cells. Quantitative PCR profiles targeting Tb*ntr* and Tb*tert* from wild type (white bar) and $RH1^R$ (grey bar) cells were compared using thecomparative C_T method. The values shown are the average $2^{-(\Delta\Delta C_T)}$ from reactions performed in triplicate ± standard deviation.

As described in Chapter 4, reduction of Tb*ntr* expression in heterozygous lines leads to resistance towards RH1 and many other ABQs. To establish whether changes in the expression level of this prodrug activator promotes resistance in the selected line, we conducted qRT-PCR on cDNA generated from total RNA extracted from both wild type and $RH1^R$ lines. As with the qPCR described above, amplifications targeting internal fragments within Tb*ntr* and Tb*tert* were performed with the resultant fluorescence profiles obtained from each reaction for each DNA fragment and from each parasite line compared using the comparative C_T method (Figure 6.8). Following normalization of the Tb*ntr* signal with respect to Tb*tert*, the level of the

NTR mRNA transcript was ~2-fold lower in the RH1^{R} line compared to wild type. This strongly suggests that reduction in Tb*ntr* expression in selected cells leads to RH1 resistance with this data complementing the data presented in Chapter 4.

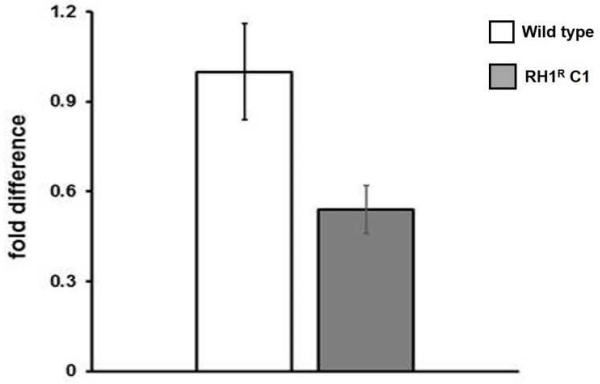

Figure 6.8: Tb*ntr* expression is lower in RH1^{R} cells. Quantitative RT-PCR profiles targeting Tb*ntr* and Tb*tert* from wild type (white bar) and RH1^{R} (grey bar) cells were compared using thecomparative C_T method and the average fold difference (as judged by $2^{-(\Delta\Delta Ct)}$from reactions performed in triplicate ± standard deviation) plotted as a measure of the relative expression level of Tb*ntr*. The difference in relative expression levels between the two lines was judged to be statistically significant (P <0.01), as assessed by Student's *t* test.

6.5Are DNA repair pathways implicated with the RH1r phenotype?

As the RH1^{R} selected line shows cross resistance to a range of compounds including several ICL forming agents that do not function as NTR activated prodrugs, it is implicit that additional factors besides TbNTR are involved in generating the phenotype observed. In Chapter 5, it was shown that in *T. brucei* RH1 to promote DNA damage that can be repaired by a pathway involving TbSNM1.To evaluate whether DNA repair enzymes play a role in generating RH1 resistance, the gene copy number and mRNA expression levels of Tb*snm1*, Tb*mre11* and Tb*rad51* was investigated. Initial amplification reactions using genomic DNA indicated that the copy number of these open reading frames were equivalent in resistant and wild type cells (data not shown).

When these studies were extended to look at mRNA expression, there was no apparent difference in any transcript abundance. These preliminary studies indicate that TbSNM1, TbMRE11 and TbRAD51 are not involved in mediating resistance to RH1 although a more in-depth analysis, possibly involving transcriptomic or proteomic approaches, would shed more light on what factors are responsible for the observed RH1 resistance phenotype.

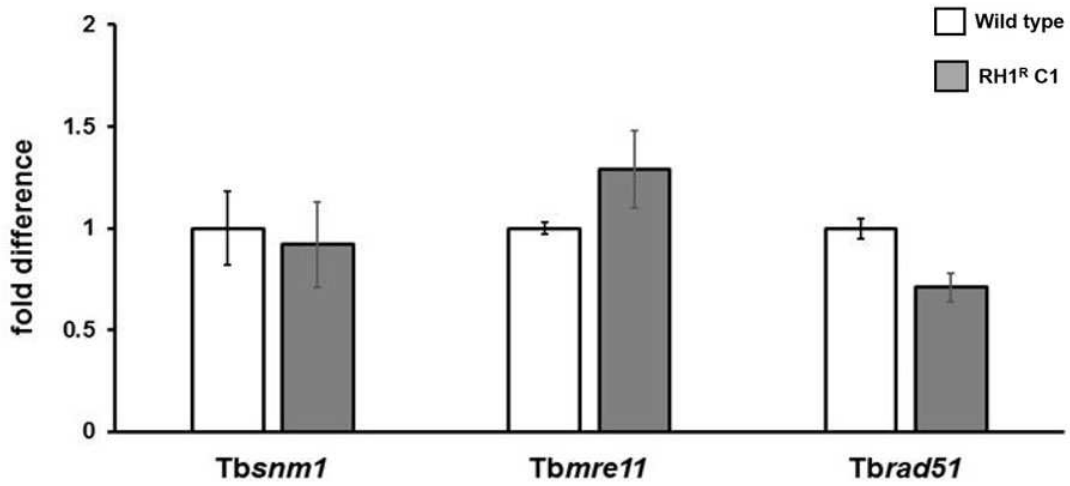

Figure 6.9: Selected DNA repair enzymes appear not be involved in mediating RH1 resistance. Quantitative RT-PCR profiles targeting Tb*snm1*, Tb*mre11*,Tb*rad51* and Tb*tert* from wild type (white bar) and $RH1^R$ (grey bar) cells were compared using thecomparative C_T method and the average fold difference (as judged by $2^{-(\Delta\Delta Ct)}$from reactions performed in triplicate ± standard deviation) plotted as a measure of the relative expression level of Tb*snm1*, Tb*mre11* andTb*rad51*.

Chapter 6 summary

In this Chapter we have explored how RH1 resistance may arise in *T. brucei.* Specifically we have shown that:

1. *T. brucei* resistant to RH1 can be selected *in vitro*.
2. The resultant $RH1^R$ lines display a ~4-fold increase in resistance to this particular ABQ.
3. The RH1 resistance phenotype is stable and can be maintained for up to 100 generations in the absence of selective pressure.
4. The $RH1^R$ lines displays cross resistance to a number of other compounds including aziridinyl- and nitrogen mustard-based compounds, and the trypanocidal nitroheterocyclic compounds nifurtimox and megazol.
5. Based on the phenotypic screens, the mechanism(s) underlying this resistance appears to be multifactorial.
6. One mechanism underlying RH1 resistance involves reduction in Tb*ntr* expression.

Chapter 7: Investigating the mechanism of action of trypanocidal nitroheterocycles

A number of nitroaromatics have been reported to display anti-trypanosomatid properties (reviewed by Raether & Hänel 2003; Wilkinson *et al*. 2011; Patterson & Wyllie 2014). Unravelling how such compounds actually go about exerting their toxic affects represents a major challenge in bringing a potential compound from the bench to the bedside. In this thesis we have previously described how biological approaches can be used to dissect the function of a given antimicrobial agent with the application of high throughput strategies speeding up this process. Techniques that have facilitated such studies in *T. brucei* are the development of whole genome loss of function (RNAi) and gain of function (over expression) screening strategies with the former being extremely informative in understanding how all the clinically used anti-HAT drugs work (Baker *et al*. 2011; Alsford *et al*. 2011; Alsford *et al*. 2012; Begolo *et al*. 2014).

Using the whole genome loss of function assay coupled, where appropriate, with next generation sequencing (Baker *et al*. 2011; Alsford *et al*. 2011; Alsford *et al*. 2012), we explored the mechanism(s) of action of the aziridinyl dinitrobenzamide CB1954 (also known as Tretazicar), a compound closely related to RH1 (Figure 6.1) and BG-M2**,** a nitroaromatic derivative of O^6-benzylguanine (Zhu *et al*. 2011). To confirm whether any of the "hits" identified are genuinely involved in mediating resistance to the selective agent, RNAi constructs specifically targeting the "hit" transcript were generated, cell lines established and growth studies and phenotypic screens performed to 1) determine whether the target is essential for viability of BSF

trypanosomes and 2) validate if reduction of target gene expression confers resistance to the selective agent.

7.1. CB1954 and its antiparasitic activity

CB1954 (5-(aziridin-1-yl)-2,4-dinitrobenzamide) (Figure 7.1) was initially developed as an anti-cancer prodrug therapeutic in the ChesterBeatty Laboratories that, following activation, generates cytotoxic metabolites that promote ICL formation (Helsby *et al*. 2003). Preliminary studies revealed that this dintrobenzamide was efficiently metabolised by rat NQO1 although this activity did not translate across to its human counterpart (Chen *et al*. 1997; Prosser *et al*. 2010). As such, interest in CB1954 as an anti-cancer agent waned although it has been patented as a rodenticide (US 8785428 B2). However, at the beginning of the 21st century, CB1954 as an anti-cancer agent has been revisited following observations that bacterial type I NTRs can interact with this compound (Prosser *et al*. 2010). As a result, strategies termed gene-directed or antibody-directed enzyme prodrug therapy were been developed that involve targeting anti-cancer cells with a DNA construct containing *E. coli* or a tumour specific antibody conjugated to the NTR protein prior to treatment with the prodrug (Chung-Faye *et al*. 2001; Palmer *et al*. 2003; Helsby *et al*. 2004; Patel *et al*. 2009; Prosser *et al*. 2010). Again initial *in vitro* studies using either system were encouraging although when transferred into an *in vivo* situation, off targeting was observed resulting in unwanted side effects (Knox *et al*. 1993).

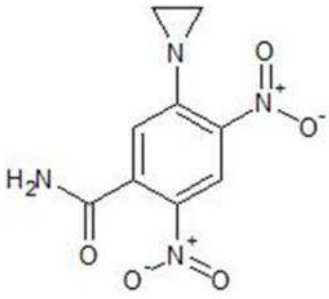

Figure 7.1: Structure of CB1954

Recently, it has been shown that CB1954 also exhibits antimicrobial activities against BSF *T. brucei*, *T. cruzi* amastigotes and *L. major* amastigotes (Bot *et al*. 2010; Sokolova *et al*., 2010; Voak *et al*. 2013). In all cases, significant potency was observed with the prodrug active at concentrations lower than 3 µM: the IC_{50} of CB1954 towards *T. brucei*, *T. cruzi* and *L. major* was calculated to be 2.97 ± 0.25, 0.57 ± 0.05 and 0.05 ± 0.02 µM respectively (Bot *et al*. 2010; Voak *et al*. 2013). In constrast, little/no toxicity was observed in the Chinese hamster fibroblasts (V79), African green monkey kidney epithelial (Vero) or human macrophage-like (THP-1) mammalian cells: IC_{50} values of 543, > 250 and > 100 µM were recorded, respectively (Helsby *et al* 2005;Bot *et al*. 2010; Voak *et al*. 2013).

7.2 Evaluating the mechanism of CB1954's trypanocidal activity

Using a similar approach as discussed in Chapter 4, collaborators at the London School of Hygiene and Tropical Medicine performed a whole genome loss of function assay using CB1954 as selective agent. A *T. brucei* RNAi library stock population was treated with tetracycline (1 µg ml^{-1}) one day (-1 day) prior to challenging the parasites with the dinitrobenzamide (3 µM) (day 0). Cell numbers were then monitored over a 16 day period with the cultures passaged as appropriate into *T. brucei* growth medium containing the fresh inducer tetracycline and CB1954. Over the first 3 days of selection, the parasites grew at a rate equivalent to that of

non-induced and non-CB1954 treated controls (Figure 7.2). This was then followed by a dramatic fall in the cumulative cell density as the selective agent killed off the trypanosomes, followed by an outgrowth from day 12 onwards of a CB1954 resistant *T. brucei* population.

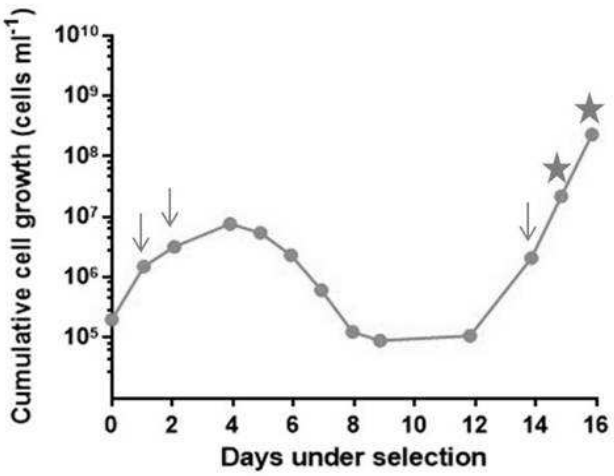

Figure 7.2:Screening for CB1954 resistant determinants using a genome wide *T. brucei* RNAi library. The BSF *T. brucei* RNAi library (Alsford *et al*. 2012; Glover *et al*. 2015) was co-treated with tetracycline (1 µg ml^{-1}) to induce RNAi, and CB1954 (3 µM) with the cumulative cell growth of the culture followed**.** The arrows correspond to culture dilution and addition of fresh CB1954 (3 µM) and tetracycline (1 µg ml^{-1}). Genomic DNA (as indicated by stars) was extracted from parasites at days 15 and 16. The above data was collected by Dr S. Alsford, LSHTM.

On days 15 and 16 genomic DNA was extracted from the CB1954 selected parasite population and used as template in a PCR-based low resolution screen (Figure 7.3A). Analysis of the resultant amplification products identified one major fragment of ~1.1 kbp, comparable to the major band size observed in the RH1 RNAi library screen. Sequence analysis of this fragment and comparison against the TriTryp genome database revealed that this mapped to a region that spanned the 3' region of the type I nitroreductase (Tb*ntr*) gene (Gene ID: Tb927.7.7230) (Figure 7.3B). This result was unsurprising given that previous studies have shown that dinitrobenzamidine readily undergoes activation by this type of oxidoreductase

enzyme (Bot *et al* 2010; Voak *et al* 2014). In addition to the Tb*ntr*-containing fragment, several other bands were also observed in amplification reactions especially when using higher concentration of the oligonucleotide primers (Figure 7.3A). Sequencing of these identified a series of non-specific DNA sequences (e.g. *vsg* genes, telomere associated regions) that were not analysed further.

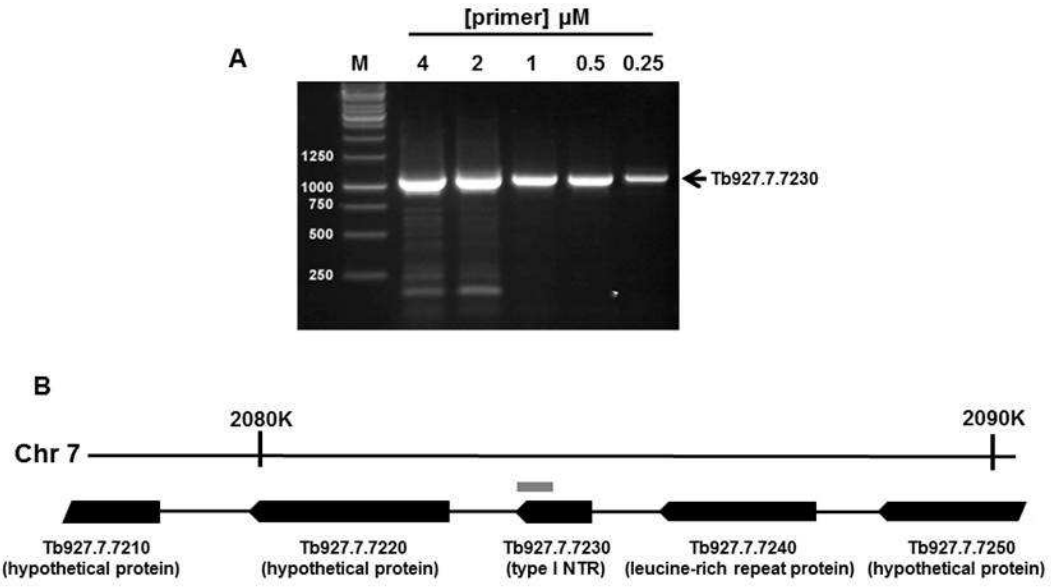

Figure 7.3: Identification of CB1954 resistance determinants. (A) Amplification of the RNAi target from the CB1954 screen using gDNA extracted on days 15 or 16 of the selection using PCR conditions described (Alsford *et al*. 2012; Glover *et al*. 2015). M indicates the size markers (in bp). Arrow indicate the DNA fragmented obtained from the screen (image contributed by Dr S Alsford, LSHTM). (B) The position of the DNA fragments recovered from the CB1954 RNAi screen relative to the genome location is shown by the grey box.

To confirm that TbNTR was the key activator of CB1954 we evaluated the susceptibility of *T. brucei* cells engineered to express reduced levels of the encoding gene. Initially, an RNAi based approach was used to down regulate gene expression. However as noted in Chapter 4, cells undergoing RNAi were viable, in contrast to reports that the TbNTR activity is essential for BSF *T. brucei* growth (Wilkinson *et al* 2008), and displayed the same susceptible to CB1954 as controls: when these the

studies were extended to nifurtimox no effect on parasite susceptibility was observed. Based on these observations we hypothesize that under the conditions used here, RNAi does not sufficiently reduced the Tb*ntr* transcript to a level that affects the sensitivity of *T. brucei* to CB1954 (RH1 or nifurtimox). In contrast, when the susceptibility of the *T. brucei* Tb*ntr* heterozygote line towards CB954 was assessed, the recombinant line displayed an IC_{50} approximately 3-fold greater than that observed towards wild type cells (Figure 7.4). This confirmed that reduction of TbNTR expression through loss of one of the Tb*ntr* encoding alleles is sufficient to generate resistance to CB1954.

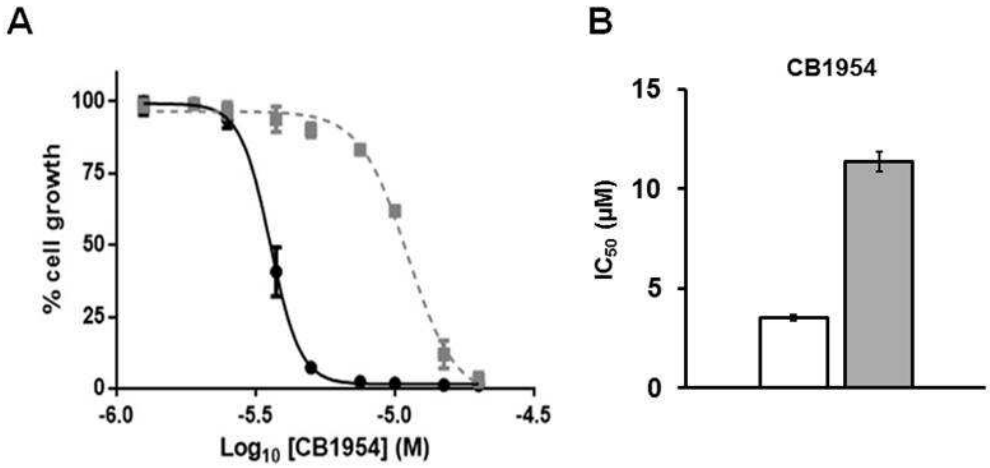

Figure 7.4: Susceptibility of *T. brucei* Tb*ntr* heterozygotes to CB1954. (A). Dose response curve of wild type *T. brucei* (solid line) and parasites that are haploid for Tb*ntr* (dotted line) to CB1954. (B). Susceptibility of wild type *T. brucei* (white bar) and TbNTR heterozygotes(grey bar) to CB1954as judged by the IC_{50} values (in µM). All data are means for experiments performed in quadruplicate ± standard deviation. The differences in susceptibility of wild type and TbNTR over expressing cells to CB1954 was statistically significant ($P < 0.01$), as assessed by Student's *t* test.

7.3 High resolution screening of CB1954 selected cells

As discussed in Chapter 4, the DNA template used in the low resolution PCR screens can also be used for a more in-depth analysis to potentially identify addition determinants that may play a role in mediating CB1954's trypanocidal mode of action. Using the criteria previously outlined, the inducibility of the CB1954 selected RNAi library was determined and shown to be 67%. This value indicates that the resistance phenotype displayed by the selected parasite population was most likely due to an RNAi effect rather than the acquisition and selection of background mutations. Given this, amplification reactions were sent for high throughput DNA sequencing carried out at Beijing Genome Institute and bioinformatic analysis of the resultant data performed by Dr S Alsford (LSHTM) in accordance to Glover *et al*. (2015).

Out of the ~450,000 total sequence reads, of which ~80,000 were deemed to be tagged reads (*i.e*. reads where one of the "signature" primer sequence used in the initial PCR was identified), 96% of the total number of reads and 82% of the tagged number of reads identified three distinct DNA fragments that all mapped to Tb*ntr* (Table 7.1). This represented the only open reading frame generated from this analysis that meets the "at least 2 tagged hit per gene" criteria laid out by Glover *et al* (2015) for the identification of a valid hit.

Gene ID	Study name	Reads/kbp/cds		Tagged hits/CDS
		Total Reads	Tagged Reads	
Tb927.7.7230	Tb*ntr*	439624	63501	3
Tb927.11.6370	Tb*ORFa*	5661	4919	1
Tb927.7.7310	Tb*ORFb*	3217	2828	1
Tb927.3.3670	Tb*ORFc*	2281	2044	1
Tb927.10.3130	Tb*ORFd*	2876	1250	1
Tb927.8.8070	Tb*ORFe*	1229	900	1
Tb927.8.8110	Tb*ORFe*	975	862	1
Tb927.8.4050	Tb*ORFf*	1165	535	1
Tb927.10.3910	Tb*ORFg*	403	363	1
Tb927.9.9600	Tb*mcm9*	290	101	2
Tb927.9.11760	Tb*rad2*	136	44	---

Table 7.1: The hits identified in the next generation sequencing sequence analysis of CB1954 RNAi library screen and the frequency of reads.

In addition to Tb*ntr*, several other potential hits that did not meet the "at least 2 tagged hit per gene" criteria were taken forward for further analysis. These were selected on the basis that >100 total reads were obtained and/or they constituted >1% tagged number of reads. Based on the TriTryp database most of these hits (designated Tb*ORFa-g*) encode for hypothetic proteins, several of which have a predicted nuclear localisation, with Tb927.9.9600 and Tb927.9.11760 coding for sequences annotated as Tb*mcm9* and Tb*rad2*, respectively (Table 7.2).

Table 7.2: Description of the hits obtained from the high throughput sequence analysis of CB1954 RNAi library screen. The information presented was obtained from the TriTryp database. Protein localisation was determined using PsortII where M: mitochondria; C: cytoplasm; N: nucleus; ER: Endoplasmic reticulum; V: vacuole; PM: Plasma membrane. Protein features and functional domains were identified using BlastP.

Study name	chromosome	Molecular mass (kDa)	Predicted localisation	Protein features and functional domains
Tb*ORFa*	11	96	35% C 30% N	1. Ribonuclease inhibitor (RI)-like domains with leucine-rich repeats 2. 28% identity to *Capsaspora* hypothetical protein.
Tb*ORFb*	7	25	44% PM 26% V	1. A signal peptide 2. 2 transmembrane domains located towards the amino-terminal 3. 37% identity towards DNA mismatch repair protein MutS from *Dethiobacter alkaliphilus*
Tb*ORFc*	3	67	70% N	1. 3 RNA recognition motifs (RRMs) involved with RNA processing (Wurst *et al*. 2009).
Tb*ORFd*	10	87	74% N	1. Calponin-homology domain, CH-domain towards the amino-terminal 2. 3-PAP Myotubularin-associated protein domain 3. No significant identity to proteins from other organisms
Tb*ORFe* Tb*ORFe*	8 8	56 62	52% M 39% N 70% M 22% N	1. 2 coding sequences are almost identical 2. 4 phosphorylation sites on 56-kDa protein/3 on the 62 kDa protein 3. 32-35% identity to *Eurpyga* (bird) and *Zootermopsis* (termite) hypothetical proteins
Tb*ORFf*	8	83	33% V 33% ER	1. 2 transmembrane domains at either end of protein sequence. 2. YWTD domain maybe involved in lipid metabolism and/or transport 3. No significant identity to proteins from other organisms
Tb*ORFg*	10	53	44% ER	1. 6 transmembrane domains 2. Homology to thiol:disulfide interchange proteins from marine bacteria and beta-lactamase like proteins from fungi.
Tb*mcm9*	9	85	57% N	Mini chromosome maintenance complex (MCM) protein (Tiengwe *et al*. 2012; Tiengwe *et al*. 2014)
Tb*rad2*	9	82	44% ER 35% M	XPG (Machado *et al* 2014).

To assess whether a reduction in activity of any of the above "hits" plays a role in resistance to CB1954, an RNAi based approach was taken. Using the RNAit algorithm, DNA fragments containing sequences internal to each of the open reading frames were amplified from *T. brucei* genomic DNA and the resultant fragments cloned into the p2T7^{Ti} RNAi vector. Each construct was then linearized before being transfected into *T. brucei*SMB. Following selection, the growth of each RNAi cell line was monitored to determine whether RNAi targeting a given transcript affected parasite viability (Figure 7.5). In all cases, cells induced to undergo RNAi were viable and grew at the same rate as non-induced controls, with most having a doubling time of around 8 hours: for cells where the Tb*ORFa* or Tb*rad2* mRNA was targeted, an increase in doubling time to ~10 and ~13 hours, respectively, was observed although this property was shown by tetracycline treated and untreated parasites.

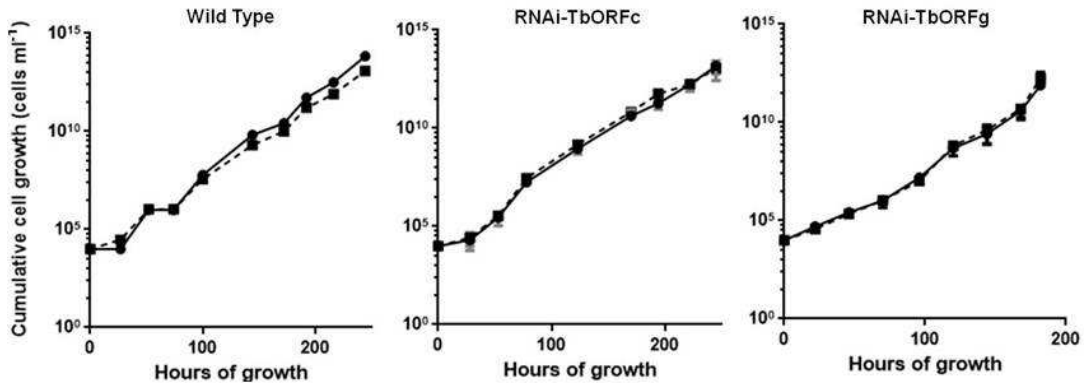

Figure 7.5: Growth of selected *T. brucei* RNAi lines. The growth of tetracycline induced (dashed line) and noninduced (solid line) BSF *T. brucei* was monitored daily over a 10-day period. For all the transformed lines, cell counts were performed on three independent cultures from which the mean cell density ± standard deviation was determined. All other RNAi lines behaved similarly.

The susceptibility of each of the cell lines towards CB1954 while undergoing RNAi was evaluated. From the resultant dose response curves (Figure 7.6), the IC_{50} of each cell line to dinitrobenzamidine was determined (Figure 7.7). In all cases, cells

undergoing RNAi, irrespective of which transcript was being targeted, exhibited a similar sensitivity to CB1954 as wild type cells. This suggests that loss of function of any lesser "hit" identified from the high throughput sequence analysis does not lead to resistance to the dinitrobenzamidine.

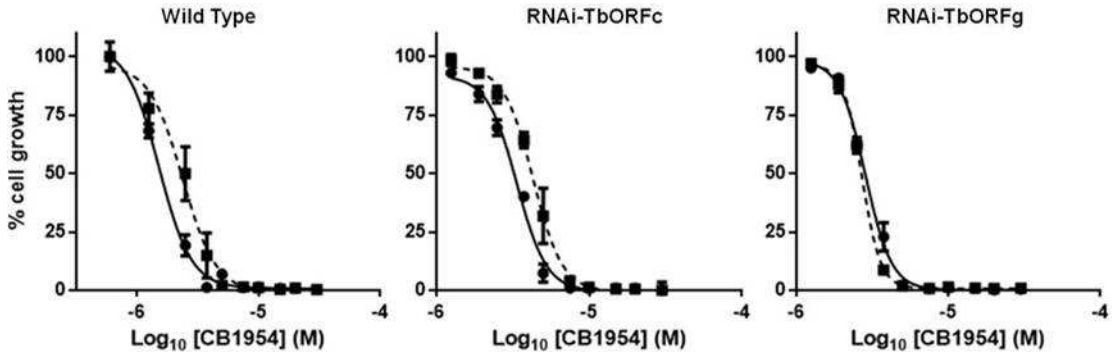

Figure 7.6: Susceptibility of selected *T. brucei* RNAi lines to CB1954. Dose response curve of tetracycline induced (dashed line) and noninduced (solid line) BSF *T. brucei* to CB1954. All data are means for experiments performed in quadruplicate ± standard deviation. All other RNAi lines behaved similarly.

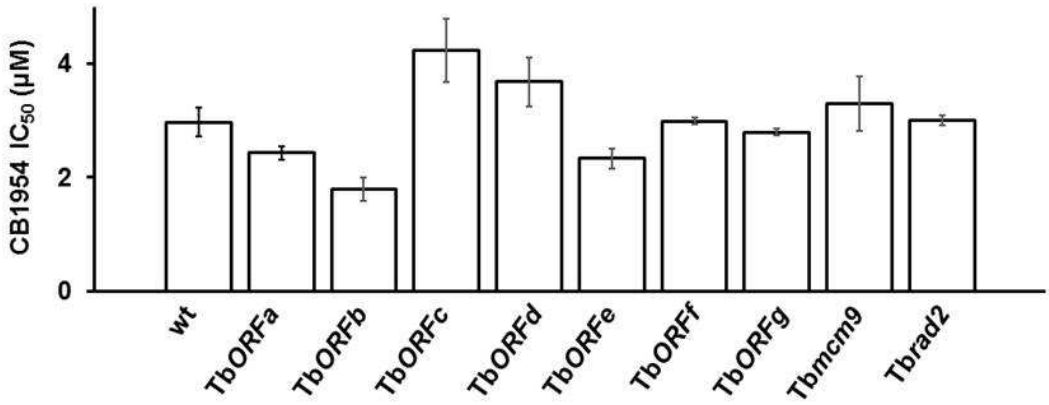

Figure 7.7: Susceptibility of *T. brucei* RNAi lines to CB1954. Susceptibility of wild type *T. brucei* and parasites undergoing RNAi targeting various transcripts to CB1954 as judged by the IC_{50} values (in µM). All data are means for experiments performed in quadruplicate ± standard deviation. The differences in susceptibility of wild type and recombinant lines was not judged to be statistically significant, as assessed by Student's *t* test.

7.4 Trypanocidal activity of BG-M2

O^6-Alkylguanine-DNA alkyltransferase (MGMT) is a ubiquitous DNA repair protein that plays a key role in mediating resistance to guanine *O*-6 chloroethylating agents in certain types of tumour cell (Pegg & Byers 1992; Pegg *et al*. 1993). This enzyme removes alkyl groups from guanine residues added by alkylating agents, thus reversing the action of the drug. To prevent this enzymatic response, several inhibitors including O^6–benzylguanine and its derivatives (Figure 7.8) have been developed to inhibit the function of MGMT(Zhu *et al*. 2011).

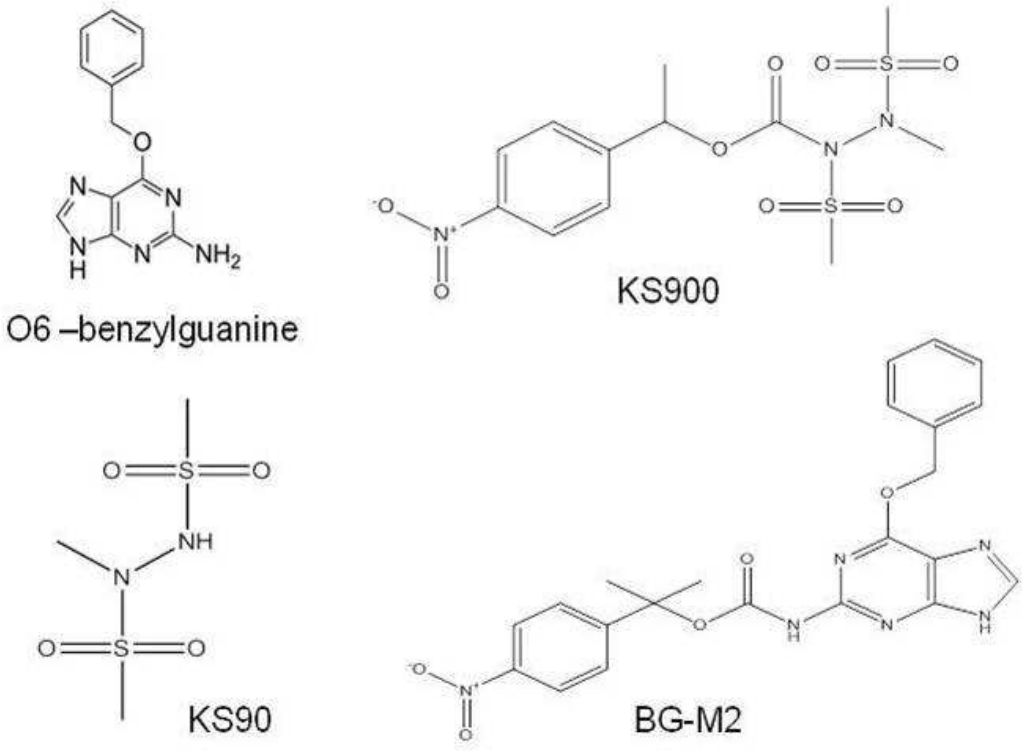

Figure 7.8: Structures of O^6-alkylguanine DNA alkytransferase inhibitors. KS90, KS900 and BG-M2 are 4-nitrobenzyloxycarbonyl derivatives of the MGMT inhibitor O^6–benzylguanine (Zhu *et al* 2011)

Here, the nitrobenzyl prodrug BG-M2 and two compounds, KS90 and KS900, used in its synthesis, were tested for trypanocidal activity (Zhu *et al*. 2011). For each agent, dose response curves against wild type BSF *T. brucei* were plotted (Figure

7.9) from which each compound's IC_{50} value was determined. This demonstrated that KS90 and KS900 did not display anti-trypanosomal at concentrations up to 10 µM and were not studied further.In contrast, BG-M2 displayed growth inhibitory activity against BSF *T. brucei* yielding an IC_{50} value of 1.96 ± 0.01 µM.

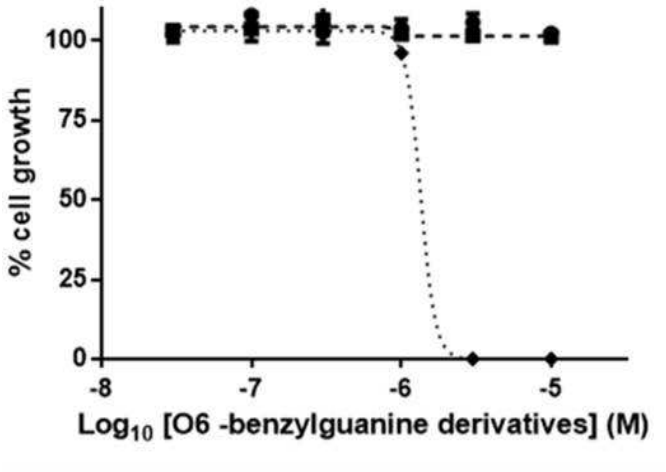

Figure 7.9: Dose response of *T. brucei* to MGMT inhibitors. The susceptibility of wild type BSF *T. brucei* to KS90 (black circles), KS900 (black squares) and BG-M2 was evaluated. All data points are means for experiments performed in quadruplicate ± standard deviation.

7.4.1 Evaluating BG-M2 as a trypanocidal prodrug

As BG-M2 is designed to function as a prodrug and contains a nitrobenzyl substituent, we initially postulated that this compound could undergo TbNTR mediated activation. To determine whether this was the case the susceptibility of Tb*ntr* over expressing parasites towards this structure was tested (Figure 7.10). From the resultant dose response curves and IC_{50} values it was clear that BG-M2 displayed equal potency against the Tb*ntr* over expressing line as towards wild type. This indicates that contrary to our initial hypothesis BG-M2 is not activated by TbNTR within the parasite itself.

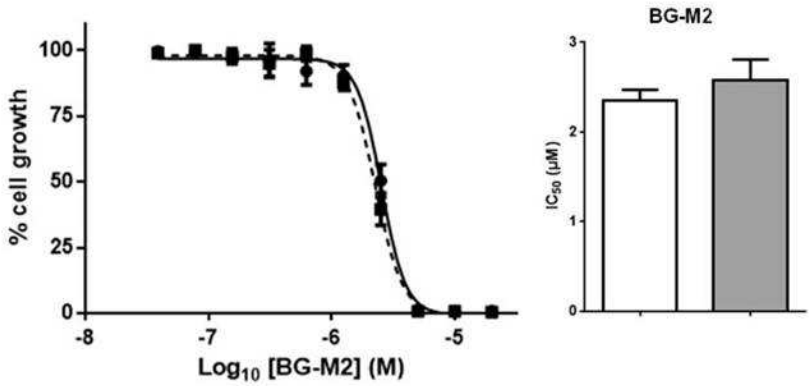

Figure 7.10: Susceptibility of *T. brucei* expressing elevated levels of TbNTR to BG-M2. (A) Dose response curve of wild type *T. brucei* (solid line) and parasites engineered to express elevated levels of TbNTR (dotted line) to BG-M2. (B) Susceptibility of wild type *T. brucei* (white bar) and TbNTR overexpressing line (grey bar) to BG-M2 as judged by the IC_{50} values (in µM). All data are means for experiments performed in quadruplicate ± standard deviation. The difference in IC_{50} values was not statistically significant, as assessed by Student's *t* test. Data provided by Dr Shane Wilkinson.

To shed light on BG-M2's trypanocidal mechanism of action a whole genome loss of function assay was performed. During the selection process BG-M2 exhibited no discernible effect on parasite growth until day 6. At this point and until day 10, parasite numbers remained relatively static. From day 10 onwards a BG-M2 resistant parasite population was selected.

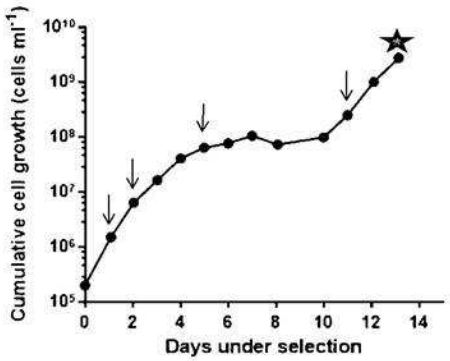

Figure 7.11:Screening for BG-M2 resistant determinants using a genome wide *T. brucei* RNAi library. The BSF *T. brucei* RNAi library (Alsford *et al*. 2012; Glover *et al*. 2015) was co-treated with tetracycline (1 µg ml^{-1}) to induce RNAi, and BG-M2 (3 µM) with the cumulative cell growth of the culture followed**.** The arrows correspond to culture dilution and addition of fresh BG-M2 (3 µM) and tetracycline (1 µg ml^{-1}). Genomic DNA (as indicated by stars) was extracted from parasites at days 13. The above data was collected by Dr S. Alsford, LSHTM.

Genomic DNA was extracted from the BG-M2 selected parasite population and used as template in a PCR-based low resolution screen (Figure 7.12). Sequence analysis of the resultant fragments demonstrated that the major (brightest) ~1.2 kbp band spanned the 3' region of Tb927.10.1740 and 5' region of Tb927.10.1750 (designated here as TbORF1 and TbORF2, respectively) while a 0.8 kbp fragment represented the 5' region of Tb927.11.11380(designated here TbORF3). Several other fragments were also sequenced but as before these correlated to a series of non-specific DNA sequences (e.g. *vsg* genes, telomere associated regions) and were not analysed further.

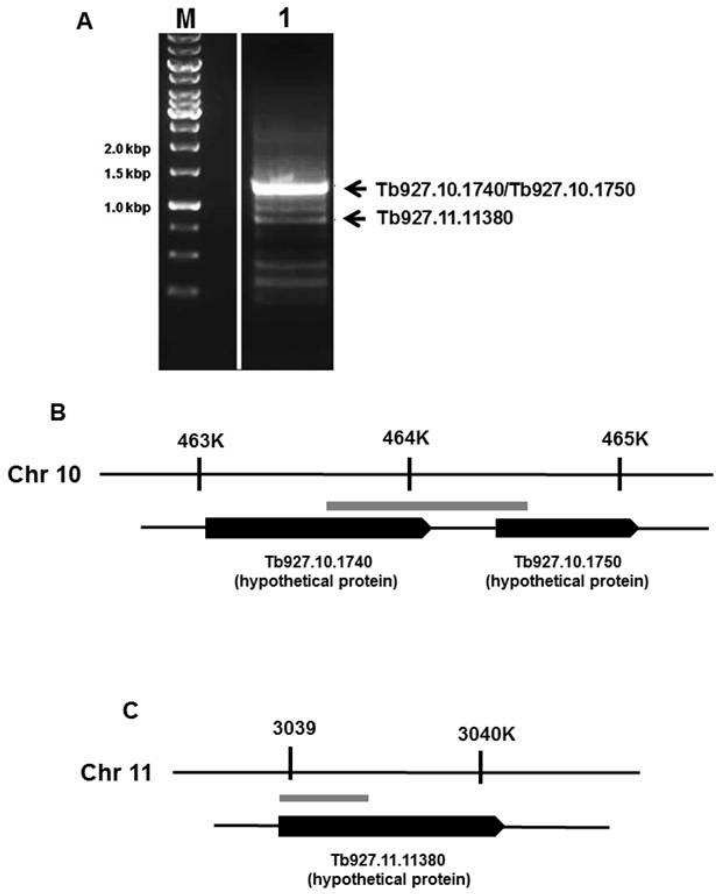

Figure 7.12:Identification of BG-M2 resistance determinants. (A) Amplification of the RNAi targets from the BG-M2 screen using gDNA extracted on day 14 of the selection using PCR conditions described (Alsford *et al*. 2012; Glover *et al*. 2015) (lane 1). M indicates a size marker in base pairs. Arrows indicate the DNA fragments obtained from the screen. (B) and (C) The position of the DNA fragments recovered from the BG-M2 RNAi relative to the genome locations are shown by the grey boxes.

Bioinformatic analysis of the three BG-M2 resistance determinants were carried out as described previously, however no putative domains were identified. Using the RNAit algorithm, DNA fragments containing sequences internal to Tb*ORF1*, Tb*ORF2* and Tb*ORF3* were amplified from *T. brucei* genomic DNA and the resultant fragments cloned into the $p2T7^{Ti}$ RNAi vector. Each construct was then processed before being transfected into *T. brucei*SMB. Following selection of recombinant parasites, the growth of each line was followed (in triplet) (data not shown) and in all cases cells induced to undergo RNAi were viable and grew at the same rate as non-induced controls, having a doubling time of around 8 hours. The susceptibility of each cell line towards BG-M2 while induced to undergo RNAi was then evaluated (Figure 7.13). From the resultant dose response curves and IC_{50} values, parasites undergoing RNAi, irrespective of which transcript was being targeted, exhibited a similar sensitivity to BG-M2 as wild type. This suggests that loss of function of TbORF1 to 3 does not lead to resistance to the O^6–benzylguanine derivative. As no potential activator was identified from the above RNAi library screen, BG-M2 appears not to function as a prodrug in *T. brucei*.

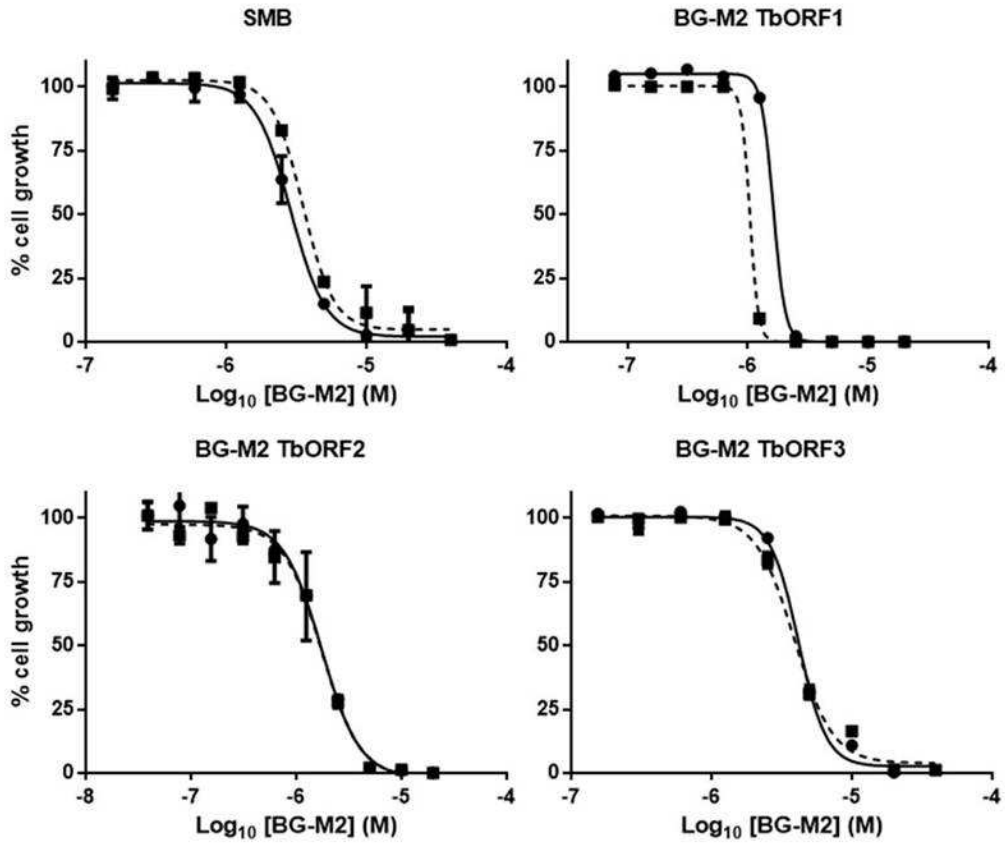

Figure 7.13: Susceptibility of *T. brucei* RNAi lines to BG-M2. Dose response curve of tetracycline induced (dashed line) and non-induced (solid line) BSF *T. brucei* to BG-M2. All data are means for experiments performed in quadruplicate ± standard deviation.

Chapter 7 summary

This chapter has focused on trying to unravel the mechanism of action of two nitrobenzyl based compounds, CB1954 and BG-M2. We have demonstrated that:

1. Screening of an RNAi library using CB1954 as a selective agent identified TbNTR as the major resistance determinant to this compound resistant parasites, confirming previous findings (Bot *et al* 2010).
2. *T. brucei* Tb*ntr* heterozygote parasites are resistant to CB1954, with these recombinant cells having an IC_{50} value ~3-fold greater than wild type
3. Other possible determinants identified from the CB1954 selected RNAi library parasite population were shown not to be involved in mediating resistance to CB1954.
4. The O^6-alkylguanine-DNA alkyltransferase inhibitor BG-M2 displays trypanocidal activity.
5. Screening of an RNAi library using BG-M2 as selective agent indicates that this compound does not function as a prodrug in *T. brucei*despite containing a nitrobenzyl grouping.

Chapter 8. Discussion

Estimates indicate that as many as 50 million people living in sub-Saharan Africa are at risk of contracting HAT. The arsenal of drugs currently used to combat this infection are problematic as they cause adverse side effects, have limited efficacy and require medical supervision with lengthy treatment times. To further complicate drug therapy, resistance is on the raise (Barrett *et al*. 2003; Delespaux & de Koning 2007; Wilkinson & Kelly 2009). Against this backdrop there is an urgent call for new antitrypanosomatid therapies to enter the market.

The natural world has provided us with a range of medicinal agents that can be used to treat infectious diseases (e.g. quinine, penicillin, artemisinin), cancer (e.g. taxol, bleomycin) and as analgesics (e.g. salicin, morphine) (Kayser *et al*. 2003). One group of natural compounds that have been exploited for their pharmacological properties are the quinones. Frequently used in folk medicine, structures such as plumbagin, emodin, lapachol, senna, menatetrenone, nigrosporin have been chemically derivatized to generate synthetic agents that function on a variety of different biological pathways.

Here, we investigated the antiparasitic properties of a library of quinone based chemicals against the three trypanosomatid species *Trypanosoma brucei*, *Trypanosoma cruzi* and *Leishmania major* with these structures spanning a range of carbocyclic backbones. Together, 24, 15 and 22 quinones yielded IC_{50}'s of < 1 µM against *T. brucei*, *T. cruzi* and *L. major* respectively, with 6, 6 and 3 of these generating values below 100 nM. When comparing the potency of each compound class, representative members of each demonstrated significant activity against one

or more of the pathogens tested. For example, the natural product mitomycin c, an indolequinone, exhibited activity against all three parasites having a high level of potency towards *T. brucei* (IC_{50} value of 20 nM) but was less effective against *T. cruzi* (IC_{50} of 2.1 µM) and *L. major* (IC_{50} of 4.2 µM) while the 1,4 benzoquinone RH1 displayed an equivalent activities against all parasites (IC_{50}'s ranging from 20 nM against *T. brucei* to 68 nM against *L. major* (Table 3.1)). Based on the entire growth inhibition data sets, no one single group of quinone exhibited a greater antiparasitic activity than any of the others.

More than half of the quinones tested belong to a related sub-group with all members containing a 1,4 benzoquinone backbone and two aziridinyl groups at the 2 and 5 positions. The sheer number of compounds available gave us scope to conduct SAR studies with these focusing on the medically relevant BSF *T. brucei*: such studies were not performed using the *T. cruzi* and *L. major* growth inhibitory data as these screens were carried out on insect form parasites.

For most of the 1,4 benzoquinone structures, the 3 and 6 positions contained equivalent substitutions (e.g., H for DZQ, **22**&**23**, CH_3 for MeDZQ, aziridinyl for **22** etc.), although in some cases divergent groupings were present (e.g., CH_2OH and CH_3 in RH1, aziridinyl and H in TZQ, or morpholinyl and F in **14**). Whether a compound does or does not possess equivalent substitutions at these sites played no role in determining the potency of the compound: MeDZQ and RH1 both generate IC_{50}'s of around 20 nM. When comparing the effect of compounds containing simple side chains at the 3 and 6 positions, the presence of small hydrocarbon chains such as methyl and/or hydroxymethyl (see MeDZQ and RH1 in Table 3.1) resulted in the

greatest trypanocidal activity relative those that containing hydrogen (DZQ), halogen (**3**, **4**) or amine (**9**) substituents. This may be because these small hydrocarbon chains may promote interaction of enzymes such as the trypanosomal type I NTR with the substrate or could help these structures (or their products) accessing their site(s) of action (Hall *et al* 2012).

For most (thirteen) compounds containing an amine or amide grouping attached *via* the nitrogen atom to the 3 and 6 positions no activity against *T. brucei* at 10 µM was observed, with some of these reported to be poor substrates for the trypanosomal type I NTR (Hall *et al*. 2012). By analogy with the situation in mammalian toxicity studies, the presence of such bulky side chains may decrease the ability of the prodrug to produce DNA damage by hindering access to the oxygen on the carbonyl groupings on the 1,4 benzoquinone backbone thus minimising their conversion to the corresponding hydroxyl or by reducing electron movement around the carbocyclic backbone following activation that then facilitates unfolding of the aziridine (Fourie *et al*2004).

By analysis of the *T. brucei* IC_{50} data there appears to be a direct correlation between the number of aziridine groupings attached to the 1,4 benzoquinone backbone and the trypanocidal activity such that compounds that possess more of these motifs generates increased potency. For the tetra- (**22**), tri- (TZQ) and bi- (DZQ) aziridinyl compounds IC_{50}'s of ~ 150, 180 and 270 nM was observed. This increased activity may be due to the ability of the compound to form interstrand and intrastrand DNA crosslinks, such that the presence of three or more aziridinyl substituents may

promote multiple mutagenic lesions within DNA whereas those that contain a pair of these groups can only form a single crosslink.

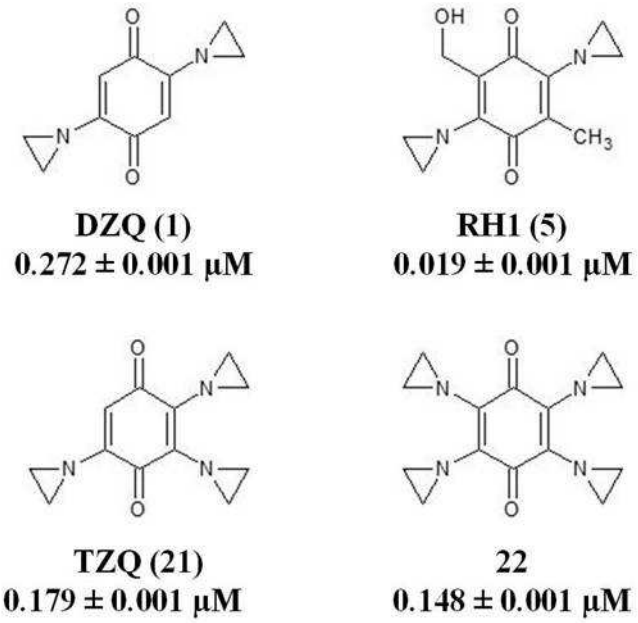

Figure 8.1: The effect of the aziridine motif upon the benzoquinone backbone and trypanocidal properties. IC_{50} values shown are the compound activity against BSF *T. brucei* displayed in Table 3.1.

Based on whether the aziridine groupings at the 2 and 5 positions on the 1,4 benzoquinone backbone contain substituent groupings, these compounds can be split into those that do not have any attached motifs (**1**-**22**; designated here as ABQs) from those that have methyl substituent(s) (**23**-**34**; designated here as MeABQs). In general the MeABQs, irrespective of the number (1 or 2) of methyl attachments, displayed a lower activity against *T. brucei* than their non-substituted counterparts. For example the three 2,5-dibromo ABQs **3**, **25** and **26** contain 0, 1 and 2 methyl groups upon each of the aziridine groups respectively, with the trypanocidal effect of the agents decreasing as the number of methyl groups increases (Figure 8.2). Similarly, DZQ (**1**) which does not contain a methyl substitution is more potent towards *T. brucei* than its methyl containing counterparts (**23**, **24**) with this effect extending to other quinone such as the naphthoquinones: compare the IC_{50} values of

41, **42** and **49** (Figure 8.2). This pattern is in keeping with observations made in high throughput oncological assays where the MeABQs were deemed inactive whereas the unsubstituted ABQ counterparts had significant anti-cancer properties (see Pubchem BioAssay results). One possible explanation accounting for such a trend may be that following prodrug activation, the methyl groups upon the aziridine ring hinders the unfolding of the aziridine ring to form an alkyl group that then promotes DNA adduct formation.

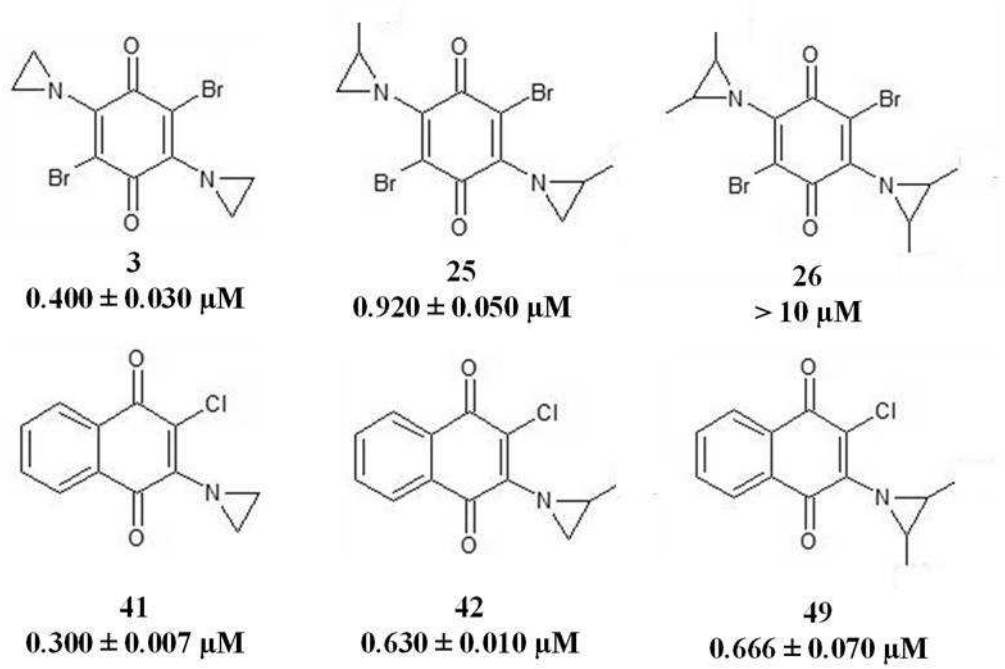

Figure 8.2: The effect of methyl addition on the aziridine ring. IC_{50} values shown are the compound activity against BSF *T. brucei*.This effect is also observed in chloride containing ABQ and MeABQs.

As ABQs tended to show activity against all three trypanosomatid lines tested, the toxicity of selected members was investigated against the immortal THP-1 mammalian cell line (Table 3.2). For all structures, growth inhibitory effects were observed with all except one generating a LD_{50} value below 10 µM with some yielding values < 100 nM. Given that many of the available ABQs have been

selected and trialled for use against hypoxic cancers it is probably not surprising that these compounds did exert such a potent effect on a mammalian line derived from a patient with acute monocytic leukaemia (Schilsky *et al*. 1982; Tan *et al*. 1984; Falletta *et al*. 1990; Danson *et al*. 2011). To determine whether this toxicity was limited to immortal cells some of the ABQ were screened against peritoneal macrophages extracted from BALB/c mice (in collaboration with Dr K Seifert (LSHTM)). This demonstrated that all compounds tested blocked cell growth at concentrations < 1 μM thus showing that *in vitro* even against primary cells ABQs show significant toxicity. As such this type of compound is unlikely to be beneficial in targeting systemic trypanosomal/leishmanial infections although may still be of use in treating cutaneous lesions. Against this disappointing result we begun to view quinones as a whole and ABQs in particular not as potential anti-trypanosomatid drugs but rather as chemical tools for dissecting biochemical pathways in the parasite.

Many nitroaromatic compounds can function as prodrugs, which require activation before exerting their effect. One enzyme that has been linked to the activation of nitro based compounds is the type I nitroreductase (NTR) (Wilkinson *et al*. 2008; Sokolova *et al*. 2010). This oxidoreductase is present in prokaryotes and absent from eukaryotes with some protozoan parasites being an exception to this rule (de Oliveira *et al*. 2007; Wilkinson *et al*. 2008; Pal *et al*. 2009; Hall *et al*. 2010; Voak *et al*. 2013). The trypanosomatid type I NTRs are FMN containing, oxygen insensitive enzymes that using NADH to mediate a 2 electron reduction of the conserved nitro group to generate cytotoxic products (Wilkinson *et al*. 2008; Hall *et al*. 2010; Hall & Wilkinson 2011; Hall *et al*. 2011; Hall *et al*. 2012). The mammalian equivalent to

this activity is NQO1, a protein known to be upregulated in many hypoxic cancers (Ross *et al*. 2000; Siegel *et al*. 2012; Parkinson *et al*. 2013). Several of the quinones evaluated in this thesis as anti-trypanosomatid agents have been demonstrated to be undergo NQO1 mediated activation with this mechanism of activation being key to their anti-cancer activity (Nemeikait-Čniene *et al*. 2003; Tudor *et al*. 2005; Siegel *et al*. 2012). As many of these quinones display antimicrobial activity against BSF *T. brucei* we decided to investigate their mechanism of action by selecting a whole genome loss of function library developed by Sam Alsford and David Horn (Alsford *et al*. 2012) for resistance to RH1, the archetypal ABQ. From this screen a resistant parasite population was selected (Figure 4.1). A low resolution PCR-based analysis of the genomes of this polyclonal population revealed that the major transcript undergoing down regulation was the trypanosomal type I NTR (Figure 4.1) with reduction of the encoded activity sufficient to generate the resistance phenotype. As a link between the level of this enzyme and prodrug activation has been previously reported (Wilkinson *et al*. 2008; Alsford *et al*. 2012; Hall *et al*. 2012) then this observation provides evidence that RH1 functions as a prodrug in *T. brucei* with this particular oxidoreductase playing a key role in the metabolism of this particular ABQ. To conclusively demonstrate this link between NTR and the trypanocidal activity of RH1 the susceptibility of parasites engineered to express altered levels of Tb*ntr* to this compound was investigated (Figures 4.4 and 4.5). This demonstrated that trypanosomes expressing reduced levels of TbNTR displayed a 2.5-fold level of resistance to this ABQ relative to controls while cells with elevated levels of the enzyme were ~ 4-fold more susceptible. This indicates that the trypanosomal type I NTR does indeed activate RH1 *in vivo*. Furthermore kinetic studies using purified recombinant TbNTR and quinone based compounds demonstrated that the enzyme

showed a greater affinity (K_{cat}/K_m) towards the quinones than the nitroaromatic compounds (Hall *et al*. 2012). The overexpression and kinetic studies lead us to conclude that TbNTR can function as a quinone oxidoreductase.

Additional evidence relating to the anti-trypanosomal mechanism of action of ABQs stemmed from selection of RH1 resistant clonal lines generated from wild type *T. brucei*. The parasites obtained from this experiment displayed a statistically significant increase in their IC_{50} values relative to wild type with this phenotype being stable in the absence of selective pressure. Previous studies using *T. cruzi* has shown that there is a direct link between benznidazole or nifurtimox resistance and TcNTR activity with two distinct mechanism leading to this phenotype: reduction of this oxidoreductase activity can arise *via* 1. loss of one of the alleles containing Tc*ntr* or 2. the acquisition of missense mutations in the Tc*ntr* coding sequence resulting in production of non-functional TcNTR protein (Wilkinson *et al*. 2008; Mejia *et al*. 2012; Bot and Wilkinson unpublished). Analysis of the copy number and sequence of Tb*ntr* revealed that neither of these had been altered in the *T. brucei* RH1 resistance lines. However, when these studies were extended to look at expression, a three-fold reduction in Tb*ntr* mRNA was observed (Figure 5.7). The mechanism that led to a decrease of this transcript was not investigated here but could be due to sequence differences in the 5' and/or 3' untranslated regions of Tb*ntr* affecting mRNA processing or stability. This does warrant further attention as it may inform as to how *T. brucei* can acquire resistance to other drugs.

Once the above link between RH1 and NTR had been established we next evaluated whether other ABQs could also undergo a similar mechanism of activation within

the parasite (Figure 4.6). For five of the six compounds tested a similar hypersensitivity profile to that observed using RH1 was displayed by trypanosomes expressing elevated levels of TbNTR, with all five of these structures also being thus deemed good substrates for this enzyme *in vitro* (Hall *et al* 2013). The only quinone that did not follow this pattern was the tetra-aziridinyl compound **22** (Figure 8.1), which also happened to be one structure previously shown not to be metabolized by TbNTR *in vitro* (Hall *et al* 2013). The reasons why **22** does not interact with TbNTR may be due to a steric hindrance effect of multiple (four) aziridinyl groupings attached to the 1,4 benzoquinone core or an electronic inductive and resonance properties exerted by all six substituents on the carbocyclic backbone (Figure 8.3). In either case, the two carbonyl oxygen atoms are blocked or electronically neutralized thereby preventing their reduction by the trypanosomal type I NTR. Based on our observations, compound **22** appears to mediate its activity *via* an another mechanism to all the other ABQs analysed here possibly using another alternative activation system, assuming that this particular agent does function as a prodrug.

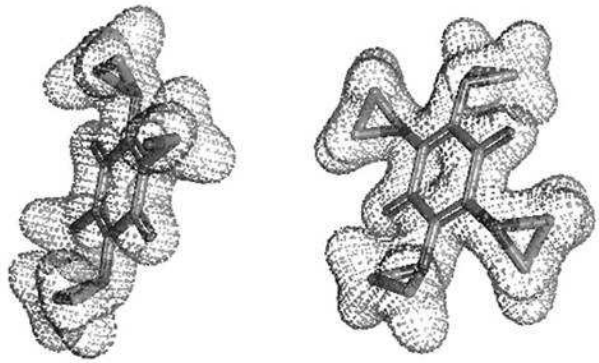

Figure 8.3: Space arrangement of RH1 and 22. The presence of four nitrogen containing side groups forces compound **22** into the orientation observed here. The resultant shape may prevent the reduction of **22** by TbNTR. Images obtained using PubChem3D (Bolton *et al*. 2011)

Cytochrome P450 reductases (CPRs) represent a class of membrane bound, FNM- and FAD-containing enzyme that utilize NADPH to mediate reduction of cytochrome P450 (Iyanagi 2005; Masters 2005; Portal *et al*. 2008). Their activity can be subverted such that they can catalyse the one electron reduction of other substrates such as nitroaromatic and quinone-based compound that in the presence of oxygen results in formation of reactive oxygen species which can then promote oxidative stress. As such CPRs are representative of the so-called type II NTRs. In trypanosomes several CPRs have been identified (Portal *et al*. 2008; Hall *et al*. 2011) with the role of at least one of these being implicated in the sterol biosynthesis pathway (De Vas *et al*. 2011). As noted, **22** is the only structure tested that does not interact TbNTR *in vitro* and *in vivo*(Hall *et al*. 2012). As we hypothesized that this compound most likely functions as a prodrug we evaluated whether it could undergo activation *via* a one electron reduction mechanism by evaluating the susceptibility of two *T. brucei* lines engineered to express ectopic copies of CPR (isoforms 2 or 3) (Figures 4.7 and 4.8). This demonstrated that trypanosomes expressing elevated levels of either of these enzymes were up to 25-fold more susceptible to **22** than controls indicating that the trypanosomal CPRs are indeed involved in the activation of this particular ABQ *in vivo*. This activity was specific to **22** as these recombinant parasite lines exhibited the same sensitivities to the other ABQs (and to nitroaromatic produgs – see Hall & Wilkinson 2011; Bot *et al*. 2013) as wild type.

The ABQs evaluated here for their anti-trypanosomatid properties were initially designed to function as anti-cancer agents that following activation promote double stranded DNA breaks *via* the formation of interstrand DNA cross links (ICLs)

(Figure 1.10 and 1.11) (Fourie *et al*. 2004; Pierce *et al*. 2011). Following activation by an oxidoreductase(s), the carbonyl oxygen atoms are reduced to the corresponding hydroxyl to form a hydroquinone intermediate having the knock on effect of causing an increase in the pKa of the aziridine nitrogen. This facilitates protonation of this atom to form an aziridinium cation that is attracted to nucleophilic DNA strand. Interaction of the aziridinium cation with the nucleic acid promotes unfolding to form aziridinyl ring exposing an alkyl group that then covalently bonds to DNA, preferentially targeting guanine residues. This then triggers the same process to occur at the second aziridine group present on the ABQ eventually leading to a linkage across onto a residue on the complementary strand (Figure 1.11). Once this cross linkage has been formed, the "activated" hydroxyl groups undergo oxidation to reform the carbonyl oxygen groups of the 1,4 benzoquinone core (Rajski & Williams 1998). If not repaired, this covalent link blocks any process that requires separation of the DNA strands that can lead to double stranded DNA breaks. The lethality of this resultant lesion is such that a single ICL can induce cell death in unicellular organisms whilst as little as 20 can be fatal to a mammalian cell (Magaña-Schwencke *et al*. 1982; Lawley & Phillips 1996). To combat such insults, all cells have evolved a series of complementary and overlapping pathways that function to repair this damage thus preserving a genome's integrity with members of the so-called PSO2p/SNM1 family of nucleases playing a key role in one arm of these processes (Li *et al*. 2005; Barber *et al*. 2005; Dudáš *et al*. 2007). Recently, we have identified and characterised a *T. brucei* homologue of this protein, designated as TbSNM1 (Sullivan *et al*. 2015). An *in silico* analysis reveal that this protein possessed many of the key functional domains exhibited by the yeast and human orthologues including MBL, β-CASP and ubiquitin zinc finger

domains (Sullivan *et al*. 2015). Gene deletion studies revealed that the encoded activity was not essential for the growth of the clinically relevant stage of the African trypanosome although cells lacking TbSNM1 were hypersensitive towards multifunctional DNA alkylating agents such as the nitrogen mustards and aziridine based therapies. Here, we have shown that ABQs exhibit a similar phenotype to the previously screened ICL inducing agents such that trypanosomes null for Tb*snm1* are ~3-fold more sensitive towards the di- and tri-functional aziridine compounds (DZQ, RH1 and TZQ) and ~ 6-fold more sensitive towards the tetra aziridine compound **22** than wild type, a phenotype that can be reversed by expression of ectopic copies of the repair enzyme (Table 5.2) It is well documented that bi-, tri- and tetra- alkylating agents are clastogenic therefore integration of these agents within the DNA duplex results in structural chromosomal changes with this promoting double strand breaks (Noll *et al*. 2006). The difference in sensitivity of the Tb*snm1* null mutant trypanosomes to the different types of ABQs tested could reflect the degree of lesions that each agent can induce within the parasite's genome. In this context DZQ, RH1 and TZQ contain sufficient aziridine substituents (two) to generate a single ICL, with RH1 and TZQ also having the potential to form intrastrand cross links *via* an additional reactive grouping: for RH1 this is a hydroxyl and TZQ a third aziridine. For **22**, two pairs of the aziridinyl could potentially generate two ICLs within close proximity to each other, inducing severe structural changes to the DNA helix.

The susceptibility of Tb*snm1* null mutant *T. brucei* to ICL inducing ABQ produgs was exacerbated by manipulation of the bioreductive activation mechanism. To achieve this, the Tb*snm1* alleles in *T. brucei* expressing ectopic copies

ofmitochondrial prodrug activators Tb*ntr*, Tb*cpr2* and Tb*cpr3* were disrupted (Hall *et al*. 2011; Sullivan *et al*. 2015). In line with previous data (Sullivan *et al* 2015), parasites lacking TbSNM1 activity but expressing elevated TbNTR were ~ 15- and ~ 5-fold more susceptible towards the TbNTR activated compounds ABQs than wild type and Tb*snm1* null mutant parasites, respectively (Figure 5.3; Table 5.3). When this analysis was extended to **22** using parasites lacking TbSNM1 activity but expressing elevated TbCPR2 or 3, a similar trend was observed (Figure 5.4; Table 5.4). Together this indicates that upon activation by TbNTR (RH1 and TZQ) or TbCPR (**22**) the resultant ABQ hydroquinone products are able to leave the organelles where the above enzymes are/postulated to be located (TbNTR is found in the mitochondrion while TbCPRs are believed to in the endoplasmic reticulum) and access the parasites nucleus where they can interact with the nuclear genome to promote ICL formation. By elevating the level of the activator (TbNTR or TbCPRs) the rate and hence amount of hydroquinone formed is increased leading to a degree of DNA damage that can then be exacerbated in the absence of the nuclear ICL repair protein SNM1.

The whole genome loss of function (RNAi) assay developed by Alsford (LSHTM) and Horn (University of Dundee) has greatly aided in our understanding of how all the clinically used anti-HAT drugs mediate their activities being especially useful in identifying uptake mechanisms and prodrug activators (Baker *et al*. 2011; Alsford *et al*. 2012). Here, we have used this approach to inform us as to the mechanism of action of not only RH1 but also of CB1954, an aziridine benzamide. As with RH1, a low resolution screen of the CB1954 resistant populations identified TbNTR as the key player in resistance, in agreement of the previous findings (Bot *et al* 2010).

Intriguingly, RH1 or CB1954 selection failed to identify sequences encoding for any obvious transporter, the type of transcript normally enriched in this sort of study (Baker *et al*. 2011; Alsford *et al*. 2012), suggesting that these two compounds can readily cross biological membranes without the need for a transporter. Indeed the indices of polar surface area (PSA), a measure of the hydrophobicity of a given agent, and partition coefficient (LogP), a measure of the affinity of a molecule for a lipophilic environment, of both RH1 and CB1954 meet the parameters defined by Lipinski's rule of five and more recent computational drug models suggest that these moieties can readily pass through the biological membrane without the aid of a transporter (Clark & Pickett 2000) (Table 8.1).

Drug	**Hydrogen bond**		**Molecular weight**	**LogP3**	**Polar surface area (PSA) (A^2)**
	acceptors	**donors**			
RH1	1	5	234	0.1	60.4
CB1954	6	1	252	0	138
Nifurtimox	7	0	287	1.3	117
Lipinski's rule	≤ 10	≤ 5	< 500	-0.4 - +5.6	≤ 140

Table 8.1: Physiochemical properties of RH1, CB1954 and nifurtimox in accordance to Lipinski's rule of five for drug likeness.

When the CB1954 selected population was subject to an indepth deep sequence analysis, a number of additional 'hits' were identified. When these sequences were analysed further by using RNAi to target specific transcripts all of the resultant *T. brucei* cell lines exhibited similar sensitivities to CB1954 as to the controls. This indicates that either the RNAi vector used (a head to head promoter arrangement)

was not down regulating gene expression sufficiently to generate a resistance phenotype (unlikely) or that all of the “hits” were false positives and have nothing to do with the biology underlying CB1954’s mode of action (more likely). Ideally, a northern blot analysis of the RNAi cell lines would confirm whether down regulation of the transcript had occurred but we were unable to establish this due to the lack of facilities in the department at present.

Chapter 9: Future work

This project has explored the potential use of quinone based compounds as anti-trypanosomatid therapies with our primary focus being on the ABQs. Our work has shown that these agents displayed potent anti-parasitic activity although their mammalian toxicity may hinder their use as treatment for systematic parasitic infections. Therefore, we came to the conclusion that these structures should be viewed as chemical tools to explore trypanosome biology.

In Chapter 4, we considered the mode of action of selected ABQ compounds. In most cases these chemicals were metabolised by a trypanosomal type I NTR both *in vivo* and *in vitro*. Further studies using these structures could revolve around the identification and characterisation of the reduction products generated following NTR-mediated activation. This could involve performing enzyme assays using the ABQ as substrate then the fractionation and identification of the resultant material using LC/MS similar to that previously conducted by Hall *et al*. (2011) and Hall & Wilkinson (2012). It may be possible to purify the reduction products by modification of the above procedure such that these activation structures could be used in anti-proliferation screens against trypanosomatid and mammalian cells. Additionally, *in silico* docking of the trypanosomal type I NTR with the selected ABQs could be performed following the determination of the structure of this enzyme (work being performed in conjunction with Dr Nonato, University of Sao Paulo) or by fitting the parasite protein onto an existing bacterial homologue framework. This would aid in drug design targeting this particular oxidoreductase, potentially highlighting differences between the human NQO1 and parasitic NTR that can be exploited to develop specific quinone-based compounds that can

discriminate between the host and pathogen activities. A similar type of analysis to this could be performed using compound **22**, the only ABQ identified here as undergoing an alternative mechanism of activation. In these studies we would use the trypanosomal CPRs in place of NTR to conduct the above experiments.

Regarding mechanism of action following activation, all the ABQs tested in this thesis appear to function as DNA alkylating agents promoting nucleic acid damage. Our primarily focus in this area replied on phenotypic screens using trypanosomes null for the DNA repair protein SNM1(Sullivan *et al*. 2015)with these recombinant cells being more susceptibility to a specific set of damaging agents that promote ICL formation. To conclusively demonstrate this link *in vitro* the NTR (or CPR) activated ABQs could be used to treat double stranded DNA with the resultant products analysed by various means including Isothermal titration calorimetry or by LC/MS. Additionally, *in vivo* studies using wild type and TbSNM1 null mutant parasites treated with an ICL inducing agent could be undertaken using a qPCR based technique similar to that described by Machado and colleagues (2014).

Further studies aimed at evaluating the role of SNM1 could be undertaken to ascertain whether, in response to DNA damage, the localisation of this protein changes, if this protein undergoes post translational modification, characterisation of SNM1 interacting partners and identification of potential inhibitors of this activity. In the latter case this could potentially lead to structures that exacerbate the DNA damaging activity of compounds such as the ABQs and could help improve these compounds selectivity against the trypanosome relative to the mammalian cell. Furthermore, additional proteins involved in the ICL repair pathway could be

identified following informatics screens (*e.g.* trypanosomal homologues of the mammalian fanconi anaemiaDNA interstand cross-link repair pathway, homologous repair *etc*) with functional studies conducted aimed at unravelling whether these have an eptistatic or non-eptistatic effect in relation to SNM1.

In Chapter 6, we reported the selection of an RH1 resistance *T. brucei* line and were able to determine that *ntr* played a role in mediating the phenotypes displayed by these cells. The mechanism responsible for these properties *via* the down regulation of the encoded transcript was not established here but could warrant further attention as this process could explain how resistance to other NTR activated (and non-activated) drugs may arise. Intriguingly not all of the phenotypic properties shown by the RH1 resistant*T. brucei* line could be explained by down regulation of this oxidoreductase. Therefore a more in depth analysis of these cells would be required based around using high throughput genomic or transcriptomic sequence analysis. This could provide a global insight into how these cells respond to the damage caused by ICL forming agents.

Thesis findings

1. A range of compounds possessing a quinone core display significant anti-parasitic activity against the medically and veterinary relevant form of *T. brucei* and against the replicative *T. cruzi* and *L. major* stages found in the insect vector.
2. Several compounds yielded very low IC_{50} values (< 100nM) indicating that these were of promise in treatment development targeting trypanosomiasis and leishmaniasis.
3. Unfortunately further evaluation of one particular grouping, the ABQs, which display potent anti-trypanosomatid activity revealed that they also exhibited significant toxicity against primary and secondary mammalian cell lines (macrophages and macrophage-like cells). As such these agents could not be considered as therapies for the systemic forms of trypanocidal infections.
4. Using ABQs as chemical tools to understand biological function we demonstrated that these compounds function as prodrugs with different mechanisms operating to activate different types of closely related compounds: TbNTR functions as activator of ABQs such as RH1, DZQ and TZQ while TbCPR2 and TbCPR3 can metabolize compound **22**.
5. Following activation (by which ever mechanism) the ABQs then mediate their trypanocidal activity by promoting DNA damage *via* the formation of ICLs in the trypanosome nuclear genome with the DNA repair protein SNM1 playing a key role in fixing this type of damage.

Appendix 1:Structures of the compounds used in this project

Aziridinyl 1,4-benzoquinones

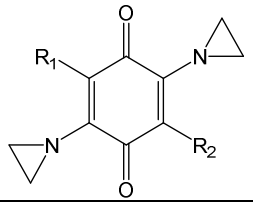

Compound	NSC#	IUPAC	Structure
DZQ (**1**)	30706	2,5-bis(1-aziridinyl)-1,4-benzoquinone	R_1=R_2=H
MeDZQ (**2**)	646714	2,5-dimethyl-3,6-diaziridinyl-1,4-benzoquinone	R_1=R_2=CH_3
3	197039	2,5-bis(aziridin-1-yl)-3,6-dibromocyclohexa-2,5-diene-1,4-dione	R_1=R_2=Br
4	208829	3,6-difluoro-2,5-bis(aziridinyl)-1,4-benzoquinone	R_1=R_2=F
RH1 (**5**)	697726	2,5-bis(aziridin-1-yl)-3-(hydroxymethyl)-6-methylcyclohexa-2,5-diene-1,4-dione	R_1=CH_2OH; R_2=CH_3
6	95139	2,5-bis(aziridin-1-yl)-3,6-dimethoxycyclohexa-2,5-diene-1,4-dione	R_1=R_2=OCH_3
7	18270	2,5-bis(aziridin-1-yl)-3,6-diethoxycyclohexa-2,5-diene-1,4-dione	R_1=R_2=OCH_2CH_3
8	17261	2,5-bis(aziridin-1-yl)-3,6-dipropoxycyclohexa-2,5-diene-1,4-dione	R_1=R_2=$O(CH_2)_2CH_3$
9	246111	2,5-diamino-3,6-bis(aziridin-1-yl)cyclohexa-2,5-diene-1,4-dione	R_1=R_2=NH_2
10	220267	2,5-bis(aziridin-1-yl)-3,6-bis(methylamino)cyclohexa-2,5-diene-1,4-dione	R_1=R_2=$NHCH_3$
11	224066	2,5-bis(aziridin-1-yl)-3,6-bis(ethylamino)cyclohexa-2,5-diene-1,4-dione	R_1=R_2=$NHCH_2CH_3$
12	328408	2,5-bis(aziridin-1-yl)-3,6-bis(heptylamino)cyclohexa-2,5-diene-1,4-dione	R_1=R_2=$NH(CH_2)_6CH_3$
13	249989	2,5-bis(aziridin-1-yl)-3,6-bis(dimethylamino)cyclohexa-2,5-diene-1,4-dione	R_1=R_2=$NH(CH_3)CH_3$
14	251728	2,5-bis(aziridin-1-yl)-3-fluoro-6-morpholin-4-ylcyclohexa-2,5-diene-1,4-dione	R_1=morpholinyl; R_2=F
15	18269	N-[4-acetamido-2,5-bis(aziridin-1-yl)-3,6-dioxocyclohexa-1,4-dien-1-yl]acetamide	R_1=R_2=$NHCOCH_3$
16	18271	N-[2,5-bis(aziridin-1-yl)-3,6-dioxo-4-(propanoylamino)cyclohexa-1,4-dien-1-yl]propanamide	R_1=R_2=$NHCOCH_2CH_3$
17	18274	N-[2,5-bis(aziridin-1-yl)-4-(butanoylamino)-3,6-dioxocyclohexa-1,4-dien-1-yl]butanamide	R_1=R_2=$NHCO(CH_2)_2CH_3$
18	51916	-[2,5-bis(aziridin-1-yl)-4-(heptanoylamino)-3,6-dioxocyclohexa-1,4-dien-1-yl]heptanamide	R_1=R_2=$NHCO(CH_2)_5CH_3$
19	51915	N-[2,5-bis(aziridin-1-yl)-4-(cyclohexanecarbonylamino)-3,6-dioxocyclohexa-1,4-dien-1-yl]cyclohexanecarboxamide	R_1=R_2=NHCOPhenyl
AZQ (**20**)	182986	ethyl N-[2,5-bis(aziridin-1-yl)-4-(ethoxycarbonylamino)-3,6-dioxocyclohexa-1,4-dien-1-yl]carbamate	R_1=R_2=$NHC(O)OCH_2CH_3$
TZQ (**21**)	29215	2,3,5-tris(aziridin-1-yl)cyclohexa-2,5-diene-1,4-dione	R_1=aziridinyl; R_2=H
22	31717	2,3,5,6-tetrakis(aziridin-1-yl)cyclohexa-2,5-diene-1,4-dione	R_1=R_2=aziridinyl

Methyl and di-methyl substituted aziridinyl 1,4-benzoquinones

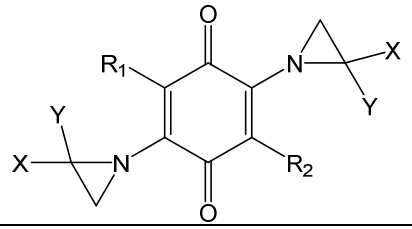

Compound	NSC#	IUPAC	Structure
23	83705	2,5-bis[(2r)-2-methylaziridin-1-yl]cyclohexa-2,5-diene-1,4-dione	R_1=R_2=X=H;Y=CH_3 (r orientation)
24	83706	2,5-bis[(2s)-2-methylaziridin-1-yl]cyclohexa-2,5-diene-1,4-dione	R_1=R_2=X=H;Y=CH_3 (s orientation)
25	197038	2,5-dibromo-3,6-bis(2-methylaziridin-1-yl)cyclohexa-2,5-diene-1,4-dione	R_1=R_2=Br; X=H; Y=CH_3
26	199106	2,5-dibromo-3,6-bis(2,2-dimethylaziridin-1-yl)cyclohexa-2,5-diene-1,4-dione	R_1=R_2=Br; X=Y=CH_3
27	200115	2,5-dichloro-3,6-bis(2-methylaziridin-1-yl)cyclohexa-2,5-diene-1,4-dione	R_1=R_2=Cl; X=H;Y=CH_3
28	202394	2,5-dichloro-3,6-bis(2,2-dimethylaziridin-1-yl)cyclohexa-2,5-diene-1,4-dione	R_1=R_2=Cl; X=Y=CH_3
29	208830	2,5-dichloro-3,6-bis(2,2-dimethylaziridin-1-yl)cyclohexa-2,5-diene-1,4-dione	R_1=R_2=Fl; X=H;Y=CH_3
30	208831	2,5-bis(2,2-dimethylaziridin-1-yl)-3,6-difluorocyclohexa-2,5-diene-1,4-dione	R_1=R_2=Fl; X=Y=CH_3
31	18273	N-[4-acetamido-2,5-bis(2-methylaziridin-1-yl)-3,6-dioxocyclohexa-1,4-dien-1-yl]acetamide	R_1=R_2=$NHCOCH_3$; X=H; Y=CH_3
32	199377	N-[4-acetamido-2,5-bis(2,2-dimethylaziridin-1-yl)-3,6-dioxocyclohexa-1,4-dien-1-yl]acetamide	R_1=R_2=$NHCOCH_3$; X=Y=CH_3
33	18272	N-[2,5-bis(2-methylaziridin-1-yl)-3, 6-dioxo-4-(propanoylamino)cyclohexa-1,4-dien-1-yl]propanamide	R_1=R_2=$NHCO(CH)CH_3$; X=H;Y=CH_3
34	199378	Ethyl N-[2,5-bis(2,2-dimethylaziridin-1-yl)-4-(ethoxycarbonylamino)-3,6-dioxocyclohexa-1,4-dien-1-yl]carbamate	R_1=R_2=$NHCOO(CH)CH_3$; X=Y=CH_3

1,4-naphthoquinones

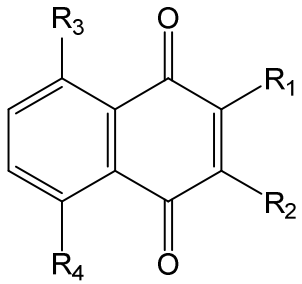

Compound	MTL/NSC#	IUPAC	Structure
Menadione (**35**)	-	2-methylnaphthalene-1,4-dione	R_1=CH_3,R_2=R_3=R_4=H
Plumbagin (**36**)	NSC236613	5-hydroxy-2-methylnaphthalene-1,4-dione	R_1=CH3, R_2=H, R_3=R_4=OH
37	MTL6-022	2,5,8 trimethylnaphthalene-1,4-dione	R_1=R_3=R_4=CH_3, R_2=H,
38	MTL6-023	5,8-dihydroxy-1,4-dihydronaphthalene-1,4-dione	R_1 =R_2 =H, R_3=R_4=OH
39	MTL6-026	2-[(2-chloroethyl)amino]-8-hydroxy-1,4-dihydronaphthalene-1,4-dione	R_1=R_4=H, R_3=OH. R_2=(2-chloroethyl)(methyl)amine,
40	MTL6-027	5,8-dioxo-5,8-dihydronapthalen-1-yl-acetate	R_1=R_2=R_4=H, R_3=$C_2H_4O_2$
41	MTL6-030	2-(aziridin-1-yl)-3-chloro-1,4-dihydronaphthalene-1,4-dione	R_1=Cl, R_2=aziridine, R_3=R_4=H
42	MTL6-031	2-chloro-3-(2-methylaziridin-1-yl)-1,4-dihydronaphthalene-1,4-dione	R_1=Cl, R_2=2-methylaziridine, R_3=R_4=H
43	MTL6-032	3-(aziridin-1-yl)-2-chloro-5-hydroxy-1,4-dihydronaphthlene-1,4-dione	R1=R_4=H, R_2=aziridine, R_3=OH
44	MTL6-033	2-chloro-5-hydroxy-3-(2-methylaziridin-1-yl)-1,4-dihydronaphthalene-1,4-dione	R1=R_4=H, R_2=methylaziridine, R_3=OH
45	-	5-hydroxy-1,4-dihydronaphthalene-1,4-dione	R_1=R_2=R_4=H, R_3=OH
Lapachol (**46**)	MTL6-038	2-hydroxy-3-(3-methylbut-2-en-1-yl)-1,4-dihydronaphthalene-1,4-dione	R_1=OH, R_2=C_6H_{12} , R_3=R_4=H
47	NSC39051	2-(aziridin-1-yl)-3-methoxynaphthalene-1,4-dione	R_1=OCH_3,R_2=aziridine, R_3=R_4=H
48	NSC139346	2-(aziridin-1-yl)-3-methylnaphthalene-1,4-dione	R_1=CH_3, R_2=aziridine, R_3=R_4=H
49	NSC35852	2-chloro-3-(2,3-dimethylaziridin-1-yl)naphthalene-1,4-dione	R_1=Cl, R_2=aziridine, R_3=R_4=H
50	NSC260640	2-[bis(2-chloroethyl)amino]naphthalene-1,4-dione	R_1=R_3=R_4=H, R_2=$N(CH_2CH_2Cl)_2$
51	NSC35854	N-[3-[bis(2-chloroethyl)amino]-1,4-dioxonaphthalen-2-yl]acetamide	R_1=$NOHCH_3$, R_3=R_4=H R_2=$N(CH_2CH_2Cl)_2$

1,4-benzoquinone mustards

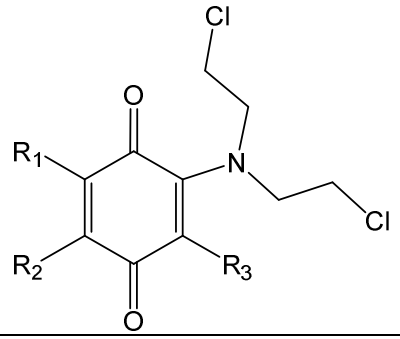

Compound	Alternative name	IUPAC	Structure
52	BM	2-[di(chloroethyl)amino]-1,4-benzoquinone	$R_1=R_2=R_3=H$
53	5MeBM	5-methyl-2-[di(chloroethyl)amino]-1,4-benzoquinone	$R_1=R_3=H$, $R_2=CH_3$
54	5MeOBM	5-methoxy-2-[di(chloroethyl)amino]-1,4-benzoquinone	$R_1=R_3=H$, $R_3=OCH_3$
55	6MeBM	6-methyl-2-[di(chloroethyl)amino]-1,4-benzoquinone	$R_1=CH_3$, $R_2= R_3=H$
56	6PhBM	6-phenyl-2-[di(chloroethyl)amino]-1,4-benzoquinone	R_1=Phenyl, $R_2= R_3=H$

Other aziridinyl-containing quinone.

Compound	NSC#	IUPAC
Mitomycin C (**57**)	26980	[6-Amino-8a-methoxy-5-methyl-4,7-dioxo-1,1a,2,4,7,8,8a,8b-octahydroazireno[2',3':3,4]pyrrolo[1,2-a]indol-8-yl]methyl carbamate
58	651080	[6-(aziridin-1-yl)-7-methyl-5,8-dioxo-2,3-dihydro-1H-pyrrolo[1,2-a]benzimidazol-3-yl] 2-chloroacetate
59	651079	[6-(aziridin-1-yl)-7-methyl-5,8-dioxo-2,3-dihydro-1H-pyrrolo[1,2-a]benzimidazol-3-yl] propanoate

Appendix 2: Chemical and physical properties of the compounds

The values were obtained from the PubChem database (http://pubchem.ncbi.nlm.nih.gov/) or calculated using Molinspiration chemoinformatics software (http://www.molinspiration.com/)

1. Aziridinyl 1,4-benzoquinones

Compound	NSC#	MW (Daltons)	H-bond donors	H-acceptors	Rotatable bonds	clogP	PSA (Å)
DZQ (**1**)	30706	190.20	0	4	2	0.2	40.2
MeDZQ (**2**)	646714	218.25	0	4	2	0.8	40.2
3	197039	347.99	0	4	2	2.0	40.2
4	208829	226.18	0	6	2	0.3	40.2
RH1 (**5**)	697726	234.25	1	5	3	0.1	60.4
6	95139	250.25	0	6	4	0.2	58.6
7	18270	278.30	0	6	6	0.9	58.6
8	17261	306.36	0	6	8	2.0	58.6
9	246111	220.23	2	6	2	-0.7	92.2
10	220267	248.28	2	6	4	0.1	64.2
11	224066	276.33	0	6	6	0.6	64.2
12	328408	416.60	2	6	16	5.6	64.2
13	249989	276.33	0	6	4	1.0	46.6
14	251728	293.29	0	7	3	0.0	52.6
15	18269	304.30	2	6	4	-1.6	98.4
16	18271	332.35	2	6	6	-0.6	98.4
17	18274	360.41	2	6	8	0.1	98.4
18	51916	444.57	2	6	14	3.3	98.4
19	51915	440.54	2	6	6	2.6	98.4
AZQ (**20**)	182986	364.35	2	8	8	0.0	117.0
TZQ (**21**)	29215	231.25	0	5	3	-0.1	43.2
22	31717	272.30	0	6	4	0.8	46.2

2. Methyl and di-methyl substituted aziridinyl 1,4-benzoquinones

Compound	NSC#	MW (Daltons)	H-bond donors	H-acceptors	Rotatable bonds	clogP	PSA (Å)
23	83705	218.25	0	4	2	1.1	40.2
24	83706	218.25	0	4	2	1.1	40.2
25	197038	376.04	0	4	2	2.8	40.2
26	199106	404.10	0	4	2	3.3	40.2
27	200115	287.14	0	4	2	2.7	40.2
28	202394	315.20	0	4	2	3.2	40.2
29	208830	254.23	0	6	2	1.6	40.2
30	208831	282.29	0	6	2	2.1	40.2
31	18273	332.35	2	6	4	-0.2	98.4
32	199377	360.41	2	6	4	-0.3	98.4
33	18272	360.41	2	6	6	0.8	98.4
34	199378	420.46	2	8	8	1.2	117.0

3. 1,4-naphthoquinones

Compound	MTL/NSC#	MW (Daltons)	H-bond donors	H-acceptors	Rotatable bonds	clogP	PSA (Å)
Menadione (**35**)	-	172.18	0	2	0	2.2	34.1
Plumbagin (**36**)	NSC236613	188.18	1	3	0	2.3	54.4
37	MTL6-022	200.23	0	2	0	2.8	34.1
38	MTL6-023	190.15	2	4	0	1.1	74.6
39	MTL6-026	251.66	2	4	3	1.8	66.4
40	MTL6-027	216.19	0	4	2	1.2	60.4
41	MTL6-030	233.65	0	3	1	2.2	37.1
42	MTL6-031	247.68	0	3	1	2.8	37.2
43	MTL6-032	215.20	1	4	1	1.3	27.4
44	MTL6-033	229.23	1	4	1	1.7	27.4
45	-	174.15	1	3	0	1.4	54.4
Lapachol (**46**)	MTL6-038	242.27	1	3	2	2.8	54.4
47	NSC39051	229.23	0	4	2	1.9	46.4
48	NSC139346	213.23	0	3	1	1.5	37.2
49	NSC35852	261.70	0	3	1	3.3	37.2
50	NSC260640	298.16	0	3	5	3.1	37.4
51	NSC35854	355.22	1	4	6	2.3	66.5

4. 1,4-benzoquinone mustards

Compound	Alternative name	MW (Daltons)	H-bond donors	H-acceptors	Rotatable bonds	clogP	PSA (Å)
52	BM	248.11	0	3	5	1.8	37.4
53	5MeBM	262.14	0	3	5	2.2	37.4
54	5MeOBM	278.14	0	4	6	1.1	46.6
55	6MeBM	262.14	0	3	5	2.2	37.4
56	6PhBM	324.21	0	3	6	3.5	37.4

5. Other quinone containing compounds

Compound	NSC#	MW (Daltons)	H-bond donors	H-acceptors	Rotatable bonds	clogP	PSA (Å)
Mitomycin C (**57**)	26980	334.32	3	8	4	-0.4	147.0
58	651080	335.74	0	6	4	1.1	81.3
59	651079	315.32	0	6	4	1.0	81.3

Lipinski's rule states that, in general, an orally active drug has no more than one violation of the following criteria:

- No more than 5 hydrogen bond donors (the total number of nitrogen–hydrogen and oxygen–hydrogen bonds)
- Not more than 10 hydrogen bond acceptors (all nitrogen or oxygen atoms)
- A molecular mass less than 500 daltons (Da)
- An octanol-water partition coefficient log *P* not greater than 5

Polar surface area no greater than 140 $Å^2$

10 or fewer rotatable bonds

Appendix 3: Primers

Primers used to amplify type I nitroreductases and fragments from RNAi library screen. The sequence in lower case italics refers to restriction sites incorporated into the primer to facilitate DNA cloning. The non-italicised, lower case sequence corresponds to a clamp that aids binding of the DNA polymerase to the primer. The identifiers given after a gene name correspond to accession numbers on the Kinetoplastid genome resource TritrypDB (http://tritrypdb.org/tritrypdb/).

Gene & primer name	**Sequence 5' to 3'**
RNAi library screen	
L1B2F	TAGCCCCTCGAGGGCCAGT
L1B2R	GGAATTCGATATCAAGCTTGGC
TbNTR(Tb927.7.7230)	
TbNTR-3	ggg*aagctt*ATGAACGTGAGCCGCGCTGCCGT
TbNTR-4	*gggtctaga*GAAGCGATTCCATCGGACGAG
LmNTR (LmjF.05.0660)	
LmNTR-1	*aaaggatcc*CTCGACGCCGTCGAGGCCGTCG
LmNTR-2	*gggaagctt*CTAGAACTTGTTCCACCGCAC

Primers used to generate RNAi constructs. The sequence in lower case italics refers to restriction sites incorporated into the primer to facilitate DNA cloning. The non-italicised, lower case sequence corresponds to a clamp that aids binding of the DNA polymerase to the primer. The identifiers given after a gene name correspond to accession numbers on the Kinetoplastid genome resource TritrypDB (http://tritrypdb.org/tritrypdb/).

Gene & primer name	Sequence 5' to 3'
TbNTR(Tb927.7.7230)	
TbNTR-RNAi-1	ttt*ggatcc*CCCGTCGACCACACTCTTATC
TbNTR-RNAi-2	ggg*ctcgag*AGCCCACAACCTCCCTAACTT
TbORFa (Tb927.11.6370)	
CB1954-RNAi-1	ttt*ggatcc*AGCGCTGGACCTTTCTGATAA
CB1954-RNAi-2	ggg*ctcgag*CGAGTTGGTTCCGACGTAATA
TbORFb (Tb927.7.7310)	
CB1954-RNAi-3	ttt*ggatcc*TCTCTTGCTTTCCTCGTGCTG
CB1954-RNAi-4	ggg*ctcgag*ACAAACAGGGGCAATTAACGA
TbORFc (Tb927.3.3670)	
CB1954-RNAi-5	ttt*ggatcc*GATGACCTCCAAGAATCGGAA
CB1954-RNAi-6	ggg*ctcgag*GCAGCATAAGCAGGGATAGCG
TbORFd (Tb927.10.3130)	
CB1954-RNAi-7	ttt*ggatcc*GAGTGCCTCAAGAGACAGGGG
CB1954-RNAi-8	ggg*ctcgag*TCAGCGAGCACACCATTAAGC
TbORFe (Tb927.8.8070 & Tb927.8.8110)	
CB1954-RNAi-9	ttt*ggatcc*CTGTCAAGCCTCCCAGCCGTT
CB1954-RNAi-10	ggg*ctcgag*TGTTAATCGTAGTAACGCTCA
TbORFf (Tb927.8.4050)	
CB1954-RNAi-11	ttt*ggatcc*ATCGCCTGAGTCTTGATGCTC
CB1954-RNAi-12	ggg*ctcgag*GCGATACCGTGCGGTTCGTTA
TbORFg (Tb927.10.3910)	
CB1954-RNAi-13	ttt*ggatcc*CCTGCACCGTGCCTTCGCTGA
CB1954-RNAi-14	ggg*ctcgag*GGATCACTACCACCACGCCTT
TbMCM9 (Tb927.9.9600)	
CB1954-RNAi-15	ttt*ggatcc*CACCCTCATGGACGCGCTCAG

CB1954-RNAi-16	ggg*ctcgag*GCGGTAGGAGTCCATCACGTT
TbRad2 (XPG) (Tb927.9.11760)	
TbRAD2 RNAi-1	ttt*ggatcc*AACCTGGTGAAAGTGTGGAGG
TbRAD2-RNAi-2	ggg*ctcgag*CTGAATTGATTCAGCTTCCCC
BG-M2 TbORF1 (Tb927.10.1740)	
TbBGM2-RNAi-1	aaa*ggatcc*TTGCACGGTGATGAAGGAAT
TbBGM2-RNAi-2	aaa*ctcgag*AAGGGCCGCCACTCACCGCCT
BG-M2 TbORF2 (Tb927.10.1750)	
TbBGM2-RNAi-3	aaa*ggatcc*CCGCGAGGAGCGAAGGTAC
TbBGM2 RNAi-4	aaa*ctcgag*AACTCCTGCCGTGCGCTGCTC
BG-M2 TbORF3 (Tb927.11.11380)	
TbBGM2 RNAi-5	aaa*ggatcc*GCCTGGCTCAAATGGAAGGAT
TbBGM2 RNAi-6	aaa*ctcgag*TGGGTTGAAACAACCAA

Primers used in qPCR. Each primer set was predicted to yield a band of between 100-150 base pairs. The sequence in lower case italics refers to restriction sites incorporated into the primer to facilitate DNA cloning. The non-italicised, lower case sequence corresponds to a clamp that aids binding of the DNA polymerase to the primer. The identifiers given after a gene name correspond to accession numbers on the Kinetoplastid genome resource TritrypDB (http://tritrypdb.org/tritrypdb/).

Gene & primer name	Sequence 5' to 3'
TbNTR (Tb927.7.7230)	
TbNTR-1	ttt*ctcgag*GGTACCTTGATGCATTTATACGTGTT
TbNTR-6	TCATGTACGACAATGGCAAC
TbSNM1(Tb427.04.1480)	
TbSNM1-seq1	CACCAGATCACCATTGCGGAG
TbSNM1-q2	GGTATTACTGAGAAGTGGTCG
TbTERT (Tb11.01.1950)**(Brenndörfer & Boshart 2010)(Brenndörfer & Boshart 2010)(Brenndörfer & Boshart 2010)**(Brenndörfer & Boshart 2010)(Brenndörfer & Boshart 2010)(Brenndörfer & Boshart 2010)	
TbTERT-R	AGGAACTGTCACGGAGTTTGC
TbTERT-f	GAGCGTGTGACTTCCGAAGG
TbCPR2(Tb927.9.15380)	
TbCYPRII-4	ggg*ggatcc*ACGAAGCGATATTAGTGATCT
TbCYPRII-6	GTTGAGGAGTATGTTGAGCAA
TbCPR3 (Tb11.02.5420)	
TbCYPRIV-4	*gggggatcc*GACTCGACGTTCGCGTTCTCT
TbCYPRIV-6	CGTGGCGCAGATAATAATGAC
TbMRE11 (Tb927.2.4390)	
TbMRE11-q1	GGGTTTGACATCATTCAGCCG
TbMRE11-q2	CCGGACGACAGGACGAATACT
TbRad51 (Tb427.03.5230)	
TbRad51-q1	AGTGTGTCGGACATGCTGGCA
TbRad51-q2	CGGGGTTCCTGCGAGCAGGCG
TbRad2 (XPG)(Tb927.9.11760)	
TbRAD2-q1	GCTGAGCCCTACGCCGTTGCT
TbRAD2-RNAi-2	ggg*ctcgag*CTGAATTGATTCAGCTTCCCC
TbMSH3 (Tb927.9.5240)	

TbMSH3-qPCR-1	AAGGCTATCGAGCTGCTGTGT
TbMSH3-qPCR-2	CACACGGTAACCACACGCTAC
TbHP1 (Tb927.9.11810)	
Tb11810-qpcr-1	ATGCTAGTCAGCACCAGTCCA
Tb11810-qpcr-2	CAATGTCCATCCCAAGCATTA
TbHP2 (Tb927.9.11670)	
Tb11670-qpcr-1	GAGGGTCTTGTGCATGGCAGT
Tb11670-qpcr-2	ATCACAGGCACGGACAACATC
TbXPF (Tb927.5.3670)	
TbXPF-qPCR-f	CAACCTACCGTCACCCAATGC
TbXPF-qPCR-r	ACCACTGCCACCGAGTTATCA

Appendix 4: Summaries of trypanosome mutant sensitivities towards ABQ agents.

Table 5.2 (Expanded): Susceptibility of *T. brucei* lines expressing altered levels of Tb*snm1* to ABQ compounds. Data represents the IC_{50} values in μM of *T. brucei* wild type, Tb*snm1*$^{-/-}$ null mutants (Tb*snm1*$^{-/-}$), Tb*snm1*$^{-/-}$ expressing an ectopic copy of Tb*snm1* (Tb*snm1*$^{-/-}$ Tb*snm1*^{RV}) and *T. brucei* wild type expressing elevated levels of Tb*snm1* (Tb*snm1*^{RV}) to selected ABQs. All values are means ± standard deviation of four independent experiments. The fold difference in IC_{50} values between the two treatments are given. The differences in susceptibility of wild type and Tb*snm1*$^{-/-}$ lines to DZQ, RH1, TZQ or 22 was statistically significant ($P < 0.01$), as assessed by Student's *t* test.

Compound	IC_{50} values (μM) ± standard deviation				Ratios		
	wild type	Tb*snm1*$^{-/-}$	Tb*snm1*$^{-/-}$ Tb*snm1*^{RV}	Tb*snm1*^{RV}	Wild type: Tb*snm1*$^{-/-}$	Tb*snm1*$^{-/-}$: Tb*snm1*$^{-/-}$ Tb*snm1*^{RV}	wild type: Tb*snm1*^{RV}
DZQ	0.157 ± 0.023	0.043 ± 0.002	0.204 ± 0.022	0.206 ± 0.017	3.7	4.7	1.3
RH1	0.019 ± 0.001	0.005 ± 0.001	0.012 ± 0.001	0.011 ± 0.001	3.0	2.4	0.6
TZQ	0.253 ± 0.033	0.046 ± 0.001	0.376 ± 0.006	0.300 ± 0.023	2.7	8.2	1.2
22	0.091 ± 0.008	0.012 ± 0.001	0.069 ± 0.007	0.056 ± 0.007	6.6	5.8	0.6
DFMO	24.150 ± 3.940	24.240 ± 6.710	26.960 ± 1.400	25.410 ± 6.440	1.0	1.1	1.1

Table 5.3 (Expanded): The growth inhibitory effects of selected ABQ compounds on *T. brucei snm1*$^{-/-}$ null mutants over expressing TbNTR. Data represents the IC_{50} values in μM of *T. brucei* wild type, *T. brucei* expressing elevated levels of TbNTR (Tb*ntr*), TbSNM1 null mutants (Tb*snm1*$^{-/-}$) and TbSNM1 null mutants expressing an ectopic copy of Tb*ntr* (Tb*snm1*$^{-/-}$ Tb*ntr*) to RH1, TZQ and DFMO. All values are means ± standard deviation of four independent experiments. [a] valve for DFMO taken from Sullivan *et al* (2015).

Compound	IC_{50} values (μM) ± standard deviation				Ratios		
	Wild Type	Tb*ntr*	Tb*snm1*$^{-/-}$	Tb*snm1*$^{-/-}$ Tb*ntr*	Wild type: Tb*ntr*	Tb*snm1*$^{-/-}$: Tb*snm1*$^{-/-}$ Tb*ntr*	Wild type: Tb*snm1*$^{-/-}$ Tb*ntr*
RH1	0.015 ± 0.001	0.003 ± 0.001	0.005 ± 0.001	0.001 ± 0.001	5.0	5.0	15.0
TZQ	0.202 ± 0.006	0.060 ± 0.009	0.076 ± 0.004	0.013 ± 0.001	3.4	5.8	15.5
DFMO[a]	27.500 ± 0.108	30.720 ± 1.330	27.100 ± 0.850	26.710 ± 2.060	0.9	0.9	1.0

Table 5.4 (Expanded): The growth inhibitory effects of selected ABQ compounds on *T. brucei snm1*$^{-/-}$ null mutants over expressing TbCPR2. Data represents the IC_{50} values in μM of *T. brucei* wild type, *T. brucei* expressing elevated levels of TbCPR2 (Tb*cpr2*), TbSNM1 null mutants (Tb*snm1*$^{-/-}$) and TbSNM1 null mutants expressing an ectopic copy of Tb*cpr2* (Tb*snm1*$^{-/-}$ Tb*cpr2*) to **22** and DFMO. All values are means ± standard deviation of four independent experiments.

Compound	IC_{50} values (μM) ± standard deviation				Ratios		
	wild type	Tb*cpr2*	Tb*snm1*$^{-/-}$	Tb*snm1*$^{-/-}$ Tb*cpr2*	Wild type: Tb*cpr2*	Tb*snm1*$^{-/-}$: Tb*snm1*$^{-/-}$ Tb*cpr2*	Wild type: Tb*snm1*$^{-/-}$ Tb*cpr2*
22	0.138 ± 0.025	0.020 ± 0.003	0.021 ± 0.001	0.011 ± 0.004	7.0	1.9	12.5
DFMO	27.500 ± 0.108	33.250 ± 5.123	27.100 ± 0.850	29.250 ± 3.862	0.8	1.1	0.9

Table 5.5: The growth inhibitory effects of selected ABQ compounds on *T. brucei snm1*$^{-/-}$ null mutants over expressing TbCPR3. Data represents the IC_{50} values in μM of *T. brucei* wild type, *T. brucei* expressing elevated levels of TbCPR3 (Tb*cpr3*), TbSNM1 null mutants (Tb*snm1*$^{-/-}$) and TbSNM1 null mutants expressing an ectopic copy of Tb*cpr3* (Tb*snm1*$^{-/-}$ Tb*cpr3*) to **22** and DFMO. All values are means ± standard deviation of four independent experiments. Ratios can be found in Appendix 4.

Compound	IC_{50} values (μM) ± standard deviation						
	wild type	Tb*cpr3*	Tb*snm1*$^{-/-}$	Tb*snm1*$^{-/-}$ Tb*cpr3*	Wild type: Tb*cpr3*	Tb*snm1*$^{-/-}$: Tb*snm1*$^{-/-}$ Tb*cpr3*	Wild type: Tb*snm1*$^{-/-}$ Tb*cpr3*
22	0.138 ± 0.025	0.019 ± 0.003	0.021 ± 0.001	0.010 ± 0.001	7.3	2.1	13.8
DFMO	27.500 ± 0.108	36.500 ± 3.697	27.100 ± 0.850	39.125 ± 2.170	0.75	0.7	0.7

Flow diagrams to summarise the results shown in Chapter 5 (part 2). These results are shown in tables 5.2, 5.3, 5.4 and 5.5

Tb*ntr* activation in *snm1*$^{-/-}$ background

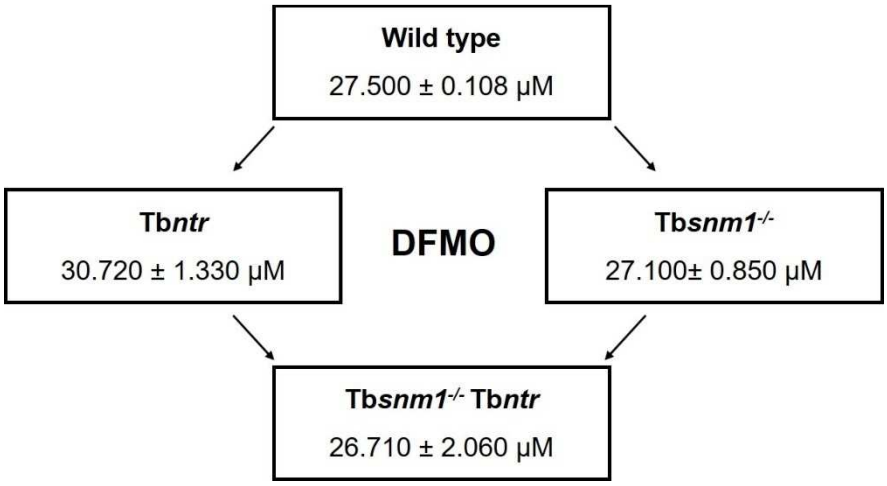

Tb*cpr2* activation in *snm1*$^{-/-}$ background

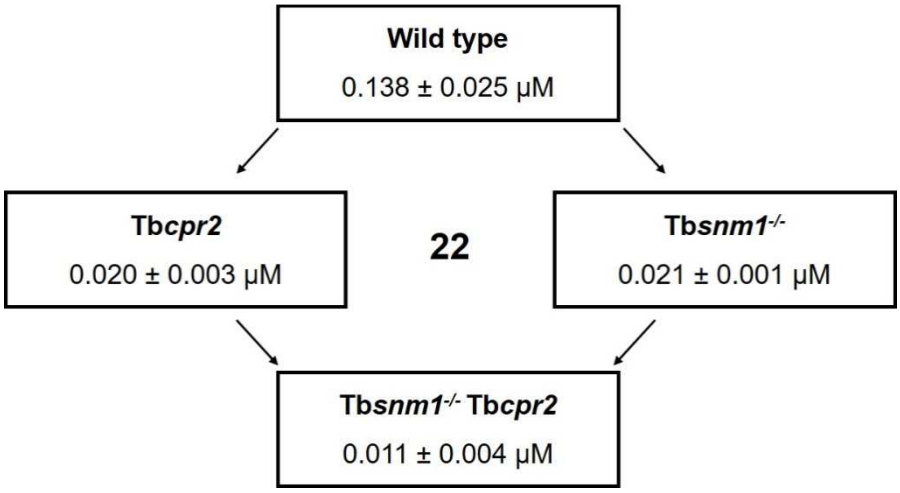

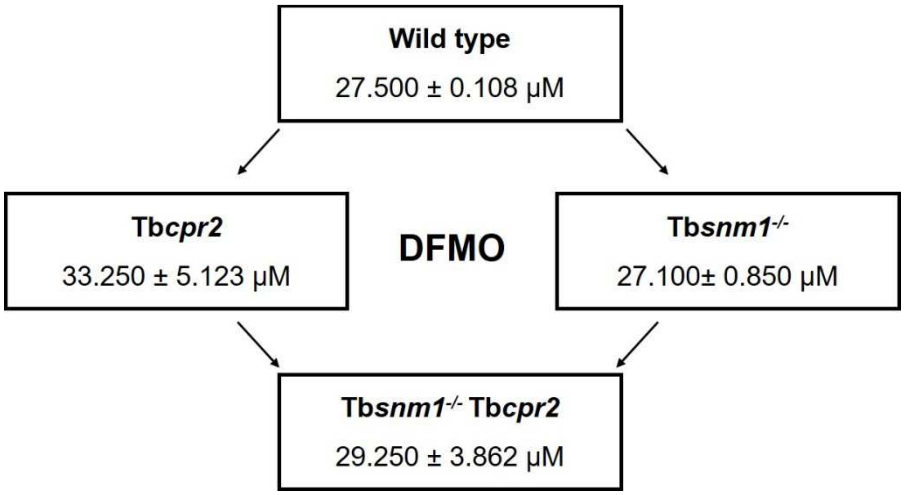

Tb*cpr3* activation in *snm1*$^{-/-}$ background

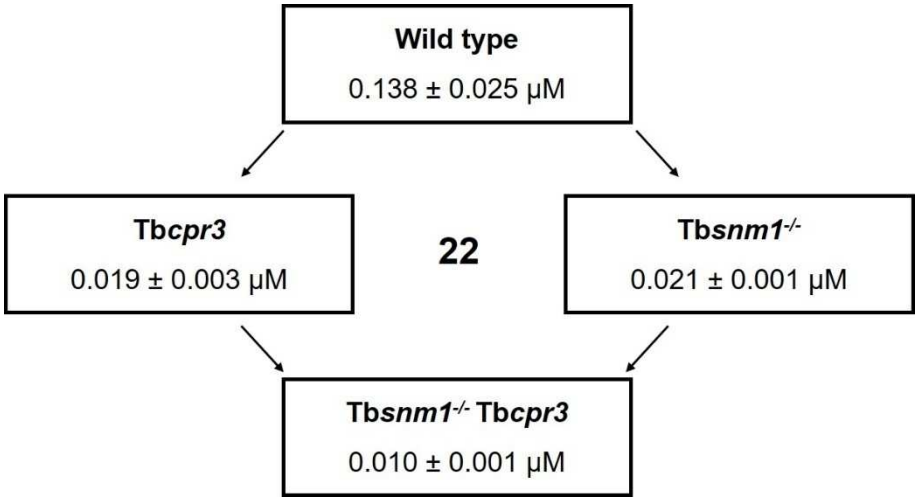

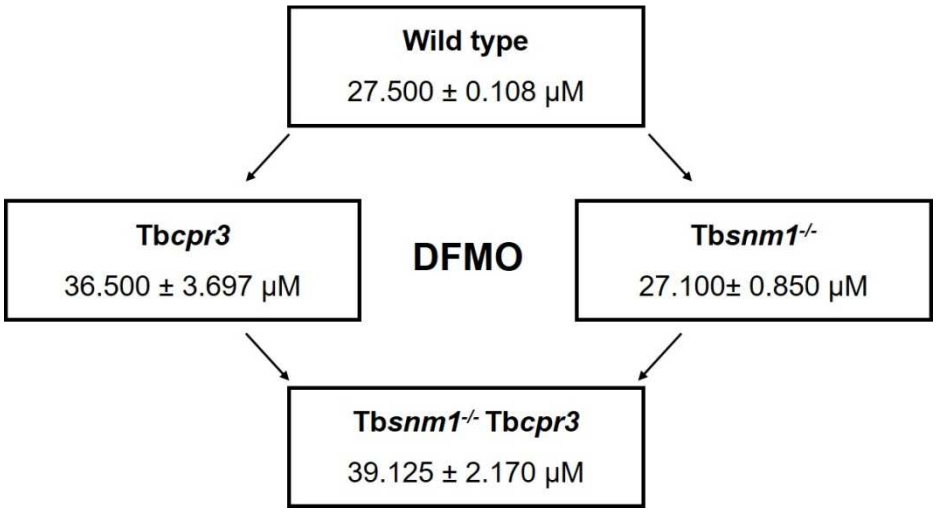

Appendix 5: Published papers

AAC
Journals.ASM.org

Targeting the Substrate Preference of a Type I Nitroreductase To Develop Antitrypanosomal Quinone-Based Prodrugs

Belinda S. Hall,* Emma Louise Meredith, and Shane R. Wilkinson

Queen Mary Pre-Clinical Drug Discovery Group, School of Biological & Chemical Sciences, Queen Mary University of London, London, United Kingdom

Nitroheterocyclic prodrugs are used to treat infections caused by *Trypanosoma cruzi* and *Trypanosoma brucei*. A key component in selectivity involves a specific activation step mediated by a protein homologous with type I nitroreductases, enzymes found predominantly in prokaryotes. Using data from determinations based on flavin cofactor, oxygen-insensitive activity, substrate range, and inhibition profiles, we demonstrate that NTRs from *T. cruzi* and *T. brucei* display many characteristics of their bacterial counterparts. Intriguingly, both enzymes preferentially use NADH and quinones as the electron donor and acceptor, respectively, suggesting that they may function as NADH:ubiquinone oxidoreductases in the parasite mitochondrion. We exploited this preference to determine the trypanocidal activity of a library of aziridinyl benzoquinones against bloodstream-form *T. brucei*. Biochemical screens using recombinant NTR demonstrated that several quinones were effective substrates for the parasite enzyme, having K_{cat}/K_m values 2 orders of magnitude greater than those of nifurtimox and benznidazole. In tests against *T. brucei*, antiparasitic activity mirrored the biochemical data, with the most potent compounds generally being preferred enzyme substrates. Trypanocidal activity was shown to be NTR dependent, as parasites with elevated levels of this enzyme were hypersensitive to the aziridinyl agent. By unraveling the biochemical characteristics exhibited by the trypanosomal NTRs, we have shown that quinone-based compounds represent a class of trypanocidal compound.

Over 10 million people are infected with *Trypanosoma cruzi* and *Trypanosoma brucei*, the causative agents of Chagas' disease and human African trypanosomiasis, respectively (8, 52). Together, these pathogens are responsible for around 40,000 deaths per year and represent a major public health problem in the regions of the world least able to deal with the associated economic burden (54). As a consequence of concerted surveillance, insect vector control, and improved housing programs, there has been a significant decline in the prevalence of infections by both species. However, as a result of blood transfusion, organ transplantation, illicit drug usage, and population migration, these trypanosomiases are emerging as a problem in areas of nonendemicity, including in Europe and the United States (5, 22, 23, 60). Currently, drugs are the only viable option to treat these diseases. For *T. cruzi*, treatment is based on nifurtimox and benznidazole, whereas suramin, pentamidine, melarsoprol, eflornithine, and nifurtimox-eflornithine combinational therapy are used against HAT (64). In addition to the problems represented by toxicity, resistance, and cost, therapy is further complicated by the fact that the effectiveness of some drugs is dependent on the subspecies and the disease stage. Therefore, there is an urgent requirement for alternative chemotherapies.

Quinone-based compounds encompass a range of molecules, characterized by two carbonyl groups linked to a carbocyclic backbone. They are widely distributed in nature and are able to participate in a number of crucial biological oxidoreductase cascades. Additionally, both natural and synthetic quinones have been extensively used in medicine as antimicrobial and anticancer agents, functioning either as inhibitors of essential redox pathways or as prodrugs. In the latter case, the compound must undergo activation by quinone reductases before mediating their cytotoxic effects. Quinone reductases can broadly be divided into two groups based on the number of reducing equivalents transferred to their target substrate. Some enzymes mediate the $1e^-$ reduction of the quinone carbonyl oxygens to form an unstable semiquinone radical. Under hypoxic conditions, the radical then undergoes further reduction to produce the hydroquinone derivative. However, in the presence of O_2, formation of the hydroquinone product is inhibited, with the semiquinone radical undergoing futile cycling to produce superoxide and regeneration of the parent compound (42, 47). In contrast, other quinone reductases, typified by NAD(P)H:quinone oxidoreductase, catalyze the $2e^-$ reduction of the quinone to form the hydroquinone directly (15, 33, 57). Interestingly, expression of these enzymes in normal tissue is low but is elevated in cancer cells, a difference that has been exploited in the development of anticancer therapies (34). During the $2e^-$ reduction of the quinone to its hydroquinone form, a redistribution of electrons occurs within the compound's backbone that can lead to exposure of a prodrug's cytotoxic component. For azirinidyl anticancer agents, such as mitomycin C, EO9, and AZQ, the cytotoxic agent remains attached to the hydroquinone core, whereas in other compounds, for example, phosphoramidate mustards and indolequinone-camptothecins, this "electronic switch" promotes cleavage of specific bonds in the structure's backbone, resulting in compound fragmentation and drug release (11).

Trypanosomal screening programs using natural and synthetic quinones have identified a number of lead compounds (31, 46). However, the mechanism(s) by which such agents mediate their antiparasitic activity is unclear. Based on *in vitro* enzyme studies

Received 13 June 2012 **Returned for modification** 1 August 2012
Accepted 19 August 2012
Published ahead of print 4 September 2012
Address correspondence to Shane R. Wilkinson, s.r.wilkinson@qmul.ac.uk.
* Present address: B. S. Hall, Faculty of Health and Medical Sciences, University of Surrey, Guildford, Surrey, United Kingdom.

doi:10.1128/AAC.01227-12

and the belief that protozoan parasites have a limited enzymatic capacity to metabolize reactive oxygen species, it had been postulated that some quinones may function by inhibiting key essential enzymes such as trypanothione reductase or lipoamide dehydrogenase, while others are thought to induce oxidative stress within the parasite (18, 19, 21, 29, 37, 51). However, no demonstration of a functional link between the antiparasitic activity of any quinone-based agent and a proposed protein target within the pathogen has been reported and it is now well established that trypanosomatids possess a series of novel enzymatic oxidative defense pathways.

In many regards, the situation concerning quinone reduction mirrors the confusion that surrounded investigations of the trypanocidal mechanism of action of nifurtimox and benznidazole. It is now clear that trypanosomes activate such nitro-based drugs using a mitochondrially targeted, oxygen-insensitive type I NTR, leading to the formation of cytotoxic reduction products (26, 27, 65). This class of oxidoreductase is largely restricted to bacteria and absent from most eukaryotes, with a subset of protozoan parasites being major exceptions. The differences between the pathogens and human host in NTR distribution are believed to form the basis for the drug selectivity of nitroheterocyclic prodrugs. Here, we show that TbNTR and TcNTR display many of the characteristics displayed by their bacterial counterparts and reveal that both parasite enzymes have a preference for quinone-based substrates. Exploiting this property, we evaluated the trypanocidal activities of an aziridinyl 1,4-benzoquinone series, identifying several compounds that display high activity against bloodstream-form *T. brucei*.

MATERIALS AND METHODS

Abbreviations. AZQ, 2,5-diaziridinyl-3,6-bis(carboethoxy-amino)-1,4-benzoquinone: BCA, bicinchoninic acid; BSF, bloodstream form; DCPIP, dichlorophenolindolephenol; DZQ, 2,5-diaziridinyl-1,4-benzoquinone; FAD, flavin adenine dinucleotide; FMN, flavin mononucleotide; GPDH, glycerol-3-phosphate dehydrogenase; HAT, human African trypanosomiasis; IC_{50}, drug concentration that inhibits cell growth by 50%; IPTG, isopropyl-β-D-thiogalactopyranoside; MeDZQ, 2,5 dimethyl-3,6 diaziridinyl-1,4-benzoquinone; Ni-NTA, nickel-nitrilotriacetic acid; NTR, nitroreductase; NQO1, NAD(P)H:quinone oxidoreductase; RH1, 2,5-diaziridinyl-3-(hydroxymethyl)-6-methyl-1,4-benzoquinone; TbNTR, type I NTR from *T. brucei*; TcNTR, type I NTR from *T. cruzi*; TZQ, triaziquone [2,3,5-tris(aziridin-1-yl)cyclohexa-2,5-diene-1,4-dione].

Compounds. The compounds used in this study were obtained from the following sources: nitrofurazone, nitrofurantoin, CB1954, ubiquinone 5, duroquinone, and DCPIP were purchased from Sigma-Aldrich. Metronidazole was a gift from Nubia Boechat (Far Manguinhos, Rio de Janeiro, Brazil), megazol from Mike Barrett (University of Glasgow), LH7 and LH37 from Longqin Hu (Rutgers University), and amino-824 from Clifton Barry III (National Institute of Allergy and Infectious Diseases) and Ujjini Manjunatha (Novartis Institute for Tropical Diseases, Singapore). Benznidazole and nifurtimox were provided by Simon Croft (London School of Hygiene and Tropical Medicine). The aziridinyl benzoquinones (Table 1) were supplied by the Department of Therapeutics, NCI, except for RH1, which was donated by Frank Guziec, Jr. (Southwestern University, Georgetown, TX).

Parasite culturing. *T. brucei brucei* (Lister 427; clone 221a and a derivative [2T1] engineered to constitutively express the tetracycline repressor protein) BSF parasites were grown in modified Iscove's medium at 37°C under a 5% CO_2 atmosphere (2, 30). The 2T1 parasites transformed to overexpress TbNTR were grown in the presence of 1 μg ml^{-1} phleomycin and 2.5 μg ml^{-1} hygromycin (65).

TABLE 1 Structure of aziridinyl 1,4-benzoquinones used in this study

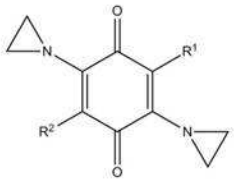

Compound	NSC no.	Structure
DZQ (1)	30706	$R^1 = R^2 = H$
MeDZQ (2)	646714	$R^1 = R^2 = CH_3$
RH1 (3)	697726	$R^1 = CH_2OH$; $R^2 = CH_3$
AZQ (4)	182986	$R^1 = R^2 = NHCOOCH_2CH_3$
TZQ (5)	29215	R^1 = aziridinyl; $R^2 = H$
6	95139	$R^1 = R^2 = OCH_3$
7	18270	$R^1 = R^2 = OCH_2CH_3$
8	246111	$R^1 = R^2 = NH_2$
9	220267	$R^1 = R^2 = NHCH_3$
10	18269	$R^1 = R^2 = NHCOCH_3$
11	31717	$R^1 = R^2$ = aziridinyl
12	251728	R^1 = morpholinyl; $R^2 = F$

Growth inhibition assays. *T. brucei brucei* BSF parasites were seeded at 1×10^3 cells ml^{-1} in 200 μl of growth medium containing different concentrations of aziridinyl benzoquinone. After incubation at 37°C for 3 days, 20 μl alamarBlue (Invitrogen, Paisley, United Kingdom) was added to each well and the plates were incubated for a further 8 to 16 h. Cell densities were determined by monitoring the fluorescence of each culture using a Gemini Fluorescent Plate Reader [Molecular Devices (UK) Ltd., Wokingham, United Kingdom] at excitation λ = 530 nm, emission λ = 585 nm, and a filter cutoff at 550 nm, and the IC_{50} was established.

Expression constructs. A DNA fragment encoding the catalytic domain of TcNTR (amino acids 78 to 312) was amplified from *T. cruzi* Sylvio X10/6 genomic DNA using the primers ggatccTGGATGCCATGAAACG TGTA and aagcttTCAAAACTTTCCCCACCGAAC (lowercase type corresponds to restriction sites incorporated into the primers to facilitate cloning). The product was digested using BamHI and HindIII and cloned into the corresponding sites of pTrcHisC. Construction of the expression vector containing the equivalent region from TbNTR is described elsewhere (28).

Oligonucleotide site-directed mutagenesis was carried out using a Stratagene QuikChange mutagenesis kit (Agilent Technologies, Stockport, United Kingdom) with pTrcHis-TcNTR as the template for DNA. Amplifications were performed in accordance with the manufacturer's instructions using primers (Eurofins) to generate each of the desired mutations. The forward primer sequences were R90A (GTGTAGTACACGA GGCACGCTCCTGCAAGCG), K94A (GAGCGTCGCTCCTGCGCGCG ATTTGACCCAAC), Q124A (GCTCCTACCGCCCTGAACTTAGCGCC ATGGGTGG), and R302A (CCGTACGCAGCCCAGCATTTCCCACGA AGC). The relevant substitution sites, incorporating the required base change, are underlined.

Protein purification. His-tagged TcNTR (wild type and mutants) and TbNTR were expressed and purified as described previously (28). Briefly, overnight cultures of *Escherichia coli* BL21(+) containing the expression plasmid were diluted 1:50 in NZCYM (Sigma-Aldrich) medium containing 100 μg ml^{-1} ampicillin and grown for 2 to 4 h at 37°C. The culture was transferred to 16°C for 30 min, and then protein expression was induced by the addition of 100 μM IPTG. Cultures were incubated at 16°C for a further 20 h. Cells were formed into pellets and then lysed in a reaction mixture consisting of 50 mM NaH_2PO_4 (pH 7.8) and 500 mM NaCl

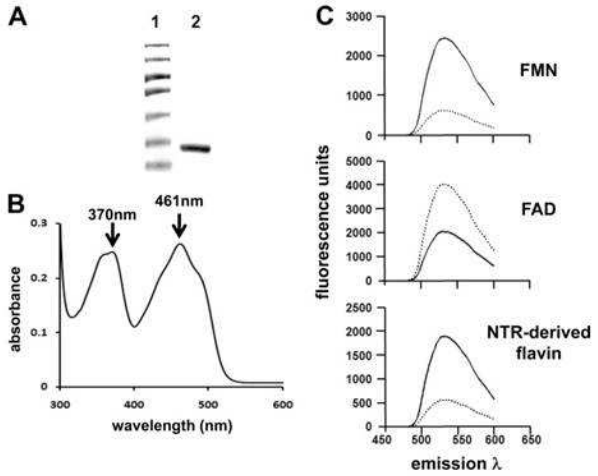

FIG 1 Trypanosomal NTRs contain FMN as a cofactor. (A) Coomassie-stained SDS-PAGE gel (10%) containing purified, recombinant TbNTR (lane 2). Lane 1, size standards. (B) Absorption spectrum (300 to 550 nm) of purified TbNTR (2 mg) in 50 mM NaH_2PO. (C) Fluorescence spectra of FMN and FAD (both 25 μM) and of supernatant from boiled and purified recombinant TbNTR (0.45 μg) at pH 7.6 (solid line) and pH 2.2 (dashed line) with excitation λ at 450 nm and emission λ between 480 and 600 nm. All the fluorescence analyses were carried out in triplicate; the profiles are derived from the mean values. When TcNTR was used in place of TbNTR, similar absorption and fluorescence profiles were observed.

(buffer A) containing 1% (vol/vol) Triton X-100, 1 mg ml^{-1} lysozyme, and a cocktail of protease inhibitors (Roche Diagnostics, Burgess Hill, United Kingdom). The clarified lysate was passed through a Ni-NTA column (Qiagen, Crawley, United Kingdom) and recombinant protein eluted using buffer A supplemented with 500 mM imidazole and 0.5% (vol/vol) Triton X-100. The protein concentration was determined using a BCA assay system (Thermo Fisher Scientific, Cramlington, United Kingdom) and the purity level confirmed by SDS-PAGE.

Flavin characterization. The flavin cofactor bound to trypanosomal NTRs was established by determining the fluorescence spectrum in acidic and neutral buffers (16). Purified protein was desalted and boiled for 5 min. In a total volume of 100 μl, clarified supernatants (90 μl) containing 0.5 mg NTR were mixed with 10 μl 50 mM NaH_2PO_4 (pH 7.6) or 1 M HCl (final pH = 2.2). The fluorescence profile for each treatment was then determined using a Gemini Fluorescent Plate Reader [Molecular Devices (UK) Ltd., Wokingham, United Kingdom] with excitation λ = 450 nm and emission λ = 480 to 600 nm. The resultant patterns were compared with profiles obtained using FMN and FAD standards.

Enzyme activity. NTR activity was measured using several electron acceptors as the substrate. A standard reaction mixture (1 ml) containing 50 mM Tris-Cl (pH 7.5), 100 μM NADH, and 100 μM electron acceptor was incubated at room temperature for 5 min. The background reaction rate was determined and the assay initiated by addition of the trypanosomal NTR (20 μg). For reaction mixtures containing nitroimidazoles, nitrobenzyl phosphoramides, or most quinones, activity was measured by following the change in absorbance at 340 nm corresponding to NADH oxidation (ε = 6,200 M^{-1} cm^{-1}), whereas for assays involving nitrofurans, the direct reduction of the substrate itself was monitored at 435 nm for nifurtimox (ε = 18,000 M^{-1} cm^{-1}) or at 400 nm for nitrofurazone and nitrofurantoin (ε = 12,000 and 15,000 M^{-1} cm^{-1}, respectively). DCPIP reduction was measured by following the decrease in absorbance at 600 nm (ε = 21,000), and CB1954 activity was determined by the increase in absorbance at 420 nm, corresponding to production of the hydroxylamine (ε = 1,200 M^{-1} cm^{-1}). Kinetic analysis was performed using GraphPad Prism 5 software.

RESULTS

Trypanosomal type I nitroreductases are FMN binding proteins. Based on cofactor and oxygen sensitivity, NTRs can be divided into two groups: type I and type II (45). To evaluate which class the trypanosomal enzymes fall into, recombinant protein containing the catalytic domains from *T. brucei* or *T. cruzi* NTR was expressed in *E. coli* and purified after one round of affinity chromatography (Fig. 1A). Elutions containing recombinant proteins were yellow, and analysis of their absorbance spectra identified peaks at 370 and 461 nm (Fig. 1B), both characteristic of flavin binding type I NTRs (62, 67, 68). To determine the nature of the NTR/cofactor interaction and identify which flavin was present, recombinant protein (TbNTR and TcNTR) was denatured and the fluorescence profile of supernatants analyzed. Flavin was released from both enzymes, indicating a noncovalent association with the protein backbone (9, 62, 68), and the fluorescence profiles under conditions of neutral and acidic pHs identified FMN as a cofactor (Fig. 1C); at neutral pH and excitation at 450 nm, flavin derived from TbNTR and TcNTR had a peak emission at 535 nm, representing a signal quenched under acidic conditions, typical of FMN and distinct from FAD (Fig. 1C) (16).

The overall level of conservation among type I NTRs is low, although certain key residues are highly conserved. Comparison of the trypanosomal enzymes with their bacterial counterparts identified several such amino acids, including R90, K94, and R302, which may play a role in FMN binding, and Q124, which could influence interactions with the substrate (note that the numbering

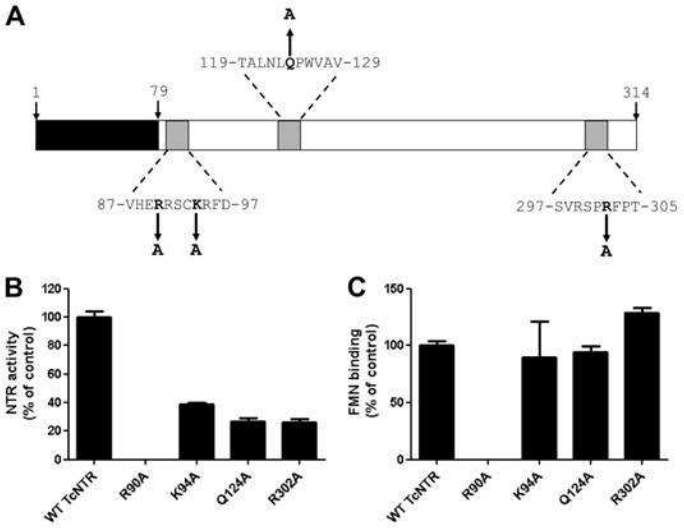

FIG 2 Site-directed mutagenesis of TcNTR. (A) Schematic of TcNTR from *T. cruzi* Silvio X10/6 showing the amino-terminal extension (residues 1 to 79), FMN binding motifs (residues 87 to 97 and 297 to 305), and substrate binding regions (residues 119 to 129) (44, 48, 65). Residues selected for mutagenesis are in bold, with arrows indicating the new amino acid substitution. Numbers refer to positions of amino acids in the TcNTR sequence (GenBank accession no. EFZ30370). (B) NTR activity was determined by following the reduction of nifurtimox (0 to 100 μM) at a fixed concentration of NADH (100 μM) in the presence of purified wild-type (WT) or mutant TcNTR protein (4 μg). All assays were carried out in triplicate. The apparent V_{max} for each protein was calculated, and the results are presented as a percentage of the wild-type activity ± standard deviation. (C) The flavin recovered from the boiled, clarified supernatants of purified wild-type or mutant TcNTR (0.45 μg) was identified as described for Fig. 1. The fluorescence of each supernatant was measured at pH 7.6 using excitation λ = 450 nm and emission λ = 535 nm. For each protein, the fluorescence value from three independent readings was taken, and the data are presented as a percentage of the wild-type value ± standard deviation.

is in accordance with the TcNTR sequence) (Fig. 2A) (44, 49). To evaluate the importance of these four residues in TcNTR activity, they were converted to alanine and His-tagged mutant proteins purified by affinity chromatography on a Ni^{2+}-NTa column. After determination of the size and purity of each protein by SDS-PAGE, activity was monitored using nifurtimox as a substrate (Fig. 2B). In one mutant (R90A), a complete loss of NTR activity was observed, and this correlated with a total loss of FMN binding (Fig. 2C). The other three mutants all showed a partial (60% to 75%) inhibition of reductase activity but no significant change in their FMN binding capacity (Fig. 2B and C). Presumably, the K94, Q124, and R302 residues play some role in substrate (either NADH or nitroaromatic) binding.

Substrate preference of the trypanosomal NTRs. To investigate their substrate specificity, trypanosomal NTR activity was monitored by following NADH oxidation at 340 nm or, when a compound's absorbance spectra precluded this, by following reduction of the substrate itself (Fig. 3A). This demonstrated that both TbNTR and TcNTR functioned as typical bacterial type I NTRs, able to catalyze the aerobic reduction of a wide range of nitroaromatics and quinones (Table 2). For some 5-nitroimidazole compounds, such as the metronidazole-like drugs and a PA-824-based antituberculosis agent, no or low activity was detected using either of the parasite enzymes whereas other structures, such as those of the anti-Chagas' disease drugs nifurtimox and ben-

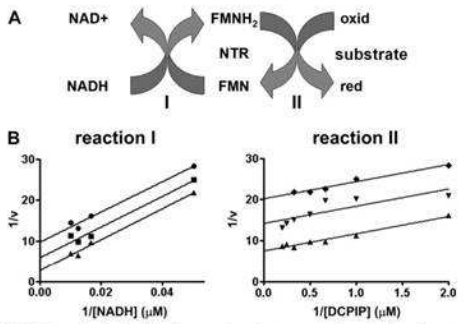

FIG 3 Investigating the kinetic properties of trypanosomal type I nitroreductase toward quinones. (A) Proposed scheme for the reduction of quinone- and nitroaromatic-based substrates by NTRs using NADH as the electron donor; "red" represents the reduced and "oxid" the oxidized form of the compound. The interactions of the trypanosomal NTR with NADH (reaction I) and the substrate (reaction II) are indicated. (B) NTR activity was assayed by following the reduction of DCPIP at 600 nm. In reaction I, assays were carried out using different concentrations of NADH (0 to 100 μM) in the presence of DCPIP (0.5 [●], 1.0 [■], and 2 [▼] μM) and TcNTR (20 μg). In reaction II, NTR activity was assayed by following the reduction of various concentrations of DCPIP (0 to 2 μM) in the presence of NADH (20 [◆], 40 [▼], and 60 [▲] μM) and TcNTR (20 μg). When TbNTR was used in place of TcNTR, similar enzyme kinetic profiles were observed.

TABLE 2 Substrate specificity of trypansomal NTRs[a]

Substrate	TbNTR			TcNTR		
	Apparent V_{max}	Apparent K_m	K_{cat}/K_m	Apparent V_{max}	Apparent K_m	K_{cat}/K_m
Nitroimidazoles						
Benznidazole	419.0 ± 35.0	60.0 ± 13.0	3.0×10^3	564.0 ± 19	43.0 ± 4.0	6.1×10^3
Megazol	476.0 ± 21.0	5.0 ± 1.0	4.0×10^4	1,358.0 ± 78.0	22.0 ± 3.0	2.7×10^4
Metronidazole	93.0 ± 9.0	55.0 ± 13.0	7.3×10^2	0		
6-Amino PA824	0			0		
Nitrofurans						
Nifurtimox	349.0 ± 22.0	41.0 ± 7.0	3.6×10^3	457.0 ± 9.0	22.0 ± 2.0	9.2×10^3
Nitrofurazone	1,167.0 ± 51.0	10.0 ± 1.0	5.2×10^4	439.0 ± 20.0	13.0 ± 2.0	3.3×10^3
Nitrofurantoin	772.0 ± 37.0	1.3 ± 0.4	2.5×10^5	1,059.0 ± 10.0	11.0 ± 1.0	4.2×10^4
Nitrobenzyls						
CB1954	318.0 ± 103.0	41.0 ± 25.0	3.5×10^3	56.0 ± 4.0	151.0 ± 2.0	1.5×10^2
LH7	245.0 ± 35.0	80.3 ± 25.0	1.3×10^3	25.0 ± 2.0	20.0 ± 8.0	5.3×10^2
LH37	1,238.0 ± 48.0	2.8 ± 0.4	1.8×10^5	151.0 ± 13.0	5.0 ± 3.0	1.3×10^4
Quinones						
Ubiquinone 5	1,227.0 ± 1.0	0.3 ± 0.0	1.6×10^6	963.0 ± 52.0	4.0 ± 0.5	1.1×10^5
Duroquinone	852.0 ± 56.0	2.0 ± 0.5	1.5×10^5	384.0 ± 27.0	10.0 ± 2.0	1.6×10^4
DCPIP	999.0 ± 183.0	3.0 ± 1.5	1.4×10^5	1,172.0 ± 40.0	0.4 ± 0.1	1.2×10^6

[a] The apparent V_{max} and K_m (± standard deviation) TbNTR and TcNTR (20 μg) values for various nitroaromatic and quinone-based substrates (0 to 200 μM) were determined in the presence of NADH (100 μM). For all nitroimidazoles, LH7, LH37, ubiquinone 5, and duroquinone, activity was followed by monitoring the rate of NADH oxidation and the kinetic values were calculated using $\varepsilon = 6{,}220\ M^{-1}cm^{-1}$. For nitrofurans, assays were carried out by following the direct reduction of the nitroheterocycle. Kinetic values were calculated using $\varepsilon = 18{,}000$, 12,000, or 15,000 $M^{-1}cm^{-1}$ for nifurtimox, nitrofurazone, or nitrofurantoin, respectively, and the amount of reductant consumed per reaction was determined, assuming that 4 molecules of NADH are oxidized per molecule of nitrofuran reduced (26). In reactions using DCPIP as the substrate, direct reduction of the indophenol was followed and activity determined using $\varepsilon = 21{,}000\ M^{-1}cm^{-1}$, assuming that 2 molecules of NADH are metabolized during reduction of 1 molecule of DCPIP (3). For CB1954, activity was monitored by detecting production of the hydroxylamine. Kinetic values were determined using $\varepsilon = 1{,}200\ M^{-1}cm^{-1}$, and the amount of NADH oxidized per reaction was determined, assuming that 4 molecules of reductant are turned over per molecule of CB1954 reduced (7, 50). The apparent V_{max} values are expressed as nanomoles of NADH oxidized per minute per milligram and apparent K_m values in micromoles. The specificity constant (K_{cat}/K_m), expressed in per molar per second, was determined and assumed one catalytic site per 30-kDa monomer. Metronidazole was not a substrate for TcNTR (n/a = no activity).

znidazole, were metabolized at equivalent rates (Table 2). The biggest difference between the two trypanosomal enzymes related to their ability to reduce nitrobenzyl-based substrates. The aziridinyl dinitrobenzamidine CB1954 and the two nitrobenzyl phosphoramide mustards LH7 and LH37 were more readily metabolized by TbNTR than by TcNTR. In the case of the mustards, this property has been shown to extend to trypanocidal activity: LH37 displays considerable growth-inhibitory activity against BSF *T. brucei*, yielding an IC_{50} of 7 nM, whereas in studies of its activity against intracellular *T. cruzi*, an IC_{50} 140-fold higher (0.99 μM) has been reported (28, 32).

When the specific activity generated by a given substrate is compared with its affinity toward the enzyme (K_{cat}/K_m), both trypanosomal NTRs appear to have a preference for quinones over nitroaromatics: TbNTR exhibited an apparent K_{cat}/K_m for ubiquinone 5 (coenzyme Q1) of 1.6×10^6, whereas for nifurtimox and benznidazole, values of 9.2×10^3 and $6.1 \times 10^3\ M^{-1}s^{-1}$ were calculated, respectively. Such preferential reduction of quinoid compounds is common among bacterial type I NTRs (9, 40, 67, 68). Interestingly, TbNTR could use NADPH and NADH as electron donors, although the apparent K_m values indicate a preference for NADH: using nifurtimox (100 μM) as the substrate, TbNTR had an apparent K_m value of 71 μM for NADH compared to 198 μM for NADPH. In contrast, TcNTR could use only NADH as a reductant, with a K_m of 86 μM (65).

To further investigate the type of kinetics that the parasite NTRs display toward NADH, assays were carried out using various concentrations of reductant against a fixed concentration of substrate (Fig. 3B shows data relating to TcNTR reduction of DCPIP; similar results were obtained using TbNTR). For most substrates, double-reciprocal plots were linear at all concentrations of electron acceptor, with the slopes remaining parallel, a pattern characteristic of a ping-pong mechanism. Likewise, reciprocal assays using a fixed concentration of NADH and various amounts of substrate generated a similar pattern of parallel slopes (Fig. 3B). This mechanism of kinetics, typical for oxidoreductase cascades, has previously been observed when using benznidazole as an electron acceptor under normoxic conditions but not when employing nifurtimox as the substrate (26, 27). When reduced by the trypanosomal NTRs, this 5-nitrofuran forms a cytotoxic open chain nitrile while undergoing limited futile cycling. No oxygen consumption was detected during the reduction of the quinone derivatives studied here (data not shown), suggesting that such reactions, if they do occur, are negligible when using these compounds as the substrate.

Like NAD(P)H:quinone oxidoreductases, bacterial type I NTRs are highly susceptible to inhibition by dicoumarol (36, 40, 56). When using NADH and nifurtimox (both at 100 μM) as the electron donor/acceptor, dicoumarol inhibited TbNTR activity with a K_i of 14 nM (Fig. 4A), indicating that this parasite enzyme is particularly sensitive to the 4-hydroxycoumarin derivative. TcNTR was less sensitive, with a K_i of 258 nM. Double-reciprocal plots indicated that inhibition was competitive for NADH (Fig. 4B).

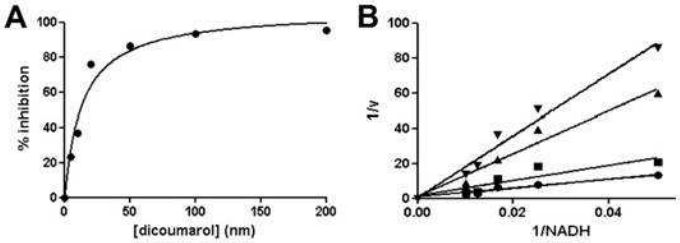

FIG 4 Inhibition of trypanosomal NTR quinone reductase activity by dicoumarol. (A) DCPIP (5 μM) reduction by TbNTR (20 μg) in the presence of NADH (100 μM) was readily inhibited by dicoumarol (0 to 200 nM). Inhibitory activity is expressed as a percentage compared to uninhibited control results. (B) NTR activity was assayed by following DCPIP (5 μM) reduction in the presence of NADH (0 to 100 μM) and 0 (●), 5 (■), 10 (▲), and 20 (▼) nM dicoumarol. All reactions were initiated by addition of TbNTR (20 μg), and activity (v) is expressed in micromoles of DCPIP reduced per minute per milligram.

Taken together, the FMN binding, aerobic activity, substrate range, kinetics, and inhibition profiles of the two trypanosomal NTRs confirm that both function as classic type I NTRs.

Aziridinyl benzoquinones as TbNTR substrates and trypanocidal agents. Aziridinyl benzoquinones have long been of interest in the treatment of cancer. These compounds are activatable by the enzyme NQO1, which is rarely expressed in most normal human tissues but is highly upregulated in many tumor cells. RH1 (compound 3), AZQ (compound 4), and TZQ (compound 5) have been shown to be effective anticancer agents in preclinical studies, with RH1 recently completing phase I trials (4, 14, 61). All appear to induce cell damage primarily by DNA alkylation and cross-linking following reductive activation (13, 66). To determine whether the trypanosomal NTR could activate aziridinyl benzoquinones, a series of compounds (Table 1) were biochemically screened to determine whether they could drive NADH oxidation (fixed at 100 μM) in the presence of TbNTR (20 μg) (Table 3). Under these conditions, seven compounds (compounds 1 to 6 and 12) were metabolized by TbNTR at respectable rates, with some displaying high affinities for the enzyme, resulting in K_{cat}/K_m values ranging from 1.6×10^4 (compound 4) to 6.4×10^5 (compound 3). For the remaining compounds, two (compounds 9 and 10) generated relatively low activities, resulting in K_{cat}/K_m values equivalent to those determined using benznidazole and nifurtimox, while three (compounds 7, 8, and 11) were not metabolized.

All 12 compounds were then screened to determine whether they displayed growth-inhibitory activity toward BSF *T. brucei* (Table 4). For all except one (compound 8), IC_{50}s < 10 μM were calculated. Those compounds that were poor TbNTR substrates (compounds 7 to 11) generally displayed the highest IC_{50}s, with only the tetra-aziridinyl benzoquinone (compound 11) showing significant antiparasitic activity (IC_{50} of 87 ± 6 nM). All the other compounds found to be effective TbNTR substrates (compounds 1 to 6 and 12) were also shown to have trypanocidal activities, with IC_{50}s ranging from 21 nM (RH1 [compound 3]) to 1.5 μM (AZQ [compound 4]). To evaluate whether TbNTR plays a role in activating the six most potent aziridinyl benzoquinones (DZQ [compound 1], MeDZQ [compound 2], RH1 [compound 3], TZQ [compound 5], compound 6, and compound 11) within the par-

TABLE 3 Activity of TbNTR toward aziridinyl benzoquinones[a]

Compound	Apparent V_{max}	Apparent K_m	K_{cat}/K_m
DZQ (1)	3,340.0 ± 267.0	2.9 ± 0.3	5.0×10^5
MeDZQ (2)	2,334.0 ± 221.0	6.9 ± 1.5	1.5×10^5
RH1 (3)	3,080.0 ± 110.0	2.1 ± 0.2	6.4×10^5
AZQ (4)	750.0 ± 30.0	20.6 ± 2.3	1.6×10^4
TZQ (5)	1,799.0 ± 180.0	6.5 ± 2.1	1.2×10^5
6	1,080.0 ± 30.0	9.9 ± 0.9	4.7×10^4
7	n/a		
8	n/a		
9	120.0 ± 20.0	30.2 ± 11.5	1.7×10^3
10	430.0 ± 50.0	66.7 ± 16.3	2.8×10^3
11	n/a		
12	2,377.0 ± 231.0	5.2 ± 1.3	2.0×10^5

[a] The apparent V_{max} and K_m (± standard deviation) TbNTR (20 μg) values for various aziridinyl benzoquinone substrates (0 to 100 μM) were determined in the presence of NADH (100 μM). TbNTR activity was followed by monitoring NADH oxidation, and the kinetic values were calculated using ε = 6,220 M^{-1} cm^{-1}. The apparent V_{max} values are expressed as nanomoles of NADH oxidized per minute per milligram, and apparent K_m values are expressed in micromoles. The specificity constant (K_{cat}/K_m), expressed in per molar per second, was determined by assuming one catalytic site per 30-kDa monomer. Compounds 7, 8, and 11 were not metabolized by TbNTR (n/a = no activity).

TABLE 4 Trypanocidal activity of aziridinyl benzoquinones[a]

Compound	*T. brucei* IC_{50} (nM)			
	Wild type	Transformed (− tet)	Transformed (+ tet)	Ratio (− tet/+ tet)
DZQ (1)	272 ± 1	318 ± 38	90 ± 3	3.5
MeDZQ (2)	698 ± 57	740 ± 18	115 ± 3	6.4
RH1 (3)	21 ± 1	12 ± 2	3 ± 1	4.0
AZQ (4)	1,590 ± 110			
TZQ (5)	179 ± 1	184 ± 10	60 ± 9	3.1
6	283 ± 41	310 ± 40	140 ± 20	2.2
7	7,733 ± 1030			
8	>10,000			
9	2,450 ± 328			
10	6,293 ± 15			
11	87 ± 6	121 ± 21	148 ± 9	0.8
12	1,253 ± 77			

[a] Data represent the growth-inhibitory effect (as judged by their IC_{50}s) of aziridinyl benzoquinones on wild-type *T. brucei* (Lister 427; clone 221a). For the six most potent compounds, IC_{50}s (± standard deviations [SD]) against parasites transformed to express elevated levels of *TbNTR* under tetracycline (1 μg ml^{-1}) control were also determined. The data in columns 2 to 4 represent mean IC_{50}s (± SD) determined in growth assays performed in triplicate.

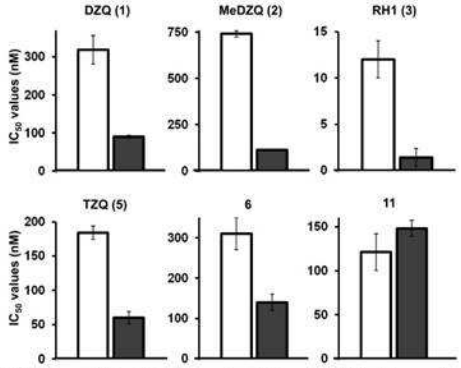

FIG 5 Susceptibility of bloodstream-form *T. brucei* to aziridinyl benzoquinones. IC_{50} values of the most potent aziridinyl benzoquinones on *T. brucei* cells induced to express elevated levels of TbNTR (black bars) compared to noninduced control values (white bars) are shown. Data represent means ± standard deviations (SD) of the results of four experiments, and the differences in susceptibility for DZQ (compound 1), MeDZQ (compound 2), RH1 (compound 3), TZQ (compound 5), and compound 6 were statistically significant ($P < 0.01$), as assessed by Student's *t* test.

asite, we made use of a cell line manipulated to express elevated levels of the enzyme (65). This revealed that, with one exception, cells induced to overexpress NTR were 2- to 6-fold more sensitive to the prodrug (DZQ [compound 1], MeDZQ [compound 2], RH1 [compound 3], TZQ [compound 5], and compound 6) than noninduced controls (Table 4, Fig. 5). In only one case (compound 11) did elevation of the NTR level fail to alter susceptibility, presumably because that compound is not a substrate for this enzyme (Tables 3 and 4).

DISCUSSION

Type I NTRs are a group of enzymes initially believed to be restricted to bacteria. They typically contain FMN as a cofactor and metabolize a wide range of nitroaromatic and quinone substrates in a reaction that is not affected by oxygen (45, 62, 67, 68). It is now clear that several eukaryotic protozoan parasites also express type I NTRs, with these orthologs playing a key role in the activation of the clinically used nitroaromatic prodrugs nifurtimox, benznidazole, and metronidazole (38, 41, 43, 65). Here, we report that the trypanosomal enzymes noncovalently bind FMN, utilize NADH as a reductant, and catalyze the reduction of a wide range of substrates via a ping-pong mechanism, an activity readily inhibited by dicoumarol. These properties are characteristic of their bacterial counterparts.

A distinct feature displayed by all bacterial type I NTRs is their ability to bind FMN as a cofactor, a characteristic shared by TbNTR and TcNTR (Fig. 1) (9, 62, 68). Overall sequence conservation between type I NTRs from different species (pro- and eukaryotic) is low, although some key residues are shared, with many being implicated in cofactor binding (44, 49, 65). For the *E. coli* nfsB sequence, nine residues located across five sites are involved in cofactor interactions (44). Two of these sites, including a characteristic R[S/T/A]X[R/H] amino-terminal cluster, mediate FMN binding via the ribityl chain. Two further regions mediate interactions via the isoalloxazine tricyclic ring, and the fifth attaches to FMN's phosphate grouping. Of these, five amino acids (R90, S92, K94, E260, and R302 [numbering based on TcNTR]) found at three locations are also present in the two trypanosomal enzymes. Site-directed mutagenesis of TcNTR revealed that only one of the mutations, R90A, prevented cofactor interaction and generated an inactive enzyme (Fig. 2). This is the only invariable residue in an amino-terminal cluster present in all nfsB-like type I NTRs from different origins, suggesting the universal importance of this arginine in FMN binding and NTR activity. In bacterial nfsB-like enzymes, reduced NTR activity *in vivo* contributes to drug resistance, with residues equivalent to K94, Q124, and R302 implicated in this process (53, 63). Alterations at these sites generated mutant proteins that bound FMN at levels equivalent to those seen with the wild type but exhibited significantly reduced enzymatic activities (Fig. 2). As K94 and R302 represent two of the residues conserved between nfsB and TcNTR, as noted above, we initially predicted that conversion of the lysine or arginine to alanine at either site would affect cofactor binding. This clearly is not the case, and our results suggest that if K94 or R302 or both are involved in TcNTR/FMN binding, then their contribution to this interaction is secondary to that of R90, with a single mutation at either site insufficient to block attachment.

The spectrum of compounds that TcNTR and TbNTR can metabolize is typical of that reported for other type I NTRs, although there are slight differences in substrate specificity (Table 2) (9, 40, 62, 67, 68). For example, 5-nitroimidazoles such as metronidazole are not readily metabolized by either of the trypanosome enzymes whereas they are efficiently reduced by bacterial and other protozoal type I NTRs (24, 39, 43). When the substrate ranges of the two trypanosomal reductases are contrasted, the two enzymes yielded equivalent specificity constant values for 2-nitroimidazoles, 5-nitrofurans, and DCPIP. However, they can be distinguished based on their ability to reduce nitrobenzyls and benzoquinones, with TbNTR generating specificity constant values ~10-fold higher than TcNTR toward the azirinidyl dinitrobenzamidine CB1954, the nitrobenzyl phosphoramide mustards LH7 and LH37, and the 1,4-benzoquinones ubiquinone 5 and duroquinone. Such disparities are not unexpected, as relatively small sequence variations can have a profound impact on substrate preference: alteration of two amino acids in the *E. coli* nfsB sequence is sufficient to enhance its ability to activate CB1954 by 100-fold (35). Despite these differences, based on specificity constant values, quinone-based compounds generally represent the preferred substrate for both TcNTR and TbNTR (Table 2).

The biological role of the trypanosomal NTRs is unknown. However, targeted gene deletion studies have clearly shown that they are essential to mammalian infective trypanosomes, as BSF *TbNTR* null mutants cannot be generated (65). Likewise, *T. cruzi* insect-form *TcNTR* null mutants are unable to differentiate into infectious metacyclic trypomastigotes and cannot infect mammalian cells (65). Based on their mitochondrial location and preference for quinone-based substrates, coupled with their similarity to FMN-dependent NADH dehydrogenases, enzymes that mediate reduction of ubiquinone to ubiquinol, the trypanosomal type I NTRs may function as ubiquinone reductases. *T. brucei* insect forms are reported to express several distinct ubiquinone reductases, but only two activities have been identified in BSF parasites (17–20, 25, 55). One is attributed to GPDH and the second to

an uncharacterized enzyme. The difference between the parasite forms is associated with the lack of cytochrome-dependent respiratory chains in the mammalian infective stage (6, 58, 59). However, *T. brucei* BSFs do possess a non-cytochrome-dependent terminal oxidase, the trypanosomal alternative oxidase (TAO), which, in concert with GPDH, functions to transfer reducing equivalents from cytosol/glycosome-generated NADH via ubiquinone to O_2, to produce H_2O (6, 10, 12). This cascade plays a key role in energy metabolism by maintaining the cytosolic/glycosomal NADH/NAD^+ balance. Potentially, TbNTR may fulfill a similar role in the parasite's single mitochondrion, helping to maintain the NADH/NAD^+ balance in this organelle. As such, it may represent the "enigmatic" BSF NADH:ubiquinone oxidoreductase activity whose presence has been vigorously debated (55). Interestingly, deep sequence analysis of *T. brucei* populations selected for nifurtimox resistance using a whole-genome loss-of-function screen provided further evidence to link TbNTR activity with ubiquinone availability, giving additional credence to the hypothesis that the biological function of TbNTR is as a ubiquinone reductase (1). Whether this pathway functions in *T. cruzi* is unclear. The mitochondrial energetics of this parasite is less well characterized than that of *T. brucei*, particularly regarding the intracellular stage. *T. cruzi* does not express a direct homologue of TAO but does possess a gene that has the potential to encode a mitochondrially targeted alternative oxidase-like protein (GenBank accession number EAN97989). However, this enzyme lacks certain key features that typify this class of oxidase, and its activity has yet to be confirmed.

The marked preference of the trypanosomal NTRs for quinone substrates suggests that this class of compound might represent an alternative to nitroheterocycles for the treatment of Chagas' disease and/or HAT. Quinones are widely used in medicine as anti-infection and anticancer agents. Trypanocidal screens using natural and synthetic quinones have shown that compounds of this class have potential as antiparasitic agents, although how these mediate their activity remains unclear. Here, we evaluated whether a series of aziridinyl benzoquinone derivatives, anticancer prodrugs designed to undergo activation by the human NQO1, displayed growth inhibitory properties against BSF *T. brucei* and then determined if TbNTR played a role in this activity. All compounds tested contained a 1,4-benzoquinone backbone and two aziridinyl groups at the 2 and 5 positions (Table 1). For most structures, the 3 and 6 positions contained equivalent substitutions (e.g., H for DZQ [compound 1], CH_3 for MeDZQ [compound 2], etc.), although in three cases divergent groupings were present (e.g., CH_2OH and CH_3 in RH1 [compound 3], aziridinyl and H in TZQ [compound 5], or morpholinyl and F in compound 12). Several compounds were identified as the substrates for the parasite enzyme, generating specificity constants 100-fold higher than those of nifurtimox and benznidazole (Tables 2 and 3), with RH1 (compound 3) yielding the highest specificity constant. Although no structure activity relationship could be determined from this limited biochemical screen, compounds containing amine-linked substitutions at positions 3 and 6 on the benzyl backbone were generally the poorest substrates for the parasite enzyme. In tests performed with *T. brucei*, the biochemical data translated into trypanocidal activity (Table 4) such that the best TbNTR substrates were the most potent against the parasite: the most effective aziridinyl quinone was RH1 (compound 3), which yielded an IC_{50} of 21 nM. The exception to this pattern was the tetra-aziridinyl benzoquinone (compound 11), which, although inactive in the biochemical assays, displayed significant potency (IC_{50} of 87 nM) against infection-form parasites. To conclusively demonstrate the link between reductase and trypanocidal activities, susceptibility to the most effective compounds was investigated using parasites engineered to overexpress TbNTR (Table 4; Fig. 5). For five of the six compounds tested, trypanosomes with elevated levels of the TbNTR were more susceptible to the aziridinyl benzoquinone than controls, indicating that this enzyme can activate those agents *in vivo*. The only quinone that failed to elicit a difference was the tetra-aziridinyl benzoquinone (compound 11), which was not metabolized by TbNTR *in vitro*.

We have now shown that the trypanosome enzymes which activate the clinically used prodrugs nifurtimox and benznidazole display many of the characteristics typical of bacterial type I NTRs: they are FMN-containing proteins that reduce a wide range of substrates via an oxygen-insensitive activity that can be readily inhibited by dicoumarol. Based on substrate preference, the trypanosomal type I NTRs can be regarded as quinone (possibly ubiquinone) reductases. We have exploited this characteristic to identify several aziridinyl benzoquinones that display significant antitrypanosomal properties. Understanding how these parasite enzymes mediate their biological function may therefore contribute to the development of novel prodrugs with improved selectivity and pharmacokinetic properties compared to those currently available.

ACKNOWLEDGMENTS

We thank John Kelly (London School of Hygiene and Tropical Medicine) for valuable discussions and comments on the manuscript.

E.L.M. is a recipient of a BBSRC Doctorial Training Studentship.

REFERENCES

1. **Alsford S, et al.** 2012. High-throughput decoding of antitrypanosomal drug efficacy and resistance. Nature **482**:232–236.
2. **Alsford S, Kawahara T, Glover L, Horn D.** 2005. Tagging a *T. brucei* rRNA locus improves stable transfection efficiency and circumvents inducible expression position effects. Mol. Biochem. Parasitol. **144**:142–148.
3. **Armstrong JM.** 1964. The molar extinction coefficient of 2,6-dichlorophenol indophenol. Biochim. Biophy. Acta **86**:194–197.
4. **Begleiter A.** 2000. Clinical applications of quinone-containing alkylating agents. Front. Biosci. **5**:E153–E171.
5. **Bern C, Montgomery SP.** 2009. An estimate of the burden of Chagas disease in the United States. Clin. Infect. Dis. **49**:e52–e54.
6. **Bienen EJ, Maturi RK, Pollakis G, Clarkson AB, Jr.** 1993. Noncytochrome mediated mitochondrial ATP production in bloodstream form *Trypanosoma brucei brucei*. Eur. J. Biochem. **216**:75–80.
7. **Bot C, et al.** 2010. Trypanocidal activity of aziridinyl nitrobenzamide prodrugs. Antimicrob. Agents Chemother. **54**:4246–4252.
8. **Brun R, Blum J, Chappuis F, Burri C.** 2010. Human African trypanosomiasis. Lancet **375**:148–159.
9. **Bryant C, DeLuca M.** 1991. Purification and characterization of an oxygen-insensitive NAD(P)H nitroreductase from *Enterobacter cloacae*. J. Biol. Chem. **266**:4119–4125.
10. **Chaudhuri M, Ott RD, Hill GC.** 2006. Trypanosome alternative oxidase: from molecule to function. Trends Parasitol. **22**:484–491.
11. **Chen Y, Hu L.** 2009. Design of anticancer prodrugs for reductive activation. Med. Res. Rev. **29**:29–64.
12. **Clarkson AB, Jr, Bienen EJ, Pollakis G, Grady RW.** 1989. Respiration of bloodstream forms of the parasite *Trypanosoma brucei brucei* is dependent on a plant-like alternative oxidase. J. Biol. Chem. **264**:17770–17776.
13. **Danson S, Ranson M, Denneny O, Cummings J, Ward TH.** 2007. Validation of the comet-X assay as a pharmacodynamic assay for measuring DNA cross-linking produced by the novel anticancer agent RH1 during a phase I clinical trial. Cancer Chemother. Pharmacol. **60**:851–861.

14. **Danson SJ, et al.** 2011. Phase I pharmacokinetic and pharmacodynamic study of the bioreductive drug RH1. Ann. Oncol. **22**:1653–1660.
15. **Ernster L, Danielson L, Ljunggren M.** 1962. DT diaphorase. I. Purification from the soluble fraction of rat-liver cytoplasm, and properties. Biochim. Biophys. Acta **58**:171–188.
16. **Faeder EJ, Siegel LM.** 1973. A rapid micromethod for determination of FMN and FAD in mixtures. Anal. Biochem. **53**:332–336.
17. **Fang J, Beattie DS.** 2003. Identification of a gene encoding a 54 kDa alternative NADH dehydrogenase in *Trypanosoma brucei*. Mol. Biochem. Parasitol. **127**:73–77.
18. **Fang J, Beattie DS.** 2002. Novel FMN-containing rotenone-insensitive NADH dehydrogenase from *Trypanosoma brucei* mitochondria: isolation and characterization. Biochemistry **41**:3065–3072.
19. **Fang J, Beattie DS.** 2002. Rotenone-insensitive NADH dehydrogenase is a potential source of superoxide in procyclic *Trypanosoma brucei* mitochondria. Mol. Biochem. Parasitol. **123**:135–142.
20. **Fang J, Wang Y, Beattie DS.** 2001. Isolation and characterization of complex I, rotenone-sensitive NADH: ubiquinone oxidoreductase, from the procyclic forms of *Trypanosoma brucei*. Eur. J. Biochem. **268**:3075–3082.
21. **Garavaglia PA, et al.** 2010. Identification, cloning and characterization of an aldo-keto reductase from *Trypanosoma cruzi* with quinone oxidoreductase activity. Mol. Biochem. Parasitol. **173**:132–141.
22. **Gascon J, Bern C, Pinazo MJ.** 2009. Chagas disease in Spain, the United States and other non-endemic countries. Acta Trop. **115**:22–27.
23. **Gautret P, et al for EuroTravNet.** 2009. Imported human African trypanosomiasis in Europe, 2005–2009. Euro. Surveill. **14**:pii=19327. http://www.eurosurveillance.org/ViewArticle.aspx? ArticleId=19327.
24. **Goodwin A, et al.** 1998. Metronidazole resistance in *Helicobacter pylori* is due to null mutations in a gene (*rdxA*) that encodes an oxygen-insensitive NADPH nitroreductase. Mol. Microbiol. **28**:383–393.
25. **Guerra DG, Decottignies A, Bakker BM, Michels PA.** 2006. The mitochondrial FAD-dependent glycerol-3-phosphate dehydrogenase of Trypanosomatidae and the glycosomal redox balance of insect stages of *Trypanosoma brucei* and *Leishmania* spp. Mol. Biochem. Parasitol. **149**:155–169.
26. **Hall BS, Bot C, Wilkinson SR.** 2011. Nifurtimox activation by trypanosomal type I nitroreductases generates cytotoxic nitrile metabolites. J. Biol. Chem. **286**:13088–13095.
27. **Hall BS, Wilkinson SR.** 2012. Activation of benznidazole by trypanosomal type I nitroreductases results in glyoxal formation. Antimicrob. Agents Chemother. **56**:115–123.
28. **Hall BS, Wu X, Hu L, Wilkinson SR.** 2010. Exploiting the drug-activating properties of a novel trypanosomal nitroreductase. Antimicrob. Agents Chemother. **54**:1193–1199.
29. **Henderson GB, et al.** 1988. "Subversive" substrates for the enzyme trypanothione disulfide reductase: alternative approach to chemotherapy of Chagas disease. Proc. Natl. Acad. Sci. U. S. A. **85**:5374–5378.
30. **Hirumi H, Hirumi K.** 1989. Continuous cultivation of *Trypanosoma brucei* blood stream forms in a medium containing a low concentration of serum protein without feeder cell layers. J. Parasitol. **75**:985–989.
31. **Hoet S, Opperdoes F, Brun R, Quetin-Leclercq J.** 2004. Natural products active against African trypanosomes: a step towards new drugs. Nat. Prod. Rep. **21**:353–364.
32. **Hu LQ, et al.** 2011. Synthesis and structure-activity relationships of nitrobenzyl phosphoramide mustards as nitroreductase-activated prodrugs. Bioorg. Med. Chem. Lett. **21**:3986–3991.
33. **Iyanagi T, Yamazaki I.** 1970. One-electron-transfer reactions in biochemical systems. V. Difference in the mechanism of quinone reduction by the NADH dehydrogenase and the NAD(P)H dehydrogenase (DT-diaphorase). Biochim. Biophys. Acta **216**:282–294.
34. **Jaiswal AK.** 2000. Regulation of genes encoding NAD(P)H:quinone oxidoreductases. Free Radic. Biol. Med. **29**:254–262.
35. **Jarrom D, et al.** 2009. Steady-state and stopped-flow kinetic studies of three *Escherichia coli* NfsB mutants with enhanced activity for the prodrug CB1954. Biochemistry **48**:7665–7672.
36. **Koder RL, Miller AF.** 1998. Steady-state kinetic mechanism, stereospecificity, substrate and inhibitor specificity of *Enterobacter cloacae* nitroreductase. Biochim. Biophys. Acta **1387**:395–405.
37. **Kubata BK, et al.** 2002. A key role for old yellow enzyme in the metabolism of drugs by *Trypanosoma cruzi*. J. Exp. Med. **196**:1241–1251.
38. **Müller J, Wastling J, Sanderson S, Muller N, Hemphill A.** 2007. A novel Giardia lamblia nitroreductase, GlNR1, interacts with nitazoxanide and other thiazolides. Antimicrob. Agents Chemother. **51**:1979–1986.
39. **Nillius D, Muller J, Muller N.** 2011. Nitroreductase (GlNR1) increases susceptibility of *Giardia lamblia* and *Escherichia coli* to nitro drugs. J. Antimicrob. Chemother. **66**:1029–1035.
40. **Nivinskas H, et al.** 2002. Two-electron reduction of quinones by *Enterobacter cloacae* NAD(P)H:nitroreductase: quantitative structure-activity relationships. Arch. Biochem. Biophys. **403**:249–258.
41. **Nixon JE, et al.** 2002. Evidence for lateral transfer of genes encoding ferredoxins, nitroreductases, NADH oxidase, and alcohol dehydrogenase 3 from anaerobic prokaryotes to *Giardia lamblia* and *Entamoeba histolytica*. Eukaryot. Cell **1**:181–190.
42. **O'Brien PJ.** 1991. Molecular mechanisms of quinone cytotoxicity. Chem.-Biol. Interact. **80**:1–41.
43. **Pal D, et al.** 2009. *Giardia*, *Entamoeba*, and *Trichomonas* enzymes activate metronidazole (nitroreductases) and inactivate metronidazole (nitroimidazole reductases). Antimicrob. Agents Chemother. **53**:458–464.
44. **Parkinson GN, Skelly JV, Neidle S.** 2000. Crystal structure of FMN-dependent nitroreductase from *Escherichia coli* B: a prodrug-activating enzyme. J. Med. Chem. **43**:3624–3631.
45. **Peterson FJ, Mason RP, Hovsepian J, Holtzman JL.** 1979. Oxygen-sensitive and -insensitive nitroreduction by *Escherichia coli* and rat hepatic microsomes. J. Biol. Chem. **254**:4009–4014.
46. **Pinto AV, de Castro SL.** 2009. The trypanocidal activity of naphthoquinones: a review. Molecules **14**:4570–4590.
47. **Powis G.** 1989. Free radical formation by antitumor quinones. Free Rad. Biol. Med. **6**:63–101.
48. **Purkayastha A, McCue LA, McDonough KA.** 2002. Identification of a Mycobacterium tuberculosis putative classical nitroreductase gene whose expression is coregulated with that of the acr aene within macrophages, in standing versus shaking cultures, and under low oxygen conditions. Infect. Immun. **70**:1518–1529.
49. **Race PR, et al.** 2005. Structural and mechanistic studies of *Escherichia coli* nitroreductase with the antibiotic nitrofurazone. Reversed binding orientations in different redox states of the enzyme. J. Biol. Chem. **280**:13256–13264.
50. **Race PR, et al.** 2007. Kinetic and structural characterisation of *Escherichia coli* nitroreductase mutants showing improved efficacy for the prodrug substrate CB1954. J. Mol. Biol. **368**:481–492.
51. **Ramos EI, et al.** 2009. 2,3-Diphenyl-1,4-naphthoquinone: a potential chemotherapeutic agent against *Trypanosoma cruzi*. J. Parasitol. **95**:461–466.
52. **Rassi A, Marin-Neto JA.** 2010. Chagas disease. Lancet **375**:1388–1402.
53. **Stein DC, Carrizosa E, Dunham S.** 2009. Use of nfsB, encoding nitroreductase, as a reporter gene to determine the mutational spectrum of spontaneous mutations in *Neisseria gonorrhoeae*. BMC Microbiol. **9**:239. doi: 10.1186/1471-2180-9-239.
54. **Stuart K, et al.** 2008. Kinetoplastids: related protozoan pathogens, different diseases. J. Clin. Invest. **118**:1301–1310.
55. **Surve S, Heestand M, Panicucci B, Schnaufer A, Parsons M.** 2012. Enigmatic presence of mitochondrial complex I in *Trypanosoma brucei* bloodstream forms. Eukaryot. Cell **11**:183–193.
56. **Tatsumi K, et al.** 1981. Studies on oxygen-insensitive nitrofuran reductase in *Escherichia coli* B/r. J. Biochem. **89**:855–859.
57. **Tedeschi G, Chen S, Massey V.** 1995. Active site studies of DT-diaphorase employing artificial flavins. J. Biol. Chem. **270**:2512–2516.
58. **Torri AF, Bertrand KI, Hajduk SL.** 1993. Protein stability regulates the expression of cytochrome c during the developmental cycle of *Trypanosoma brucei*. Mol. Biochem. Parasitol. **57**:305–315.
59. **Torri AF, Hajduk SL.** 1988. Posttranscriptional regulation of cytochrome c expression during the developmental cycle of *Trypanosoma brucei*. Mol. Cell. Biol. **8**:4625–4633.
60. **Urech K, Neumayr A, Blum J.** 2011. Sleeping sickness in travelers—do they really sleep? PLoS Negl. Trop. Dis. **5**:e1358. doi:10.1371/journal.pntd.0001358.
61. **Ward TH, et al.** 2005. Preclinical evaluation of the pharmacodynamic properties of 2,5-diaziridinyl-3-hydroxymethyl-6-methyl-1,4-benzoquinone. Clin. Cancer Res. **11**:2695–2701.
62. **Watanabe M, Nishino T, Takio K, Sofuni T, Nohmi T.** 1998. Purification and characterization of wild-type and mutant "classical" nitroreductases of *Salmonella typhimurium*. L33R mutation greatly diminishes binding of FMN to the nitroreductase of *S. typhimurium*. J. Biol. Chem. **273**:23922–23928.

63. **Whiteway J, et al.** 1998. Oxygen-insensitive nitroreductases: analysis of the roles of nfsA and nfsB in development of resistance to 5-nitrofuran derivatives in *Escherichia coli*. J. Bacteriol. **180**:5529–5539.
64. **Wilkinson SR, Kelly JM.** 2009. Trypanocidal drugs: mechanisms, resistance and new targets. Expert Rev. Mol. Med. **11**:e31. http://dx.doi.org/10.1017/S1462399409001252.
65. **Wilkinson SR, Taylor MC, Horn D, Kelly JM, Cheeseman I.** 2008. A mechanism for cross-resistance to nifurtimox and benznidazole in trypanosomes. Proc. Natl. Acad. Sci. U. S. A. **105**:5022–5027.
66. **Yan C, Kepa JK, Siegel D, Stratford IJ, Ross D.** 2008. Dissecting the role of multiple reductases in bioactivation and cytotoxicity of the antitumor agent 2,5-diaziridinyl-3-(hydroxymethyl)-6-methyl-1,4-benzoquinone (RH1). Mol. Pharmacol. **74**:1657–1665.
67. **Zenno S, et al.** 1996. Biochemical characterization of NfsA, the *Escherichia coli* major nitroreductase exhibiting a high amino acid sequence homology to Frp, a *Vibrio harveyi* flavin oxidoreductase. J. Bacteriol. **178**:4508–4514.
68. **Zenno S, Koike H, Tanokura M, Saigo K.** 1996. Gene cloning, purification, and characterization of NfsB, a minor oxygen-insensitive nitroreductase from *Escherichia coli*, similar in biochemical properties to FRase I, the major flavin reductase in *Vibrio fischeri*. J. Biochem. **120**:736–744.

Molecular Microbiology [2015] ■ doi:10.1111/mmi.12973

Unravelling the role of SNM1 in the DNA repair system of *Trypanosoma brucei*

James A. Sullivan,[1] Jie Lun Tong,[1] Martin Wong,[1] Ambika Kumar,[1] Hajrah Sarkar,[1] Sarah Ali,[1] Ikran Hussein,[1] Iqra Zaman,[1] Emma Louise Meredith,[1] Nuala A. Helsby,[2] Longqin Hu[3] and Shane R. Wilkinson[1]*

[1]*School of Biological & Chemical Sciences, Queen Mary University of London, Mile End Road, London E1 4NS, UK.*

[2]*Department of Molecular Medicine and Pathology, University of Auckland, Private Bag 92019, Auckland, New Zealand.*

[3]*Department of Medicinal Chemistry, Ernest Mario School of Pharmacy, Rutgers, The State University of New Jersey, Piscataway, NJ 08854, USA.*

Summary

All living cells are subject to agents that promote DNA damage. A particularly lethal lesion are interstrand cross-links (ICL), a property exploited by several anti-cancer chemotherapies. In yeast and humans, an enzyme that plays a key role in repairing such damage are the PSO2/SNM1 nucleases. Here, we report that *Trypanosoma brucei*, the causative agent of African trypanosomiasis, possesses a *bona fide* member of this family (called TbSNM1) with expression of the parasite enzyme able to suppress the sensitivity yeast *pso2Δ* mutants display towards mechlorethamine, an ICL-inducing compound. By disrupting the Tb*snm1* gene, we demonstrate that TbSNM1 activity is non-essential to the medically relevant *T. brucei* life cycle stage. However, trypanosomes lacking this enzyme are more susceptible to bi- and tri-functional DNA alkylating agents with this phenotype readily complemented by ectopic expression of Tb*snm1*. Genetically modified variants of the null mutant line were subsequently used to establish the anti-parasitic mechanism of action of nitrobenzylphosphoramide mustard and aziridinyl nitrobenzamide prodrugs, compounds previously shown to possess potent trypanocidal properties while exhibiting limited toxicity to mammalian cells. This established that these agents, following activation by a parasite specific type I nitroreductase, produce metabolites that promote formation of ICLs leading to inhibition of trypanosomal growth.

Accepted 16 February, 2015. *For correspondence. E-mail s.r.wilkinson@qmul.ac.uk; Tel. (+44) 20 7882 3057; Fax (+44) 20 882 7732.

Introduction

The socioeconomic development of sub-Saharan Africa has been hindered by a group of medical and veterinary infections collectively known as African trypanosomiasis. The causative agents of many of these diseases are protozoan parasites belonging to the species *Trypanosoma brucei*, organisms that live and multiply extracellularly in the bloodstream and tissue fluids of their mammalian hosts. Transmission occurs *via* the blood-feeding habits of the insect vector, the tsetse fly. Over the last 15 years implementation of improved health surveillance programmes combined with new treatment regimens has led to a dramatic fall in the estimated number of new cases of the human form of the disease, known as human African trypanosomiasis (HAT) from around 450 000 in 1997 to about 20 000 in 2012 (Barrett, 2006; WHO, 2014). This situation has resulted in World Health Organization aiming to eliminate HAT as a public health problem by 2020. In contrast, animal African trypanosomiasis, particularly in domesticated livestock, remains a major problem with these infections killing around 3 million head of cattle each year and causing an annual loss of income estimated to be about US$4.75 billion (UNFAO, 2004).

With no immediate prospect of a vaccine or chemoprophylaxis and with vector control being problematic, drug treatment represents the only option available to combat HAT. However, the current chemotherapies used are few in number and their use is controversial, as they can be costly, often require medical supervision for administration, some have limited efficacy and may cause adverse side effects, with drug resistance becoming more widespread (Wilkinson and Kelly, 2009; Alsford *et al.*, 2013). One way to facilitate the development of new drugs targeting HAT is to better understand the mechanism of action of existing treatments with the properties that underlie parasite selectivity incorporated into the development of new trypanocidal agents. For example, melamine rings have been incorporated into several compounds to exploit the substrate specificity displayed by the P2 adenosine trans-

porter, a permease implicated in the uptake of pentamidine and melarsoprol (Stewart *et al.*, 2004; Baliani *et al.*, 2005; Chollet *et al.*, 2009; Klee *et al.*, 2010; Capes *et al.*, 2012; Giordani *et al.*, 2014). Similarly, a parasite nitroreductase (NTR), an enzyme responsible for the activation of nifurtimox (Wilkinson *et al.*, 2008; Hall *et al.*, 2011), has been used to screen nitroaromatic libraries for anti-*T. brucei* properties (Bot *et al.*, 2010; 2013; Hall *et al.*, 2010; 2012; Hu *et al.*, 2011; Papadopoulou *et al.*, 2011; 2012; 2013). In the latter case, several NTR-activated chemicals containing nitrogen mustard or aziridine functional groups that promote DNA damage *via* formation of cross-linkages have been identified as having significant anti-parasitic activities and low mammalian cell toxicity (Bot *et al.*, 2010; Hall *et al.*, 2010; Hu *et al.*, 2011).

Genomes are constantly challenged by endogenous and exogenous agents that promote DNA damage, with interstrand cross-links (ICLs) representing a particularly dangerous lesion (O'Connor and Kohn, 1990). Formed when the two complementary strands within the DNA double helix become covalently linked, ICLs block essential cellular process that require DNA strand separation including DNA replication and transcription, leading to chromosomal breakage, rearrangements, or cell death (Dronkert and Kanaar, 2001; McHugh *et al.*, 2001; Deans and West, 2011; Sengerova *et al.*, 2011). Estimates indicate that a single ICL can kill a unicellular microbe with as few as 20 being fatal to a mammalian cell (Magana-Schwencke *et al.*, 1982; Lawley and Phillips, 1996). In order to preserve the integrity and functionality of DNA, eukaryotic cells have evolved a series of complementary and overlapping pathways to repair ICLs, although the precise mechanisms involved in these systems are not fully understood (Deans and West, 2011). In *Saccharomyces cerevisiae*, many of the major DNA repair pathways [nucleotide excision repair (NER), mismatch repair, post-replication repair/translesion synthesis and homologous recombination] have been implicated in fixing ICL damage, although only a few proteins specifically involved in ICL lesion repair have been identified (Barber *et al.*, 2005; Lehoczky *et al.*, 2007; Daee *et al.*, 2012; Ward *et al.*, 2012). Of these, Pso2p (also known as Snm1) is of great interest as cells lacking this activity are specifically and highly susceptible to ICL-forming agents including psoralen, cisplatin and mechlorethamine but not to any other forms of DNA damage (Henriques and Moustacchi, 1980; Ruhland *et al.*, 1981a,b). The precise role played by Pso2p in this repair system remains unknown, although biochemical studies have shown that it displays a 5′ exonuclease activity (Li *et al.*, 2005). This coupled with the observation that *pso2Δ* cells exposed to ICL-inducing compounds tend to accumulate DNA double stranded breaks indicates that Pso2p does not function in the initial incision event, which in yeast is primarily controlled by NER, but may be involved in the processing of DNA ends created during the generation of ICL-associated DNA double stranded breaks (Li and Moses, 2003; Barber *et al.*, 2005; Dudas *et al.*, 2007). Intriguingly, Pso2p also displays a structure-specific DNA hairpin opening endonuclease activity providing evidence that it may have other functions outside ICL repair (Tiefenbach and Junop, 2012).

Here, we report that *T. brucei* expresses a Pso2/Snm1 homologue that can readily complement for the susceptibility phenotype exhibited by *pso2Δ* yeast cells towards an ICL forming agent. Deletion of the gene, designated Tb*snm1*, from the parasite genome revealed that although the encoded enzyme is not essential for viability and growth of bloodstream form (BSF) trypanosomes, cells lacking this activity were more susceptible to bifunctional nitrogen mustard- and aziridine-based ICL-inducing agents. Using recombinant *T. brucei* expressing altered levels of Tb*snm1*, we establish that the trypanocidal mechanism of several potent nitroaromatic-based agents that contain ICL-promoting grouping are dependent on an initial activation catalysed by a parasite specific type I NTR that generates metabolites that then promote DNA damage.

Results

Identifying trypanocidal chemical tools for studying DNA repair

Previous screening studies have identified nitroaromatic-based azirindyl/nitrogen mustard compounds to be effective trypanocidal agents (Bot *et al.*, 2010; Hall *et al.*, 2010; Hu *et al.*, 2011). The antimicrobial activity of these involves a parasite specific activation step catalysed by a type I NTR that leads to metabolites postulated to promote DNA damage. To determine if the above compounds do function *via* this pathway, a range of anti-cancer compounds known to mediate their cytotoxicity by promoting DNA cross-linkages were screened for trypanocidal activity against BSF *T. brucei*. The structures tested included non-nitroaromatic-based aziridines and nitrogen mustards, nitrosoureas, platinum complexes, an alkyl sulfonate and non-classical DNA cross-linking agents.

Out of the non-nitroaromatic anti-cancer compounds assessed, 17 had no effect on parasite growth at concentrations of up to 30 μM, including busulfan, the only alkyl sulfonate analysed here, and all five non-classical DNA cross-linking agents (Table 1). These were not analysed further. For the remaining compounds, the concentration that inhibits parasite growth by 50% (IC_{50}'s) was determined (Table 1). For all the remaining classes of DNA cross-linking agents, two or more compounds displayed trypanocidal activities with IC_{50} values ranging from 13 nM for mitomycin C, the most potent agent identified here, to approximately 35 μM for mechlorethamine and ThioTEPA.

Table 1. Susceptibility of *T. brucei* lines to DNA damaging agents.

Compound	*T. brucei* IC_{50}	
	Wild type	Tb*snm1*$^{-/-}$
Nitrogen mustards		
Chlorambucil, cyclophosphamide, uramustine, trofosfamide, ifosfamide, bendamustine	>30.000	nd
Mechlorethamine	34.240 ± 1.270	8.210 ± 1.180
Melphalan	8.660 ± 0.660	3.960 ± 0.320
Estramustine	9.370 ± 1.150	nd
Prednimustine	13.870 ± 1.330	nd
LH7	10.870 ± 0.240	0.580 ± 0.050
LH17	4.160 ± 0.130	0.380 ± 0.040
LH32	0.245 ± 0.079	0.021 ± 0.004
LH33	0.215 ± 0.008	0.015 ± 0.000
LH34	0.067 ± 0.006	0.006 ± 0.001
LH37	0.097 ± 0.009	0.005 ± 0.000
Aziridines		
ThioTEPA	37.830 ± 1.730	13.880 ± 0.970
Triethylenemelamine	1.130 ± 0.150	0.300 ± 0.020
Mitomycin C	0.013 ± 0.001	0.010 ± 0.001
CB1954	3.900 ± 0.420	0.690 ± 0.050
NH1	0.120 ± 0.004	0.044 ± 0.013
Nitrosoureas		
Carmustine, nimustine, NSC270516	>30.000	nd
Lomustine	16.650 ± 0.440	17.310 ± 0.210
Streptozotocin	21.800 ± 5.020	nd
Semustine	4.760 ± 0.050	3.780 ± 0.070
Alkyl sulfonate		
Busulfan	>30.000	nd
Non-classical DNA cross-linking agents		
Altretamine, pipobroman, dacarbazine, temozolomide, mitobronitol	>30.000	nd
Platinum-based		
Oxaliplatin, nedaplatin	>30.000	nd
Cisplatin	2.280 ± 0.130	3.400 ± 0.280
Carboplatin	5.030 ± 0.040	nd
Other agents		
Hydroxyurea	105.970 ± 10.190	88.200 ± 7.300
H_2O_2	43.710 ± 5.950	50.06 ± 7.520
UV irradiation	214.000 ± 13.000	196.000 ± 30.000
MMS	16.125 ± 1.379	14.020 ± 1.343
DMFO	24.150 ± 3.940	24.240 ± 6.710
Nifurtimox	2.850 ± 0.020	2.250 ± 0.090
Benznidazole	46.140 ± 1.440	37.680 ± 1.630

The cell lines analysed were *T. brucei* (wild type) and *T. brucei* Tb*snm1*$^{-/-}$ null mutants (Tb*snm1*$^{-/-}$). IC_{50} values are given in μM except for UV irradiation, which is in J m^{-1}. LH7, LH17, LH32-34, LH37, CB1954 and NH1 represent structures previously identified as trypanocidal agents (Bot *et al.*, 2010; Hall *et al.*, 2010; Hu *et al.*, 2011). nd is not determined.

Identification of the DNA repair enzyme TbSNM1

In other eukaryotes, the SNM1/PSO2 family of nucleases play an important role in repairing damage caused by DNA cross-linking agents (Cattell *et al.*, 2010). Analysis of the *T. b. brucei* genome database (Aslett *et al.*, 2010) identified a single hypothetical gene (designated as Tb*snm1*) of 2163 bp located on chromosome 4 with potential to encode for a 79.5 kDa enzyme (TbSNM1; Gene ID: Tb927.4.1480) related to this family of enzymes. Full-length TbSNM1 is 42% identical to the *T. cruzi* homologue (GenBank accession no. XP_816034) and has 27–32% identity to the leishmanial enzymes LmSNM1 (XP_001686430) and LdSNM1 (XP_003864463). When compared with yeast, plant and mammalian counterparts sequence identity ranged from 15% to 24%. Based on sequence, TbSNM1 can be divided into two regions (Fig. 1). The amino terminal section (residues 36–182) constitutes a non-canonical metallo-ß-lactamase (MBL; pfam12706) domain containing four motifs (motifs 1–4), including a characteristic HxHxDH signature (motif 2), that in other SNM1/PSO2 proteins cooperate to mediate zinc cofactor binding. The second section represents a β-CASP (named after its representative members **C**PSF, **A**rtemis, **S**NM1 and **P**SO2; pfam10996) region (residues 213–519) that contains within it a stretch of 31 amino acids comprising a DRMBL (DNA repair metallo-ß-lactamase; pfam07522) domain (residues 488–519). The β-CASP region contains a fifth zinc binding motif (motif 5) but as with other SNM1/PSO2 sequences the precise location of this has yet to be defined: *in silico* analysis of TbSNM1 indicates that D220 or H497 (motifs 5′ and 5″ respectively) may fulfil this role with H497 being the most likely of the two candidate residues (Callebaut *et al.*, 2002). The β-CASP domain of TbSNM1 also contains a diagnostic valine residue (position 519) that indicates that the parasite enzyme is involved in DNA processing: DNA processing MBLs contain a valine residue at the equivalent site, whereas RNA processing MBLs contain a histidine (Callebaut *et al.*, 2002).

To investigate whether the *T. brucei* enzyme is a SNM1/PSO2 homologue, Tb*snm1* minus its ATG initiation codon was amplified and cloned into a version of the yeast expression vector pYCYlac111 that contains a DNA sequence encoding for the FLAG-tag epitope. The resultant plasmid was transformed into the *S. cerevisiae* wild type and *pso2*Δ strains and expression of recombinant TbSNM1 confirmed by western blot analysis (Fig. 2A). The susceptibility of the fungal lines to mechlorethamine, a DNA cross-linking agent, was then determined and from the resultant dose-response curves the IC_{50} value for each strain calculated (Fig. 2B and C). Yeast lacking *pso2* were clearly more susceptible to the nitrogen mustard than wild type with the null mutant displaying an IC_{50} value approximately 40% that of the control strain. When Tb*snm1* was expressed in wild type yeast a slight (1.4-fold) resistance was noted. This phenotype was also observed in the *pso2*Δ strain expressing Tb*snm1* correlating with an increase in the IC_{50} value from 1.3 μM in cells lacking Pso2p to 5.7 μM in *pso2*Δ yeast expressing FLAG-TbSNM1. These data

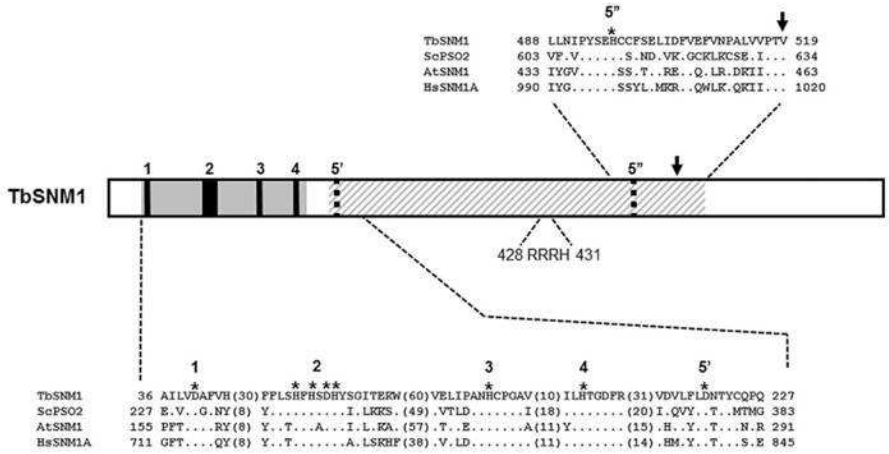

Fig. 1. Sequence analysis of TbSNM1. The sequence corresponding to the metallo-ß-lactamase (MBL; grey box) and β-CASP (hatched box) domains of TbSNM1 was aligned with other members of the SNM1A/PSO2 family of nucleases. The residues that are common with the TbSNM1 sequence are represented by dots. Sequence differences when compared with TbSNM1 are shown. In the alignments, amino acids marked with an asterisks (solid line in TbSNM1 schematic) correspond to motif 1–4, regions postulated to co-ordinate the metal (zinc) cofactor binding. The two possible residues that may represent motif 5 (5′ or 5″; dotted line in TbSNM1 schematic) are also shown. The down arrow highlights the amino acid that distinguishes DNA from RNA processing metallo-β-lactamases, whereas the RRRH sequence corresponds to a putative nuclear 'pattern 4' targeting signal. The sequences aligned are: *T. brucei* TbSNM1 (GenBank AAZ10739), *Saccharomyces cerevisiae* ScPSO2 (NP_013857), *Arabidopsis thaliana* AtSNM1 (NP_189302) and *Homo sapiens* HsSNM1A (NP_001258745).

clearly show that TbSNM1 can complement for the *pso2*Δ mutation and that the trypanosomal enzyme is a *bona fide* SNM1/PSO2 homologue.

TbSNM1 is targeted to the T. brucei *nucleus*

When analysed using the PSORTII and WoLFPSORT algorithms, TbSNM1 was predicted to be targeted to the nucleus *via* a 'four pattern' RRRH (residues 428–431) nuclear localisation signal. To confirm this, the full-length Tb*snm1* gene minus its ATG initiation codon was amplified and ligated in-frame and downstream of the gene encoding for the enhanced green fluorescence protein (GFP) in a trypanosomal vector that facilitated tetracycline inducible gene expression (Alsford *et al.*, 2005). The resultant construct was used to transform BSF *T. brucei*, and parasite clones were selected.

To induce expression of the tagged protein, cells were incubated in the presence of tetracycline for 48 hours. Recombinant parasites were examined by Western blotting using a monoclonal antibody against GFP (Fig. 3A), with extracts derived from these cells containing a band of the expected size (~ 105 kDa), or were fixed and examined by confocal microscopy (Fig. 3B). For parasites expressing GFP-TbSNM1, GFP fluorescence was restricted to a large single spot, a pattern reported for trypanosomal proteins localised to nucleus (Fig. 3B). To confirm this, cells were co-stained with the DNA dye, DAPI. When the images were compared, the pattern of localisation indicated that GFP-TbSNM1 was located in the larger of two compartments (the nucleus) where DAPI is found with the smaller, faint spot corresponding to the kinetoplast, the genome found in the parasites' single mitochondrion.

Functional analysis of TbSNM1 in T. brucei

To assess whether TbSNM1 was essential to BSF *T. brucei*, an RNAi-based approach was initially employed. A DNA fragment corresponding to an internal region of Tb*snm1* was cloned into p2T7^{Ti} (Wilkinson *et al.*, 2003) and the construct transformed into BSF *T. brucei*. In the absence of tetracycline, recombinant clones were found to grow at approximately the same rate as the parental cells. Addition of tetracycline to parasites harbouring the RNAi construct did not affect the growth rate suggesting that TbSNM1 is not essential to BSF *T. brucei*. To confirm this, DNA fragments corresponding to the 5′ flank of Tb*snm1* and the 3′ region of the Tb*snm1* gene were cloned either side of a cassette containing blasticidin or puromycin resistance markers. The integration constructs were trans-

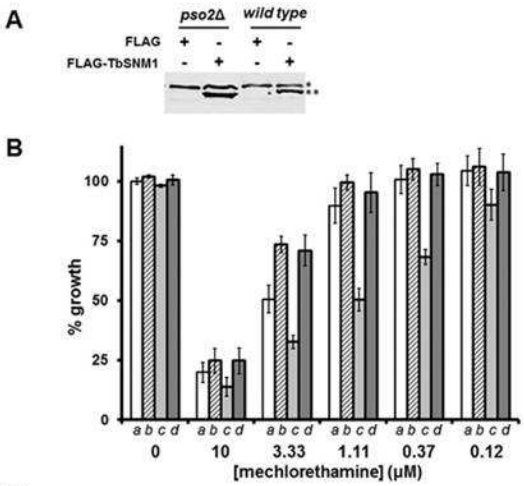

C

	Yeast IC_{50} (μM)			
	wild type + FLAG	wild type + FLAG-TbSNM1	*pso2*Δ + FLAG	*pso2*Δ + FLAG-TbSNM1
mechlorethamine	3.6 ± 0.4	5.1 ± 0.5 (1.4)	1.3 ± 0.6 (0.4)	5.7 ± 0.7 (1.6)

Fig. 2. Complementation of the yeast *pso2*Δ mutation.
A. Western blot analysis was carried out using a monoclonal antibody to the FLAG-tag epitope on cell extracts made from *S. cerevisiae* BY4742 (wild type) and *pso2*Δ strains expressing the FLAG epitope (control) or FLAG-TbSNM1. A band of ~ 80 kDa (indicated by **) was observed in lysates derived from cell expressing the recombinant trypanosomal protein. A cross-reactive epitope (*) and Ponceau S staining of the membrane (not shown) were used as loading controls.
B and C. The susceptibility of wild type (*a* and *b*) and *pso2*Δ (*c* and *d*) yeast strains expressing FLAG (*a* and *c*) or FLAG-TbSNM1 (*b* and *d*) to different concentrations of mechlorethamine. All data are mean values ± standard deviations from experiments performed in triplicate. In C, the values given in parenthesis represent the fold difference in IC_{50} values (in μM) relative to wild-type controls.

formed into BSF *T. brucei* with heterozygote (Tb*snm1*$^{+/-}$) and then null mutant (Tb*snm1*$^{-/-}$) lines selected. Southern hybridisation was used to confirm each integration event demonstrating that both copies of the *Tbsnm1* gene could readily be deleted from the parasite genome (Fig. 4A and B), whereas quantitative RT-PCR data analysed using the comparative C_T method showed that a full-length Tb*snm1* mRNA was not expressed (data not shown) (Schmittgen and Livak, 2008). Reduction or lack of TbSNM1 had no effect on trypanosome growth (data not shown). Therefore, TbSNM1 is non-essential to BSF *T. brucei* under normal culture conditions confirming the RNAi observations.

To evaluate whether deletion of both copies of Tb*snm1* from the *T. brucei* genome altered sensitivity to chemicals that promote DNA cross-linkage, null mutant cells were grown in the presence of these agents, and the IC_{50} values for each compound were determined (Table 1). Cells lacking TbSNM1 were more susceptible to a range of nitrogen mustard and aziridinyl compounds, including several of the trypanocidal nitroaromatic structures previously identified (Bot *et al.*, 2010; Hall *et al.*, 2010; Hu *et al.*, 2011). Intriguingly, Tb*snm1*$^{-/-}$ cells exhibited a larger difference in their sensitivities to the nitrogen mustards screened than that observed when using the aziridinyl compounds. When these growth assays were extended to look at other DNA damaging agents including mitomycin C, semustine, cisplatin, methyl methanesulphonate (MMS), H_2O_2, hydroxyurea and UV light, and to the clinically used trypanocidal drugs nifurtimox, benznidazole or *difluoromethylornithine* (DFMO), no difference in IC_{50} was observed.

In order to demonstrate conclusively that the altered susceptibility phenotypes were specifically due to lack of TbSNM1, a complementation strategy was used. In

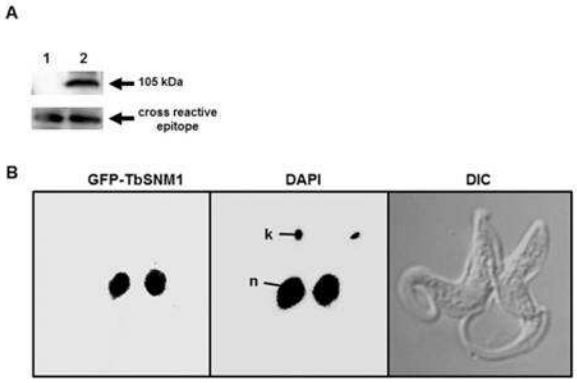

Fig. 3. Localisation of TbSNM1 in bloodstream form *T.brucei*.
A. Expression of GFP-TbSNM1 was examined by probing a blot containing cell lysates from *T. brucei* wild type (lane 1) and GFP-TbSNM1 expressing cells (lane 2) using an anti-GFP antibody (upper panel). Protein from 1.5×10^7 cells was loaded in each track and a cross-reactive epitope (lower panel) and by Coomassie staining (not shown) were used as loading controls.
B. Parasites expressing GFP-TbSNM1 were co-stained with DAPI (DNA) and the cells examined by confocal microscopy. The TbSNM1 signal is coincidental with the nucleus (n; large DAPI spot); the smaller DAPI spot corresponds to the kinetoplast (k), the trypanosome mitochondrial genome.

these experiments, Tb*snm1*$^{-/-}$ cells were transformed with a vector that facilitates constitutive expression of an ectopic copy of Tb*snm1* integrated into one of the parasite's tubulin arrays: wild-type cells also expressing this vector were also generated. The IC_{50} of these parasites towards selected nitrogen mustard and aziridinyl compounds was determined and compared with values obtained using wild type and Tb*snm1* null mutant lines (Fig. 5A). When the susceptibility of the complemented line to the nitrobenzyl-containing nitrogen mustard (LH34) and aziridinyl (NH1) compounds was tested, the resultant dose response curves (and associated IC_{50} values) were distinct from the Tb*snm1*$^{-/-}$ cells, which displayed increased sensitivity to both agents, and equivalent to the plots observed using Tb*snm1* expressing parasites (wild type and wild-type cells engineered to express elevated levels of TbSNM1) (Fig. 5A). When the screens were extended to investigate the complemented line's susceptibility to non-nitroaromatic nitrogen mustard (mechlorethamine) and aziridinyl (triethylenemelamine) compounds, a resistance phenotype was noted, with the dose response curves (and associated IC_{50} values) in the complemented line mirroring that obtained for wild-type parasites expressing elevated levels of TbSNM1 (Fig. 5A): trypanosomes (wild type and Tb*snm1* null mutants) expressing an ectopic copy of Tb*snm1* were up

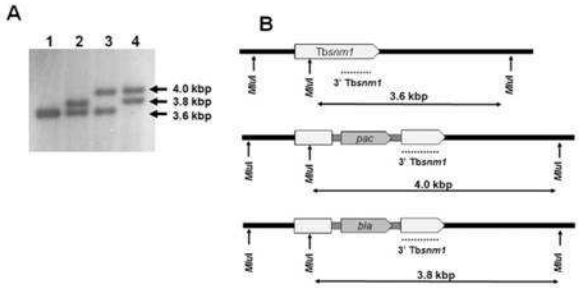

Fig. 4. Disruption of Tb*snm1* in *T. brucei*.
A. Diagram of the Tb*snm1* alleles and the effects of gene disruption. A 5′ Tb*snm1* flanking sequence and a 3′ Tb*snm1* coding region were amplified and cloned sequentially either side of a puromycin (*pac*) or blasticidin (*bla*) cassette (plus *T. brucei* tubulin intergenic elements required for processing of mRNA (hashed boxes). The dotted lines correspond to the probe used to check integration. The position of the predicted *MluI* sites plus the band sizes (in kbp) obtained after hybridisation are shown.
B. Southern blot analysis of *MluI* digested genomic DNA from *T. brucei* (lane 1), Tb*snm1*$^{+/-}$ *bla* and Tb*snm1*$^{+/-}$ *pac* heterozygous clones (lanes 2 and 3 respectively) and a Tb*snm1*$^{-/-}$ null mutant line (lane 4). Blots were hybridised with labelled 3′ region of sequences. Sizes given are in kbp.

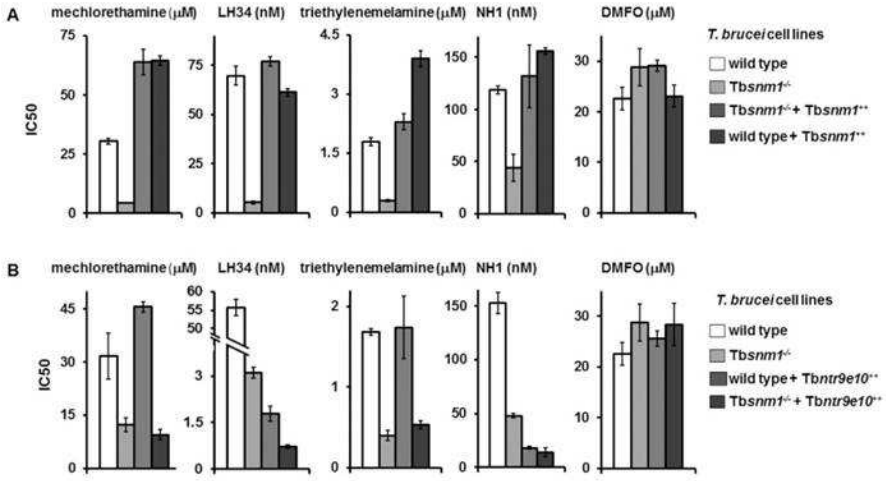

Fig. 5. Susceptibility of *T. brucei* lines expressing altered levels of TbSNM1 to DNA damaging agents.
A. Growth inhibitory effects (expressed as IC_{50} values in μM or nM) of the *T. brucei* wild type, Tb*snm1*$^{-/-}$ null mutant, Tb*snm1*$^{-/-}$ expressing an ectopic copy of Tb*snm1* (Tb*snm1*$^{-/-}$ + Tb*snm1*$^{++}$) and *T. brucei* expressing elevated levels of Tb*snm1* (wild type + Tb*snm1*$^{++}$) lines towards DNA damaging agents. Integration of the Tb*snm1* expression vector into a single tubulin array was confirmed by Southern hybridisation and expression evaluated through qPCR (data not shown).
B. Growth inhibitory effects (expressed as IC_{50} values in μM or nM) of *T. brucei* wild type, Tb*snm1*$^{-/-}$ null mutant, *T. brucei* expressing an ectopic copy of Tb*ntr* (wild type + Tb*ntr9e10*$^{++}$ and Tb*snm1*$^{-/-}$ expressing elevated levels of Tb*ntr* (Tb*snm1*$^{-/-}$ + Tb*ntr9e10*$^{++}$) towards DNA damaging agents. Expression of Tb*ntr* was evaluated through qPCR (data not shown). Data in panels A and B are mean values ± standard deviations from experiments performed in quadruplicate.

to 2.1-fold more resistant to mechlorethamine and triethylenemelamine than wild type.

The above complementation studies indicate that parasites (wild type or Tb*snm1*$^{-/-}$) ectopically expressing Tb*snm1* are resistant to non-nitroaromatic DNA cross-linking agents but not to the nitroaromatic-containing compounds. One reason for this could reflect that the latter structures function as prodrugs and must undergo an NTR catalysed activation step before mediating their trypanocidal DNA damaging activities.

Linking prodrug activation with DNA damage

To identify any link between the DNA damaging and the NTR-activating pathways, both copies of the Tb*snm1* gene were deleted from *T. brucei* cells, expressing an ectopic copy of Tb*ntr* and the susceptibilities of these recombinant cells towards selected nitrogen mustard and aziridinyl compounds determined (Fig. 5B). When treated with mechlorethamine or triethylenemelamine, both Tb*snm1* expressing cell lines (wild type and trypanosomes expressing elevated levels of Tb*ntr*) displayed similar dose response curves and therefore had similar IC_{50}s to either agent (Fig. 5B). When these studies were expanded to investigate the susceptibility of parasites lacking TbSNM1, the Tb*snm1*$^{-/-}$ null mutant line and Tb*snm1*$^{-/-}$ cells expressing the ectopic copy of Tb*ntr* displayed equivalent IC_{50} values, with both being more sensitive to mechlorethamine and triethylenemelamine than wild type (Fig. 5B). Importantly, no difference in IC_{50} was observed using either of the lines lacking Tb*snm1* indicating that Tb*ntr* plays no role in metabolising either mechlorethamine or triethylenemelamine.

When the nitrobenzyl-containing DNA cross-linking agents LH34 and NH1 were tested against the parasite lines expressing altered levels of Tb*snm1* and/or Tb*ntr*, a different outcome was observed (Fig. 5B). For Tb*snm1*$^{-/-}$ parasites or wild-type cells expressing an ectopic copy of Tb*ntr*, treatment with either damaging agents resulted in increased susceptibility when compared against controls, with Tb*ntr* overexpressing trypanosomes being more sensitive to LH34 and NH1 than the null mutant lines: Tb*snm1*$^{-/-}$ cells and *T. brucei* overexpressing Tb*ntr* were 18.0- and 24.0-fold more susceptible to LH34, respectively, with a 2.7- and 31.1-fold increase in sensitivity noted towards NH1. For Tb*snm1*$^{-/-}$ null parasites express-

ing an ectopic copy of Tb*ntr*, this increase in potency was magnified further with these cells showing a 80.0- and 38.7-fold increase in susceptibility towards LH34 and NH1, respectively, when as compared against wild type.

Discussion

Currently, very little is known about the mechanisms *T. brucei* employs to repair ICL damage even though this parasite is exposed to such deleterious insults throughout its cell and life cycles. In other unicellular eukaryotes such as budding and fission yeast, the processing of ICLs occurs through the concerted activities of several major DNA repair pathways with one enzyme, Pso2p, playing a central and specific role in fixing such lesions. Although non-essential for yeast viability, the importance of Pso2p is only apparent in its absence on exposure to ICL-inducing, bifunctional alkylating agents but not to monofunctional alkylating agents, ionising radiation or ultraviolet light (Henriques and Moustacchi, 1980; Ruhland *et al.*, 1981a,b). Here, we report the characterisation of TbSNM1, a trypanosomal Pso2p homologue, and demonstrate that this enzyme plays a key role in processing ICL lesions when generated by bifunctional nitrogen mustard and aziridinyl compounds including several nitroaromatic-based agents previously shown to have potent anti-trypanosomal properties with low toxicity to mammalian cells (Bot *et al.*, 2010; Hall *et al.*, 2010; Hu *et al.*, 2011).

In terms of its sequence, TbSNM1 displays the main characteristics found in other PSO2/SNM1 proteins, possessing adjacent MBL and β-CASP domains that together form the enzyme's zinc-binding central catalytic core (Cattell *et al.*, 2010). To confirm the *in silico* identification, a complementation approach was undertaken. This involved ectopically expressing the trypanosomal enzyme in a yeast *pso2Δ* line and then evaluating the susceptibility of the resultant cells to mechlorethamine, a bifunctional alkylating agent routinely used as an ICL-inducing agent. In this genetic background, the parasite protein was able to revert the susceptibility phenotype displayed by the *pso2Δ* line resulting in an additional slight (approximately twofold) resistance towards this nitrogen mustard. This confirmed that the trypanosomal enzyme is a genuine Pso2p homologue and that it plays a role in the processing of ICL lesions. Furthermore, as TbSNM1 can complement for the *pso2* mutation then the parasite enzyme may interact with the same partner proteins as its yeast counterpart. For example, Pso2p contains an ubiquitin binding zinc finger (UBZ) C2HC motif upstream of its catalytic core (Yang *et al.*, 2010). By analogy with hSNM1A, the only human PSO2/SNM1 homologue able to complement the yeast *pso2* mutation (Hazrati *et al.*, 2008), this signature sequence is able to facilitate binding to monoubiquinated PCNA leading to recruitment of this repair enzyme to ICL-stalled replication forks (Yang *et al.*, 2010). Interestingly, *in silico* searches failed to identify any known UBZ C2HC domain or any other type of ubiquitin interaction motifs (UIMs) in the parasite protein sequence. Therefore, if formation of PSO2/SNM1-containing DNA repair complexes at the site of ICL damage does involve PCNA ubiquitylation, then the molecular mechanisms underlying TbSNM1 recruitment to such lesions occurs through an as yet uncharacterised UIM or *via* interactions involving a conserved adapter protein. Recently, it has been shown that the β-CASP domain of Pso2p can be phosphorylated leading to the suggestion that this event may play a role in modulating the enzyme's exo- or endo-nucleolytic activity (Munari *et al.*, 2014). Whether TbSNM1 undergoes a similar post-translational modification, and how this effects its nuclease activity has yet to be established.

The endogenous function of TbSNM1 is non-essential to replicating *T. brucei*: both copies of *Tbsnm1* could be deleted from the genome of BSF trypomastigote parasites. However, the importance of this enzyme to the trypanosome only became evident following exposure to ICL-inducing compounds: null mutant cells were more susceptible to bi- and tri-functional alkylating agents as compared with controls, whereas these recombinant cells display an equivalent sensitivity to wild type when exposed to MMS, UV irradiation and H_2O_2, treatments normally repaired by homologous recombination, nucleotide excision repair or base excise repair pathways. This trait was solely due to loss of TbSNM1 activity as expression of an ectopic copy of Tb*snm1* in the null mutant genetic background restored the recombinant parasites IC_{50} near to wild-type levels. Intriguingly, the range of compounds that elicits the change in susceptibility in the Tb*snm1*$^{-/-}$ trypanosomes although similar to that noted for the yeast *pso2Δ* line does have some notable differences (Henriques and Moustacchi, 1980; Ruhland *et al.*, 1981a,b). For example, yeast *pso2* mutants are reported to be more susceptible to cisplatin and mitomycin C, whereas *T. brucei* lacking TbSNM1 displays sensitivities similar to that exhibited by wild-type parasites. This may be because that although both compounds can function as ICL-inducing agents they can also mediate their cytotoxic activities *via* other mechanisms including promoting formation of intrastrand cross-links, activating signal transduction pathways, stimulating redox cycling, acting as enzyme inhibitors or alkylating other biological molecules (Sharma and Tomasz, 1994; Pagano *et al.*, 2003; Siddik, 2003; Rabik and Dolan, 2007; Paz *et al.*, 2012). One (or a combination) of these alternative modes of action (or possibly another unidentified mechanism) may account for cisplatin's and mitomycin C's trypanocidal properties, therefore negating the requirement for a TbSNM1-dependent ICL repair pathway.

Previous trypanocidal screening programmes have identified nitrobenzylphosphoramide mustards and aziridi-

nyl nitrobenzamides as having potent anti-parasitic activity (Bot *et al.*, 2010; Hall *et al.*, 2010; Hu *et al.*, 2011). These agents function as prodrugs and must be activated before they can mediate their cytotoxic effects, a reaction catalysed a NADH-dependent type I NTR. This reduction causes the conversion of a conserved electron withdrawing nitro-group present on the compound's benzyl ring to an electron donating hydroxylamine derivative (Bot *et al.*, 2010; Hall *et al.*, 2010; Hu *et al.*, 2011). This action effectively acts as an electronic switch that is believed to turn on the alkylating ability of the nitrogen mustard or aziridinyl moiety causing ICL-mediated DNA damage. Using Tb*snm1* null mutant parasites engineered to express elevated levels of TbNTR, we have now demonstrated a link between prodrug activation and ICL formation. Here we observed that wild-type parasites exhibited the highest IC_{50} values towards LH34 (a nitrobenzylphosphoramide mustard) and NH1 (an aziridinyl nitrobenzamide), whereas trypanosomes lacking TbSNM1 and cells overexpressing TbNTR had intermediate sensitivities. Interestingly, Tb*snm1* null mutants that also express elevated levels of TbNTR were the most prone to both compounds. This implies that following uptake, LH34 and NH1 are transported into mitochondrion where they undergo TbNTR-mediated reduction to form the bioactive products. These observations suggest that in parasites where the NTR activity is overexpressed, this conversion occurs at a faster rate than in wild-type cells resulting in increased sensitivity to the compound. A portion of the resulting metabolites are then able to access the nucleus where they induce ICL formation. In the absence of TbSNM1, mutant cells are less able to repair this type of DNA damage, resulting in an increased susceptibility to the ICL-inducing agent. In parasites where both TbSNM1 and TbNTR levels have been altered, this susceptibility phenotype is exacerbated. Intriguingly, the difference in sensitivities between Tb*snm1*$^{-/-}$ cells expressing elevated TbNTR levels from those over expressing TbNTR alone was greater for LH34 than for NH1. This may be attributable to properties of the substrate/TbNTR-generated metabolites, possibly reflecting differences in cell and/or organelle uptake [TbNTR is a mitochondrial protein (Wilkinson *et al.*, 2008)] or how the substrates interact with, or how the metabolites are released from, TbNTR [*in vitro* nitrobenzyl phosphoramide nitrogen mustard-based compounds interact with TbNTR more readily than the aziridinyl nitrobenzamide (Hall *et al.*, 2012)]. Additionally, as this study only considers ICL formation and repair in the nuclear genome, it is plausible that LH34 and NH1 reduction products may also affect the mitochondrial genome with the NH1 metabolites preferentially affecting this DNA containing region and not the nucleus.

We have now demonstrated that *T. brucei* expresses a *bona fide* homologue of the PSO2/SNM1 nuclease family. The trypanosomal enzyme displays characteristics of its yeast counterpart and is able to repair the DNA damage caused by bi- and tri-functional alkylating agents. By exploiting parasites lacking this enzyme we were able to demonstrate that following TbNTR-mediated activation nitrobenzylphosphoramide mustard and aziridinyl nitrobenzamide agents, compounds previously shown to have potent trypanocidal properties with little/no cytotoxicity in mammalian cells, generate metabolites that promote ICL formation. Although not essential to survival of the medically relevant form of *T. brucei*, in the future TbSNM1 could be targeted through the use of inhibitors to improve the potency of other drugs that do cause parasite death through formation of the extremely lethal ICL.

Experimental procedures

Cell culturing

Bloodstream form *Trypanosoma brucei brucei* [MITat 427 strain; clone 221a and a derivative (2T1) engineered to express elevated levels of TbNTR-myc] was maintained in HMI-9 (Invitrogen) medium supplemented with 3 g l^{-1} sodium bicarbonate, 0.014% (v/v) β-mercaptoethanol and 10% (v/v) foetal calf serum (Hirumi and Hirumi, 1989; Wilkinson *et al.*, 2008) at 37°C under a 5% (v/v) CO_2 atmosphere. The 2T1 cells were grown in the presence of 1 μg ml^{-1} phleomycin and 2 μg ml^{-1} puromycin. Transformed *T. brucei* cells were grown in the presence of 2.5 μg ml^{-1} hygromycin, 10 μg ml^{-1} blasticidin and/or 2 μg ml^{-1} puromycin.

Saccharomyces cerevisiae strains BY4742 (*MATα his3-Δ1 leu2-Δ0 lys2-Δ0 ura3-Δ0*) and a *pso2Δ* derivative obtained from the Open Biosystems (Thermo Scientific) knock-out collection were maintained in yeast extract-peptone broth containing 2% (w/v) glucose. Transformed cells were grown in Synthetic Complete Dropout medium lacking leucine (Sigma).

Chemicals

The DNA damaging agents were obtained from Drug Synthesis and Chemistry Branch, Developmental Therapeutics Program, Division of Cancer Treatment and Diagnosis, National Cancer Institute except CB1954, H_2O_2, MMS and hydroxyurea (all Sigma-Aldrich), NH1 (Helsby *et al.*, 2004) and LH7, LH17, LH32-34 and LH37 (Hu *et al.*, 2003; 2011; Li *et al.*, 2003). Nifurtimox and benznidazole were obtained from Simon Croft (London School of Hygiene and Tropical Medicine) and DFMO from Mike Barrett (University of Glasgow).

Plasmids

The vectors used to delete Tb*snm1* from the *T. brucei* genome were generated as follows. Primers were designed to amplify 897 or 909 bp fragments from the 5′ Tb*snm1* untranslated region and 3′ region of the Tb*snm1* gene respectively. These

were cloned sequentially either side of a puromycin- (*pac*) or blasticidin- (*bla*) containing resistance cassette. The constructs were linearised (SacI/KpnI for the *pac* vector or SacII/KpnI for the *bla* vector) then introduced into BSF *T. brucei* using the Human T-cell Nucleofector® kit and an Amaxa® Nucleofector™ (Lonza AG) set to program X-001. Integration of the DNA constructs into the *T. brucei* genome results in deletion of 60% of the Tb*snm1* open reading frame (amino acids 1 to 425) including all of the non-canonical MBL domain. As this region is essential for Pso2p/SNM1 function (Li and Moses, 2003), removal of the MBL encoding DNA sequence from the trypanosomal genome would generate parasites lacking TbSNM1 activity, effectively producing Tb*snm1* null mutant cells.

The Tb*snm1* trypanosomal expression vector was generated as follows: a 2166 bp DNA sequence corresponding to full-length Tb*snm1* was amplified from *T. brucei* genomic DNA using the primers *cctgcagg*ATGGCAGGTGGA GCTGCAGGT and *gcgcgcc*TTATTCTGAGTC ACTACTCAG (lower-case italics correspond to restriction sites incorporated into the primers to facilitate cloning), digested with SdaI/SgsI and ligated into the corresponding sites of vector pTubEX-LmSpSyn (Taylor *et al.*, 2008), replacing Lm*spsyn*. The NotI/XhoI digested construct was introduced into *T. brucei* wild type and *Tbsnm1*$^{-/-}$ cells using nucleofection and recombinant clones selected.

For the localisation construct, a 2166 bp DNA sequence corresponding to full-length Tb*snm1* was amplified from *T. brucei* genomic DNA using the primers *tctaga*GCAGGTGGAGCTGC AGGTAAG and *gagatct*TTATTCTGAGTCACT ACTCAG (lower-case italics correspond to restriction sites incorporated into the primers to facilitate cloning), the fragment digested with XbaI/BglII and ligated into the XbaI/BamHI sites of vector pRPa$^{GFP\text{-}AT2}$ (Alsford *et al.*, 2005) to replace the Tb*at2* coding sequence. The cloning was carried out such that the gene coding for the GFP was inserted in-frame at the 5′ end of the *Tbsnm1*-derived DNA fragment. The AscI-digested construct was introduced into *T. brucei* 2T1 parasites.

To construct the yeast complementation vector Tb*snm1* was amplified from the trypanosomal localisation plasmid using the primers *tctaga*GCAGGTGGAGCTGCAGGTAA G and *aagctt*TTATTCTGAGTCACTACTCAG (lower-case italics correspond to restriction sites incorporated into the primers to facilitate cloning). The resultant fragment was digested with XbaI/HindIII and ligated into the corresponding sites of a pYCYlac111 derivative containing a DNA sequence encoding for the FLAG-tag epitope (Novoselova *et al.*, 2013). The plasmid was transformed into yeast strains BY4742 and *pso2*Δ. In this system recombinant TbSNM1 is tagged at its amino-terminus with a FLAG-tag epitope detectable with the anti-FLAG monoclonal antibody (Sigma).

Localisation

BSF trypanosomes expressing GFP-TbSNM1 were washed twice in phosphate-buffered saline (PBS), fixed in 2% (w/v) paraformaldehyde/PBS and washed again in PBS. Aliquots of the cell suspension (10^5 cells) were then air dried onto microscope slides. Parasite DNA was stained using Vectashield Mounting Medium containing 4′,6-diamidino-2-phenylindole (DAPI) (Vectorshield Laboratories), and slides were viewed using a Leica SP5 confocal microscope (Leica Microsystems (UK) Ltd).

Antiproliferative assays

All assays were performed in a 96-well plate format. *T. brucei* BSF parasites were seeded at 1×10^4 ml^{-1} in 200 µl growth medium containing different concentrations of compound. For UV irradiation, parasites were exposed to doses up to 900 J m^{-2} using a Stratalinker® UV crosslinker (Stratagene). After incubation at 37°C for 3 days, 2.5 µg resazurin (20 µl of 0.125 µg ml^{-1} stock in phosphate buffered saline) was added to each well, and the plates were incubated for a further 6–8 hours (Jones *et al.*, 2010). Cell densities were determined by monitoring the fluorescence of each culture using a Gemini Fluorescent Plate Reader (Molecular Devices (UK) Ltd, Wokingham, UK) at an excitation wavelength of 530 nm, emission wavelength of 585 nm and a filter cutoff at 550 nm. The drug/treatment concentration that inhibits cell growth by 50% (IC_{50}) was established using the non-linear regression tool on GraphPad Prism (GraphPad Software).

Yeast complementation assay

All assays were performed in a 96-well plate format. The cell density of overnight yeast cultures were equalised according to absorbance at 405 nm in medium containing different concentrations of mechlorethamine. The growth of each strain was then followed by monitoring the change in absorbance at 405 nm using an Absorbance Microplate Reader (BioTek Instruments Ltd). The % growth for each mechlorethamine-treated culture after 18 hours relative to untreated samples was determined.

Acknowledgements

Emma Louise Meredith is a recipient of a BBSRC Doctorial Training Studentship. We would like to thank Martin Taylor (London School of Hygiene and Tropical Medicine) for valuable discussions and comments on the manuscript.

References

Alsford, S., Kawahara, T., Glover, L., and Horn, D. (2005) Tagging a *T. brucei* RRNA locus improves stable transfection efficiency and circumvents inducible expression position effects. *Mol Biochem Parasitol* **144:** 142–148.

Alsford, S., Kelly, J.M., Baker, N., and Horn, D. (2013) Genetic dissection of drug resistance in trypanosomes. *Parasitology* **140:** 1478–1491.

Aslett, M., Aurrecoechea, C., Berriman, M., Brestelli, J., Brunk, B.P., Carrington, M., *et al.* (2010) TriTrypDB: a functional genomic resource for the Trypanosomatidae. *Nucleic Acids Res* **38:** D457–D462.

Baliani, A., Bueno, G.J., Stewart, M.L., Yardley, V., Brun, R., Barrett, M.P., and Gilbert, I.H. (2005) Design and synthesis of a series of melamine-based nitroheterocycles with activ-

ity against Trypanosomatid parasites. *J Med Chem* **48:** 5570–5579.
Barber, L.J., Ward, T.A., Hartley, J.A., and McHugh, P.J. (2005) DNA interstrand cross-link repair in the *Saccharomyces cerevisiae* cell cycle: overlapping roles for PSO2 (SNM1) with MutS factors and EXO1 during S phase. *Mol Cell Biol* **25:** 2297–2309.
Barrett, M.P. (2006) The rise and fall of sleeping sickness. *Lancet* **367:** 1377–1378.
Bot, C., Hall, B.S., Bashir, N., Taylor, M.C., Helsby, N.A., and Wilkinson, S.R. (2010) Trypanocidal activity of aziridinyl nitrobenzamide prodrugs. *Antimicrob Agents Chemother* **54:** 4246–4252.
Bot, C., Hall, B.S., Alvarez, G., Di Maio, R., Gonzalez, M., Cerecetto, H., and Wilkinson, S.R. (2013) Evaluating 5-nitrofurans as trypanocidal agents. *Antimicrob Agents Chemother* **57:** 1638–1647.
Callebaut, I., Moshous, D., Mornon, J.P., and de Villartay, J.P. (2002) Metallo-beta-lactamase fold within nucleic acids processing enzymes: the beta-CASP family. *Nucleic Acids Res* **30:** 3592–3601.
Capes, A., Patterson, S., Wyllie, S., Hallyburton, I., Collie, I.T., McCarroll, A.J., *et al.* (2012) Quinol derivatives as potential trypanocidal agents. *Bioorg Med Chem* **20:** 1607–1615.
Cattell, E., Sengerova, B., and McHugh, P.J. (2010) The SNM1/Pso2 family of ICL repair nucleases: from yeast to man. *Environ Mol Mutagen* **51:** 635–645.
Chollet, C., Baliani, A., Wong, P.E., Barrett, M.P., and Gilbert, I.H. (2009) Targeted delivery of compounds to *Trypanosoma brucei* using the melamine motif. *Bioorg Med Chem* **17:** 2512–2523.
Daee, D.L., Ferrari, E., Longerich, S., Zheng, X.F., Xue, X., Branzei, D., *et al.* (2012) Rad5-dependent DNA repair functions of the *Saccharomyces cerevisiae* FANCM protein homolog Mph1. *J Biol Chem* **287:** 26563–26575.
Deans, A.J., and West, S.C. (2011) DNA interstrand crosslink repair and cancer. *Nat Rev Cancer* **11:** 467–480.
Dronkert, M.L., and Kanaar, R. (2001) Repair of DNA interstrand cross-links. *Mutat Res* **486:** 217–247.
Dudas, A., Vlasakova, D., Dudasova, Z., Gabcova, D., Brozmanova, J., and Chovanec, M. (2007) Further characterization of the role of Pso2 in the repair of DNA interstrand cross-link-associated double-strand breaks in *Saccharomyces cerevisiae*. *Neoplasma* **54:** 189–194.
Giordani, F., Buschini, A., Baliani, A., Kaiser, M., Brun, R., Barrett, M.P., *et al.* (2014) Characterisation of a melamino nitroheterocycle as a potential lead for the treatment of human African trypanosomiasis. *Antimicrob Agents Chemother* **58:** 5747–5757.
Hall, B.S., Wu, X., Hu, L., and Wilkinson, S.R. (2010) Exploiting the drug-activating properties of a novel trypanosomal nitroreductase. *Antimicrob Agents Chemother* **54:** 1193–1199.
Hall, B.S., Bot, C., and Wilkinson, S.R. (2011) Nifurtimox activation by trypanosomal type I nitroreductases generates cytotoxic nitrile metabolites. *J Biol Chem* **286:** 13088–13095.
Hall, B.S., Meredith, E.L., and Wilkinson, S.R. (2012) Targeting the substrate preference of a type I nitroreductase to develop antitrypanosomal quinone-based prodrugs. *Antimicrob Agents Chemother* **56:** 5821–5830.
Hazrati, A., Ramis-Castelltort, M., Sarkar, S., Barber, L.J., Schofield, C.J., Hartley, J.A., and McHugh, P.J. (2008) Human SNM1A suppresses the DNA repair defects of yeast pso2 mutants. *DNA Repair (Amst)* **7:** 230–238.
Helsby, N.A., Atwell, G.J., Yang, S., Palmer, B.D., Anderson, R.F., Pullen, S.M., *et al.* (2004) Aziridinyldinitrobenzamides: synthesis and structure-activity relationships for activation by *E. coli* nitroreductase. *J Med Chem* **47:** 3295–3307.
Henriques, J.A., and Moustacchi, E. (1980) Isolation and characterization of pso mutants sensitive to photo-addition of psoralen derivatives in *Saccharomyces cerevisiae*. *Genetics* **95:** 273–288.
Hirumi, H., and Hirumi, K. (1989) Continuous cultivation of *Trypanosoma brucei* blood stream forms in a medium containing a low concentration of serum protein without feeder cell layers. *J Parasitol* **75:** 985–989.
Hu, L., Yu, C., Jiang, Y., Han, J., Li, Z., Browne, P., *et al.* (2003) Nitroaryl phosphoramides as novel prodrugs for *E. coli* nitroreductase activation in enzyme prodrug therapy. *J Med Chem* **46:** 4818–4821.
Hu, L.Q., Wu, X.H., Han, J.Y., Chen, L., Vass, S.O., Browne, P., *et al.* (2011) Synthesis and structure-activity relationships of nitrobenzyl phosphoramide mustards as nitroreductase-activated prodrugs. *Bioorg Med Chem Lett* **21:** 3986–3991.
Jones, D.C., Hallyburton, I., Stojanovski, L., Read, K.D., Frearson, J.A., and Fairlamb, A.H. (2010) Identification of a κ-opioid agonist as a potent and selective lead for drug development against human African trypanosomiasis. *Biochem Pharmacol* **80:** 1478–1486.
Klee, N., Wong, P.E., Baragana, B., Mazouni, F.E., Phillips, M.A., Barrett, M.P., and Gilbert, I.H. (2010) Selective delivery of 2-hydroxy APA to *Trypanosoma brucei* using the melamine motif. *Bioorg Med Chem Lett* **20:** 4364–4366.
Lawley, P.D., and Phillips, D.H. (1996) DNA adducts from chemotherapeutic agents. *Mutat Res* **355:** 13–40.
Lehoczky, P., McHugh, P.J., and Chovanec, M. (2007) DNA interstrand cross-link repair in *Saccharomyces cerevisiae*. *FEMS Microbiol Rev* **31:** 109–133.
Li, X., and Moses, R.E. (2003) The beta-lactamase motif in Snm1 is required for repair of DNA double-strand breaks caused by interstrand crosslinks in *S. cerevisiae*. *DNA Repair (Amst)* **2:** 121–129.
Li, X., Hejna, J., and Moses, R.E. (2005) The yeast Snm1 protein is a DNA 5′-exonuclease. *DNA Repair (Amst)* **4:** 163–170.
Li, Z., Han, J., Jiang, Y., Browne, P., Knox, R.J., and Hu, L. (2003) Nitrobenzocyclophosphamides as potential prodrugs for bioreductive activation: synthesis, stability, enzymatic reduction, and antiproliferative activity in cell culture. *Bioorg Med Chem* **11:** 4171–4178.
McHugh, P.J., Spanswick, V.J., and Hartley, J.A. (2001) Repair of DNA interstrand crosslinks: molecular mechanisms and clinical relevance. *Lancet Oncol* **2:** 483–490.
Magana-Schwencke, N., Henriques, J.A., Chanet, R., and Moustacchi, E. (1982) The fate of 8-methoxypsoralen photoinduced crosslinks in nuclear and mitochondrial yeast DNA: comparison of wild-type and repair-deficient strains. *Proc Natl Acad Sci USA* **79:** 1722–1726.
Munari, F.M., Revers, L.F., Cardone, J.M., Immich, B.F.,

Moura, D.J., Guecheva, T.N., *et al.* (2014) Sak1 kinase interacts with Pso2 nuclease in response to DNA damage induced by interstrand crosslink-inducing agents in *Saccharomyces cerevisiae*. *J Photochem Photobiol B* **130:** 241–253.

Novoselova, T.V., Rose, R.S., Marks, H.M., and Sullivan, J.A. (2013) SUMOylation regulates the homologous to E6-AP carboxyl terminus (HECT) ubiquitin ligase Rsp5p. *J Biol Chem* **288:** 10308–10317.

O'Connor, P.M., and Kohn, K.W. (1990) Comparative pharmacokinetics of DNA lesion formation and removal following treatment of L1210 cells with nitrogen mustards. *Cancer Commun* **2:** 387–394.

Pagano, G., Manini, P., and Bagchi, D. (2003) Oxidative stress-related mechanisms are associated with xenobiotics exerting excess toxicity to Fanconi anemia cells. *Environ Health Perspect* **111:** 1699–1703.

Papadopoulou, M.V., Trunz, B.B., Bloomer, W.D., McKenzie, C., Wilkinson, S.R., Prasittichai, C., *et al.* (2011) Novel 3-nitro-1H-1,2,4-triazole-based aliphatic and aromatic amines as anti-chagasic agents. *J Med Chem* **54:** 8214–8223.

Papadopoulou, M.V., Bloomer, W.D., Rosenzweig, H.S., Chatelain, E., Kaiser, M., Wilkinson, S.R., *et al.* (2012) Novel 3-nitro-1H-1,2,4-triazole-based amides and sulfonamides as potential antitrypanosomal agents. *J Med Chem* **55:** 5554–5565.

Papadopoulou, M.V., Bloomer, W.D., Rosenzweig, H.S., Ashworth, R., Wilkinson, S.R., Kaiser, M., *et al.* (2013) Novel 3-nitro-1H-1,2,4-triazole-based compounds as potential anti-Chagasic drugs: in vivo studies. *Future Med Chem* **5:** 1763–1776.

Paz, M.M., Zhang, X., Lu, J., and Holmgren, A. (2012) A new mechanism of action for the anticancer drug mitomycin C: mechanism-based inhibition of thioredoxin reductase. *Chem Res Toxicol* **25:** 1502–1511.

Rabik, C.A., and Dolan, M.E. (2007) Molecular mechanisms of resistance and toxicity associated with platinating agents. *Cancer Treat Rev* **33:** 9–23.

Ruhland, A., Kircher, M., Wilborn, F., and Brendel, M. (1981a) A yeast mutant specifically sensitive to bifunctional alkylation. *Mutat Res* **91:** 457–462.

Ruhland, A., Haase, E., Siede, W., and Brendel, M. (1981b) Isolation of yeast mutants sensitive to the bifunctional alkylating agent nitrogen mustard. *Mol Gen Genet* **181:** 346–351.

Schmittgen, T.D., and Livak, K.J. (2008) Analyzing real-time PCR data by the comparative C(T) method. *Nat Protoc* **3:** 1101–1108.

Sengerova, B., Wang, A.T., and McHugh, P.J. (2011) Orchestrating the nucleases involved in DNA interstrand cross-link (ICL) repair. *Cell Cycle* **10:** 3999–4008.

Sharma, M., and Tomasz, M. (1994) Conjugation of glutathione and other thiols with bioreductively activated mitomycin C. Effect of thiols on the reductive activation rate. *Chem Res Toxicol* **7:** 390–400.

Siddik, Z.H. (2003) Cisplatin: mode of cytotoxic action and molecular basis of resistance. *Oncogene* **22:** 7265–7279.

Stewart, M.L., Bueno, G.J., Baliani, A., Klenke, B., Brun, R., Brock, J.M., *et al.* (2004) Trypanocidal activity of melamine-based nitroheterocycles. *Antimicrob Agents Chemother* **48:** 1733–1738.

Taylor, M.C., Kaur, H., Blessington, B., Kelly, J.M., and Wilkinson, S.R. (2008) Validation of spermidine synthase as a drug target in African trypanosomes. *Biochem J* **409:** 563–569.

Tiefenbach, T., and Junop, M. (2012) Pso2 (SNM1) is a DNA structure-specific endonuclease. *Nucleic Acids Res* **40:** 2131–2139.

UNFAO (2004) *Programme against African trypanosomosis – the disease*. URL http://www.fao.org/ag/againfo/programmes/en/paat/disease.html

Ward, T.A., Dudasova, Z., Sarkar, S., Bhide, M.R., Vlasakova, D., Chovanec, M., and McHugh, P.J. (2012) Components of a Fanconi-like pathway control Pso2-independent DNA interstrand crosslink repair in yeast. *PLoS Genet* **8:** e1002884.

WHO (2014) Human African trypanosomiasis (sleeping sickness). *Factsheet* **259:**. URL http://www.who.int/mediacentre/factsheets/fs259/en/

Wilkinson, S.R., and Kelly, J.M. (2009) Trypanocidal drugs: mechanisms, resistance and new targets. *Expert Rev Mol Med* **11:** e31.

Wilkinson, S.R., Horn, D., Prathalingam, S.R., and Kelly, J.M. (2003) RNA interference identifies two hydroperoxide metabolizing enzymes that are essential to the bloodstream form of the African trypanosome. *J Biol Chem* **278:** 31640–31646.

Wilkinson, S.R., Taylor, M.C., Horn, D., Kelly, J.M., and Cheeseman, I. (2008) A mechanism for cross-resistance to nifurtimox and benznidazole in trypanosomes. *Proc Natl Acad Sci USA* **105:** 5022–5027.

Yang, K., Moldovan, G.L., and D'Andrea, A.D. (2010) RAD18-dependent recruitment of SNM1A to DNA repair complexes by a ubiquitin-binding zinc finger. *J Biol Chem* **285:** 19085–19091.

References

Alirol, E., Schrumpf, D., Amici Heradi, J., Riedel, A., De Patoul, C., Quere, M. & Chappuis, F.,(2013) Nifurtimox-eflornithine combination therapy for second-stage gambiense human African trypanosomiasis: Médecins Sans Frontières experience in the Democratic Republic of the Congo. *Clinical Infectious Diseases*, 56, pp.195–203.

Alley, S.C., Brameld, K.A. & Hopkins, P.B.,(1994) DNA interstand cross-linking by 2,5-Bis(1-aziridinyl)-1,4-benzoquinone: Nucleotide sequence Preferences and Covalent Structure of dG-to-dG Cross-links at 5-d' (GNnC) in Synthethic Oligonucleotide Duplexes. *Journal of American Chemical Society*, 116(7), pp.2734–2741.

Alsford, S., Currier, R.B., Guerra-Assunção, J.A., Clark, T.G. & Horn, D.,(2014) Cathepsin-L can resist lysis by human serum in Trypanosoma brucei brucei. *PLoS pathogens*, 10(5), p.e1004130.

Alsford, S., Eckert, S., Baker, N., Glover, L., Sanchez-Flores, A., Leung, K.F., Turner, D.J., Field, M.C., Berriman, M. & Horn, D.,(2012) High-throughput decoding of antitrypanosomal drug efficacy and resistance. *Nature*, pp.1–6.

Alsford, S. & Horn, D.,(2008) Single-locus targeting constructs for reliable regulated RNAi and transgene expression in Trypanosoma brucei. *Molecular and biochemical parasitology*, 161(1), pp.76–9.

Alsford, S., Kelly, J.M., Baker, N. & Horn, D.,(2013) Genetic dissection of drug resistance in trypanosomes. *Parasitology*, 140(12), pp.1478–91.

Alsford, S., Turner, D.J., Obado, S.O., Sanchez-Flores, A., Glover, L., Berriman, M., Hertz-Fowler, C. & Horn, D.,(2011) High-throughput phenotyping using parallel sequencing of RNA interference targets in the African trypanosome. *Genome research*, 21(6), pp.915–24.

Avendano, C. & Menendez, J.C.,(2008) *Medicinal Chemistry of Anticancer drugs* 1st ed., Amsterdam: Elsevier Science and Technology.

Bacchi, C.J.,(2009) Chemotherapy of human african trypanosomiasis. *Interdisciplinary perspectives on infectious diseases*, 2009, p.195040.

Baggish, A.L. & Hill, D.R.,(2002) Antiparasitic agent atovaquone. *Antimicrobial Agents and Chemotherapy*, 46(5), pp.1163–1173.

Baker, N., Alsford, S. & Horn, D.,(2011) Genome-wide RNAi screens in African trypanosomes identify the nifurtimox activator NTR and the eflornithine transporter AAT6. *Molecular and biochemical parasitology*, 176(1), pp.55–7.

Baker, N., de Koning, H.P., Mäser, P. & Horn, D.,(2013) Drug resistance in African trypanosomiasis: the melarsoprol and pentamidine story. *Trends in parasitology*, 29(3), pp.110–8.

Barber, L.J., Ward, T.A., Hartley, J.A. & McHugh, P.J.,(2005) DNA interstrand cross-link repair in the Saccharomyces cerevisiae cell cycle: overlapping roles for PSO2 (SNM1) with MutS factors and EXO1 during S phase. *Molecular and cellular biology*, 25(6),

pp.2297–2309.

Barrett, M.P., Burchmore, R.J.S., Stich, A., Lazzari, J.O., Frasch, A.C., Cazzulo, J.J. & Krishna, S.,(2003) The trypanosomiases. *Lancet*, 362(9394), pp.1469–80.

Begleiter, A. & Leith, M.K.,(1990) Activity of quinone alkylating agents in quinone-resistant cells. *Cancer Research*, 50, pp.2872–2876.

Begleiter, A., Leith, M.K., Patel, D. & Hasinoff, B.B.,(2007) Role of NADPH cytochrome P450 reductase in activation of RH1. *Cancer chemotherapy and pharmacology*, 60(5), pp.713–23.

Begolo, D., Erben, E. & Clayton, C.,(2014) Drug target identification using a trypanosome overexpression library. *Antimicrobial agents and chemotherapy*, 58(10), pp.6260–4.

Benoit, C.-E., Bastianetto, S., Brouillette, J., Tse, Y., Boutin, J.A., Delagrange, P., Wong, T., Sarret, P. & Quirion, R.,(2010) Loss of quinone reductase 2 function selectively facilitates learning behaviors. *The Journal of neuroscience : the official journal of the Society for Neuroscience*, 30(38), pp.12690–12700.

Berardini, M.D., Souhami, R.L., Lee, C.S., Gibson, N.W., Butler, J. & Hartley, J.A.,(1993) Two structurally related diaziridinylbenzoquinones preferentially cross-link DNA at different sites upon reduction with DT-diaphorase. *Biochemistry*, 32(13), pp.3306–12.

Berger, B.J., Carter, N.S. & Fairlamb, a H.,(1995) Characterisation of pentamidine-resistant Trypanosoma brucei brucei. *Molecular and biochemical parasitology*, 69(2), pp.289–298.

Bernhard, S.C., Nerima, B., Mäser, P. & Brun, R.,(2007) Melarsoprol- and pentamidine-resistant Trypanosoma brucei rhodesiense populations and their cross-resistance. *International Journal for Parasitology*, 37(13), pp.1443–1448.

Berriman, M., Ghedin, E., Hertz-Fowler, C., Blandin, G., Renauld, H., Bartholomeu, D.C., Lennard, N.J., Caler, E., Hamlin, N.E., Haas, B., Böhme, U., Hannick, L., Aslett, M.A., Shallom, J., Marcello, L., Hou, L., Wickstead, B., Alsmark, U.C.M., Arrowsmith, C., Atkin, R.J., Barron, A.J., Bringaud, F., Brooks, K., Carrington, M., Cherevach, I., Chillingworth, T.-J., Churcher, C., Clark, L.N., Corton, C.H., Cronin, A., Davies, R.M., Doggett, J., Djikeng, A., Feldblyum, T., Field, M.C., Fraser, A., Goodhead, I., Hance, Z., Harper, D., Harris, B.R., Hauser, H., Hostetler, J., Ivens, A., Jagels, K., Johnson, D., Johnson, J., Jones, K., Kerhornou, A.X., Koo, H., Larke, N., Landfear, S., Larkin, C., Leech, V., Line, A., Lord, A., Macleod, A., Mooney, P.J., Moule, S., Martin, D.M.A., Morgan, G.W., Mungall, K., Norbertczak, H., Ormond, D., Pai, G., Peacock, C.S., Peterson, J., Quail, M.A., Rabbinowitsch, E., Rajandream, M.-A., Reitter, C., Salzberg, S.L., Sanders, M., Schobel, S., Sharp, S., Simmonds, M., Simpson, A.J., Tallon, L., Turner, C.M.R., Tait, A., Tivey, A.R., Van Aken, S., Walker, D., Wanless, D., Wang, S., White, B., White, O., Whitehead, S., Woodward, J., Wortman, J., Adams, M.D., Embley, T.M., Gull, K., Ullu, E., Barry, J.D., Fairlamb, A.H., Opperdoes, F., Barrell, B.G., Donelson, J.E., Hall, N., Fraser, C.M., Melville, S.E. & El-Sayed, N.M.,(2005) The genome of the African trypanosome Trypanosoma brucei. *Science (New York, N.Y.)*, 309(5733), pp.416–22.

Bolton, E.E., Chen, J., Kim, S., Han, L., He, S., Shi, W., Simonyan, V., Sun, Y., Thiessen, P.A., Wang, J., Yu, B., Zhang, J. & Bryant, S.H.,(2011) PubChem3D: A new resource for scientists. *Journal of Cheminformatics*, 3(9), pp.1–15.

Bolton, J.L., Trush, M.A., Penning, T.M., Dryhurst, G. & Monks, T.J.,(2000) Role of quinones in toxicology. *Chemical research in toxicology*, 13(3), pp.135–60.

Bonatto, D., Brendel, M. & Henriques, J.A.P.,(2005) The eukaryotic Pso2p/Snm1p family revisited: in silico analyses of Pso2p A, B and Plasmodium groups. *Computational biology and chemistry*, 29(6), pp.420–33.

Bonatto, D., Revers, L.F., Brendel, M. & Henriques, J.A.P.,(2005) The eukaryotic Pso2/Snm1/Artemis proteins and their function as genomic and cellular caretakers. *Brazilian journal of medical and biological research*, 38(3), pp.321–34.

Bot, C., Hall, B.S., Alvarez, G., Di Maio, R., González, M., Cerecetto, H. & Wilkinson, S.R.,(2013) Evaluating 5-nitrofurans as trypanocidal agents. *Antimicrobial agents and chemotherapy*, 57(57), pp.1638–47.

Bot, C., Hall, B.S., Bashir, N., Taylor, M.C., Helsby, N.A. & Wilkinson, S.R.,(2010) Trypanocidal activity of aziridinyl nitrobenzamide prodrugs. *Antimicrobial agents and chemotherapy*, 54(10), pp.4246–52.

Bouteille, B., Oukem, O., Bisser, S. & Dumas, M.,(2003) Treatment perspectives for human African trypanosomiasis. *Fundamental & clinical pharmacology*, 17(2), pp.171–81.

Boveris, A., Sies, H., Martino, E.E., Docampo, R., Turrens, J.F. & Stoppani, A.O.,(1980) Deficient metabolic utilization of hydrogen peroxide in Trypanosoma cruzi. *The Biochemical journal*, 188(3), pp.643–648.

Brenndörfer, M. & Boshart, M.,(2010) Selection of reference genes for mRNA quantification in Trypanosoma brucei. *Molecular and biochemical parasitology*, 172(1), pp.52–5.

Brun, R., Blum, J., Chappuis, F. & Burri, C.,(2010) Human African trypanosomiasis. *Lancet*, 375(9709), pp.148–59.

Burri, C.,(2010) Chemotherapy against human African trypanosomiasis: is there a road to success? *Parasitology*, 137(14), pp.1987–94.

Buschini, A., Ferrarini, L., Franzoni, S., Galati, S., Lazzaretti, M., Mussi, F., Northfleet de Albuquerque, C., Maria Araújo Domingues Zucchi, T. & Poli, P.,(2009) Genotoxicity revaluation of three commercial nitroheterocyclic drugs: nifurtimox, benznidazole, and metronidazole. *Journal of parasitology research*, 2009, p.463575.

Campos, M.C.O., Leon, L.L., Taylor, M.C. & Kelly, J.M.,(2014) Benznidazole-resistance in Trypanosoma cruzi: evidence that distinct mechanisms can act in concert. *Molecular and biochemical parasitology*, pp.2–4.

Carter, N.S. & Fairlamb, A.H.,(1993) Arsenical-resistant trypanosomes lack an unusual adenosine transporter. *Nature*, 363(361), pp.173–176.

Cattell, E., Sengerová, B. & McHugh, P.J.,(2010) The SNM1/Pso2 Family of ICL Repair

Nucleases: From Yeast to Man. *Environmental and molecular mutagenesis*, 51(3), pp.635–645.

CDC,(2011) Neglected Tropical diseases. Available at: http://www.cdc.gov/globalhealth/ntd/ [Accessed June 14, 2017].

Center for disease control (CDC),(2015) Parasites - African Trypanosomiasis (also known as Sleeping Sickness). Available at: http://www.cdc.gov/parasites/sleepingsickness/biology.html [Accessed April 24, 2015].

Checchi, F., Piola, P., Ayikoru, H., Thomas, F., Legros, D. & Priotto, G.,(2007) Nifurtimox plus eflornithine for late-stage sleeping sickness in Uganda: A case series. *PLoS Neglected Tropical Diseases*, 1(2), pp.1–6.

Chen, S., Knox, R., Wu, K., Deng, P.S.K., Zhou, D., Bianchet, M.A. & Amzel, L.M.,(1997) Molecular basis of the catalytic differences among DT-diaphorase of human, rat, and mouse. *Journal of Biological Chemistry*, 272(13), pp.1437–1439.

Chung-Faye, G., Palmer, D., Anderson, D., Clark, J., Downes, M., Baddeley, J., Hussain, S., Murray, P.I., Searle, P., Seymour, L., Harris, P.A., Ferry, D. & Kerr, D.J.,(2001) Virus-directed , Enzyme Prodrug Therapy with Nitroimidazole Reductase : A Phase I and Pharmacokinetic Study of its Virus-directed , Enzyme Prodrug Therapy with Nitroimidazole Reductase : A Phase I and Pharmacokinetic Study of its. *Clinical Cancer Research*, 7, pp.2662–2668.

Clark, D. & Pickett, S.,(2000) Computational methods for the prediction of “drug-likeness”. *Drug discovery today*, 2(1), pp.49–58.

Daee, D.L., Ferrari, E., Longerich, S., Zheng, X.F., Xue, X., Branzei, D., Sung, P. & Myung, K.,(2012) Rad5-dependent DNA repair functions of the Saccharomyces cerevisiae FANCM protein homolog Mph1. *Journal of Biological Chemistry*, 287(32), pp.26563–26575.

Danson, S., Ranson, M., Denneny, O., Cummings, J. & Ward, T.H.,(2007) Validation of the comet-X assay as a pharmacodynamic assay for measuring DNA cross-linking produced by the novel anticancer agent RH1 during a phase I clinical trial. *Cancer chemotherapy and pharmacology*, 60(6), pp.851–61.

Danson, S., Ward, T.H., Butler, J. & Ranson, M.,(2004) DT-diaphorase: a target for new anticancer drugs. *Cancer treatment reviews*, 30(5), pp.437–49.

Danson, S.J., Johnson, P., Ward, T.H., Dawson, M., Denneny, O., Dickinson, G., Aarons, L., Watson, A., Jowle, D., Cummings, J., Robson, L., Halbert, G., Dive, C. & Ranson, M.,(2011) Phase I pharmacokinetic and pharmacodynamic study of the bioreductive drug RH1. *Annals of oncology : official journal of the European Society for Medical Oncology / ESMO*, 22(7), pp.1653–60.

Deans, A.J. & West, S.C.,(2011) DNA interstrand crosslink repair and cancer. *Nature reviews. Cancer*, 11(7), pp.467–480.

Dehn, D.L., Inayat-Hussain, S.H. & Ross, D.,(2005) RH1 induces cellular damage in an

NAD(P)H:quinone oxidoreductase 1-dependent manner: relationship between DNA cross-linking, cell cycle perturbations, and apoptosis. *The Journal of pharmacology and experimental therapeutics*, 313(2), pp.771–779.

Delespaux, V. & de Koning, H.P.,(2007) Drugs and drug resistance in African trypanosomiasis. *Drug Resistance Updates*, 10, pp.30–50.

Dighiero, G., Maloum, K., Desablens, B., Cazin, B., Navvro, M., Leblay, R., Leporrier, M., Jaubert, J., Lepeu, G., Dreyfus, B., Binet, J. & Travade, P.,(1998) Chlorambucil in Indolent Chronic Lymphocytic Leukemia. *The New England Journal of Medicine*, 338(21), pp.1506–1514.

Drabløs, F., Feyzi, E., Aas, P.A., Vaagbø, C.B., Kavli, B., Bratlie, M.S., Peña-Diaz, J., Otterlei, M., Slupphaug, G. & Krokan, H.E.,(2004) Alkylation damage in DNA and RNA - Repair mechanisms and medical significance. *DNA Repair*, 3, pp.1389–1407.

Dronkert, M.L. & Kanaar, R.,(2001) Repair of DNA interstrand cross-links. *Mutation research*, 486(4), pp.217–47.

Dudáš, a., Vlasáková, D., Dudášová, Z., Gabčová, D., Brozmanová, J. & Chovanec, M.,(2007) Further characterization of the role of Pso2 in the repair of DNA interstrand cross-link-associated double-strand breaks in Saccharomyces cerevisiae. *Neoplasma*, 54(3), pp.189–194.

Dufour, M., Yan, C., Seigel, D., Colucci, M., Jenner, M., Oldham, N., Gomez, J., Reigan, P., Li, Y., De Matteis, C., Ross, D. & Moody, C.,(2012) Mechanism-based inhibition of quinone reductase 2 (NQO2). Selectivity for NQO2 over NQO1 and structural basis for flavoprotein inhibition. *ChembioChem*, 29(8), pp.997–1003.

Dzielendziak, A., Butler, J., Hoey, B.M., Lea, J.S. & Ward, T.H.,(1990) Comparison of the structural and cytotoxic activity of novel 2,5-bis(carboethoxyamino)-3,6-diaziridinyl-1,4-benzoquinone analogues. *Cancer Research*, 50, pp.2003–2008.

Enanga, B., Ariyanayagam, M.R., Stewart, M.L. & Barrett, M.P.,(2003) Activity of Megazol, a Trypanocidal Nitroimidazole, Is Associated with DNA Damage. *Antimicrobial agents and chemotherapy*, 47(10), pp.3368–3370.

Fairlamb, A.H. & Cerami, A.,(1992) Metabolism and functions of trypanothione in the Kinetoplastida. *Annual review of microbiology*, 46, pp.695–729.

Fairlamb, A.H., Henderson, G.B. & Cerami, A.,(1989) Trypanothione is the primary target for arsenical drugs against African trypanosomes. *Proceedings of the National Academy of Sciences of the United States of America*, 86(8), pp.2607–11.

Falletta, J.M., Cushing, B., Lauer, S., Bell, B., Mahoney, D.H., Castleberry, R. & Krance, R.A.,(1990) Phase I evaluation of diaziquone in childhood cancer. *Investigational New Drugs*, 8, pp.167–170.

Fang, J. & Beattie, D.S.,(2002a) Novel FMN-containing rotenone-insensitive NADH dehydrogenase from Trypanosoma brucei mitochondria: Isolation and characterization. *Biochemistry*, 41(9), pp.3065–3072.

Fang, J. & Beattie, D.S.,(2002b) Rotenone-insensitive NADH dehydrogenase is a potential source of superoxide in procyclic Trypanosoma brucei mitochondria. *Molecular and Biochemical Parasitology*, 123(2), pp.135–142.

Feasey, N., Wansbrough-Jones, M., Mabey, D.C.W. & Solomon, A.W.,(2010) Neglected tropical diseases. *British medical bulletin*, 93, pp.179–200.

Fourie, J., Guziec, F., Guziec, L., Monterrosa, C., Fiterman, D.J. & Begleiter, A.,(2004) Structure-activity study with bioreductive benzoquinone alkylating agents: effects on DT-diaphorase-mediated DNA crosslink and strand break formation in relation to mechanisms of cytotoxicity. *Cancer chemotherapy and pharmacology*, 53(3), pp.191–203.

Franco, J., Pere, S., Diarra, Ruiz-Postigo, Samo & Jannin,(2012) Monitoring the use of nifurtimox-eflornithine combination therapy (NECT) in the treatment of second stage gambiense human African trypanosomiasis. *Research and Reports in Tropical Medicine*, p.93.

Franco, J., Simarro, P., Diarra, A. & Jannin, J.,(2014) Epidemiology of human African trypanosomiasis. *Clinical epidemiology*, (6), pp.257–275.

Garavaglia, P. a, Cannata, J.J.B., Ruiz, A.M., Maugeri, D., Duran, R., Galleano, M. & García, G.A.,(2010) Identification, cloning and characterization of an aldo-keto reductase from Trypanosoma cruzi with quinone oxido-reductase activity. *Molecular and biochemical parasitology*, 173(2), pp.132–141.

Genois, M.-M., Paquet, E.R., Laffitte, M.-C.N., Maity, R., Rodrigue, A., Ouellette, M. & Masson, J.-Y.,(2014) DNA repair pathways in trypanosomatids: from DNA repair to drug resistance. *Microbiology and molecular biology reviews : MMBR*, 78(1), pp.40–73.

Glover, L., Alsford, S., Baker, N., Turner, D.J., Sanchez-Flores, A., Hutchinson, S., Hertz-Fowler, C., Berriman, M. & Horn, D.,(2015) Genome-scale RNAi screens for high-throughput phenotyping in bloodstream-form African trypanosomes. *Nature protocols*, 10(1), pp.106–33.

Graf, F.E., Ludin, P., Wenzler, T., Kaiser, M., Brun, R., Pyana, P.P., Büscher, P., de Koning, H.P., Horn, D. & Mäser, P.,(2013) Aquaporin 2 Mutations in Trypanosoma brucei gambiense Field Isolates Correlate with Decreased Susceptibility to Pentamidine and Melarsoprol. *PLoS Neglected Tropical Diseases*, 7(10).

Graves, P.R., Kwiek, J.J., Fadden, P., Ray, R., Hardeman, K., Coley, A.M., Foley, M. & Haystead, T.A.J.,(2002) Discovery of novel targets of quinoline drugs in the human purine binding proteome. *Molecular pharmacology*, 62(6), pp.1364–1372.

Grellier, P., Maroziene, A., Nivinskas, H., Sarlauskas, J., Aliverti, A. & Cenas, N.,(2010) Antiplasmodial activity of quinones: roles of aziridinyl substituents and the inhibition of Plasmodium falciparum glutathione reductase. *Archives of biochemistry and biophysics*, 494(1), pp.32–9.

Guise, C.P., Mowday, A.M., Ashoorzadeh, A., Yuan, R., Lin, W.H., Wu, D.H., Smaill, J.B.,

Patterson, A. V. & Ding, K.,(2014) Bioreductive prodrugs as cancer therapeutics: Targeting tumor hypoxia. *Chinese Journal of Cancer*, 33, pp.80–86.

Hall, B.S., Bot, C. & Wilkinson, S.R.,(2011) Nifurtimox activation by trypanosomal type I nitroreductases generates cytotoxic nitrile metabolites. *The Journal of biological chemistry*, 286(15), pp.13088–95.

Hall, B.S., Meredith, E.L. & Wilkinson, S.R.,(2012) Targeting the substrate preference of a type I nitroreductase to develop antitrypanosomal quinone-based prodrugs. *Antimicrobial agents and chemotherapy*, 56(11), pp.5821–30.

Hall, B.S. & Wilkinson, S.R.,(2011) Activation of benznidazole by trypanosomal type I nitroreductases results in glyoxal formation. *Antimicrobial agents and chemotherapy*, 56(1).

Hall, B.S., Wu, X., Hu, L. & Wilkinson, S.R.,(2010) Exploiting the drug-activating properties of a novel trypanosomal nitroreductase. *Antimicrobial agents and chemotherapy*, 54(3), pp.1193–9.

Hashimoto, T. & Nakai, M.,(2011) Increased hippocampal quinone reductase 2 in Alzheimer's disease. *Neuroscience Letters*, 502(1), pp.10–12.

Helsby, N. a, Atwell, G.J., Yang, S., Palmer, B.D., Anderson, R.F., Pullen, S.M., Ferry, D.M., Hogg, A., Wilson, W.R. & Denny, W. a,(2004) Aziridinyldinitrobenzamides: synthesis and structure-activity relationships for activation by E. coli nitroreductase. *Journal of medicinal chemistry*, 47(12), pp.3295–307.

Helsby, N.A., Wheeler, S.J., Pruijn, F.B., Palmer, B.D., Yang, S., Denny, W.A. & Wilson, W.R.,(2003) Effect of nitroreduction on the alkylating reactivity and cytotoxicity of the 2,4-dinitrobenzamide-5-aziridine CB 1954 and the corresponding nitrogen mustard SN 23862: Distinct mechanisms of bioreductive activation. *Chemical Research in Toxicology*, 16(4), pp.469–478.

Henderson, G.B., Ulrich, P., Fairlamb, A.H., Rosenberg, I., Pereira, M., Sela, M. & Cerami, A.,(1988) "Subversive" substrates for the enzyme trypanothione disulfide reductase: alternative approach to chemotherapy of Chagas disease. *Proceedings of the National Academy of Sciences of the United States of America*, 85(15), pp.5374–5378.

Henriques, J.A. & Moustacchi, E.,(1981) Interactions between mutations for sensitivity to psoralen photoaddition (pso) and to radiation (rad) in Saccharomyces cerevisiae. *Journal of bacteriology*, 148(1), pp.248–56.

Henriques, J.A.P. & Moustacchi, E.,(1980) Isolation and characterization of pso mutants sensitive to photo-addition of psoralen derivatives in Saccharomyces cerevisiae. *Genetics*, 95, pp.273–288.

Hu, L., Wu, X., Han, J., Chen, L., Vass, S.O., Browne, P., Hall, B.S., Bot, C., Gobalakrishnapillai, V., Searle, P.F., Knox, R.J. & Wilkinson, S.R.,(2011) Synthesis and structure-activity relationships of nitrobenzyl phosphoramide mustards as nitroreductase-activated prodrugs. *Bioorganic and Medicinal Chemistry Letters*, 21, pp.3986–3991.

Irigoín, F., Cibils, L., Comini, M. a., Wilkinson, S.R., Flohé, L. & Radi, R.,(2008) Insights into the redox biology of Trypanosoma cruzi: Trypanothione metabolism and oxidant detoxification. *Free Radical Biology and Medicine*, 45(6), pp.733–742.

Iyanagi, T.,(2005) Structure and function of NADPH-cytochrome P450 reductase and nitric oxide synthase reductase domain. *Biochemical and Biophysical Research Communications*, 338(1), pp.520–528.

Iyer, V. & Szybalski, W.,(1963) A molecular mechanism of mitomycin action: linking of complementary DNA strands. *Proceedings of the National Academy of …*, 50(1961), pp.355–362.

Iyer, V.N. & Szybalski, W.,(1964) Mitomycins and Porfiromycin: Chemical Mechanism of Activation and Cross-Linking of Dna. *Science (New York, N.Y.)*, 145(3627), pp.55–58.

Jamonneau, V., Ilboudo, H., Kaboré, J., Kaba, D., Koffi, M., Solano, P., Garcia, A., Courtin, D., Laveissière, C., Lingue, K., Büscher, P. & Bucheton, B.,(2012) Untreated human infections by Trypanosoma brucei gambiense are not 100% fatal. *PLoS neglected tropical diseases*, 6(6), p.e1691.

Kayser, O., Kiderlen, a. F. & Croft, S.L.,(2003) Natural products as antiparasitic drugs. *Parasitology Research*, 90, pp.55–62.

Kelly, J.M., Taylor, M.C., Smith, K., Hunter, K.J. & Fairlamb, A.H.,(1993) Phenotype of recombinant Leishmania donovani and Trypanosoma cruzi which overexpress trypanothione reductase. *European Journal of Biochemistry*, 37, pp.29–37.

Kennedy, P.G.E.,(2013) Clinical features, diagnosis, and treatment of human African trypanosomiasis (sleeping sickness). *The Lancet Neurology*, 12(2), pp.186–194.

Keyes, S.R., Rockwell, S. & Sartorelli, A.C.,(1985) Porfiromycin as a bioreductive alkylating agent with selective toxicity to hypoxic EMT6 tumor cells in vivo and in vitro. *Cancer Research*, 45(8), pp.3642–3645.

Knox, R.J., Friedlos, F. & Boland, M.P.,(1993) The bioactivation of CB 1954 and its use as a prodrug in antibody-directed enzyme prodrug therapy (ADEPT). *Cancer metastasis reviews*, 12(2), pp.195–212.

Koster, A.S.,(1991) Bioreductive activation of quinones: a mixed blessing. *Pharmaceutisch weekblad. Scientific edition*, 13(3), pp.123–6.

Kubata, B.K., Kabututu, Z., Nozaki, T., Munday, C.J., Fukuzumi, S., Ohkubo, K., Lazarus, M., Maruyama, T., Martin, S.K., Duszenko, M. & Urade, Y.,(2002) A Key Role for Old Yellow Enzyme in the Metabolism of Drugs by Trypanosoma cruzi. *Journal of Experimental Medicine*, 196(9), pp.1241–1251.

Kumar, P., Lodge, R., Raymond, F., Ritt, J.-F., Jalaguier, P., Corbeil, J., Ouellette, M. & Tremblay, M.J.,(2013) Gene expression modulation and the molecular mechanisms involved in Nelfinavir resistance in Leishmania donovani axenic amastigotes. *Molecular microbiology*.

Lam, C.F.C., Pearce, A.N., Tan, S.H., Kaiser, M. & Copp, B.R.,(2013) Discovery and

evaluation of thiazinoquinones as anti-protozoal agents. *Marine drugs*, 11(9), pp.3472–99.

Lawley, P.D. & Phillips, D.H.,(1996) DNA adducts from chemotherapeutic agents. *Mutation research*, 355, pp.13–40.

Lee, E.J., Van Echo, D.A., Egorin, M.J., Nayar, M.S., Shulman, P. & Schiffer, C.A.,(1986) Diaziquone given as a continuous infusion is an active agent for relapsed adult acute nonlymphocytic leukemia. *Blood*, 67(1), pp.182–187.

Legros, D., Ollivier, G., Gastelluetchegorry, M., Paquet, C., Burri, C., Jannin, J. & Buscher, P.,(2002) Treatment of human African trypanosomiasis?present situation and needs for research and development. *The Lancet Infectious Diseases*, 2(7), pp.437–440.

Lehoczký, P., McHugh, P.J. & Chovanec, M.,(2007) DNA interstrand cross-link repair in Saccharomyces cerevisiae. *FEMS Microbiology Reviews*, 31(2), pp.109–133.

Leoni, L.M., Bailey, B., Reifert, J., Bendall, H.H., Zeller, R.W., Corbeil, J., Elliott, G. & Niemeyer, C.C.,(2008) Bendamustine (Treanda) displays a distinct pattern of cytotoxicity and unique mechanistic features compared with other alkylating agents. *Clinical Cancer Research*, 14(1), pp.309–317.

Leprohon, P., Légaré, D., Raymond, F., Madore, E., Hardiman, G., Corbeil, J. & Ouellette, M.,(2009) Gene expression modulation is associated with gene amplification, supernumerary chromosomes and chromosome loss in antimony-resistant Leishmania infantum. *Nucleic acids research*, 37(5), pp.1387–99.

Leung, K.K.K. & Shilton, B.H.,(2013) Chloroquine binding reveals flavin redox switch function of quinone reductase 2. *Journal of Biological Chemistry*, 288(16), pp.11242–11251.

Li, X., Hejna, J. & Moses, R.E.,(2005) The yeast Snm1 protein is a DNA 5'-exonuclease. *DNA repair*, 4(2), pp.163–70.

Li, X. & Moses, R.E.,(2003) The beta-lactamase motif in Snm1 is required for repair of DNA double-strand breaks caused by interstrand crosslinks in S. cerevisiae. *DNA repair*, 2(1), pp.121–9.

Lin, A.J., Cosby, L., Shansky, C. & Sartorelli, A.,(1972) Potential Bioreductive Alkylating Agents. 1.Benzoquinone Derivatives. *Journal of medicinal chemistry*, 1(Scheme I), pp.2–7.

Lizzi, F., Veronesi, G., Belluti, F., Bergamini, C., López-Sánchez, A., Kaiser, M., Brun, R., Krauth-Siegel, R.L., Hall, D.G., Rivas, L. & Bolognesi, M.L.,(2012) Conjugation of Quinones with Natural Polyamines: Toward an Expanded Antitrypanosomatid Profile. *Journal of medicinal chemistry*, 55(23), pp.10490–500.

Long II, D. & Jaiswal, A.K.,(2000) NRH:quinone oxidoreductase 2 (NQO2). *Chemico-biological interactions*, 129, pp.99–112.

Lopes, A.,(2010) Trypanosomatids: Odd Organisms, Devastating Diseases. *The Open Parasitology Journal*, 4(1), pp.30–59.

Lundkvist, G.B., Kristensson, K. & Bentivoglio, M.,(2004) Why trypanosomes cause sleeping sickness. *Physiology (Bethesda, Md.)*, 19, pp.198–206.

Lusthof, K.K.J., De Mol, N.J., Janssen, L.H.M., Verboom, W., Reinhoudt, D.N. & Mol, N. De,(1989) DNA alkylation and formation of DNA interstrand cross-links by potential antitumour 2, 5-bis (1-aziridinyl)-1, 4-benzoquinones. *Chemico-biological interactions*, 70(3-4), pp.249–262.

Machado, C.R., Vieira-da-Rocha, J.P., Mendes, I.C., Rajão, M.A., Grynberg, P., Oliveira, D.A.A., Marques, C., Van Houten, B. & McCulloch, R.,(2014) Nucleotide excision repair in Trypanosoma brucei: specialization of transcription-coupled repair due to multigenic transcription. *Molecular microbiology*, 92(4), pp.756–76.

Magaña-Schwencke, N., Henriques, J.A., Chanet, R. & Moustacchi, E.,(1982) The fate of 8-methoxypsoralen photoinduced crosslinks in nuclear and mitochondrial yeast DNA: comparison of wild-type and repair-deficient strains. *Proceedings of the National Academy of Sciences of the United States of America*, 79(March), pp.1722–1726.

Maliepaard, M., Wolfs, A., Groot, S.E., de Mol, N.J., Janseen, L. & Janssen, L.H.,(1995) Indoloquinone E09: DNA interstrand cross-linking upon reduction by DT-diaphorase or xanthine oxidase. *British journal of cancer*, 71(November 1994), pp.836–839.

Malvy, D. & Chappuis, F.,(2011) Sleeping sickness. *Clinical microbiology and infection : the official publication of the European Society of Clinical Microbiology and Infectious Diseases*, 17(7), pp.986–95.

Masters, B.S.S.,(2005) The journey from NADPH-cytochrome P450 oxidoreductase to nitric oxide synthases. *Biochemical and Biophysical Research Communications*, 338(1), pp.507–519.

Mather, M.W., Darrouzet, E., Valkova-Valchanova, M., Cooley, J.W., McIntosh, M.T., Daldal, F. & Vaidya, A.B.,(2005) Uncovering the molecular mode of action of the antimalarial drug atovaquone using a bacterial system. *The Journal of biological chemistry*, 280(29), pp.27458–65.

Matovu, E., Stewart, M.L., Geiser, F., Brun, R., Mäser, P., Wallace, L.J.M., Burchmore, R.J., Enyaru, J.C.K., Barrett, M.P., Kaminsky, R., Seebeck, T. & De Koning, H.P.,(2003) Mechanisms of arsenical and diamidine uptake and resistance in Trypanosoma brucei. *Eukaryotic Cell*, 2(5), pp.1003–1008.

McHugh, P., Spanswick, V. & Hartley, J.,(2001) Repair of DNA interstrand crosslinks: molecular mechanisms and clinical relevance. , 44(0), pp.483–490.

Mejia, A.M., Hall, B.S., Taylor, M.C., Gómez-Palacio, A., Wilkinson, S.R., Triana-Chávez, O. & Kelly, J.M.,(2012) Benznidazole-resistance in Trypanosoma cruzi is a readily acquired trait that can arise independently in a single population. *The Journal of infectious diseases*, 206(2), pp.220–8.

Mejía-Jaramillo, A.M., Fernández, G.J., Palacio, L. & Triana-Chávez, O.,(2011) Gene expression study using real-time PCR identifies an NTR gene as a major marker of resistance to benznidazole in Trypanosoma cruzi. *Parasites & Vectors*, 4(1), p.169.

Menna-Barreto, R.F.S., Beghini, D.G., Ferreira, A.T.S., Pinto, A. V, De Castro, S.L. & Perales, J.,(2010) A proteomic analysis of the mechanism of action of naphthoimidazoles in Trypanosoma cruzi epimastigotes in vitro. *Journal of proteomics*, 73(12), pp.2306–15.

Mohapatra, S.,(2014) Drug resistance in leishmaniasis: Newer developments. *Tropical parasitology*, 4(1), pp.4–9.

Molyneux, D.H., Hotez, P.J. & Fenwick, A.,(2005) "Rapid-impact interventions": how a policy of integrated control for Africa's neglected tropical diseases could benefit the poor. *PLoS medicine*, 2(11), p.e336.

Mony, B.M., MacGregor, P., Ivens, A., Rojas, F., Cowton, A., Young, J., Horn, D. & Matthews, K.,(2014) Genome-wide dissection of the quorum sensing signalling pathway in Trypanosoma brucei. *Nature*, 505(7485), pp.681–5.

Mony, B.M. & Matthews, K.R.,(2015) Assembling the components of the quorum sensing pathway in African trypanosomes. *Molecular Microbiology*, 96(2), pp.220–232.

Moore, B.J.O., Dodge, R.K., Amrein, P.C., Kolitz, J., Lee, E.J., Powell, B., Godfrey, S., Robert, F. & Schiffer, C.A.,(1997) Granulocyte-Colony Stimulating Factor (Filgrastim) Accelerates Granulocyte Recovery After Intensive Postremission Chemotherapy for Acute Myeloid Leukemia With Aziridinyl Benzoquinone and Mitoxantrone: Cancer and Leukemia Group B Study 9022. *Blood*.

Moore, D.A.J., Edwards, M., Escombe, R., Agranoff, D., Bailey, J.W., Squire, S.B. & Chiodini, P.L.,(2002) African Trypanosomiasis in Travelers Returning to the United Kingdom. , 8(1), pp.74–76.

Moreau, P., Milpied, N., Mahé, B., Juge-Morineau, N., Rapp, M.J., Bataille, R. & Harousseau, J.L.,(1999) Melphalan 220 mg/m2 followed by peripheral blood stem cell transplantation in 27 patients with advanced multiple myeloma. *Bone marrow transplantation*, 23, pp.1003–1006.

Mouridsen, H.T., Kristensen, D., Nielsen, J.H. & Dombernowsky, P.,(1980) Phase II trial of prednimustine, L-1031, (NSC-134087) in advanced breast cancer. *Cancer*, 46(L 1031), pp.253–255.

Mukherjee, A., Boisvert, S., Monte-Neto, R.L. Do, Coelho, A.C., Raymond, F., Mukhopadhyay, R., Corbeil, J. & Ouellette, M.,(2013) Telomeric gene deletion and intrachromosomal amplification in antimony-resistant Leishmania. *Molecular microbiology*, 88(1), pp.189–202.

Nemeikait-Čniene, A., Šarlauskas, J., Anusevičius, Ž., Nivinskas, H. & Č-Nas, N.,(2003) Cytotoxicity of RH1 and related aziridinylbenzoquinones: involvement of activation by NAD(P)H:quinone oxidoreductase (NQO1) and oxidative stress. *Archives of Biochemistry and Biophysics*, 416(1), pp.110–118.

Nerima, B., Matovu, E., Lubega, G.W. & Enyaru, J.C.K.,(2007) Detection of mutant P2 adenosine transporter (TbAT1) gene in Trypanosoma brucei gambiense isolates from northwest Uganda using allele-specific polymerase chain reaction. *Tropical Medicine*

and International Health, 12(11), pp.1361–1368.

Nok, A.J.,(2003) Arsenicals (melarsoprol), pentamidine and suramin in the treatment of human African trypanosomiasis. *Parasitology research*, 90(1), pp.71–9.

Noll, D., McGregor Mason, T. & Miller, P.,(2006) Formation and Repair of Interstand Cross-Links in DNA. *Chemical research in toxicology*, 106(2), pp.277–301.

de Oliveira, I.M., Henriques, J. a P. & Bonatto, D.,(2007) In silico identification of a new group of specific bacterial and fungal nitroreductases-like proteins. *Biochemical and Biophysical Research Communications*, 355(4), pp.919–925.

Pal, D., Banerjee, S., Cui, J., Schwartz, A., Ghosh, S.K. & Samuelson, J.,(2009) Giardia, Entamoeba, and Trichomonas enzymes activate metronidazole (nitroreductases) and inactivate metronidazole (nitroimidazole reductases). *Antimicrobial Agents and Chemotherapy*, 53(2), pp.458–464.

Palmer, D.H., Milner, A.E., Kerr, D.J. & Young, L.S.,(2003) Mechanism of cell death induced by the novel enzyme-prodrug combination, nitroreductase/CB1954, and identification of synergism with 5-fluorouracil. *British journal of cancer*, 89(5), pp.944–50.

Papadopoulou, M. V, Bloomer, W.D., Lepesheva, G.I., Rosenzweig, H.S., Kaiser, M., Aguilera-venegas, B., Wilkinson, S.R., Chatelain, E. & Ioset, J.,(2015) Novel 3-Nitrotriazole-Based Amides and Carbinols as Bifunctional Antichagasic Agents. *Journal of medicinal chemistry*, 58, pp.1307–1319.

Papadopoulou, M. V, Bloomer, W.D., Rosenzweig, H.S., Chatelain, E., Kaiser, M., Wilkinson, S.R., Mckenzie, C. & Ioset, J.,(2012) Novel 3-Nitro-1H-1,2,4-triazole-based Amides and Sulfonamides as Potential anti-Trypanosomal Agents. *Journal of medicinal chemistry*, 55(11), pp.5554–5565.

Papadopoulou, M. V, Trunz, B.B., Bloomer, W.D., Mckenzie, C., Wilkinson, S.R., Prasittichai, C., Brun, R., Kaiser, M. & Torreele, E.,(2011) Novel 3-Nitro-1H-1,2,4-triazole-Based Aliphatic and Aromatic Amines as Anti-Chagasic Agents. *Journal of medicinal chemistry*, 54, pp.8214–8223.

Papadopoulou, M. V., Bloomer, W.D., Rosenzweig, H.S., Kaiser, M., Chatelain, E. & Ioset, J.R.,(2013) Novel 3-nitro-1H-1,2,4-triazole-based piperazines and 2-amino-1,3-benzothiazoles as antichagasic agents. *Bioorganic and Medicinal Chemistry*, 21(21), pp.6600–6607.

Parkinson, E.I., Bair, J.S., Cismesia, M. & Hergenrother, P.J.,(2013) Efficient NQO1 Substrates are Potent and Selective Anticancer Agents. *ACS Chemical biology*, (8), pp.2173–2183.

Parsons, M.,(2004) Glycosomes: parasites and the divergence of peroxisomal purpose. *Molecular microbiology*, 53(3), pp.717–24.

Patel, P., Young, J.G., Mautner, V., Ashdown, D., Bonney, S., Pineda, R.G., Collins, S.I., Searle, P.F., Hull, D., Peers, E., Chester, J., Wallace, D.M., Doherty, A., Leung, H., Young, L.S. & James, N.D.,(2009) A phase I/II clinical trial in localized prostate

cancer of an adenovirus expressing nitroreductase with CB1954 [correction of CB1984]. *Molecular therapy : the journal of the American Society of Gene Therapy*, 17(7), pp.1292–9.

Patterson, S. & Wyllie, S.,(2014) Nitro drugs for the treatment of trypanosomatid diseases: past, present, and future prospects. *Trends in parasitology*, 30(6), pp.289–298.

Peacock, L., Ferris, V., Bailey, M. & Gibson, W.,(2014) Mating compatibility in the parasitic protist Trypanosoma brucei. *Parasites & vectors*, 7(1), p.78.

Pécoul, B.,(2004) New drugs for neglected diseases: from pipeline to patients. *PLoS medicine*, 1(1), p.e6.

Pegg, A. & Byers, T.,(1992) Repair of DNA containing O6-alkylguanine. *The FASEB journal*, 6, pp.2302–2310.

Pegg, A.E., Boosalis, M., Samson, L., Mosche, R.C., Byers, T.L., Swenn, K. & Dolanl, M.E.,(1993) Mechanism of Inactivation of Human 06-Alkylguanine-DNA Alkyltransferase by 06-Benzylguanine. *Biochemistry*, 32, pp.11998–12006.

Pérez-victoria, F.J., Castanys, S., Pe, F.J. & Gamarro, F.,(2003) Leishmania donovani Resistance to Miltefosine Involves a Defective Inward Translocation of the Drug Leishmania donovani Resistance to Miltefosine Involves a Defective Inward Translocation of the Drug. *Antimicrobial agents and chemotherapy*.

Perez-Victoria, J., Perez-Victoria, F.J., Parodi-talice, A., Ravelo, A.G., Castanys, S., Jime, I. a & Gamarro, F.,(2001) Alkyl-Lysophospholipid Resistance in Multidrug-Resistant Leishmania tropica and chemosensitization by a novel P-Glycoprotein-like transporter modulator. *Antimicrobial agents and chemotherapy*, 45(9), pp.2468–2474.

Phillips, R.M., Hendriks, H.R. & Peters, G.J.,(2013) EO9 (Apaziquone): from the clinic to the laboratory and back again. *British journal of pharmacology*, 168(1), pp.11–18.

Picozzi, K., Fèvre, E.M., Odiit, M., Carrington, M., Eisler, M.C., Maudlin, I. & Welburn, S.C.,(2005) Sleeping sickness in Uganda: a thin line between two fatal diseases. *BMJ (Clinical research ed.)*, 331(7527), pp.1238–1241.

Pierce, S., Guziec, L., Guziec, F. & Brodbelt, J.,(2011) Characterization of Aziridinylbenzoquinone DNA cross-links by LC-IPRMPD-MS. *Chemical research in toxiciology*, 23(6), pp.1097–1104.

Pieretti, S., Haanstra, J.R., Mazet, M., Perozzo, R., Bergamini, C., Prati, F., Fato, R., Lenaz, G., Capranico, G., Brun, R., Bakker, B.M., Michels, P. a M., Scapozza, L., Bolognesi, M.L. & Cavalli, A.,(2013) Naphthoquinone derivatives exert their antitrypanosomal activity via a multi-target mechanism. *PLoS neglected tropical diseases*, 7(1), p.e2012.

Pinto, A.V. & de Castro, S.L.,(2009) The trypanocidal activity of naphthoquinones: a review. *Molecules (Basel, Switzerland)*, 14(11), pp.4570–90.

Poli, P., Aline de Mello, M., Buschini, A., Mortara, R.A., Northfleet de Albuquerque, C., Da Silva, S., Rossi, C. & Zucchi, T.M.A.D.,(2002) Cytotoxic and genotoxic effects of megazol, an anti-Chagas' disease drug, assessed by different short-term tests.

Biochemical Pharmacology, 64(11), pp.1617–1627.

Portal, P., Villamil, S.F., Alonso, G.D., De Vas, M.G., Flawiá, M.M., Torres, H.N. & Paveto, C.,(2008) Multiple NADPH-cytochrome P450 reductases from Trypanosoma cruzi suggested role on drug resistance. *Molecular and biochemical parasitology*, 160(1), pp.42–51.

Prosser, G.A., Copp, J.N., Syddall, S.P., Williams, E.M., Smaill, J.B., Wilson, W.R., Patterson, A. V & Ackerley, D.F.,(2010) Discovery and evaluation of Escherichia coli nitroreductases that activate the anti-cancer prodrug CB1954. *Biochemical pharmacology*, 79(5), pp.678–87.

Puri, R., Palit, V., Loadman, P.M., Flannigan, M., Shah, T., Choudry, G.A., Basu, S., Double, J.A., Lenaz, G., Chawla, S., Beer, M., Van Kalken, C., de Boer, R., Beijnen, J.H., Twelves, C.J. & Phillips, R.M.,(2006) Phase I/II pilot study of intravesical apaziquone (EO9) for superficial bladder cancer. *The Journal of urology*, 176(4 Pt 1), pp.1344–8.

Pyana, P.P., Lukusa, I.N., Ngoyi, D.M., van Reet, N., Kaiser, M., Shamamba, S.K. Bin & Büscher, P.,(2011) Isolation of Trypanosoma brucei gambiense from cured and relapsed sleeping sickness patients and adaptation to laboratory mice. *PLoS Neglected Tropical Diseases*, 5(4), pp.1–6.

Raether, W. & Hänel, H.,(2003) Nitroheterocyclic drugs with broad spectrum activity. *Parasitology research*, 90 Supp 1, pp.S19–S39.

Rahlfs, S., Schirmer, R. & Becker, K.,(2002) The thioredoxin system of Plasmodium falciparum and other parasites. *Cell molecular life sciences*, 59, pp.1024–1041.

Rajski, S.R. & Williams, R.M.,(1998) DNA Cross-Linking Agents as Antitumor Drugs. *Chemical Reviews*, 98, pp.2723–2796.

Ralston, K.S., Kabututu, Z.P., Melehani, J.H., Oberholzer, M. & Hill, K.L.,(2009) The Trypanosoma brucei flagellum: moving parasites in new directions. *Annual review of microbiology*, 63, pp.335–362.

Redmond, S., Vadivelu, J. & Field, M.C.,(2003) RNAit: an automated web-based tool for the selection of RNAi targets in Trypanosoma brucei. *Molecular and Biochemical Parasitology*, 128(1), pp.115–118.

Reigan, P., Siegel, D., Guo, W. & Ross, D.,(2011) A mechanistic and structural analysis of the inhibition of the 90-kDa heat shock protein by the benzoquinone and hydroquinone ansamycins. *Molecular pharmacology*, 79(5), pp.823–832.

Ritt, J.F., Raymond, F., Leprohon, P., Légaré, D., Corbeil, J. & Ouellette, M.,(2013) Gene Amplification and Point Mutations in Pyrimidine Metabolic Genes in 5-Fluorouracil Resistant Leishmania infantum. *PLoS Neglected Tropical Diseases*, 7(11), pp.1–11.

Robays, J., Nyamowala, G., Sese, C., Betu, V., Mesu, K., Lutumba, P. & Veken, W. Van Der,(2008) High Failure Rates of Melarsoprol for Democratic Republic of Congo. *Emerging Infectious Diseases*, 14(6), pp.966–967.

Romas, E., KM, G., Krauth-Siegel, R., Bader, J., Martinez, L. & Maldonado, R.,(2009) 2,3-Diphenyl-1,4-naphthoquinone: A potential chemotherapeutic agent against Trypanosoma cruzi. *Journal of parasitology*, 27(5), pp.417–428.

Ross, D., Kepa, J.K., Winski, S.L., Beall, H.D., Anwar, A. & Siegel, D.,(2000) NAD(P)H:quinone oxidoreductase 1 (NQO1): Chemoprotection, bioactivation, gene regulation and genetic polymorphisms. *Chemico-Biological Interactions*, 129(1-2), pp.77–97.

Salomão, K., De Santana, N. a, Molina, M.T., De Castro, S.L. & Menna-Barreto, R.F.S.,(2013) Trypanosoma cruzi mitochondrial swelling and membrane potential collapse as primary evidence of the mode of action of naphthoquinone analogues. *BMC microbiology*, 13, p.196.

Schilsky, R.L., Kelley, J.A., Inde, D.C., Howser, D.M., Cordes, R.S. & Young, R.C.,(1982) Phase I Trial and Pharmacokinetics (NSC 182986) in Humans of Aziridinylbenzoquinone. , 42(April), pp.1582–1586.

Schmittgen, T.D. & Livak, K.J.,(2008) Analyzing real-time PCR data by the comparative CT method. *Nature Protocols*, 3(6), pp.1101–1108.

Schumann Burkard, G., Jutzi, P. & Roditi, I.,(2011) Genome-wide RNAi screens in bloodstream form trypanosomes identify drug transporters. *Molecular and biochemical parasitology*, 175(1), pp.91–4.

Sengerová, B., Wang, A.T. & McHugh, P.J.,(2011) Orchestrating the nucleases involved in DNA interstrand cross-link (ICL) repair. *Cell Cycle*, 10(23), pp.3999–4008.

Sereno, D. & Lemesre, J.L.,(1997) In vitro life cycle of pentamidine-resistant amastigotes: Stability of the chemoresistant phenotypes is dependent on the level of resistance induced. *Antimicrobial Agents and Chemotherapy*, 41(9), pp.1898–1903.

Shapiro, T.A. & Englund, P.T.,(1990) Selective cleavage of kinetoplast DNA minicircles promoted by antitrypanosomal drugs. *Proceedings of the National Academy of Sciences of the United States of America*, 87(3), pp.950–4.

Siegel, D., Gibson, N.W., Preusch, P.C. & Ross, D.,(1990) Metabolism of Mitomycin C by DT-Diaphorase : Role in Mitomycin C-induced DNA Damage and Cytotoxicity in Human Colon Carcinoma Cells Metabolism of Mitomycin C by DT-Diaphorase : Role in Mitomycin C-induced DNA Damage and Cytotoxicity in Human Colon Carcino. , (31), pp.7483–7489.

Siegel, D., Yan, C. & Ross, D.,(2012) NAD(P)H:quinone oxidoreductase 1 (NQO1) in the sensitivity and resistance to antitumor quinones. *Biochemical pharmacology*, 83(8), pp.1033–40.

Simarro, P.P., Diarra, A., Ruiz Postigo, J.A., Franco, J.R., Jannin, J.G., Postigo, J.A.R., Franco, J.R. & Jannin, J.G.,(2011) The Human African trypanosomiasis control and surveillance programme of the World Health Organization 2000-2009: the way forward. *PLoS neglected tropical diseases*, 5(2), p.e1007.

Skinner, M., Sanchorawala, V., Seldin, D., Dember, L., Falk, R., Berk, J., Anderson, J.,

O'Hara, C., KT, F., CA, L., Wiesman, J., Quillen, K., Swan, N. & DG, W.,(2004) High-Dose Melphalan and Autologous Stem-Cell Transplantation in Patients with AL Amyloidosis: An 8-year study. *Annals of Internal medicine*, 140(2), pp.85–94.

Sokolova, A.Y., Wyllie, S., Patterson, S., Oza, S.L., Read, K.D. & Fairlamb, A.H.,(2010) Cross-resistance to nitro drugs and implications for treatment of human African trypanosomiasis. *Antimicrobial agents and chemotherapy*, 54(7), pp.2893–900.

Southern, E.,(1975) Detection of specific sequences among DNA fragments separated by gel electrophoresis. *Journal of molecular biology*, pp.503–517.

Srivastava, I.K., Morrisey, J.M., Darrouzet, E., Daldal, F. & Vaidya, A.B.,(1999) Resistance mutations reveal the atovaquone-binding domain of cytochrome b in malaria parasites. *Molecular Microbiology*, 33(4), pp.704–711.

Srivastava, I.K., Rottenberg, H. & Vaidya, A.B.,(1997) Atovaquone, a Broad Spectrum Antiparasitic Drug, Collapses Mitochondrial Membrane Potential in a Malarial Parasite. *Journal of Biological Chemistry*, 272(7), pp.3961–3966.

Stevens, J., Noyes, H., Schofield, C. & Gibson, W.,(2001) The Molecular Evolution of Trypanosomatidae. *Advances in parasitology*, 48, pp.1–53.

Steverding, D.,(2008) The history of African trypanosomiasis. *Parasites & vectors*, 1(1), p.3.

Stich, A., Abel, P.M. & Krishna, S.,(2002) Human African trypanosomiasis. *British Medical Journal (BMJ)*, 325(July), pp.203–206.

Stuart, K., Brun, R., Croft, S., Fairlamb, A., Gürtler, R.E., Mckerrow, J., Reed, S. & Tarleton, R.,(2008) Review series Kinetoplastids : related protozoan pathogens , different diseases. , 118(4), pp.1301–1310.

Sudarshi, D., Lawrence, S., Pickrell, W.O., Eligar, V., Walters, R., Quaderi, S., Walker, A., Capewell, P., Clucas, C., Vincent, A., Checchi, F., MacLeod, A. & Brown, M.,(2014) Human African Trypanosomiasis Presenting at Least 29 Years after Infection—What Can This Teach Us about the Pathogenesis and Control of This Neglected Tropical Disease? *PLoS Neglected Tropical Diseases*, 8(12), p.e3349.

Sullivan, J.A., Tong, J.L., Wong, M., Kumar, A., Sarkar, H., Ali, S., Hussein, I., Zaman, I., Meredith, E.L., Helsby, N.A., Hu, L. & Wilkinson, S.R.,(2015) Unravelling the role of SNM1 in the DNA repair system of Trypanosoma brucei 1. *Molecular microbiology*, pp.1–39.

Tan, C., Hancock, C., Mondora, A. & Hoffman, N.,(1984) Phase I study of aziridinylbenzoquinone (AZQ, NSC 182986) in children with cancer. *Cancer research*, 1(February), pp.831–835.

Tashkin, D.P., Elashoff, R., Clements, P.J., Goldin, J., Roth, M.D., Furst, D.E., Arriola, E., Silver, R., Strange, C., Bolster, M., Seibold, J.R., Riley, D.J., Hsu, V.M., Varga, J., Schraufnagel, D.E., Theodore, A., Simms, R., Wise, R., Wigley, F., White, B., Steen, V., Read, C., Mayes, M., Parsley, E., Mubarak, K., Connolly, M.K., Golden, J., Olman, M., Fessler, B., Rothfield, N. & Metersky, M.,(2006) Cyclophosphamide versus

placebo in scleroderma lung disease. *The New England journal of medicine*, 354, pp.2655–2666.

Tiefenbach, T. & Junop, M.,(2012) Pso2 (SNM1) is a DNA structure-specific endonuclease. *Nucleic Acids Research*, 40(5), pp.2131–2139.

Tiengwe, C., Marcello, L., Farr, H., Gadelha, C., Burchmore, R., Barry, J.D., Bell, S.D. & McCulloch, R.,(2012) Identification of ORC1/CDC6-interacting factors in trypanosoma brucei reveals critical features of origin recognition complex architecture. *PLoS ONE*, 7(3), pp.22–24.

Tiengwe, C., Marques, C.A. & McCulloch, R.,(2014) Nuclear DNA replication initiation in kinetoplastid parasites: new insights into an ancient process. *Trends in parasitology*, 30(1), pp.27–36.

Tran, T., Saheba, E., Arcerio, A. V, Chavez, V., Li, Q.-Y., Martinez, L.E. & Primm, T.P.,(2004) Quinones as antimycobacterial agents. *Bioorganic & medicinal chemistry*, 12(18), pp.4809–13.

Tudor, G., Alley, M., Nelson, C.M., Huang, R., Covell, D.G., Gutierrez, P. & Sausville, E.A.,(2005) Cytotoxicity of RH1: NAD(P)H:quinone acceptor oxidoreductase (NQO1)-independent oxidative stress and apoptosis induction. *Anti-cancer drugs*, 16(4), pp.381–91.

Tufts Center for the Study of Drug Development,(2014) Cost to Develop and Win Marketing Approval for a New Drug Is $2.6 Billion. Available at: http://csdd.tufts.edu/research [Accessed April 23, 2015].

Valavanis, C., Boussiotis, V.A. & Pangalis, G.A.,(1993) Accumulation of O6-methylguanine in Human DNA after therapeutic exposure to methylating agents and its relationship with biological effects. *Environmental health perspectives*, 99, pp.143–147.

De Vas, M.G., Portal, P., Alonso, G.D., Schlesinger, M., Flawiá, M.M., Torres, H.N., Fernández Villamil, S. & Paveto, C.,(2011) The NADPH-cytochrome P450 reductase family in Trypanosoma cruzi is involved in the sterol biosynthesis pathway. *International journal for parasitology*, 41(1), pp.99–108.

Vincendeau, P. & Bouteille, B.,(2006) Immunology and immunopathology of African trypanosomiasis. *Anais da Academia Brasileira de Ciências*, 78(4), pp.645–65.

Vincent, I.M., Creek, D., Watson, D.G., Kamleh, M.A., Woods, D.J., Wong, P.E., Burchmore, R.J.S. & Barrett, M.P.,(2010) A molecular mechanism for eflornithine resistance in African trypanosomes. *PLoS pathogens*, 6(11), p.e1001204.

Voak, A. a, Gobalakrishnapillai, V., Seifert, K., Balczo, E., Hu, L., Hall, B.S. & Wilkinson, S.R.,(2013) An essential type I nitroreductase from Leishmania major can be used to activate leishmanicidal prodrugs. *The Journal of biological chemistry*, 288(40), pp.28466–76.

Voak, A.A., Seifert, K., Helsby, N.A. & Wilkinson, S.R.,(2014) Evaluating aziridinyl nitrobenzamide compounds as leishmanicidal prodrugs. *Antimicrobial Agents and*

Chemotherapy, 58(1), pp.370–377.

Ward, T.A., Dudášová, Z., Sarkar, S., Bhide, M.R., Vlasáková, D., Chovanec, M. & McHugh, P.J.,(2012) Components of a Fanconi-Like Pathway Control Pso2-Independent DNA Interstrand Crosslink Repair in Yeast. *PLoS Genetics*, 8(8).

Wastling, S.L., Picozzi, K., Wamboga, C., Von Wissmann, B., Amongi-Acup, C., Wardrop, N.A., Stothard, J.R., Kakembo, A. & Welburn, S.C.,(2011) Latent Trypanosoma brucei gambiense foci in Uganda: a silent epidemic in children and adults? , (2008), pp.1480–1487.

Whitesell, L., Mimnaugh, E.G., De Costa, B., Myers, C.E. & Neckers, L.M.,(1994) Inhibition of heat shock protein HSP90-pp60v-src heteroprotein complex formation by benzoquinone ansamycins: essential role for stress proteins in oncogenic transformation. *Proceedings of the National Academy of Sciences of the United States of America*, 91(18), pp.8324–8328.

Wilkinson, S.R., Bot, C., Kelly, J.M. & Hall, B.S.,(2011) Trypanocidal activity of nitroaromatic prodrugs: current treatments and future perspectives. *Current topics in medicinal chemistry*, 11(16), pp.2072–84.

Wilkinson, S.R., Horn, D., Prathalingam, S.R. & Kelly, J.M.,(2003) RNA interference identifies two hydroperoxide metabolizing enzymes that are essential to the bloodstream form of the african trypanosome. *The Journal of biological chemistry*, 278(34), pp.31640–6.

Wilkinson, S.R. & Kelly, J.M.,(2003) The role of glutathione peroxidases in trypanosomatids. *Biological Chemistry*, 384(4), pp.517–525.

Wilkinson, S.R. & Kelly, J.M.,(2009) Trypanocidal drugs: mechanisms, resistance and new targets. *Expert reviews in molecular medicine*, 11(October), p.e31.

Wilkinson, S.R., Prathalingam, S.R., Taylor, M.C., Ahmed, A., Horn, D. & Kelly, J.M.,(2006) Functional characterisation of the iron superoxide dismutase gene repertoire in Trypanosoma brucei. *Free radical biology & medicine*, 40(2), pp.198–209.

Wilkinson, S.R., Taylor, M.C., Horn, D., Kelly, J.M. & Cheeseman, I.,(2008) A mechanism for cross-resistance to nifurtimox and benznidazole in trypanosomes. *Proceedings of the National Academy of Sciences of the United States of America*, 105(13), pp.5022–7.

Winger, J.A., Hantschel, O., Superti-Furga, G. & Kuriyan, J.,(2009) The structure of the leukemia drug imatinib bound to human quinone reductase 2 (NQO2). *BMC structural biology*, 9, p.7.

Wirtz, E., Leal, S., Ochatt, C. & Cross, G.A.,(1999) A tightly regulated inducible expression system for conditional gene knock-outs and dominant-negative genetics in Trypanosoma brucei. *Molecular and biochemical parasitology*, 99(1), pp.89–101.

Wiser, M.F.,(2011) *Protozoa and Human disease*, New York and London: Garland Science.

Wolburg, H., Mogk, S., Acker, S., Frey, C., Meinert, M., Schönfeld, C., Lazarus, M., Urade,

Y., Kubata, B.K. & Duszenko, M.,(2012) Late stage infection in sleeping sickness. *PloS one*, 7(3), p.e34304.

World Health Organisation,(2011) African trypanosomiasis (sleeping sickness). Available at: http://www.who.int/mediacentre/factsheets/fs259/en/.

World Health Organisation,(2015) Neglected tropical diseases. Available at: http://www.who.int/neglected_diseases/en/ [Accessed April 13, 2015].

World Health Organisation,(2014) Trypanosomiasis, human African (sleeping sickness). *Factsheet N°259*. Available at: http://www.who.int/mediacentre/factsheets/fs259/en/ [Accessed April 23, 2015].

World Health Organisation,(2013) WHO to roll out implementation strategy to eliminate sleeping sickness Title. Available at: http://www.who.int/neglected_diseases/HAT_roll_out_strategy_2013/en/ [Accessed April 23, 2015].

Wu, K., Knox, R., Sun, X.Z., Joseph, P., Jaiswal, A.K., Zhang, D., Deng, P.S. & Chen, S.,(1997) Catalytic properties of NAD(P)H:quinone oxidoreductase-2 (NQO2), a dihydronicotinamide riboside dependent oxidoreductase. *Archives of biochemistry and biophysics*, 347(2), pp.221–228.

Wurst, M., Robles, A., Po, J., Luu, V.-D., Brems, S., Marentije, M., Stoitsova, S., Quijada, L., Hoheisel, J., Stewart, M., Hartmann, C. & Clayton, C.,(2009) An RNAi screen of the RRM-domain proteins of Trypanosoma brucei. *Molecular and biochemical parasitology*, 163(1), pp.61–5.

Yan, C., Dufour, M., Siegel, D. & Reigan, P.,(2011) Indolequinone Inhibitors of NRH: Quinone Oxidoreductase 2. Characterization of the Mechanism of Inhibition in both Cell-Free and Cellular Systems. *Biochemistry*, pp.6678–6688.

Yan, C., Kepa, J.K., Siegel, D., Stratford, I.J. & Ross, D.,(2008) Dissecting the Role of Multiple Reductases in Bioactivation and Cytotoxicity of the Antitumor Agent 2 , 5-Diaziridinyl-3-. *Molecular pharmacology*, 74, pp.1657–1665.

Yang, Y., Voak, A., Wilkinson, S.R. & Hu, L.,(2012) Design, synthesis, and evaluation of potential prodrugs of DFMO for reductive activation. *Bioorganic and Medicinal Chemistry Letters*, 22(21), pp.6583–6586.

Zhu, R., Liu, M.-C., Luo, M.-Z., Penketh, P.G., Baumann, R.P., Shyam, K. & Sartorelli, A.C.,(2011) 4-nitrobenzyloxycarbonyl derivatives of O(6)-benzylguanine as hypoxia-activated prodrug inhibitors of O(6)-alkylguanine-DNA alkyltransferase (AGT), which produces resistance to agents targeting the O-6 position of DNA guanine. *Journal of medicinal chemistry*, 54(21), pp.7720–8.